SYNTHESIS AND CHARACTERIZATION OF DISULFONATED POLY(ARYLENE ETHER SULFONE) RANDOM COPOLYMERS AS MULTIPURPOSE MEMBRANES FOR REVERSE OSMOSIS AND FUEL CELL APPLICATIONS

Natalie Yolanda Arnett

Dissertation submitted to the faculty of Virginia Polytechnic Institute and State University in partial fulfillment of the requirements for the degree of

DOCTOR OF PHILOSOPHY
In
Macromolecular Science and Engineering

James E. McGrath, Chair
Judy S. Riffle
Robert B. Moore
John G. Dillard
William L. Harrison

March 26, 2009
Blacksburg, Virginia

Keywords: proton exchange membrane, fuel cell, reverse osmosis, disulfonated copolymers, copolymer blends, asymmetric membranes, diffusion induced phase separation (DIPS), phase diagrams, thin film composites, random, morphology, poly(arylene ether sulfone)

SYNTHESIS AND CHARACTERIZATION OF DISULFONATED POLY(ARYLENE ETHER SULFONE) RANDOM COPOLYMERS AS MULTIPURPOSE MEMBRANES FOR REVERSE OSMOSIS AND FUEL CELL APPLICATIONS

Natalie Yolanda Arnett

ABSTRACT

The results described in this dissertation focus on the synthesis and utilization of several disulfonated poly(arylene ether) random copolymer membranes in fuel cell and reverse osmosis applications. Poly(arylene ether)s were prepared by direct step copolymerization using a third monomer 3,3'-disulfonated 4,4'-dichlorodiphenylsulfone. The membrane properties of a 4,4'-biphenol-based disulfonated poly (arylene ether sulfone) random copolymer (BPS-35), optionally blended with various fluorine containing polymers or unsulfonated biphenol-based poly (arylene ether sulfone)s (Radel R) were investigated for fuel cell applications. Fluorine containing copolymers used included with 2,2'-hexafluoroisopropylidene 4,4'-biphenol based unsulfonated (6F-00) or disulfonated (6FS-35 and 6FS-60) PAES, hexafluoroisopropylidene biphenol based 4,4'-difluoro phenyl phosphine oxide) (6FPPO), and poly(vinylidene fluoride) (Kynar®). Tapping mode atomic force microscopy (TM-AFM) images of the membranes with 10 wt% of fluorinated copolymers showed macroscopic phase separation. Good miscibility between the copolymers at low concentrations was also confirmed by the observation of only one glass transition temperature. Compared to the benchmark Nafion 1135, the 10wt% blends of the fluorinated copolymers afforded a considerable reduction in the

methanol permeabilities, which is important for direct methanol fuel cells (DMFC). The best DMFC performance with 0.5 M methanol fuel was illustrated with blends containing 10 wt% 6FS-00. At higher methanol concentrations (up to 2.0 M) BPS-35/6FS-00 (90/10) membranes outperformed both Nafion membranes.

Blends of BPS-35 blends with 6FS-35 or Radel R were also used as RO membranes. The highest salt rejections of 97.2 and 98.0% were obtained from BPS35/Radel R (90:10) and BPS-35/6FS-35 (95:5) blends, respectively in the salt form.

A systematic study of the preparation of BPS-20 random copolymer skin-core asymmetric membranes by diffusion induced phase separation (DIPS) from various polar aprotic solvent or cosolvent systems is reported. The best aprotic solvents to generate an asymmetric structure were NMP and DMAc whereas tetrahydrofuran (THF)/ formamide (FAm) (80/20 v/v) mixtures proved to be the best co-solvent systems. Acetone was the best non-solvent to prepare asymmetric membranes from both aprotic solvents and co-solvent mixtures. Overall, asymmetric membranes prepared from THF/FAm co-solvent mixtures illustrated the most stable phase separated morphology that was free of macrovoids. However, thicker skins (~5 μm) were formed due to the high volatility of THF. Therefore, ultra-thin skin thin film composites (TFC) based on BPS-20 in diethylene glycol (Di(EG) were prepared. Thermal treatment of these TFC was conducted at 90 ^{o}C and the addition of 20 wt% glycerin to the casting formulation helped to prevent pore collapse in the porous Udel polysulfone. A minimum of three coats was required to obtain a dense, smooth, and pinhole free skin layer. The generation of three dimensional (ternary) solubility parameter phase diagrams based on experimental data

was formulated and a region of solubility based on the solubility parameters of the aprotic solvents and the different co-solvent systems was established for BPS-20.

Dedicated to my loving husband, Ron and precious daughter Nasya for their patience, understanding, support, and love.

ACKNOWLEDGEMENTS

I would first like to give my heartfelt appreciation to my advisor, Dr. James E. McGrath for his guidance, encouragement, and patience. I would especially thank him for going beyond what is expected of him to make my graduate years as unforgettable as possible. His involvement in my life and wonderful personality has been a great inspiration to me; I will never forget his kindness. I would also like to thank the members of my advisory committee, Dr. Judy S. Riffle, Dr. John G. Dillard, Dr. Robert Moore, and Dr. William Harrison for their valuable teachings and expertise that have allowed me to grow as a student and a professional. The time and attention that you have given me will always be remembered. Special thanks go to Dr. William Harrison for his mentoring, encouragement, and advice over my graduate years.

Many thanks go to my colleagues past and present for their assistance, discussions, suggestions, and friendship: Dr. Chang Lee, Dr. Abhishek Roy, Dr. Anand S. Badami, Dr. Mou Paul, Dr. Hang Wang, Dr. Melinda Einsla, Dr. Brian Einsla, Dr. Charles Tchatchoua, Dr. Kent Wiles, Dr. Zhongbiao Zhang, Dr. Xiang Yu, Hae-Seung Lee, Rachael VanHouten, and Juan Yang. Your suggestions and discussions over the years have helped me tremendously. I would especially like to thank Miss Ozma Lane for all her help, your late nights have not gone unnoticed. Thank you all so much

I would like to thank Mrs. Laurie Good, Mrs. Millie Ryan, and Mrs. Tammy Jo Hiner their encouragement, kindness, and help with various tasks over the years.

I would like to extend my deepest gratitude to my parents Mr. Philip and Rosalie Arnett for their love and support. Your unchanging presence and endless love in my life have

made me the person that I am today. I could not have attained this accomplishment without you. You have been there from the beginning and I am blessed to have you in my life. Thank you to my sibling Philippa, Nicole, Rosevelt, Nathan, and Jonathan for always being there when I needed anything. Also to my nephew Juwan whose laugh and intelligence always brings a joy to my heart. I would also like to thank my entire family for their love, prayers, and assistance that have aided me to this point of my life. I love you all so much.

I would also like to express my appreciation to all of my friends primarily Tuesday, Antorn, Rosalind, and Keisha who have being there from the start. Also I would like to thank Dana for all your love, support and for taking care of my baby when no one else would. Thanks to you all for believing that I could do this.

My devoted husband, Ron who played a large part in helping me acquire this significant accomplishment, is worthy of the greatest recognition by far. His love, wisdom, and sense of humor really keep me going and I have been extremely blessed to have him in my life. I would also like to thank my baby Nasya whose curious nature has kept me smiling and great hugs have given me strength to move forward. I love you both so much.

To the greatest love, my Lord and Savior Jesus Christ, thank you for being the source of my strength, joy, love, and blessings. It is through you, Lord, that all this is possible. I could not have finished this journey without you.

ATTRIBUTION

Several colleagues and coworkers aided in the writing and research behind several of the chapters of this dissertation. A brief description of their contributions is included here.

Prof. James E. McGrath (Department of Chemistry, Virginia Tech) is the primary advisor and committee chair. Prof. McGrath gave the author tremendous help and guidance on this work.

William L. Harrison (NanoSonic, Inc.) is a committee member and mentor. Dr. Harrison helped the author with the blend preparation and discussion in chapters 2, 3, and 4.

Frank Cromer (Department of Chemistry, Virginia Tech) helped the author with X-ray Photoelectron Spectroscopy (XPS) measurements in Chapter 2.

Anand Badami (Department of Chemistry, Virginia Tech) currently at Dow Chemicals helped with tapping mode atom force microscopy (TP-AFM) measurements in chapter 2.

Limin Dong (deceased) contributed to the preliminary blend preparation in chapter 2.

Ozma Lane (Department of Chemistry, Virginia Tech) provided TP-AFM, proton conductivity, and relative humidity measurements in chapter 3; SEM measurements and discussion in chapters 6, 7, and 8.

Dr. Ho Bum Park (University of Texas at Austin, Department of Chemical Engineering) carried out reverse osmosis measurements in chapter 5.

Bryan McCloskey (University of Texas at Austin, Department of Chemical Engineering) carried out reverse osmosis measurements and bubble tests in chapter 8.

Dr. Benny Freeman (University of Texas at Austin, Department of Chemical Engineering) was the primary advisor to Dr. Park and Mr. McCloskey and contributed to the discussion of the reverse osmosis measurements in chapters 5 and 8.

Abhishek Roy (Department of Chemistry, Virginia Tech) currently at Dow Water Solutions aided in the discussion and measurements of proton exchange membrane properties in chapters 2 and 3.

Dr. Melinda Einsla (Los Almos National Laboratories) currently at Rohm & Haas contributed to chapter 4 by performing direct methanol fuel cell performance measurements.

Dr. Chung Hyun Lee (Department of Chemistry, Virginia Tech) was instrumental in formulating three dimensional phase diagram in chapters 6, 7, and 8. Dr. Lee also aided in the preparation and reverse osmosis measurements of thin film composites in chapter 8

TABLE OF CONTENTS

LIST OF FIGURES

LIST OF TABLES

CHAPTER 1. LITERATURE REVIEW

1. INTRODUCTION TO POLY(ARYLENE ETHER)S

High temperature polymers such as poly (arylene ether)s are an important group of commercially available thermoplastics with a wide range of desirable properties. [1] Poly (arylene ether)s are well known engineering thermoplastics that were first successfully prepared in high molecular weight by R. N. Johnson, *et al* in 1967. [2] The general structure of poly(arylene ethers) is given in Figure 1-1. These amorphous or semi-crystalline high performance engineering thermoplastics exhibit a variety of properties including high thermal, hydrolytic, and oxidative stability, good mechanical strength, and high glass transition temperatures.[3]

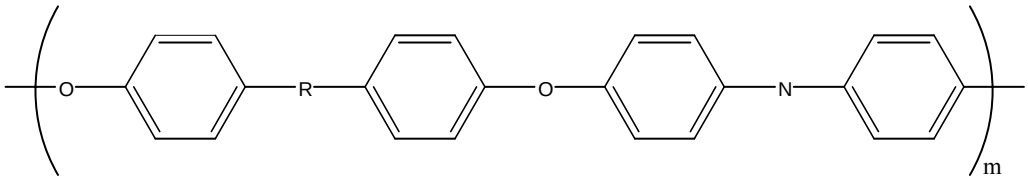

Figure 1-1. A basic structure of poly(arylene ether).

.

Initial interests in poly (arylene ether)s begin with the synthesis of polysulfone condensation polymers from p, p'- dihalodiphenyl sulfones and p-phenylenedithiols by

[1] Hedrick, J.L.; Labadie, J.W., *Step-Growth Polymers for High Performance Materials: New Synthetic Methods*, ACS Symp. Ser. 624, 1996.
[2] Johnson, R.N., Farnham, A.G., Clendinning, R.A., Hale, W.F., Merriam C.N., *J. Polym. Sci.: Part A-1* **1967,** (5), 2399-2414.
[3] a) Cotter, R.J. *Engineering Plastics: Handbook of Polyarylethers*, Gordan and Breach Publishers: Basel, Switzerland, 1995. b) Johnson, R.N. in *Encyclopedia of Polymer Science and Technology*, N.M. Bikales, Ed., John Wiley & Sons: New York, 1969.

Kreuchunas in 1958.[4] Since then several variations of poly(arylene ethers) such as UDEL® (polysulfone), PEEK® (polyetheretherketone), and Victrex® PES (polyethersulfone) have become commercially available. Consequently, enhancements in polymer properties due to polymer structural changes have led to the utilization of these polymers in automobiles, membranes, electronics, and aerospace industries.[5]

1.1. Synthesis of Poly(arylene ether)s

Poly(arylene ether)s have been synthesized by several techniques including Ullmann ether synthesis, nickel coupling reactions, electrophilic aromatic substitution via Friedel-Crafts reactions and nucleophilic aromatic substitution, with the latter clearly being the most important.

1.1.1. The Ullman Reaction

Ullman reactions involve the reaction of a phenol (phenolate) with an aromatic halide in the presence of a copper catalyst. Typically, Ullman reactions have been thoroughly investigated for small molecules. However, the potential of forming unique poly(arylene ether)s structures is possible in Ullmann reactions due to the utilization of non-activated aromatic halides.[6,7,8,9,10] The halide reactivity was determined to be the

[4] Algird Kreuchunas. Polysulfone condensation polymers. *US Patent 2822351*, 1958.
[5] a) R.N. Johnson, Encyclopedia of Polymer Science and Technology, N.M. Bikales, Ed., Wiley, New York, (1969); b) D.C. Clagett, Encyclopedia of Polymer Science and Engineering, Mark, H. F.; Bikales, N. M.; Overberger, C. G.; Menges, G., Ed., John Wiley & Sons: New York, , Vol. 6, 94 (1986).
[6] S. Wang and J. E. McGrath, " Polyarylene Ethers": A Review, in M. Rogers and T.E. Long, eds., Step Polymerization, Wiley, 2002.
[7] Farnham, A.G.; Johnson, R.N., *US Patent 3,332, 909* , 1967.

opposite of that observed for classical step addition nucleophilic aromatic substitution reactions I > Br > Cl >> F. This implies that the diiodo and dibromo monomers were the most reactive since the breaking of the aryl halide bond was the fastest rate determining step under Ullmann conditions.

The synthesis of high molecular weight poly arylene ethers utilizing Ullmann-like reactions was reported by several investigation, including Stamatoff,[11,12] Burgoyne,[13] Robeson,[13] and Jurek et al.[8,9] Stamaoff successfully utilized cuprous chloride and an organic base as cocatalyst to prepare condensed p-bromo-sodium phenolate in inert organic solvents such as nitrobenzene and benzophenone at high temperatures. However, benzophenone was proven to be a better solvent with a cuprous chloride-pyridine complex catalyst because the resulting polymers demonstrated thermal stability and low dielectric constants.[14] An oxygen free polymerization system must be maintained to produce high molecular weight polymers dry, since oxygen promotes a free radical side reaction leading to non-linear and/or crosslinked polymers.[13]

Jurek et al[9] also synthesized high molecular weight poly(arylene ether)s via Ullmann coupling reactions of bisphenols and dibromoarylenes in the presence of a copper catalyst. Unfortunately, this approach had poor reproducibility, required special brominated monomers, and final removal of the copper salts was difficult.

1.1.2. Nickel Coupling Reactions

---

[8] Jurek, M.J., McGrath, J.E., *ACS Polymer Preprints* **198**7, 28(1), 180-182.
[9] Jurek, M.J., Ph.D. Thesis, VPI &SU, 1987.
[10] Jennings, B.E.; Jones, M.E.B.; Rose, J.B., *J. Polym. Sci.: Part C* **1967**, 16, 715-724.
[11] (a) Stamatoff, G.S., *French Patent 1,301,174* , 1962, (b) Stamatoff, G.S., *US Patent 3,228,910* , 1966.
[12] Stamatoff, G.S., *Chem Abstracts 66*, 56009q.
[13] Burgoyne, W.; Robeson, L. M. US Patent *5,658,994*, 1997.
[14] Pankova, E.S.; Martsenitsena, S.V.; Derlin, A.A., *Vysokomol Soyed A*, 1975, 17(7), 1415-1420.

A relatively new approach for preparing poly(arylene ethers) employed nickel (Ni^0)-catalyzed coupling reactions to form aromatic carbon-carbon bonds from halogenated aromatic compounds.[15] Originally the coupling reaction of Ni^0 with aryl halides was utilized to synthesizing biphenyl quantitatively from chlorobenzene. Some advantages associated with Ni^0 coupling reactions, unlike Ullmann reactions, are that these reactions can proceed with both chloro and fluoro compounds in the presence of an activated or unactivated halide. Additionally, milder reaction temperatures (60-80^oC) are used when the polymerization is carried out in aprotic solvents.[16,17]

Colon et al[15,16] prepared polyarylene ether sulfone from Ni^0 coupling reactions with selected aryl dichloride monomers. Metal zinc, magnesium, and manganese were used along with the nickel catalyst to drive the polymerization, resulting in high yields of coupled products. To obtain high molecular weight polymers, amorphous polymers that were soluble in the dipolar aprotic solvents at low reaction temperatures of 60-80^oC were required. This was necessary because the coupling reaction between the homogeneous active catalyst and the aryl chlorides had to take place in solution. Polymerization parameters such as zinc purity, water removal, and inert environments were carefully monitored since these factors could affect either the molecular weight of the polymers or catalyst activity.

A detailed study of the polymerization conditions utilizing nickel catalyzed coupling reactions to synthesize poly(arylene ether sulfone)s was also published[17, 18].

---

[15] Colon, I. and Kwiatkowski, G.T. *J. Polym. Sci.: Part A: Polym. Chem.* **1990**, 28, 367-383.
[16] Colon, I.; Maresca, L. M.; Kwiatkowski, G. T. *U S Patent 4, 263 466* , 1991
[17] Havelka, P. A.; Shearea, V. V. *Macromolecules* **1999**, *32*, 6418-6424.
[18] Mitsuru Ueda and Fumiaki Ichikawa Macromolecules **1990,** 23, 926-930.

Unfortunately, low molecular weight polymers were formed due to side reactions such as the reduction of the aryl chloride to ArH or the transfer of the aryl groups from triphenylphosphine to metal.

Ghassemi and McGrath[19] reported the synthesis of aromatic phosphine oxide containing polymers via nickel catalyzed coupling polymerizations of bis(4-chloro-phenyl)phosphine oxide. The dichloro monomer was added to the activated catalyst mixture instead of other polymerization reagents to achieve higher molecular weight polymers. The reduction of the phosphine oxide groups in poly(4,4'-diphenylphenylphosphine oxide) (PAPO) could be achieved using phenylsilane.

1.1.3. Friedel-Crafts Electrophilic Substitution

Friedel-Craft electrophilic substitution of aryl sulfonyl chlorides with aryl ethers is another synthetic technique used to prepare poly (arylene ethers sulfone)s.[20] This reaction method involves the self condensation of A-B monomers through a two-stage mechanism.[21] The first step of polysulfonylation is the formation of the sulfonylium cation $ArSO_2^+$, resulting from the action of the Lewis-acid catalyst with the sulfonyl halide. Next, the electrophilic cation attacks the aromatic carbon to generate an intermediate complex by losing a proton and yielding the new sulfone linkage. The electrophilic attacking agent is formed by the reaction of a Friedel –Craft catalyst with the sulfonyl chloride. The primary byproduct for these polymerizations is HCl. Electron-

[19] Ghassemi, H.; McGrath, J.E., *Polymer* **1997**, 38, 3139-3143; (b) Ghassemi, H. and McGrath, J. E. *Polymer Preprints,* **2002**, 43(2), 1021-1022.
[20] a) J.B. Rose, *Polymer* **1974**, 15, 456-465; b) Ivin, K.J.; Rose, J.B., *Advances in Macromolecular Chemistry*, W.M. Pasika, Ed., Academic Press, London, Vol. 1, 336, 1968.
[21] Suter, C.M.; in *The Organic Chemistry of Sulfur*, New York, 1944, p.670.

donating groups enhance the sulfonylation process therefore, it is important that the aromatic ring being attacked does not contain electron withdrawing substituents, such as -SO_2- or –CO-.

Several catalysts, such as $AlCl_3$, $AlBr_3$, $FeCl_3$, $SbCl_5$, or BF_3, have been utilized in Friedel- Crafts reactions.[22,23] Low concentrations of these catalysts are recommended to minimize side reactions and to allow easier catalyst removal from the polymers.

Poly(arylene ether)s prepared by this two step method can be synthesized both in bulk and in solution. Typical solvents include dimethyl sulfone, chlorinated biphenyl and nitrobenzene. Early bulk polymerizations which were conducted in the melt required low concentrations (0.1 to 4 wt% $FeCl_3$) of Lewis acids at temperatures of 120 to 250^oC.[24,10] However, variations in polymer structure due to sulfonylation on various positions on the arylene-ring[25] and branched or crosslinked material were commonly associated with bulk polymerizations via Friedel-Craft mechanisms.

In 1962, Bonner was perhaps the first to obtained low molecular weight poly(arylene ether ketone)s via Friedel-Crafts condensation.[26] It was not until over 20 years later that high molecular weight poly(arylene ether ketone ketone)s would be prepared.[27] These reactions were carried out in dichlorobenzene at room temperature under nitrogen. A large excess of $AlCl_3$ (>3 parts catalyst for every repeating unit in molecule) was also required.

---

[22] Cremlyn, R.J.; Bassin, P., *Phosphorus, Sulfur, and Silicon*, 1991, 56, 245.
[23] Olah, G.A., in *Friedel-Crafts Chemistry*, Wiley, New York, 1973, p. 488.
[24] Jones, M.E.B, *British Patent 979,111*, 1965, in Chem. Abstracts **1965**, 62, 9065h
[25] Cohen, S.M.; Young, R.H., *J. Polym. Sci., Polym. Chem. Ed.* **1966**, 4, 722.
[26] U. S. Pat. 3, 065, 205 (1962), Du Pont Co., inv.: W. H. Bonner; *Chem. Abstr*. **58**, 5806f.
[27] U. S. Pat. 4, 816, 556 (1989); Du Pont Co., invs.: F. P. Gay, C. Brunnette; *Chem. Abstr*. **106**, 5631y.

High molecular weight poly(arylene sulfone)s with good solubility have also been made via Friedel-Craft sulfonylation mechanism in solution at lower temperatures (~120^{o}C).[28] Slower polymerizations of relatively deactivated monomers were also carried out in solution; however, some branching was noted.[10]

1.1.4. Nucleophilic Aromatic Substitution

The most ideal pathway used to synthesize completely poly (arylene ether)s is nucleophilic aromatic substitution (S_NAr).[29,30,31,32] Nucleophilic aromatic substitution is composed of two step reactions of activated halide monomers with an aromatic bisphenol. The low reactivity of the resonance–stabilized aromatic leaving groups restricts the application of unactivated halide monomers.[33] The first step, which is the rate determining step, generates a resonance stabilized carboanion through nucleophilic attack on the carbon-halide bond.[34] This generates a carboanion intermediate called a Meisenheimer complex.[35] The presence of these Meisenheimer complexes has been demonstrated by Fyfe et al.[36] The second step results in the re-establishment of the phenyl ring aromaticity by the elimination of the halide ion. Stabilization of the Meisenheimer salt intermediate in the S_NAr reaction mechanism is extremely important

[28] Cudby, M. E. A.; Feasey, R. G.; Jennings, B. E.; Jones, M. E. B.; Rose, J. B. *Polymer* 1965, 6, 589-601.
[29] Rose, J. B. In Recent Advances in Mechanistic and Synthetic Aspects of Polymerization; D. Riedel Publishing: Boston, 1987.
[30] Johnson, R.N., in *Encyclopedia of Polymer Science and Engineering,* N.M. Bikales, Ed., John Wiley & Sons: New York, 1969.
[31] Hedrick, J. L.;Mohanty, D. K.; Johnson, B. C.; Viswanathan, R.; Hinkley, J. A.; McGrath, J. E. *J. Poly Sci, Part A* **1986**, *23*, 287-300.
[32] March, J. *Advanced Organic Chemistry*; 3rd ed.; John Wiley and Sons: New York, 1985.
[33] Cotter, R.J. *Engineering Plastics: Handbook of Polyarylethers*, Gorden and Breach Publishers: Basel, Switzerland, 1995.
[34] a) Bunnett, J.F., Zahler, R.F., *Chem. Rev.* **1951**, 49, 273-412.
[35] Meissenheimer, J. *Liebigs. Ann. Chem.* **1902**, *323*, 205-246.
[36] Fyfe, C. A.; Koll, A.; Damji, W. H.; Malkiewich, C. D.; Forte, P. A. *Can. J. Chem.* **1977**, *55*, 1468-1472.

to the efficiency of the overall S_NAr process mechanism. Factors including the leaving group (fluorine is better than chlorine), the nucleophile, the activating group, and the solvent influence the resonance stabilization of Meisenheimer transition state.

The reactivity of the aryl halide in S_NAr reactions is independent of the carbon-halogen bond. Therefore, the influence of the leaving group in S_NAr mechanisms is related to the polar effect of the halogen. Bunnett[34] illustrated that even though the carbon-halogen bond strength decreases, the greater bond dipole of the C-F bond results in faster attack by a nucleophile. The rate sequence of halogen leaving groups was reported as F >> Cl ≥ Br ≥ I. Better access of the nucleophile to the activated carbon could also be a factor since the small fluorine atom imparts less steric hindrance.

The Meisenheimer intermediate is further stabilized due to the greater electronegativity associated with the fluorine atom permitting more electron density to be inductively pulled away from the activated carbon atom. Other groups such as alkoxy, nitro, and sulfonyl can also act as good leaving groups. The proposed order of the leaving groups in nucleophilic aromatic substitution reaction is listed as $F^- > NO_2^- > {}^-SO_3Ph > Cl^- > Br^- \sim I^- > {}^-OAr > {}^-OR > {}^-SR$.[37]

Successful synthesis of poly (arylene ether sulfones) also depends heavily on the ease of the nucleophile to facilitate in departure of the leaving group. Properties associated with a good nucleophile in nucleophilic aromatic substitution are:[38]

1. the polarizability and electronegativity of the nucleophile;
2. the bond strength between the nucleophile and the carbon it is attacking;
3. nucleophile size; and

[37] (a) Miller, J.A., in *Aromatic Nucleophilic Substituion,* Elsevier, London, 1961, p. 61, and (b) Beck, J.R., *Tetrahedron* **1978**, 34, 2057-2068.
[38] Carey, F. A.; Sundberg, R. J. *Advanced Organic Chemistry*; 3rd ed.; Plenum Press: New York, 1990.

4. the solvation energy of the attacking atom

The order of increasing nucleophilic strength has been established as $ArS^- > RO^- > R_2NH^- > ArO^- > OH^- > ArNH_2 > NH_3 > I^- > Br^- > Cl^- > H_2O > ROH$.[119] The superior behavior of the phenoxide anion is related to better polarizability and weaker solvation of heavier atoms.

Nucleophilic aromatic substitution reactions are normally performed in polar aprotic solvents because these solvents do not solvate the nuclophile.[112] Solvation of the attacking anion takes place readily in polar solvents due to strong interaction such as hydrogen bonding that may occur between the nucleophile and the solvent. Typically, the primary polar solvent that causes several major problems in S_NAR reactions is water. Water not only solvates the nucleophile but can also act as a nucleophile which ultimately leads to low molecular weight polymers. The addition of an azeotroping agent such as o-dichlorobenzene, toluene, or xylene assists in the exclusion of water from the synthetic process.

Meisenheimer complexes are most strongly stabilized by electron withdrawing groups that are usually para to the substitution position. The ability of the activating group to accept the negative charge for the attacked rings occurs rapidly at these positions.[39] The most widely used activating groups in poly (arylene ethers) synthesis are sulfone, ketone, and nitrile groups The approximate order of the electron withdrawing group corresponds to the deactivating power of the substituent.

1.1.5. Two Approaches to Synthesis of Poly (Arylene Ether)s via Nucleophilic Aromatic Substitution

[39] Miller, J. A. *Aromatic Nucleophilic Substitution*; American Elsevier: New York, 1968.

Nucleophilic aromatic substitution of poly (arylene ether)s typically proceeds by two principal approaches; the strong base approach (e.g. sodium hydroxide) or the weak base approach (e.g. potassium carbonate). Both approaches undergo similar mechanisms that first require the formation of a phenolate or diphenolate anion from the reaction an aromatic bisphenol with a weak base or a strong base, respectively. The generated phenolate anion then reacts with an aromatic activated dihalide to produce a diaryl ether linkage.

1.1.5.1.Strong Base Approach

Synthesis of high molecular weight poly (arylene ether)s via the strong base approach was first introduced by Johnson et al. They investigated a series of polyethers prepared from different bisphenol monomers under various reaction conditions that were essential to successful synthesis of high molecular weight polyarylene ethers. The reaction employed sodium hydroxide, bisphenol A, 4,4'-dichlorodiphenyl sulfone (DCDPS), and dimethyl sulfoxide/chlorobenzene as the solvent.

The main advantage of the strong base approach was the short reaction time needed to reach high molecular weight. The disadvantage of the strong base method is the possibility of side reactions when water and oxygen is present. To obtain high molecular weight polymers, water and oxygen must be removed and the stoichiometry must be carefully controlled in the prepolymerization step. Water may be formed by the hydrolysis of the sodium phenolate groups in the presence of a strong base. The

formation of water in the reaction may essentially upset the stochiometry of the overall reaction to generate a less reactive bisphenol via hydrolysis of the activated halide. Cleavage of the activated aromatic ether linkages of the polymer and a reduced degree of polymerization may also be associated with the presence of water. Side reactions with oxygen result in oxidation of alkali phenates leading to lower molecular weights and discoloration of the polymer.

1.1.5.2. Synthesis of Poly(Arylene Ether Nitrile)s via the Weak Base Approach

Poly(arylene ether nitrile)s (PAEN) are a class of engineering thermoplastics that exhibit excellent heat, solvent, radiation, and flame resistance as well as good mechanical properties.[40] The pendant nitrile group promotes adhesion on many polymer substrates through polar interaction with other functional groups.[41] Various bisphenols have been studied for the synthesis of PAEN via nucleophilic aromatic substitution polymerization. Mohanty et al[42] studied the effects of different diphenol linking agents (sulfur, isopropylidene, and sulfone) on the properties and relative rates on PAEN synthesis. The more rigid sulfone group exhibited the highest glass transition temperature (222 ºC) but had the slowest reaction rate.

[40] A. Saxena, V.L. Rao, K.N. Ninan, *European Polymer Journal* **2003**, 39, 57-61.
[41] a) K.V. Sivaramakrishnan, C.S. Marvel, J. *Polym. Sci., Polym. Chem. Ed.* **1974,** 12, 651-662; b) T.M. Keller, *J. Polym. Sci., Polym. Chem. Ed*. **1988,** 26, 3199-3212.
[42] D.K. Mohanty, A.M. Walstrom, T.C. Ward, J.E. McGrath, *Polymer Preprints* **1986,** 24, 147-149.

Mutsuo et al.[43] prepared a series of crystalline and amorphous PAENs from 2,6 dichlorobenzonitrile (DBN) or 2,6 difluorobenzonitrile (DFBN) with various bisphenols in N-methylpyrrolidone (NMP) in the presence of potassium or sodium carbonate. Crystalline PAEN prepared from 2,6 dihalobenzonitrile with resorcinol showed similar thermal properties but higher tensile and flexural strengths compared to commercially available Victrex.

Phenolphthalein-modified PAEN copolymers with varying molar ratios of phenolphthalein (PP) and hydroquinone (HQ) have been synthesized by Li et al.[44] These polymers also exhibited high glass transition and decomposition temperatures that were dependent on increasing PP content.

1.1.5.3.Synthesis of Poly(Arylene Ether Phosphine Oxide)s via the Weak Base Approach

Poly(arylene ether phosphine oxide)s (PEPO) are high-temperature engineering thermoplastics characterized by high thermal stability and inherent flame resistance. The preparation of low molecular weight PEPOs were first recorded by Hashimoto et al[45]. Smith et al[46] synthesized PEPO homopolymers via nucleophilic aromatic substitution reactions of bis(4-fluorophenyl)phenyl (methyl) phosphine oxide with different bisphenol monomers. Intrinsic viscosities above 0.60 dL/g and glass transition temperatures

[43] S. Matsuo, T. Murakami, R.J. Takasawa, *Polym. Sci., Polym. Chem.* **1993,** 31, 3439.
[44] Li, C., Gu, Y., liu, X. *Materials Letters* **2006,** 60, 137 – 141
[45] Hashimoto, S., Furukawa, I., Ueyama, K. *Macromol. Sci. Chem.* **1977,** A11, 2167.
[46] Smith, C.D., Grubbs, H., Webster, H.F., Gungor, A., Wightman, J.P, McGrath, J.E. *High Performance Materials* **1991,** 3, 211-229.

ranging from 190 ºC for bisphenol PEPO to 282 ºC for 9,9-bis(4-hydroxyphenyl)fluorine (FL) PEPO were observed. These polymers were also self extinquishing as observed by Bunsen burner tests where complete volatilization did not occur upon removal from the flame. This was substantiated by high char yields (31 -43 %) between 600 to 800 ºC. In situ second harmonic generation (SHG) studies showed that in the F6 Bis A-PEPO poling temperatures only effected short term relaxation[47].

Riley et al have prepared PEPO copolymers from hydrolytically stable phosphorus-containing monomers[48]. High molecular weight poly(ary1ene ether)s based on 4,4'-bis(fluoropheny1)methylphosphine oxide (BFPMPO) were successfully synthesized via nucleophilic aromatic substitution. These polymers exhibited high glass transition temperatures (260°C) and decomposition temperatures well over 500°C.

The radiation chemistry of biphenol PEPO, bisphenol-A PEPO and hydroquinone PEPO prepared from bis(4-fluorophenyl)phenylphosphine oxide were also studied by electron spin resonance spectroscopy (ESR)[49]. Both neutral and anionic free radicals produced on gamma (γ)-irradiation of these polymers were detected after irradiation at 77K. At room temperature the radical yields for a given dose increased in the following order; biphenol < bisphenol- A < hydroquinone PEPO. This order of increase was due the ratio of ether bonds to aromatic groups in the polymer that undergo chain scission after exposure to ionizing radiation. Chain scission in the irradiated polymers was observed by a decrease in the molecular weight.

---

[47] Stacey Fu, C. Y., Priddy, D.B., Lyle, G.B., McGrath, J.E., Lackritz, H.S., *Mat. Res. Soc. Symp.Proc.* **1994,** 328, 547-552.

[48] Riley, D. J., Gungor, A. S., Srinivasan, A., Sankarapandian, M., Tchatchoua, C., Muggli, M. W., Ward, T.C., Kashiwagi, T., McGrath, J.E. *Polymer Engineering and Science*, **1997**, 37, 1501-1511

[49] Hopewell, J.L., Hill, D.J.T., O'Donneli, J.H., Pomery, P.J.,McGrath, J.E., Priddy, D.P., Smith, C.D. P*olymer Degradation and Stability* **1994,** 45, 293-299

1.1.5.4. Synthesis of Poly(Arylene Ether Ketone)s via the Weak Base Approach

High performance poly(arylene ether ketone)s (PAEK) with excellent mechanical properties, good resistance to acid and bases, high themal properties properties via nucleophilic aromatic substitution have been reporte[50]. Changes to the polymer chemical structure via various monomers have resulted in these polymers being used in gas separation[51] and wave guide devices[52]. Chng et al[51] prepared a series of homo/random copolymers PAEK from 4,4-difluorobenzophenone (DFBP), 2,2-bis(4-hydroxy-phenyl)propane (BPA), and 2,2-bis(4-hydroxy-3,5-dimethyl-phenyl)propane (TMBPA) in varying ratios. With the increase in TMBPA content, the gas permeation coefficients, diffusion and solubility coefficients of H_2, O_2, N_2, CO_2 and CH_4 increased due to the increased polymer free volume and chain stiffness by the tetramethyl substitution group on the phenyl rings.

Fluorinated PAEK has been developed by the synthesis of hexafluorobisphenol A (6F-BPA) with bis(pentafluorophenyl) ketone (BPK) in dimethylacetamide (DMAc) in the presence of CaH_2[53]. Unlike the conventional polycondensation of phenolate groups of hexafluorobisphenol A (6F-BPA) with para-fluorines of bis(pentafluorophenyl) ketone (BPK) no azeotropic distillation was required due to the fact that no water was produced.

---

[50] Rose, J.B in "Recent Advances in Mechanistic and Synthetic Aspects of Polymerization", M. Fontannille and A. Guyot Eds. D. Reidel Publishing Company, 1987 207-211.
[51] Chng, M.L., Xiao, Y., Chung, T.S., Toriida, M., Tarnai, S.*Polymer* **2007,** 48, 311-317
[52] Jiang, J. Callender, C. L., Noad, J. P., Qi, Y., Ding J., Day, M. *Optical Engineering* **2007,** 46, 074601-074607
[53] Ding, J., Day, M., Robertson, G. P., Roovers J., *Macromol. Chem. Phys.* **2004,** 205, 1070–1079

This ultimately improved the overall selectivity of the reaction resulting in high molecular weight polymer with low branching contents. Novel photocrosslinkable fluorinated PAEKs for waveguide devices have been also been synthesized by this procedure[52]. The fabricated waveguides from these devices show smooth surfaces and good definition.

One of the drawbacks of this group of semi-crystalline polymers is their high solvent resistance. However, this can be controlled by inserting bulky substituents onto the polymer backbone to suppress crystallinity. Poly(arylene ether ketone)s containing sulfonate groups were synthesized by aromatic nucleophilic polycondensation of 4,4'-difluorobenzophenone (DFK), sodium 2,5-dihydroxybenzensulfonate (SHQ) and phenolphthalein (PL) in dimethylsulfoxide at 175 ºC in presence of anhydrous potassium carbonate[54]. High-molecular weight (reduced viscosities above 0.68 dL/g) copolymers that were soluble in various aprotic solvents were obtained. A new series of wholly aromatic poly(ether ether ketone ketone) containing pendant sulfonic acid groups (SPAEEKK) with high intrinsic viscosities and showing good solubilities in aprotic solvents, enabling them to be cast into strong flexible films have also been prepared[55].

1.1.5.5.Synthesis of Poly(Arylene Ether Sulfone)s via the Weak Base Approach

Some of first synthetic methods to prepare poly(arylene ether sulfone)s utilizing weak bases such as potassium carbonate (K_2CO_3) as a means to possibly minimize side

[54] Wang, F., Chen, T., Xu, J., Liu, T., Jiang, H., Qi, Y., Liu, S., Li, X. *Polymer* **2006**, 47, 4148–4153
[55] Gao, Y. Robertson, G.P., Guiver, M.D., Mikhailenko, S.D., Li, X., Kaliaguine, S., *Macromolecules* **2004**, *37,* 6748-6754

reactions associated with sodium hydroxide were reported in the form of patents.[56] Poly(arylene ether sulfone)s are tough amorphous thermoplastics that have exceptional thermal and mechanical properties[57]. A beta (β) relaxations at about 100 ºC due to relaxations from the rotation in the aryl ether bond and relaxations of a sulfone-water complex are also characteristic of these copolymers[58].

Systematic studies to investigate and understand the details associated with the weak base method have been carried out extensively by McGrath et al since 1979.[59] Modifications to the polymer backbone by using other bisphenols and other diaryl sulfones to enhance thermal and other properties have also been demonstrated. A typical reaction scheme for the weak base approach is shown in Figure 1-2. McGrath and his colleagues prepared some novel poly(arylene ether)s from bisphenol type compounds by employing anhydrous potassium carbonate as a base and N,N'-dimethylacetamide as the dipolar aprotic solvent.[60] Possible reaction mechanisms were proposed. An azeotroping agent, toluene, was also used to dehydrate the reaction and avoided the problems associated with the hydrolysis of monomer and polymer. The bisphenolate insolubility for rigid systems could be avoided by deprotonating one phenol group at a time. Additionally, strict stochiometric control of the base in this procedure was not necessary since potassium carbonate did not cause any major hydrolysis of the halide. Therefore, a

[56] a) Clendinning, R.A.; Farnham, A.G.; Zutty, N. L.; Priest, D.C., *Canada Patent 847,963* , 1970.; b) Berd, B.; Claus, C.; *German Patent. 2,749,645* , 1975.; c) I. C. I. U.S.; *German Patent 2,635,101*; 1977; (b) I. C. I. Ltd.; *Japan Patent 7,812,991* , 1978.
[57] Harris, J. E., *Handbook of Plastic Materials and Technology*. Wiley: Canada, 1990.
[58] Robeson, L.M., Farnham, A.G., McGrath, J.E., "Dynamic Mechanical Characteristics of Polysulfone and Other Polyarylethers" D.J. Meier, Ed., MMI Mono Graph V 4, Gordon and Breach Sci. Pub., New York, 1978.
[59] Viswanathan, R., McGrath, J.E. *Polymer Prep*rints, **1979,** 20, 365.
[60] Viswanathan, R.; Johnson, B.C.; McGrath, J.E., *Polymer* **1984**, 12 (25), 1827.

20 mol% of potassium carbonate is the typical amount used in these polymerization reactions.

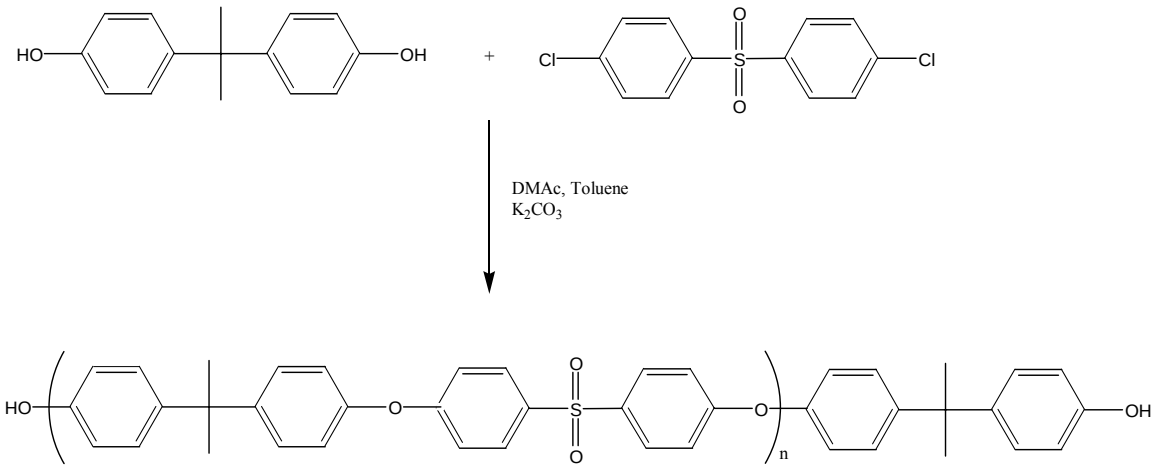

Figure 1-2. Synthetic scheme for preparation of bisphenol A based poly(arylene ether sulfone)[128].

Continuous studies of the weak base approach by this research group also alluded to the possibility of two synthetic routes to prepare poly(arylene ether sulfone). The first proposed mechanism involves the formation the bisphenate *in situ*, followed by attack on two activated dihalides whereas the second synthetic route, which is the preferred route, occurs through a monophenolate species.[61] Further kinetic studies to compare the weak and strong base approaches were also carried out by McGrath and Priddy[62]. Similar reaction conditions were used for both bases. Samples were taken from the reaction as a function of time, isolated in acetic acid and their end groups analyzed. Results from this series of experiments showed that the kinetics in the strong base reactions were dependent on the concentrations of the activated halide and the diphenolate. Therefore,

[61] Priddy, D.; Smith, C. D.; McGrath, J. E. In 43rd Annual Southeastern Regional Meeting of the American Chemical Society: Richmond, VA, 1991
[62] Priddy, D., *Ph. D. Thesis*, VPI & SU, 1994

the strong base approach yielded mono or disubstituted bisphenols. Similar reaction kinetics cannot be applied to the weak base method because only mono substituted products were detected in the first 100 minutes of the reaction. This is caused by the reduction in the formation of the diphenolate prior to reaction with the activated dihalide. The formation of disubstituted product in the weak base approach did not reach the concentration of monosubstituted product until five hours of reaction time. This phenomenon is the key to generating high molecular weight with a "rigid" bisphenol such as hydroquinone or 4,4'-biphenol where the biphenolate is highly insoluble and hence unreactive.

Radiation resistant hydroquinone (HQ), biphenol (BP), and biphenol-hydroquinone (HQ/BP) based PAESs have been synthesized[63]. HQ 50%/BP 50% and commercially available UDEL were exposed to electron radiation at doses of 120, 360, 690 Mrad. The HQ 50%/BP 50% displayed superior radiation resistance than UDEL as observed by the retention of mechanical properties and molecular weight up to 700 Mrad. The isopropylidene link in UDEL is the likely the source of free radical generation that leads to chain scission and crosslinking. The decreased radiation stability of UDEL only up to 50 Mrad has been demonstrated previously[64].

[63] Hedrick, J.L., Mohanty, D.K., Johnson, B.C., Viswanathan, R., Hinkley, J.A., McGrath, J.E. J. *Polym. Sci..: Polym. Chem. Ed*. **1986,** 23, 287-300.
[64] Brown, J.R., O'Donnell J. H., *J. Appl. Polym. Sci.* **1975,** 19, 405.

Most recently, poly(arylene ether sulfone)s have been synthesized containing pyridine and tetramethyl biphenyl groups to enhance the chemical composition[65]. Chemical modifications by sulfonation or carboxylation have allowed these polymers to be utilized in fuel cells and water purification applications.

1.2. Sulfonation of Poly(arylene ether)s

Several researchers have examined modifications to poly (arylene ether)s (PAE)s. The objective was to prepare advanced macromolecules for fuel cells or water purification by modifying (PAE)s without sacrificing their excellent physical, chemical, and mechanical properties. The aromatic rings in the polymer backbone allow for facile electrophilic or nucleophilic reactions to modify the physical properties of the polymer. Sulfonation is one of the most powerful and versatile processes used for polymer modification to increase hydrophilicity and other membrane properties such as higher water flux, improved permeability and proton conductivity.[66] Sulfonation of the poly (arylene ether)s occurs via electrophilic aromatic substitution.[67] The electrophilic aromatic substitution mechanism is reviewed in

Figure 1-3[68]. Sulfonation proceeds in the presence of more electronegative atoms than oxygen that increase the electron density at the aromatic ring causing the sulfur atom to become the electrophilic center. This allows sulfur to react at the position on the

[65] Pefkianakis, E. K.; Deimede, V.; Daletou, M. K.; Gourdoupi, N.; Kallitsis, J. K., *Macromol. Rapid Commun.* **2005,** 26, 1724-1728.
[66] Smitha, B.; Sridhar, S.; Khan, A.A.; Solid Polymer Electrolyte Membranes for Fuel Cell Applications—A Review. *J Mem. Sci.* **2005**, 259, 10-26.
[67] Kucera, F.; and Jancar, J; *Polymer Engineering and Science* **1998**, 38 (5), 783-792.
[68] Vallard, K. P. C. and Schore, N. E. *Organic Chemistry, Structure and Function, 3rd Ed.,* W. H. Freeman and Company: New York, 1999, 668.

aromatic ring with the highest electron density. However, several intermediate species are involved in sulfonation reactions which lead to complex reaction mechanisms.

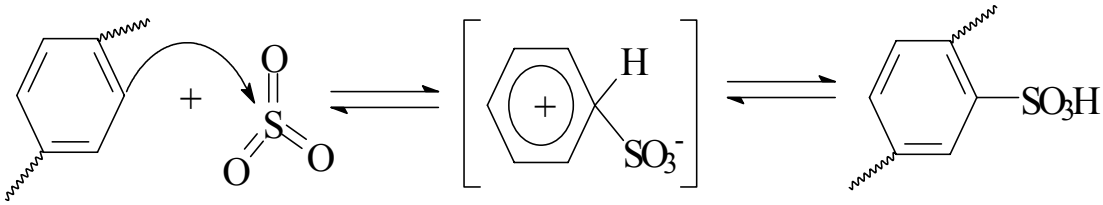

Figure 1-3. Representation of Sulfonation via Electrophilic Aromatic Substitution.

Typically, sulfonations at elevated temperatures (150 - 300ºC) are preferred because higher yields, especially at higher degrees of sulfonation are obtained. Drawbacks associated with the presence of highly reactive sulfonic acid groups included desulfonation and crosslinking. Coincidentally, the presence of these side reactions is increased at elevated temperature.

Generally, the two methods used to prepare sulfonated poly(arylene ether)s are post sulfonation or direct copolymerization reactions. In post sulfonation reactions preformed polymers are sulfonated whereas a sulfonated monomer is used to prepare the polymer via direct copolymerization. . Direct copolymerization reaction of poly(arylene ether)s proceeds by initially sulfonating the monomer, followed by the synthesis of the sulfonated polymers. The placement and amounts of the sulfonic groups on the repeat unit differ for each technique (Figure 1-4).[69]

[69] Hickner. M. A.; Ghassemi, H.; Kim, Y. S.; Einsla, B. R.; McGrath, J.,E.; Alternative Polymer Systems for Proton Exchange Membranes (PEMs) *Chem. Rev*. **2004**, 104, 4587-4612

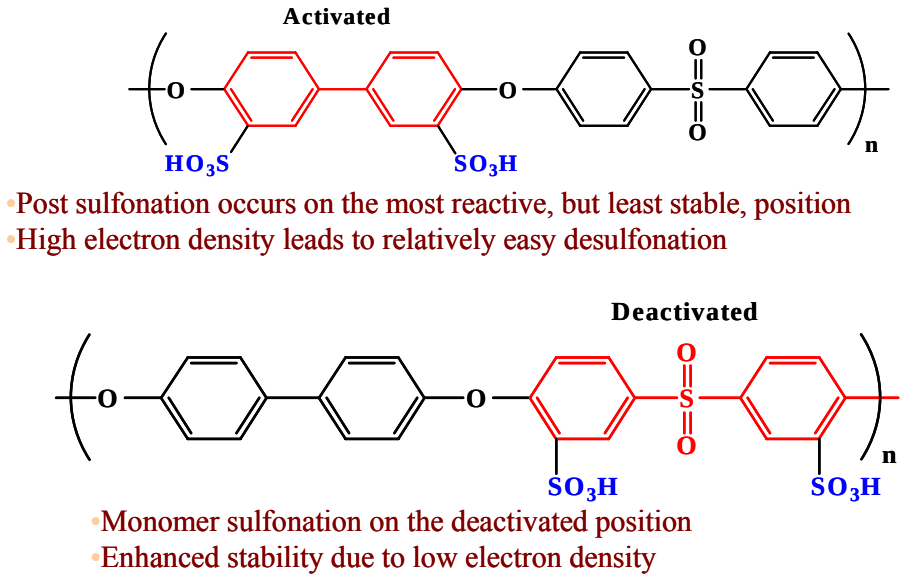

Figure 1-4. Placement of sulfonic acid group(s) from Post and Direct Sulfonation of Biphenol based Poly(arylene ether sulphone)s[70].

1.2.1. Post Sulfonation of Poly(Arylene Ether)s

Studies show that post-sulfonation reaction on the polymer result in the placement of up to one sulfonic acid group per repeat unit ortho to the activated aromatic ether linkage.[71] At this position there is a high electron density, making it the most reactive part of the polymer. Therefore, desulfonation of the polymer in aqueous acid or water occurs rather easily during a post-sulfonation reaction. The electrophilic release of the sulfonic acid groups in the presence of these reagents is due to the high concentration of $H^{\oplus}$ ions. In post sulfonation reactions, sulfonic acids are randomly introduced using

[70] Kenton Wiles., *Ph. D. Thesis*, VPI & SU, 2005
[71] M. Rikukawa and K. Sanui. *Prog. Polym. Sci.* **2000**, 25, 1463-1502.

chlorosulfonic acid ($ClSO_3H$),[72] concentrated sulfuric acid,[73,74] pure or complexed sulfur trioxide,[75,76] and methanesulfonic acid.[77]

Bishop et al,[78] illustrated the effect of various strong acids on the solubility and properties of a poly(ary1ene ether ketone). Upon dissolution in chlorosulfonic and concentrated sulfuric acids, PEEK was readily sulfonated to yield ionic polymers with modified properties. Chemical cross-linking due to the formation of sulfone links between aromatic rings on different polymer molecules has been related to varying degrees of "aggregation" observed in different solvents. The tendency of PEEK toward sulfone formation was noted by changes in molecular weight. Although dilution of H_2SO_4 minimized cross-linking, a dramatic decrease in the solubility of PEEK due to decreasing crystallinity with decreasing molar concentrations of H_2S0_4 was observed.

Previous post sulfonation research on bisphenol A poly(arylene ether sulfone) (UDEL®) and Victrex® was conducted by Quentin.[79] This researcher successfully carried out various degrees of sulfonation of these polymers at room temperature using chlorosulfonic acid. However, the presence of several adverse side reactions such as chain scission, branching and /or cross-linking at the isopropylidene group of UDEL® polymers was also apparent. Guan et al[80] showed that to suppress these side reactions associated with chlorosulfonic acid, sulfonations at lower temperatures (10ºC) should be

[72] Lee and C.S. Marvel, *J Polym. Sci., Polym. Chem. Ed*., **1984**, 22, 295.
[73] L. Jia, X. Xu, H. Zhang, and J. Xu, *J. Appl. Polym. Chem*., **1996**, 60, 123-131.
[74] X. Jin, M.T. Bishop, T.S. Ellis, and F.E. Karasz, *Br. Polym. J*., **1985**, 17, 4.
[75] M.I. Litter and S. Marvel, *J. Polym. Sci., Polym. Chem. Ed*., **1985**, 23, 2205.
[76] T, Owaga and C.S. Marvel, *J. Polym. Sci., Polym. Chem. Ed*., **1985,** 23, 1231.
[77] C. Bailly, D.J. Williams, F.E. Karasz, and W. J. MacKnight, *Polymer*, **1987**, 28, 1009-1016.
[78] Bishop, Matthew T.; Karasz,Frank E.; Langley, Kenneth H.; and Russet, Paul S. *Macromolecules* **1985**, 18, 86-93.
[79] Quentin , J. P. *Sulfonated Polyarylether Sulfones*, US 3,709,841. Rhone-Poulenc, January 9, **1973**.
[80] Guan, R.; Zou, H.; Lu, D.; Gong, C.; Liu, Y. European Polymer Journal **2005**, 41, 1554-1560.

conducted. The high reactivity of chlorosulfuric acid even at room temperature made control of the degree of sulfonation very difficult[81].

A relatively mild post sulfonation procedure utilizing sulfur trioxide and triethyl phosphate complex (SO_3-TEP) to sulfonate commercially available UDEL® was investigated by Noshay and Robeson.[82] Although the presence of a milder sulfonating agent could potentially minimize or even eliminate possible side reactions, lower reaction rates and less efficient sulfonations are associated with this process.

The success of SO_3-TEP to reduce these side reactions was illustrated by Johnson *et al.* who found no evidence of a crosslinking side reaction using sulfur trioxide in a comprehensive study on functional membranes using SO_3-TEP for water desalination.[83]

As shown in Figure 1-5**,** further studies by Nolte et al [84] illustrated that the occurrence of these reactions in the sulfonation of poly(arylene ether sulfone)s could be successfully minimized or controlled by utilizing trimethylsilyl chlorosulfonate as a protecting agent for the isopropylidene group during the sulfonation reaction. However, a degree of sulfonation of 90 mole% exhibited extreme swelling with water uptake of >400%.

Lufrano and collegues also utilized trimethylsilylchlorosulfonate as a mild sulfonation process to prepare proton exchange polysulfone membranes for PEMFC

---

[81] Trotta, F.; Drioli, E.; Moraglio,G.; Baima Poma, E. *Journal of Applied Polymer Science* **1998**, 70, 477-482.

[82] A Noshay; L.M. Robeson, *J. Appl. Polym. Sci.* **1976**, 20, 1885-1903; C.L. Brousse; R. Cheapurlet; J.P. Quentin, *Desalination* **1976**, 18, 137; V. Deimede, G.A. Voyiatzis, J.K. Kallitsis, L. Qingfeng, N.J. Bjerrum,; *Macromolecules*. **2000**, 33, 7609-7617.

[83] Johnson, B. C.; Yilgor, I.; Tran, C.; Iqbal, M.; Wightman, J.; Lloyd, D.; McGrath, J. E. *J. Polym. Sci. Polym. Chem. Ed.* **1984**, 22, 721-737.

[84] a) R. Nolte, K. Ledjeff, M. Bauer, and R. Mulhaupt, *J. Membr. Sci*., 1993, 83, 211-220; b) H.S. Chao and D.R. Kelsey, *US Patent 4,625,000*, 1986.

applications.[85] At 77 and 49% degrees of sulfonations the polysulfone membrane became swelled excessively or showed poor fuel cell performance, respectively..

Genova-Dimitrova et al [86] discouraged the use of sulfur trioxide and a triethyl phosphate complex to sulfonate due to an exothermic reaction and high toxicity associated with SO_3-TEP. Instead, trimethylsilylchlorosulfonate (TMSCS) was used for the post sulfonation reactions because it formed a perfectly homogeneous reaction mixture, with neither cleavage nor branching occurring during sulfonation. This was demonstrated by comparable intrinsic viscosity results from two SPSF samples with different cation-exchange capacities of 0.92 and 1.61 meg/kg.

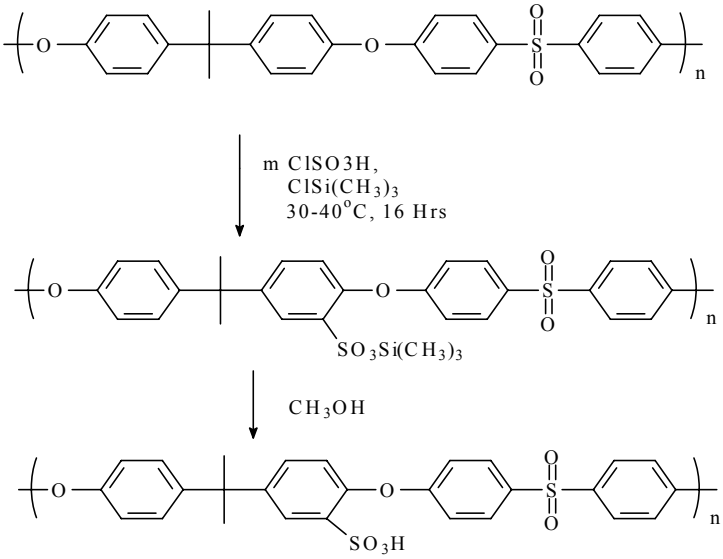

Figure 1-5. Post sulfonation reaction of bisphenol based poly(arylene ether sulfone)[84].

[85] Lufrano,F.; Gatto, I.; Staiti, P.; Antonucci, V.; Passalacqua, E. *Solid State Ionics* **2001**, 145 47–51
[86] Genova-Dimitrova, P.; Baradie, B.; Foscallo, D.; Poinsignon, C.; Sanchez, J.Y. *J. Membr.* Sci. **2001**,185, 59-71.

Kerres et al[87] investigated a novel post sulfonation approach that involves the metalation of the phenyl ring followed by sulfination and subsequent oxidation of preformed polymers. However this approach, as with the other post-sulfonation techniques, was difficult to control and reproduce.

1.2.2. Direct Copolymerization of Sulfonated Poly(Arylene Ether)s via Sulfonated Monomers

Several researchers[88,89] have avoided the harsh post-sulfonating reactions by alternatively employing direct copolymerization nucleophilic aromatic substitution reaction via sulfonated monomers. Direct polymerization of disulfonated monomers can increase proton conductivity and produce enhanced thermal, chemical, and mechanical stability since sulfonic acid moieties are less susceptible to hydrolysis because required carbocation intermediate is not easily generated.[90] Furthermore, unlike post-sulfonation reactions the acidity of the sulfonic acid moieties is increased due to direct sulfonation of the disulfonated monomer easily and reproducibly placing up to two sulfonic acid moieties per repeat unit at the meta position on the deactivated phenyl ring.

Robeson and Matzner[91] first reported the use of a sulfonated monomer primarily for its flame retarding additive properties. Udea et al[92] utilized direct copolymerization

---

[87] Kerres, J.; Cui, W; Reichle, S.; *Journal of Polymet Science:Part A: Polymer Chemistry* 1996, 34, 2421.
[88] a) Wang, F; Hickner, M; Ji, Q; Harrison, W; Mecham, J; Zawodzinski, T; McGrath, J. E. Macromol Symp 2001, 175, 387-395.; b) Einsla, Brian R.; Hong, Young-Taik; Kim, Yu Seung; Wang, Feng; Gunduz, Nazan; McGrath, James E. Journal of Polymer Science, Part A: Polymer Chemistry 42 (**2004**) 862-874.
[89] Genies, C.; Mercier, R.; Sillion, B.; Cornet, N.; Gebel, G.; Pineri, M., *Polymer* **2001**, 42, 359-373.
[90] 127 Genies, C.; Mercier, R.; Sillion, B.; Cornet, N.; Gebel, G. and Pineri, M. *Polymer* **2001**, 42, 359.
[91] Robeson, L.M., Matzner, M., Flame retardant polyarylate compositions, US Patent 4,380,598 (1983), to Union Carbide.

of preformed sulfonated monomers to prepare a series of partially sulfonated poly(ether sulfone)s (PES). 3,3'Disulfonate-4,4'-dichlorodiphenylsulfone was prepared by reacting 4,4'-dichlordiphenylsulfone (DCDPS) with fuming sulfuric acid. However, low yields (≈30%) of the monomer were obtained. A general depiction of the synthesis and purification of this sulfonated monomer is shown in Figure 1-6.

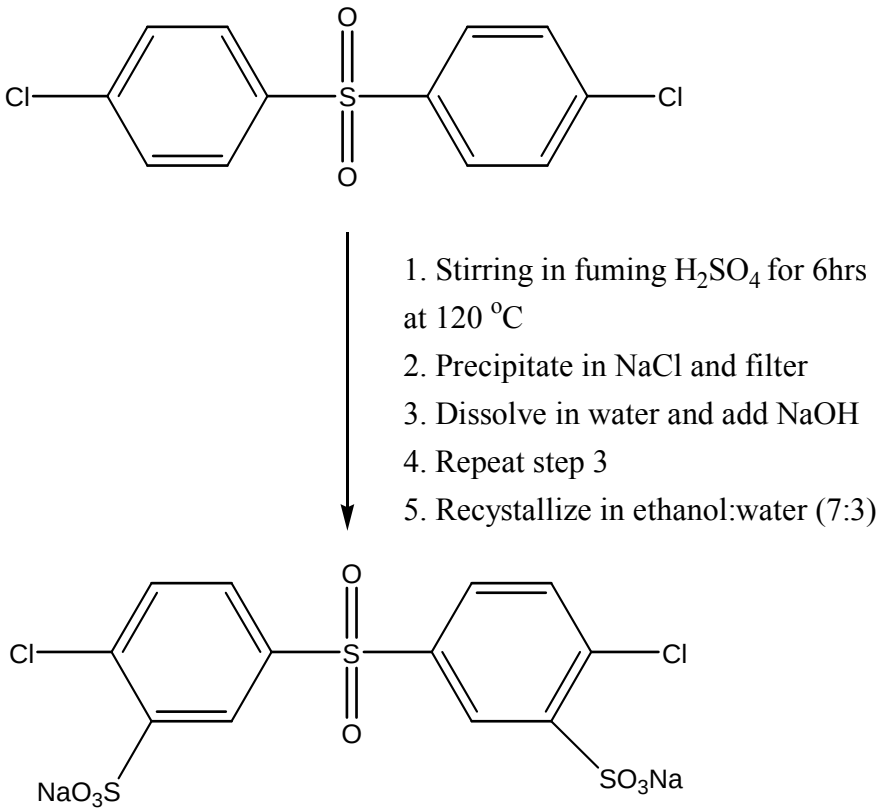

Figure 1-6. Preparation of disulfonation of DCDPS monomer used in direct sulfonated PAES

Successful step-copolymerization of the subsequent statistical disubstituted polyether sulfone (PES) was accomplished by incorporating stoichiometric amounts of the

[92] Ueda, M.; Toyota, H.; Ouchi, T.; Sugiyama, J.; Yonetake, K.; Masuko, T.; Teramoto, T. *J. Polym. Sci.:Part A: Polym. Chem.* **1993**, 31(4), 853-858.

disulfonated monomer to the non-sulfonated monomers in the presence of excess base (potassium carbonate), azeotropic agent (toluene), and dipolar aprotic solvents[93], [94].

The McGrath group at Virginia Tech has utilized 3,3'-disulfonated 4,4'-dichlorodiphenyl sulfone monomer to prepare a variety of disulfonated poly(arylene ether) random, block, crosslinked, and blended copolymers as membranes for proton exchange membrane fuel cells and reverse osmosis applications (Figure 1-7). Unlike the Udea etal procedure, modifications to the sulfonated monomer synthesis resulted in higher yields of 80-90%.

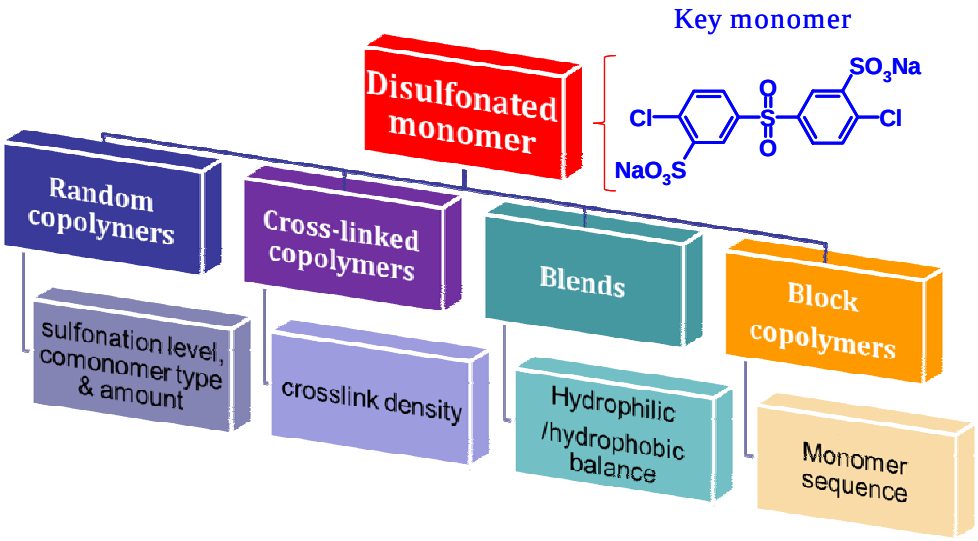

Figure 1-7. Preparation of disulfonation of DCDPS monomer used in direct sulfonated PAES

In general, recrystallization of the crude disulfonated monomer from the alcohol–water mixture was necessary to remove the monosulfonated, DCDPS impurities, and

[93] Sankir, M. Bhanu, V. A. Harrison, W. L., Ghassemi, H., Wiles, K. B. 1 Glass, T. E. A. Brink, E., Brink, M. H. McGrath, J. E. *J. Appl. Polym. Sci*., **2006**,100, 4595–4602.
[94] Li, Y., VanHouten, R. A., Brink , A. E., McGrath, J. E. *Polymer* **2008,** 49, 3014–3019

sodium chloride that lowered the yield. Recently methods to accurately determine the purity and directly use the unrecrystallized SDCDPS have been investigated.

Li et al[94] developed a novel characterization method for determining the purity of the SDCDPS via UV-visible spectroscopy. In Li's research pure SDCDPS which was recrystallized 6 times from IPA/Water (7/3 v/v) mixtures and dried in a vacuum oven at 160 ^{o}C for at least 48 h was used to establish a Beer's Law calibration curve. Consequently, this plot was used to determine the purity of the unrecrystallized product.

Sankir et al[93] reported that a one-step process to prepare disulfonated poly(arylene ether sulfone) from crude disulfonated monomer was possible. Through various characterization techniques these researchers demonstrated DCDPS could be completely converted to the disulfonated monomer and that the crude SDCDPS monomer and recrystallized SDCDPS were identical. Except for residual salt, the optimum conditions for 100% conversion of DCDPS to the disulfonated monomer was 1 : 3.3 reactant molar ratio (DCDPS : SO_3) at 110°C for 6 h. High molecular weight disulfonated poly(arylene ether sulfone) random copolymers utilizing both these procedures have been prepared.[93]

1.2.2.1.Disulfonated Poly(Arylene Ether) Random Copolymers

Wang *et al*[95] reported on the preparation of biphenol based copolymers (PBPSH-XX) with up to 60 mol% sulfonation. The proton conductivity of PBPSH-60 (0.17 S/cm) surpassed that of Nafion 1135 with a proton conductivity of 0.12 S/cm. A representation

[95] Wang, F.; Hickner, M.; Kim, Y. S.; Zawodzinski, T. A.; McGrath, J. E., *J. Membr. Sci.* **2002**, 197, 231-242.

of the general synthetic scheme to prepare these disulfonated poly(arylene ether sulfone) copolymers is presented in Figure 1-8.

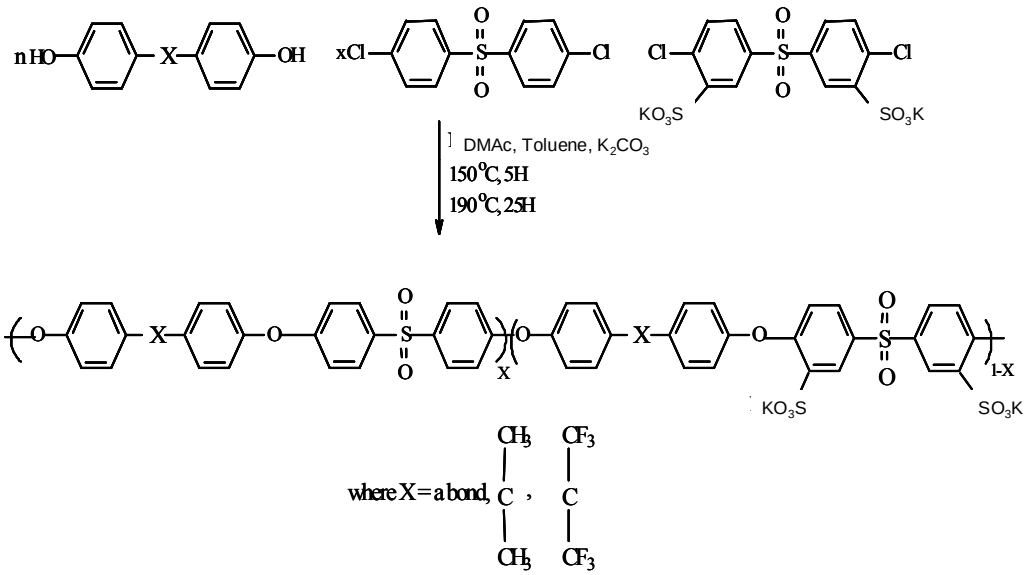

Figure 1-8. Synthesis of Disulfonated Poly(arylene ether sulfone) Copolymers via Direct Copolymerization[164].

A comprehensive study of four bisphenols (Figure 1-9) with controlled degrees of sulfonation was icompleted by Harrison et al.[96] The high molecular weight sulfonated copolymers had excellent film forming behavior, demonstrated high glass transition temperatures and proton conductivities of greater than 0.1 S/cm; this conductivity is equivalent to Nafion control membranes. Crosslinking and branching for almost all of the samples were not observed as confirmed by solubility tests in DMAc, NMP, chloroform, and water.

[96] a) Harrison, W.L.; Wang, F.; Mecham, J.B; Bhanu, V.A.; Hill, M.; Kim, Y. S.; McGrath, J. E. *J Polym Sci Part A: Polym Chem* **2003**, 41, 2264-2276.

Directly copolymerized poly(arylene sulfide sulfone) disulfonated copolymers (PATS) from SDFDPS, DFDPS, and 4,4'-thiobisbenzenethiol have also been investigated[97]. Proton conductivities as high as 0.16 S/cm were exhibited by these copolymers. However, the difluoro monomers were needed instead of the dichloro version to achieve faster reaction times and higher molecular weights.

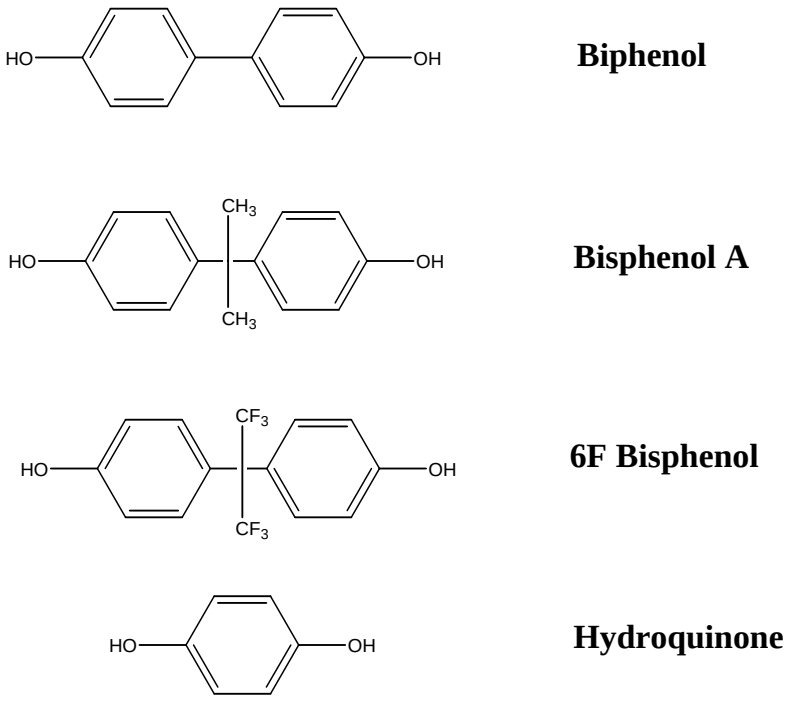

Figure 1-9. Structures of bisphenol monomers investigated by the McGrath research group at Virginia Tech.

One of the major drawbacks of direct copolymerization based on disulfonated monomers is that these random copolymers at higher degrees of sulfonation (above 50%) become mechanically unstable and exhibit excessive swelling. Generally this phenomenon, commonly called the percolation threshold, is accompanied by a

[97] Wiles, K.B., Wang, F., McGrath, J.E., *J. Polym. Sci.: Part A: Polym. Chem.* **2005,** 43, 2964-2976.

"phase inversion" of the hydrophilic and hydrophobic domains of the copolymers[98]. Crosslinking and blending are viable techniques for reducing the swelling of these membranes and improving their mechanical stability without significantly affecting proton conductivity. Paul et al[99] investigated the crosslinking effect of BPS random copolymers with high degrees of disulfonation (e.g., 50% disulfonation). A 10 wt% solution of previously synthesized phenoxide endcapped BPS50 copolymer containing various weight concentrations of tetraglycidyl bis(p-aminophenyl)methane (Araldite MY721 epoxy resin) and 2.5 wt% of triphenylphosphine (TPP) was prepared in NMP, cast on a silanized glass plate, and placed in the vacuum oven at various temperature and times. The lowest water uptake and swelling were observed for the network cured with two equivalents of epoxy per phenoxide and cured for 90 minutes. A drastic change in water uptake and swelling also occurred when the molecular weight of the copolymer was decreased from 10 kg mole^{-1} to five or three kg mole^{-1}.

Arnett et al[100] prepared a series of disulfonated random copolymer blends by mixing various weight percent biphenol based disulfonated PAES (BPS-35) with hexafluoroisopropylidene biphenol based PAES (6F-00), hexafluoroisopropylidene biphenol based disulfonated PAES (6FS-35), and Radel R. Water uptake was reduced as the ratio of the partially fluorinated moiety increased in the blend. Initially the proton conductivity also decreased however, these conductivities remained constant as the concentration of unsulfonated polymer was increased from 2 to 10 wt.%. A self-enrichment of the fluorine atoms on the both the air and glass surface of the membranes

[98] Y.S. Kim, Hickner, M. Dong, L.Pivovar, B. McGrath, J.E. *J. Membr. Sci.* **2004, ,**243, 317–326
[99] Paul, M. Park, H. Freeman, B.D., Roy, A., McGrath, J. E., Riffle, J.S. Polymer **2008**, 49, 2243-2252.
[100] Arnett, N. Y. ; Harrison, W. L.; Badami, A. S.; Roy, A.; Lane, O.; Cromer, F.; Dong, L.; McGrath, J. E. **2007**, 172, 20-29.

was also observed. Furthermore, the introduction of 10 wt% of the fluorinated copolymers led to considerable reduction in methanol permeability compared to Nafion 1135[101].

The incorporation of two different polar groups, e.g. benzonitile (CN) or phenyl phosphine oxide (PPO) in either the BP or 6F series has also been investigated. High molecular weight nitrile-functional, (hexafluoroisopropylidene) diphenol-based poly(arylene ether) copolymers with pendent sulfonic acid groups have been prepared by Sumner et al[102]. These copolymers were prepared by a similar direct copolymerization procedure utilizing the disulfonated DCDPS monomer however the diphenylsulfone unit was completely replaced with benzontrile. Lower water absorptions at equivalent IECs to BPSH-40, and Nafion 112 were observed. The decrease in water absorption is due to the complexation of the nitrile group with water molecules[103]. Higher methanol permeabilities than BPSH-40 but better DMFC performance than both Nafion and BPSH-40 were observed for benzonoitrile containing poly(arylene ether) copolymers with a 35% degree of disulfonation.

The effect of the phenyl phosphine oxide group along the main chain has also been investigated. These polymers have been prepared from 4,4'-bis(fluorophenyl)

[101] Arnett, Natalie Y.; Harrison, William L.; Roy, Abhishek; Lane, Ozma; Badami, Anand; Hill, Melinda; Frank Cromer, Dong, Limin; McGrath, James E. Hydrocarbon and partially fluorinated sulfonated copolymer blends as functional membranes for direct methanol fuel cells. Preprints of Symposia - American Chemical Society, Division of Fuel Chemistry **2008**, 53(2), 748-749.

[102] Sumner, M.J., Harrison, W.L., Weyers, R.M., Kim, Y.S., McGrath, J.E., Riffle, J.S., Brink, A., Brink, M.H. *J. Membr. Sci.* **2004**, 239, 199–211

[103] Kim, Y.S., Einsla, B, Sankir, M., Harrison, W. H., Pivovar, B.S., *Polymer* **2006,** 47 , 4026–4035

phenylphosphine oxide) (SBFPPO), BFPPO, SDCDPS, and 4,4'-biphenol[104]. A dramatic reduction in methanol crossover can be achieved from PPO incorporation[105].

1.2.2.2.Disulfonated Poly(Arylene Ether) Block Copolymers

Recently, PEMs for fuel cells based on multiblock copolymers have been considered[106,107,108]. Multiblock copolymers are interesting because the morphology of the copolymer membrane can be better controlled by varying the two sequences length in the multiblock structures. Most of the research in the McGrath group has focused on developing multiblock with hydrophobic–hydrophilic sequences where the ionic groups located within the hydrophilic blocks provide protonic conductivity and the hydrophobic blocks offer good mechanical strength. Hydrophilic blocks are synthesized from phenoxide-terminal, chloride-terminal, or amine endcapped fully disulfonated poly(arylene ether sulfone) hydrophilic oligomers (BPSH100) with different molecular weights.

Various hydrophobic telechelic oligomers have been examined to tailor the properties and structures of these hydrophilic/hydrophobic multiblocks. Lee et al utilized amine-terminated BPS-100 telechelics with anhydride terminated polyimide (PI) oligomers to prepare BPS-100/PI multiblocks[106]. The coupling reaction was conducted in

---

[104]Shobha, H. K.; Smalley, G. R.; Sankarapandian, M.; Tchatchoua, C.; Muggli, M. W.; Ward, T. C.; McGrath, J. E., ACS *Polym. Preprints*. **2000**, 41(1), 180-181.
[105] Yu Seung Kim, Brian Einsla, Mehmet Sankir, William Harrison, Bryan S. Pivovar *Polymer* **2006,** 47, 4026–4035.
[106] Lee, H.-S., Badami, A., Roy, A., McGrath, J.E. *J.Polym.Sci.: Part A: Polymer Chemistry* **2007,** 45, 4879–4890.
[107] Lee, H.-S., Roy, A., Lane, O., and McGrath, J.E. *Polymer* **2008,** 49, 715-723.
[108] Li, Y., Roy, A., Badami, A., Hill, M., Yang, J., Dunn, S., McGrath, J.E. *J. Power Sources* **2007,** 172, 30–38.

mixed solvent of m-cresol/NMP at 120 ºC for 12 h. High proton conductivities of 1.6 S/cm at IECs of 1.9 meq/g and a well developed nanophase separation were achieved.

Two series of multiblock copolymers phenoxide terminated fully disulfonated poly(arylene ether sulfone) (BPSH100) and decafluorobiphenyl (DFBP) or hexafluorobenzene (HFB) end-capped unsulfonated poly(arylene ether sulfone) (BPS0) have been synthesized[107]. The encapped reaction using highly reactive DFBP and HFB were carried out at 105 and 80 ºC for 12 h, respectively. No significant differences in membrane properties were observed between DFBP and HFB linked systems. Multiblock copolymers with fixed block lengths exhibited lower IEC values (1.2-1.4 meq/g) but comparable proton conductivities (0.065 – 0.120 S/cm) than random BPSH-35 copolymer Multiblocks copolymers of unequal block length with higher IECs and proton conductivities were also prepared.

Novel multiblock copolymers based on a fluorine terminated hydrophobic poly(arylene ether ketone) (6FK) oligomer (4 kg/mol) and BPSH-100 oligomer (4 kg/mol) been successfully synthesized by Li et al[108]. The endcapper for the fluorine terminated hydrophobic segment (6FK) was DFBP. The multiblock copolymer was synthesized via a two-step technique where the phenoxide terminated BPSH-100 was first synthesized for 16 h at 190 ºC followed by the drop wise addition of 6FK dissolved in NMP at 160 ºC. The temperature of the reaction was increased back to 190 ºC after the addition of 6FK was completed. Comparable proton conductivity to Nafion 112 as a function of temperature and under relative humidityconditions was observed. Similar hydrogen-air fuel cell performance to Nafion 1135 was also observed.

Yu et al [109] prepared three series of hydrophilic-hydrophobic, sulfonated-fluorinated multiblock copolymers. These multiblocks were prepared with different bisphenol units in the hydrophobic fluorinated blocks. The chemical structures of these multiblock copolymers are shown in Figure 1-10.

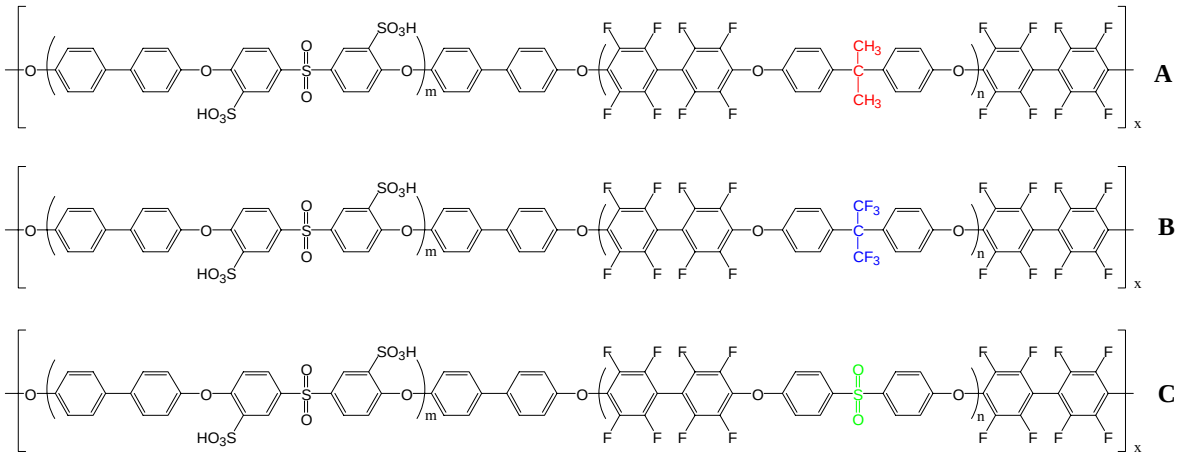

Figure 1-10. Structures of fluorinated-sulfonated, hydrophobic-hydrophilic multiblock copolymers. Structure A represents BisAF-BPSH, B represents 6FBisAF-BPSH, and C represents BisSF-BPSH

Thus far, the BisSF-BPSH (17K-12K) copolymers have displayed the highest performance/water sorption selectivity of all the multiblock copolymers synthesized. These materials were able to outperform the commercial product, Nafion 112, while still maintaining low water uptake (~40 wt%).

2. MEMBRANE SEPARATION APPLICATIONS

2.1. Introduction to Desalination

[109] Yu, X.; Roy, A.; Dunn, S.; Yang, J.; McGrath, J. E., Synthesis and characterization of sulfonated-fluorinated, hydrophilic-hydrophobic multiblock copolymers for proton exchange membranes. *Macromol. Symp.* **2006,** 439, 245-246.

Water is one of the earth's most abundant resources required for the substance of life. However, only 3% is fresh water found in the form of ice, ground water, lakes and rivers[110]. Overpopulation, exploitation of fresh water sources, higher standards of living, and increased pollution have led to water scarcity becoming one of the greatest threats to mankind. According to the World Health Organization (WHO) about 1 billion people do not have access to clean water while 41% of earth's populations live in water-stressed areas.[111] Concern about the decline to fresh water sources has prompted worldwide interest to use desalination of brackish water or seawater as a means to solving this crisis.

Desalination is the process that removes salt or suspended materials from brackish or seawater.[112] Several techniques are used to desalinate water (See Table 1-1). These technologies are classified as either a phase-change/thermal process or a membrane/single-phase process[113]. Phase-change processes, either multi-stage flash (MSF), multiple-effect boiling (MEB) or vapor compression (VC) separates salt from water by evaporation and condensation. Membrane processes such as reverse osmosis (RO) or electrodialysis (ED) on the other hand, utilize the diffusion of water through a membrane which retains most of the salts.

Seawater normally has salinity in the range of 35,000– 45,000 ppm. Brackish water has lower salinity than seawater, often ranging between 2,000-5,000 ppm. To achieve the acceptable salinity levels (500 ppm) for drinking water significant amounts of

[110] Kalogirou, S.A., *Seawater desalination using renewable energy sources.* Progress in Energy and Combustion Science, **2005,** 31(3), 242-281.
[111] R. Singh, Worldwide Water Crisis, *J. Membr. Sci.* **2008,** 313, 353-354.
[112] Service, R. F. *Science* **2006,** 313, 1088-1090.
[113]Fritzmann, C., Löwenberg , J., Wintgens, T., Melin, T., *Desalination*, **2007**, 216(1-3), 1-76.

energy are required.[114] Typically, the amount of energy required to desalinate water varies with the technique used. Membrane desalination processes generally have lowest energy consumption of all the desalination process because no energy-intensive phase changes or potentially expensive solvents or adsorbents are needed. Compared to a thermal distillation plant that requires 15 to 25 kilowatthours (kWh) of electricity to produce $1m^3$ of water, a typical seawater RO plant only requires 1.5 to 2.5 kWh/m^3 to operate[112]. Thus reverse osmosis to become one of the most dominant industrial processes for water desalination.

2.1.1. Desalination by Reverse Osmosis

Reverse osmosis (RO) desalination process is an efficient and reliable membrane technology used for the production of drinking water from seawater or brackish water[115]. Reverse osmosis offers several advantages over other desalination process such as inherently simple design and operation, and simultaneous separation and concentration of both inorganic and organic compounds that are less than 150 Daltons. It can be combined with other separation process including selective separation based on MSF or VC in order to produce highly efficient hybrid systems.[116]

[114] A) Mallevialle, J.; Odendaal, P. E.; Wiesner, M. R., Eds. Water Treatment: Membrane Processes; McGraw-Hill: New York, 1996; B) Tiwari GN, Singh HN, Tripathi R. *Solar Energy* **2003,** 75(5), 367–373.
[115] Jacob, Cyril. *Desalination* **2007**, 205, 47–52.
[116] Bhattacharyya, D., and Williams, M., "Introduction and Definitions - Reverse Osmosis", in *Membrane Handbook,* W. Ho and K. Sirkar, eds., Van Nostrand Reinhold, New York 1992, 265-268.

Table 1-1. Summary of characteristics in desalination thermal and membrane processes[117]

Technologies	*Feed Water*	*Energy Consumption (kJ/kg)*	*Advantages/ Disadvantages*
Thermal Processes			
Multi-stage flash (MSF)	SW	338	▪ Ease and reliability of process ▪ Less complicated design ▪ Tolerate large capacities ▪ Extremely high energy consumptions ▪ Expensive
Multi-effect Distillation (MED)	SW	149	▪ Less energy required than MSF ▪ Can operate using waste thermal energy ▪ Complicated design ▪ Corrosion and scaling of oversaturated compounds
Vapor Compression (VC)	SW/BW	192	▪ High performance ratios ▪ Plant size limitation due to limited compressor capacities ▪ More complicated process and design
Membrane Processes			
Reverse Osmosis (RO)	SW/BW	120	▪ Low energy consumption ▪ Simple design and operation ▪ Less expensive than distillation process ▪ Fouling of membranes ▪ Pretreatment is needed
Electrodialysis (ED)	BW	144	▪ Higher energy consumption at high salt concentrations

SW = Seawater; BW = brackish water

RO is a process that occurs when the water is moved across a semi-permeable membrane from lower concentration to higher concentration. The feed water is separated into pure water (permeate) and a concentrated salt solution (retentate) by applying a pressure difference across the membrane (Figure 1-11).

[117] Younos, T., Tulou, K.E. *J. Contemporary Water Research and Education* **2005,** 132, 3-10; Van der Bruggen, B., Vandecasteele, C. *Desalination* **2002,** 143, 207-218.

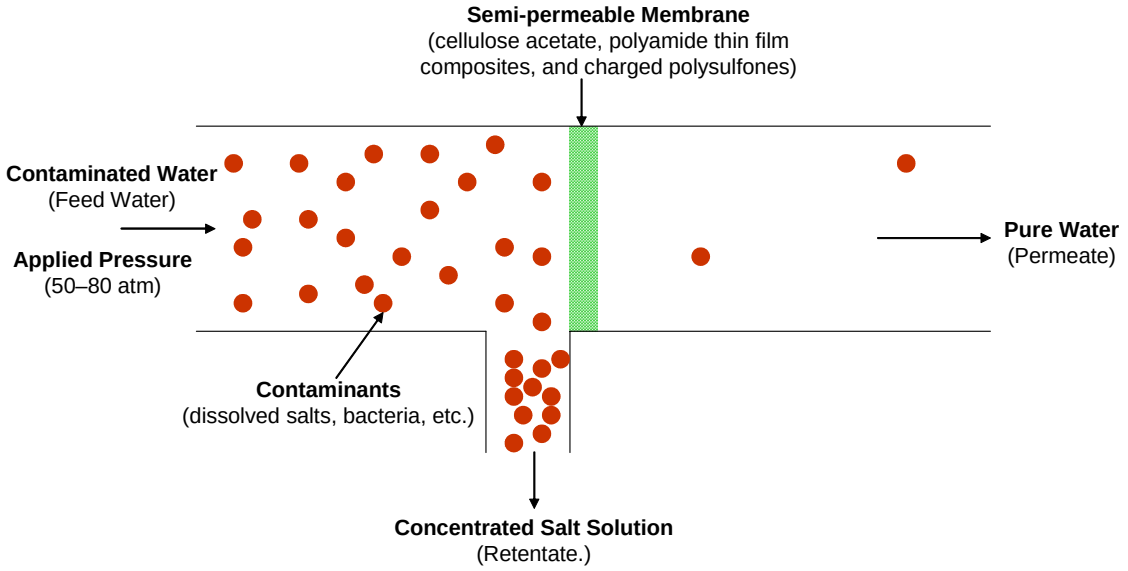

Figure 1-11. Schematic of Reverse Osmosis Process

In order for the permeate to pass into the retentate compartment, pressure higher (50–80 atm) than the osmotic pressure (π) of the system are needed. Higher pressures must be used to have a sufficient amount of water pass through a unit area of membrane[118]. Osmotic pressure is the pressure required to separate water from a solution (seawater) and permeate through a membrane. The osmotic pressure of an ideal solution is defined as:

$$\pi = CRT$$

where π represents the osmotic pressure, C is the salt ion concentration, R is the ideal gas constant, and T is the solution temperature.

[118] Dresner L. Hyperfiltration (revere osmosis). In: Spiegler KS, Laird ADK, editors. Principles of desalination, Part B. 2nd ed. New York: Academic Press; 1980. p. 401–560

One of the first RO processes was designed in the late 1940s at UCLA by Gerald Hassen[119]. Hassler's design proposed the use of two porous ceramic plates separated by a very narrow adjustable air gap between 10 to 25 microns thickness. The narrow air gap or vapor space should have functioned as a semipermeable membrane, since the design was limited due to the "bubbling pressure" of the ceramic plate which did not allow the system to operate above 4 atm. The use of cellophane sheets to cover the evaporating and condensing surfaces enabled the system to operate at pressures greater than 50 atm. Although this initial design was upgraded over the next 10 years, high yields of product water were never collected and the project ended in 1960[120].

2.1.1.1.Theory

In RO, the diffusion through the membrane occurs via a mechanism known as the solution-diffusion model (SDM).[121] In the SDM, the flow of water molecules through the membrane occurs in three steps. In the first step, water molecules are absorbed into the upstream face of the membrane. The second step, which is the rate determining step, occurs when these water molecules diffuse down the chemical potential across the membrane. Finally, these molecules are desorbed from the downstream face of the membrane.

---

[119] Glater, Julius. *Desalination* **1998,** 117, 297-309.
[120] A) G.L. Hassler, The sea as a source of fresh water, UCLA Dept. of Engineering Research Summary, 1949-1950.; B) G.L. Hassler and J.W. McCutchan, Saline Water Conversion, Advances in Chemistry, Series No. 27, Amer. Chem. Soc., Washington, DC, 1960, p. 192.
[121] Baker, Richard W. Membrane Technology and Applications **2nd ed**. John Wiley & Sons Inc. NJ, 2004.

Two assumptions govern the SDM. First the chemical potential of the feed and permeate fluids on both sides of the membranes are in equilibrium with the membrane interface. Therefore, the diffusion of fluid through the membrane is much slower than the rates of absorption and desorption at the membrane interface. The second assumption is that the pressure applied within a dense membrane is uniform at the highest pressure value and a concentration gradient is the only chemical potential gradient across the membrane. Therefore, the driving forces for permeation (flux) in reverse osmosis are mainly based on concentration and pressure differences between the feed and permeate sides.

The flux, J_i, of a water (component *i*), is described by the simple equation[122]

$$J_i = L_i \frac{d\mu_i}{dx} \qquad \textbf{Equation 1-1}$$

where $d\mu_i / dx$ is the gradient in chemical potential of water and L_i is a coefficient of proportionality linking this chemical potential driving force with flux. By reducing the concentration and pressure in RO to chemical potentials

$$d\mu_i = RTd \ln(\gamma_i c_i) + v_i dp \qquad \textbf{Equation 1-2}$$

where R is the ideal gas constant, T is ambient temperature, c_i is the molar concentration (mol/mol) of water, γ_i is the activity coefficient (mol/mol) of water linking mole fraction with activity, p is the pressure, and v_i is the molar volume of water, the effect of these components on flux can be expressed. Since no pressure gradient exist across the membrane, flow through the membrane with integrated thickness can be described as

[122] Wijmans, J.G. and Baker, R.W. *J. Membr. Sci.* **1995,** 107, 1-21.

$$J_i = D_i \frac{(c_{io(m)} - c_{il(m)})}{l} \qquad \textbf{Equation 1-3}$$

where D_i is the diffusion coefficient, $c_{io(m)}$ is the concentration of water in the membrane at the feed interface (point o), $c_{il(m)}$ is the concentration of water in the membrane at the permeate interface (point *l*), and *l* is the position of the permeate interface of the membrane.

The chemical potential in the fluid and membrane phases can be equated by

$$\mu_{io} = \mu_i^o + RT \ln(\gamma_i n_i) + \nu_i (p - p_{i_{sat}}) \qquad \textbf{Equation 1-4}$$

where n_i is the mole fraction (mol/mol) of water, and $p_{i_{sat}}$ is saturated vapor pressure of water. By rearranging this equation, the concentration of the differing species in the membrane at the fluids interface can be obtained in terms of the pressure and composition of the feed and permeate fluids.

At the feed interface, the pressure in the feed solution and within the membrane is identical. Thus equating the chemical potential of the water in contact with the membrane at the feed interface (μ_{io}) with the chemical potential of the water in the membrane at the feed interface ($\mu_{io(m)}$) gives

$$\mu_{io} = \mu_{io(m)} \qquad \textbf{Equation 1-5}$$

Substituting the expression for the chemical potential of incompressible fluids (Equation 1-4) yields

$$c_{io(m)} = \frac{\gamma_{io}}{\gamma_{io(m)}} c_{io} \qquad \textbf{Equation 1-6}$$

where c_{io} represents the concentration of water in contact with the membrane at the feed interface, γ_{io} is the activity coefficient of water in contact with the membrane at the feed interface, $\gamma_{io(m)}$ is the activity coefficient of water in the membrane at the permeate interface. The ratio of the activity coefficients $\frac{\gamma_{io}}{\gamma_{io(m)}}$ is the sorption coefficient (K_i), hence:

$$c_{io(m)} = K_i \times c_{io} \qquad \textbf{Equation 1-7}$$

At the permeate side, equating the chemical potential gives

.

$$\mu_{il} = \mu_{il(m)} \qquad \textbf{Equation 1-8}$$

where μ_{il} is the chemical potential of water in contact with the membrane at the permeate interface and $\mu_{il(m)}$ is the chemical potential of water in the membrane at the permeate interface. By taking into account that a pressure difference exists from p_o within the membrane to p_l in the permeate solution occurs at the permeate side and substituting the expression for the chemical potential of incompressible fluids (Equation 1-4) the expression for concentration of water in the membrane at the permeate interface ($c_{il(m)}$)can be described as

$$c_{il(m)} = K_i c_{il} \exp\left(\frac{-\nu_i (p_o - p_l)}{RT}\right) \qquad \textbf{Equation 1-9}$$

c_{il} represents the concentration of water in contact with the membrane at the permeate interface, ν_i is the molar volume of water, R is the ideal gas constant, and T is ambient temperature.

An expression in terms of water flux (J_i) which is defined as the volume of permeate produced per unit membrane area per unit time[123], can be generated by substituting the equations for concentration (Equation 1-7 and Equation 1-9) into Equation 1-3

$$J_i = \frac{D_i K_i}{l}\left[c_{io} - c_{il} \exp\left(\frac{-\nu_i (p_o - p_l)}{RT}\right)\right] \qquad \textbf{Equation 1-10}$$

This expression is further simplified to

$$J_i = A(\Delta p - \Delta \pi) \qquad \textbf{Equation 1-11}$$

where A is the water permeability constant to the term $\frac{D_i K_i c_{io} \nu_i}{lRT}$, Δp is the difference in hydrostatic pressure across the membrane $(p_o\text{-}p_l)$, and $\Delta\pi$ is the osmotic pressure .

Consequently the expression for salt flux (J_j) can also be expressed in a similar manner to water flux

$$J_j = \frac{D_j K_j}{l}\left[c_{jo} - c_{jl} \exp\left(\frac{-\nu_j (p_o - p_l)}{RT}\right)\right] \qquad \textbf{Equation 1-12}$$

or in more simplified terms

[123] Z hou, W. and Song, L. *Environ. Sci. Technol*. **2005,** 39, 3382-3387.

$$J_j = B\left(c_{jo} - c_{jl}\right) \qquad \textbf{Equation 1-13}$$

where B is the salt permeability constant, c_{ol} represents the concentration of salt in contact with the membrane at the feed interface, and c_{jl} represents the concentration of water in contact with the membrane at the permeate interface. In this B is given by

$$B = \frac{D_j K_j}{l} \qquad \textbf{Equation 1-14}$$

where D_j is the salt diffusivity in the membrane, K_j is the salt partition coefficient, and l is the membrane thickness. However, salt fluxes are independent of pressure and are only a function of the salt concentration. Therefore salt rejection values (R),

$$R = \frac{1 - c_{jl}}{c_{jo}} \times 100\% \qquad \textbf{Equation 1-15.}$$

which are a measure of the ability of the membrane to separate salt from the feed solution, are used.

2.1.1.2.Reverse Osmosis Membranes for Desalination

The overall efficiency of any RO system ultimately depends on the properties of the semi-permeable membrane. An ideal reverse osmosis membrane should have the following properties[124]:

- High water flux rate and salt rejection
- Tolerant of chlorine and other oxidants
- Resistant to biological attack and fouling by collidal or suspended material

[124] Amjad, Z., Ed. Reverse Osmosis: Membrane Technology, Water Chemistry, and Industrial Applications; Van Nostrand Reinhold: New York, 1993.

- Inexpensive
- Mechanically and chemically stable even at elevated temperatures
- Tolerant of high temperatures
- Easy to form into thin films or hollow fibers

Since no ideal membranes exist, modifications to the structure and properties of the semi-permeable membrane properties have been made to facilitate greater levels of efficiency in RO systems. Additionally, these membranes must undergo a number of pre-treatment and post-treatment stages, to achieve maximum RO performance.

2.1.1.2.1. Pre-treatment of Reverse Osmosis Membranes

Pre-treatment of RO membranes includes all activities to adjust the feed water in constitution and pH-value. Membrane fouling is one of the most severe problems associated with RO. In fouling, colloids accumulate on the membrane surface or within the membrane pores and adversely affect both the quantity (permeate flux) and quality (solute concentration) of the product water. The higher fouling was found to be more likely in membranes with rougher surfaces as shown in the case of most composite polyamide RO membranes[125]. Zhu et al[125] illustrated that compared to cellulose acetate RO membranes a higher degree of fouling attributed to the pronounced surface roughness was observed in polyamide composite membranes. Fouling can be classified as chemical (scaling), physical, biological, and organic. These types of foulants affect various aspects of reverse osmosis operation such as water flux and salt rejection resulting in decreased performances. Pre-treatment serves to reduce fouling potential, to increase reverse

[125] Z hu, X. and E limelech, M. Environ. Sci. Technol. **1997,** 31, 3654-3662.

osmosis membrane life, to maintain performance level and to minimize scaling on the membrane surface.[126]

Pre-treatment can be divided into two groups: the physical pre-treatment and the chemical pre-treatment. Physical pretreatment is responsible for mechanical filtration through screening, cartridge filters, sand filters or membrane filtration. This form of pre-treatment typically inhibits physical fouling of the membranes. But this mechanical treatment is supported by a rather extensive chemical treatment. Chemical pre-treatment includes the addition of scale inhibitors and pH adjustments to prevent scaling by $CaCO_3$, $CaSO_4$, $BaSO_4$, and silica, coagulants to inhibit organic foulants, and disinfectants which may prevent bio-fouling.[127]

Chlorination of feed water is a vital step of chemical pre-treatment. Chlorination in reverse osmosis is required to disinfect water and remove/prevent the biological attack on membranes[128]. Chlorine is introduced in feed water as sodium hypochlorite (NaOCl) or chlorine gas (Cl_2). As shown in Equation 1-16, NaOCl is hydrolyzed by water to hypochlorous acid:

$$NaOCl + H_2O \rightarrow HOCl + NaOH \qquad \textbf{Equation 1-16}$$

Then hypochlorous acid further dissociates to hydrogen and hypochlorite ions

$$HOCl \rightarrow H^+ + OCl^- \qquad \textbf{Equation 1-17}$$

A free residual chlorine concentration, which is the sum of NaOCl, HOCl and OCl^-, of 0.5–1.0 mg/L should be maintained along the pre-treatment line to prevent biofouling. However before coming into contact with the RO membrane manufacturers normally

[126] C.V. Vedavyasan *Desalination* **2007,** 203, 296–299.
[127] G. Migliorini and E. Luzzo, Seawater reverse osmosis plant using the pressure exchanger for energy recovery: a calculation model, Desalination, **2004,** 165, 289–298.
[128] A. R. Pitochelli, E. L. Mainz, D. B. Griffith, *Ultrapure Water* **2006,** 22(4),42 – 43.

recommend that the chlorine concentration of feed water should be lower than 0.1 ppm to prevent membrane deterioration by oxidation or hydrolysis.[129] Membrane deterioration by chlorination is most noticeable in polyamide type membranes. Polyamide type membranes have demonstrated high membrane deterioration at lower pH and higher concentration of hypochlorite solution.[130] Even at higher pH (pH 10), improvement of membrane performance was only achieved at the early stage. Thus, dechlorination is achieved by adding sodium metabisulfite ($NaHSO_3$) as a reducing agent, in order to completely neutralize the residual active chlorine and protect chlorine sensitive membranes. Furthermore, pH adjustments to alter the strength of NaOCl and to prevent hydrolysis observed primarily in cellulose acetate membranes must be implemented as a part of the pretreatment process.[131]

2.1.1.2.2. Post-treatment of Reverse Osmosis Membranes

In post-treatment permeate is re-mineralised, re-hardened, disinfected by chlorination and adjusted to drinking water standards. Since permeate water has low total dissolved solid (TDS) values, this water can be, corrosive, foul-tasting and unhealthy. Permeate has to be re-hardened in order to prevent corrosion of pipes in the distribution network. Corrosiveness of water measured by the measured pH of the water minus the equilibrium pH values (pH) of the system if saturated with $CaCO_3$ at the measured alkalinity and calcium values, also called the Langelier saturation index (LSI). To prevent corrosion a slightly positive LSI is required and can be achieved by dissolution of lime

[129] Buch, P.R., Jagan Mohan, D., Reddy, A.V.R. *J.Membr Sci* **2008,** 309, 36–44.
[130] Kang, G.-D., Gao, C-J., Chen, W.-D. Jie, X-M., Cao,Y-M., Yuan,Q. *J. Membr.Sci.* **2007,** 300, 165–171.
[131] Munoz Elguera, A., Perez Baez, S. O. *Desalination* **2005,** 184, 173–183.

[$Ca(OH)_2$]or limestone ($CaCO_3$) by carbon dioxide. Re-chlorination of permeate water by chlorine gas, on-site sodium hypochlorite generation and bulk hypochlorite is necessary to protect consumers from pollution introduced during distribution and storage. Adjustments to pH values and CO_2 content are also needed to prevent scaling that arises from precipitation and deposition of salts on the membrane surface. Overall control of the system should be maintained for continuous and reliable water production.

One of the most important aspects of post-treatment is boron removal. Boron causes abnormalities to human reproduction and to damage citrus plant production. In seawater containing 4-5 mg/L of boron, boron is usually present as boric acid H_3BO_3. However the accepted standard for boron in drinking water is 0.5 mg/L. In a single pass RO system, boron can be removed at elevated pH but this promoted precipitation of scaling layers Thus increased pH is typically used in double pass operation at the second RO pass.

Many researchers are now turning to boron specific ion resin that essentially removes only boric acid from water and has no significant effect on the concentration of other ions. A complex between boric acid and a methyl glucamine resin (Figure 1-12) has been shown to residual boron levels well below 0.5 mg/L independent of operating conditions such as temperature, pH, or salinity.[132]

[132] Jacobs, C. *Desalination* **2007,** 205, 47–52.

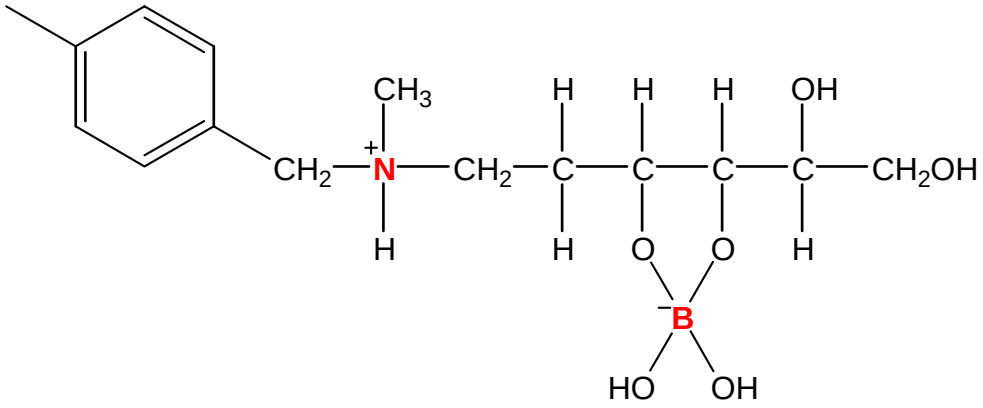

Figure 1-12. Complexation of Boric Acid and a Methyl Glucamine (Boron Specific Resin)

Kabay et al[133] showed that increasing the amounts of boron resins and decreasing particle size from 0.0125 to 0.1000 g/50 m and 0.355 mm to 75 µm, respectively, resulted in increased boron removal.

2.1.1.2.3. Candidates for Reverse Osmosis Desalination Membranes

The reverse osmosis desalination membrane market generated more than $350 million in 2000. Today, a number of commercially available desalination membranes are produced by GE Osmotics[134], Dow Chemical/ Film Tec Corp[135], Hydranautics[136], Trisep Corporation [137], and Toray Membrane America, Inc.[138] The properties of some desalination membranes are presented in Table 1-2.

---

[133] Kabay, N., Sarp, S., Yuksel, M., Arar, O., Bryjak, M. *Reactive & Functional Polymers* **2007,** 67, 1643–1650.
[134] http://www.gewater.com (2008).
[135] http://www.dow.com (2008).
[136] http://www.hydranautics.com (2008).
[137] http://www.trisep.com (2008).
[138] http://www.toraywater.com (2008).

Table 1-2. Properties of commercially available reverse osmosis desalination membranes

Name (Supplier)	Operating Pressure (psig)	Permeance (GFD/psi)	Permeance (L/m2 h bar)	Nominal NaCl Rejection (%)
Brackish Water Reverse Osmosis				
ESPA1 (Hydranautics)	150	0.24	5.88	99.3
DS-11 AG Series (GE Water)	225	0.13	3.08	99.5
BW30 (Dow FilmTec)	225	0.13	3.16	99
XLE (Dow FilmTec)	100	0.38	7.53	98
Seawater Reverse Osmosis				
SWC4+ (Hydranautics)	800	0.02	0.52	99.8
DS-3 SC (GE Water)	800	0.01	0.37	99
SW30HR (Dow FilmTec)	800	0.04	0.97	99.6

Typically, these membranes are either based on cellulose acetate or polyamide type polymers in asymmetric or thin film composite (TFC) form (Figure 1-13). Currently, most membranes are spiral wound or hollow fiber configurations. In the spiral wound configuration (Figure 1-14), a flat sheet membrane and spacers are wound around the permeate collection tube to produce flow channels for permeate and feedwater[139]. This design maximizes flow while minimizing the membrane module size. Hollow fiber systems are bundles of tiny, hair-like membrane tubes that reject ions when the feedwater permeates the walls of these tubes. The permeate was collected through the

[139] Handbook of industrial Membranes http://www.gewater.com/handbook/index.jsp (**2008**).

hollow center of the fibers while concentrated brine is produced on the outside of the fibers contained by the module housing.

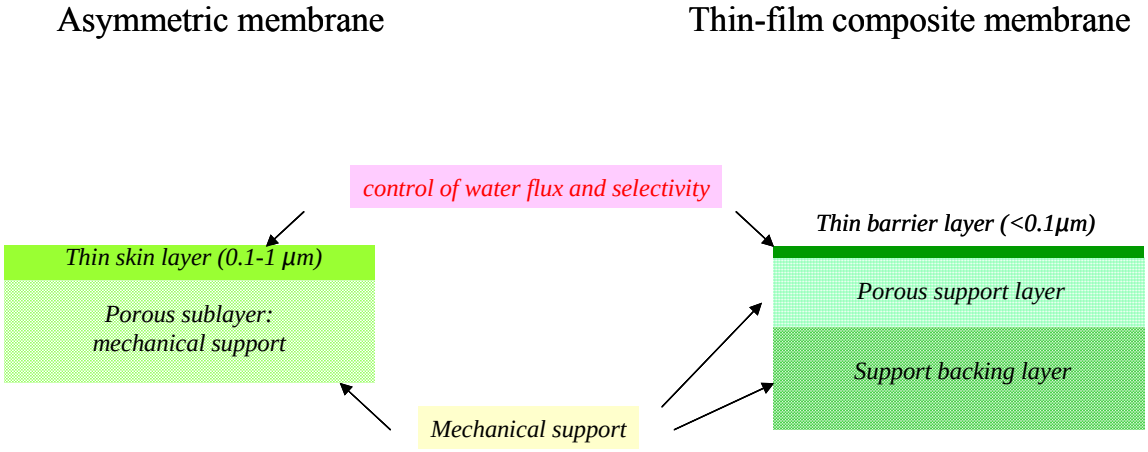

Figure 1-13. Basic schematics of asymmetric and thin film composite membranes

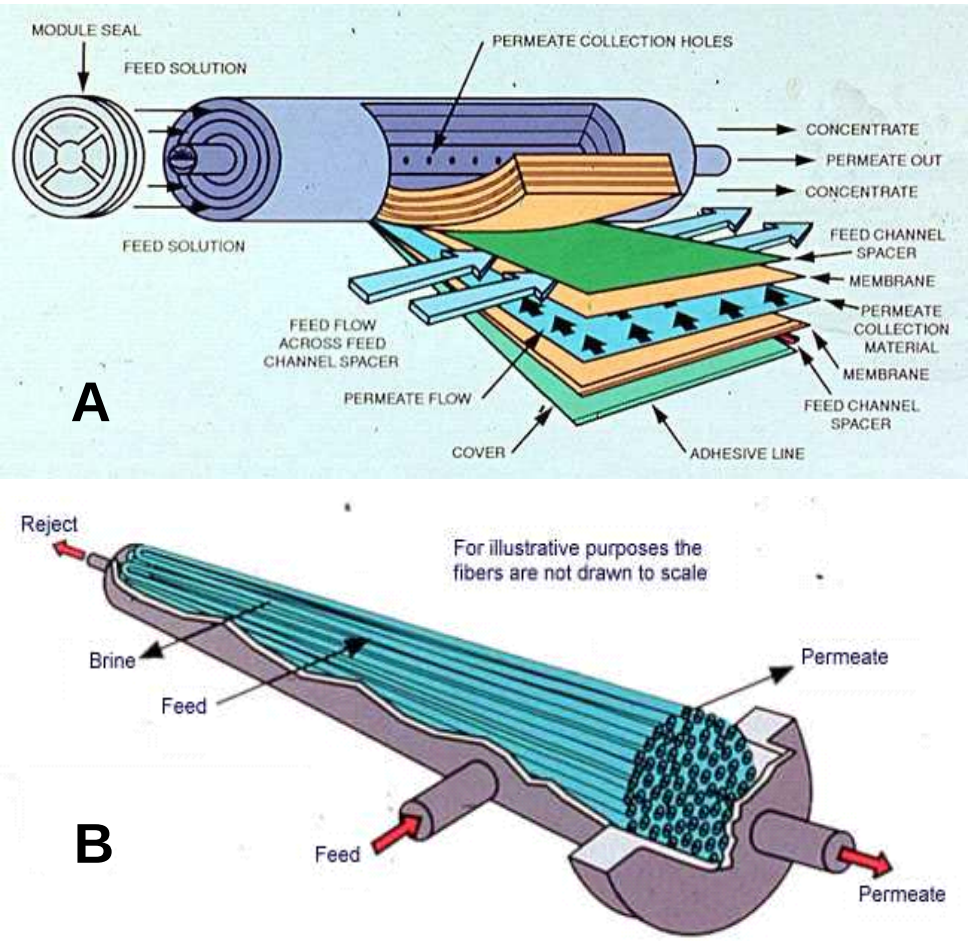

Figure 1-14. Current state of the art module used in desalination. A represents a spiral wound configuration; B depicts a hallow fiber configuration. Reprinted from [139] with permission from GE Infrastructure Water and Process Technologies.

Asymmetric membranes were first prepared by Loeb and Sourirajan[140]. The asymmetric membrane structure consists of a thin, dense top surface layer (0.1-1 μm) on a porous support sublayer about 100 μm thick (See Figure 1-13). The top layer is responsible for the membrane selectivity while the sublayer offers mechanical support. Asymmetric membranes are generally prepared by a process known as phase inversion.

[140] Loeb, S, Sourirajan, S. *Advances in Chemistry Series* **1963,** 38, 117-132.

Phase inversion/separation is the process by which a polymer solution is induced to phase separate/demix into a polymer rich phase and a polymer poor phase[141]. Usually, the polymer rich phase solidifies forming the dense top layer whereas the polymer poor phase develops into the pores. There are four main techniques used to induce phase inversion. These include thermally induced, air induced, vapor induced, and diffusion induced phase separation[142]. Thermally induced phase separation (TIPS) occurs by casting a film as a hot solution and then allowing the temperature decrease. As the temperature of the solution cool, the polymer precipitates. After demixing the solvent is removed by extraction, evaporation or freeze drying. In air-casting of a polymer solution the polymer is dissolved in a mixture of a volatile solvent and a less volatile nonsolvent. During the evaporation of the volatile solvent, the solubility of the polymer decreases due to the film becoming enriched with the nonvolatile nonsolvent inducing phase separation. During vapor induced process, phase separation of the polymer solution is induced through the penetration of nonsolvent vapor in the solution.

The most popular and widely used phase inversion technique is diffusion induced phase separation (DIPS)[121]. In this process a polymer solution is cast as a thin film on a support and is subsequently immersed in a nonsolvent bath. Precipitation can occur because the solvent in the polymer solution is exchanged for the nonsolvent. The final morphologies and properties of phase separated membranes are determined by the composition of the polymer solution (concentration, solvent, or additives), the support materials, the thickness of the cast polymer film, the non-solvents, temperature of the

[141] Luccio, M.D., Nobrega, R., Borges, C.P. *J. Applied Polym Sci* **2002,** 86, 3085-3096.
[142] Baker, Richard W. "Membranes and Module" pp 89-160 in Membrane Technology and Applications **2nd ed**. John Wiley & Sons Inc. NJ 2004.

polymer solution, non-solvent bath or environment, and drying time[143]. The effects of concentration, solvent, or additives on the structure and properties of polyethersulfone (PES) membranes prepared by the DIPS technique have been illustrated by Koussau et al[144]. The use of DMF instead of NMP resulted in thinner membranes (60 μm) with larger more spongy like macrovoids/pores. The top layer of these membranes was also much thicker (3 μm) than those prepared from NMP (~0.5 μm). Increasing the concentration of the polymer solutions from DMF results in less porous membrane with less fingerlike pores, increase in the overall membrane thickness [14 wt% (50 μm) versus 20wt% (60 μm)]and lower water permeability due to thicker skin layers. In both cases, the increase in viscosity slowed down the diffusion exchange between solvent and non-solvent and leads to a higher polymer concentration at the interphase between polymer solution and non-solvent bath.

Thin film composites (TFC) were first introduced in 1972[145]. As shown in Figure 1-13, TFCs are composed of a 20 to 100 nm thin dense polymer barrier layer formed over an approximately 100 μm thick microporous film. Since the barrier layers of the composite membranes are usually much thinner than asymmetric membranes, much higher selectivities and water fluxes can be achieved. This dense layer can be deposited onto the microporous support by various methods including casting the barrier layer separately on the surface of a water bath followed by lamination to the microporous support film; dip-coating the microporous support film in a polymer, a reactive monomer or prepolymer solution followed by drying or curing with heat or radiation; gas-phase deposition of the barrier layer of the microporous support film from a glow discharge

[143] Barth, C., Goncalves, M.C., Pires, A.T.N., Roeder, J., Wolf, B.A. *J. Membr. Sci*. **2000,** 169, 287-299.
[144] K. Boussu *, C. Vandecasteele, B. Van der Bruggen *Polymer* **2006,** 47, 3464–3476
[145] Cadotte, J.E., U.S. Pat. 4,039,440 (1977).

plasma; or interfacial polymerization, which is by far the most important technique for preparing composite membranes, of reactive monomers on the surface of the microporous support film.[146]

2.1.1.2.3.1.Cellulose Acetate

Cellulose acetate membranes were the first to offer a practical balance of selectivity and solvent permeation rate for water desalination[147]. As shown in Figure 1-15, these membranes are prepared by reacting cellulose with acetic anhydride in acetic acid in the presence of a catalyst (sulfuric acid) to give acetated cellulose[148]. The degree of acetylation depicts the amount of pendant OH groups on cellulose replaced by acetyl groups (CH_3COO^-). The water and salt permeability of cellulose acetate membranes is extremely sensitive to the degree of acetylation of the polymers. High degree of acetylation yields high salt rejections but low fluxes while low degree of acetylation have high fluxes but low salt rejections[146]**.** Although the degree of acetylation can range from 0 to 3, most commercial CA membranes have a 2.7 degree of acetylation.

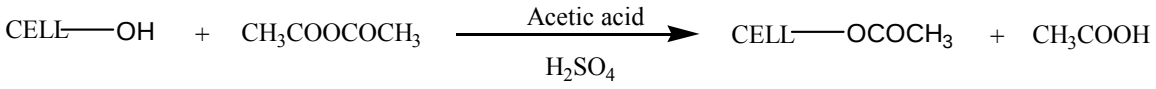

Figure 1-15. Acetylation Reaction of Cellulose Acetate

[146] Strathmann, Heiner *Synthetic Membranes and Their Preparation* in Handbook of Industrial Membranes, pp. 1-60.
[147] Muldowneyt, G. P. and Punzi, V. L. *Ind. Eng. Chem. Res* **1988**, 27, 2341-2352.
[148] Odian, G. Principles of Polymerization 3rd Ed john Wiley and Sons, NY 1991, pp. 710.

Initial interest in CA membranes as desalination membranes began with the research of Reid and Breton at the University of Florida[149]. In this RO system driven by compressed air and the feed solution was stirred convectively, Reid and Breton showed that cellulose acetate with a high salt rejection (98%) at 1000 psi was most promising. Very low fluxes attributed to the 5-20μm film thicknesses were also observed. This restricted the efficiency of these membranes in any RO systems. Nonetheless, the feasibility of cellulose acetate membranes as potential RO membrane fueled a whole new era of membrane research.

The major breakthrough in RO membrane development began in 1960 with the development of the first high-flux asymmetric reverse osmosis membrane from cellulose acetate using the DIPS technique.[140] This was called the Loeb–Sourirajan process. In this process, a solution containing 20 to 25 wt% cellulose acetate dissolved in a acetone (66.7 wt%), water (10.0 wt%), magnesium perchlorate (1.1 wt%) mixture and a film was cast from the polymer solution on a glass plate to a thickness of 0.025 cm in a cold box. While the temperature in the cold box was maintained at 0-10 °C, acetone was allowed to evaporate for 3-4 min, before the film was immersed to ice cold water. The membranes were then annealed in water at 65-85 ºC to produce a denser, more salt-rejecting skin virtually free of micropores. These membranes exhibited salt rejection values of 99.5% in 52,500 mg/L feed solution at pressures of 1500 to 2000 psig.[140]. Khulbe et al[150] illustrated this effect using Electron Spin Resonance (ESR) by showing that the pore size of the skin layer in a cellulose acetate membrane could be decreased to same size of a

[149] C.E. Reid and E.J. Breton, J. Appl. Polymer Sci. **1959**, 133.
[150] Khulbe, K.C., Matsuura, T., Lamarche. G., Lamarche, A.-M., Choi, C., Noh, S.H., *Polymer* **2001,** 42, 6479-6484.

dense membrane from the same casting solution if annealed at 90 ºC. High salt rejections (95 %) were also achieved from these asymmetric membranes.

Cellulose acetate (CA) membranes were once widely used in RO desalination industries due to several advantages such as excellent mechanical properties, cheap, easy preparation, and relatively resistant to chlorine attack[151]. One of the greatest drawbacks of these polymers that have limited further commercialization in the RO industry is their ability to hydrolyze over time especially at pHs above or below 4.7[152]. Hydrolysis caused to a reduction in the degree of acetylation leading to loss of salt rejection capacity of the RO membranes. This was mostly prominent in cellulose acetate and cellulose diacetate membranes. The most promising cellulosic materials suitable for the preparation of successful asymmetric separation membranes is cellulose triacetate (CTA), a cellulose ester with 43.7 wt% acetyl content[153]. Compared to cellulose acetate (CA) and cellulose diacetate (CDA), CTA exhibited superior hydrolytic stability and a greater resistance to free chlorine and biodegradation. However as previously discussed, at this degree of acetylation really low fluxes and insolubility in various water miscible solvents are observed. Thus, considerable effort to improve the performances of these membranes ultimately led to the development of blends of CA or CDA with CTA. King et al prepared blends of acetate polymer with small amounts of triacetate polymer or other cellulose esters such as cellulose acetate butyrate (CAB)[154]. These membranes displayed

[151] Amjad, Z., Ed. Reverse Osmosis: Membrane Technology, Water Chemistry, and Industrial Applications; Van Nostrand Reinhold: New York, 1993.
[152] Farooque, A. M., A1-Amoud, A., Numata P. K., *Desalination* **1999,**123, 165-171.
[153] Kosutic, K. and Kunst, B., *J. Appli. Polym. Sci*. **2001,** 81, 1768–1775; Kesting, R. E. In Reverse Osmosis and Synthetic Membranes; Sourirajan S., Ed.; National Research Council Canada: Ottawa, 1977; p 106.
[154] W.M. King, D.L. Hoernschemeyer and C.W. Saltonstall, Jr, Cellulose Acetate Blend Membranes, in *Reverse Osmosis Membrane Research*, H.K. Lonsdale and H.E. Podall (eds), Plenum Press, New York, pp. 131–162 (1972).

salt rejections of 99% with modest fluxes. Applied Membranes Inc., also utilizes CTA/CAB blends in their M-C2514A series. These membranes exhibit salt rejections of 96% and fluxes of 80 gpd at 225 psi[155].

2.1.1.2.3.2.Polyamide

Reverse osmosis membranes made of cellulose acetate for water desalination and purification purposes have been largely replaced with polyamide thin film composite (TFC) membranes. TFC demonstrate excellent desalination properties as higher salt rejection values, higher flux, and increased resistance to adverse water conditions such as pH and increasing temperature

John Cadotte at North Star Research is credited with the first TFC which was prepared by interfacial reaction at the membrane surface a porous polysulfone support membrane soaked in an aqueous solution of 0.5 to 1% polyethyleneimine with a 0.2 to 1% solution of toluene-2,4-diisocyanate or isophthaloyl chloride in hexane and then cured at 110°C to further crosslink the polyethyleneimine[156]. Major improvements to the chemistry were later accomplished by using aromatic diamines and triacyl chloride reactants such as m-phenylenediamine and trimesoyl chloride, respectively, produced by the Film Tec Corporation[157]. Salt rejections of 99.3–99.5% at 800 psi were also obtained. Higher rejection of 99.9% and fluxes of 12 gal/ft^{2}day at 1000 psi were obtained by

[155] http://www.appliedmembranes.com (2008).
[156] Rozelle, L.T., Cadotte, J.E., Cobian, K.E. and Kopp, C.V., Nonpolysaccharide membranes for reverse osmosis: NS-100 Membranes, in: *Reverse Osmosis and Synthetic Membranes, S.* Sourirajan (Ed.), pp. 249-261, National Research Council Canada, Ottawa, Canada (1977).
[157] Cadotte, J.E., King, R.S., Majerle, R.J. and Petersen, R.J., *J. Macromol. Sci.* Chem., 1981, Al5, 727-755.

researchers at Toray when a similar membrane from 1,3,5-tris(hydroxy ethyl) isocyanuric acid comonomer was utilized[158].

Riley *et al*. also prepared polyamide TFC based on epamine (epichlorohydrinethylenediamine adduct) crosslinked with toluene 2,4-diisocyanate[159]. These membranes were used in the first large RO seawater desalination plant in Jiddah, Saudia Arabia. However as previously mentioned, these membranes exhibited very low tolerance to oxidants especially chlorine.

Polyamide membranes are believed to degrade by chlorination first undergoing N-chlorination through chlorine attack on amidic nitrogen followed by ring chlorination through intermolecular rearrangement (

Figure **1-16**). Ring chlorination disrupts hydrogen bonding between the chains and degrades the polymer matrix via chain scission.

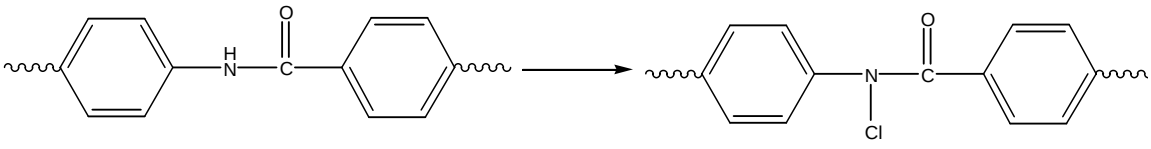

Step 1: N-Chlorination via chlorine attack on amidic nitrogen

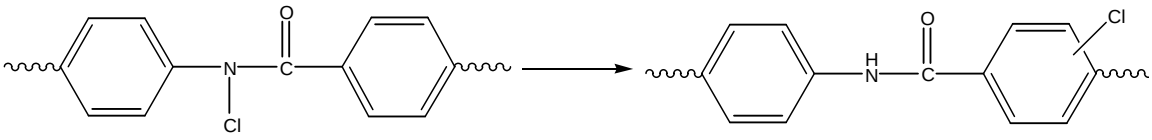

Step 2: Ring chlorination through intermolecular rearrangement

Figure 1-16. Membrane degradation mechanism of polyamide-type membranes by chlorination[160].

[158] Kurihara, M., Harumiya, N., Kannamaru, N., Tonomura, T., Nakasatomi, M. *Desalination* **1981,** 38, 449-460.
[159] Riley, R.L. Milstead, C.E., Lloyd, A.L., Seroy, M.W., Takami, M. *Desalination* **1977,** 23, 331-355.
[160] M.I., Lora, J., Alcaina, M.I., Arnal, J.M. *Desalination* **1996**, 108, 83-89.

The examination of the effect of chlorination on PA membranes was illustrated by Buch et al[129]. Scanning electron micrographs indicated the conversion of the smooth polyamide skin layer into a rough granular nature upon chlorine exposure. The change of the skin layer nature was due to the conversion of the hydrogen bonding amide N-H group to the non-hydrogen bonding N-Cl group as illustrated by FTIR spectra. Further investigations by Kwak et al[161] correlated the surface roughness with the inherent chemical nature of aromatic polyamides. In this study, four types of model TFC membranes, two crosslinked and two linear aromatic polyamides were prepared via interfacial polymerization of phenylene diamines with either tri- or di-functional acid chlorides on the polysulfone microporous supports. Surface examination by Scanning Electron Microscopy ((SEM) showed the appearance of a dense, finely dispersed nodular structure on the surface of the crossliked polyamide while surface morphology of the linear polyamides demonstrated more fully developed, widely spread polymer strands. The surface roughness and the surface area were directly correlated to the water flux of the membranes. Rougher surfaces and larger skin areas lead to higher water flux. The lack of virtual crosslinks and hydrogen bonding in the linear polyamides have reflected the rougher surface with larger area.

The influence of the diamine chemical structures on the chlorine resistance has been investigated by several researchers. Shintani et al[162] prepared various polyamides from isophthaloyl dichloride (IPC) or 1,3,5-benzenetricarbonyl trichloride (TMC) and 17 kinds of diamines. Although membranes prepared from N,N'-DMMPD and TMC exhibited higher chlorine resistance in aqueous sodium hypochlorite solution (200 ppm)

[161] Kwak, S.-Y., Jung, S.G., Yoon, Y.S., Ihm, D.W. *J.Polym. Sci.: Part B: Polym Phys* **1999,** 37, 1429–1440.
[162] Shintani,T., Matsuyama, H., Kurata, N. *Desalination* **2007,** 207, 340–348.

at 40 C for 96 h than commercial polyamide and cellulose acetate RO membranes, lower salt rejection of about 93% was observed.

Improved chlorine stability was also observed by poly-terephthalamide diphenyl sulphone (PTDS) and polyiso- phthalamide diphenyl sulphone (PIDS) copolymer membranes[160]. Compared to commercial polyamide membranes, that cannot tolerate more than 1 ppm of free chlorine, these membranes showed better resistance to chlorine attacks at higher concentration (10 ppm) of free chlorine. More chlorine-tolerant PA membranes have also been prepared by crosslinking reaction of piperazine with trimesoyl chloride[163]. The enhanced stability of these membranes in chlorine was no doubt due to the absence of hydrogen of secondary amide bonds.

2.1.1.2.3.3.Sulfonated Polysulfone

Materials for desalination membranes for reverse osmosis and other water purification areas are commonly prepared from post polysulfones have been widely studied. Sulfonated polysulfone membranes showed excellent resistance against compaction, hydrolysis and degradation and exhibited good flux and rejection characteristics Hollow fiber membranes prepared from sulfonated polysulfones with high chlorine resistance (100 ppm) have been reported[164]. Millipore developed a line of sulfonated polysulfone spiral wound membranes with salt rejections of 95% and product flux rates up to 55 gal/ft^2/day.(gfd) at 400 psi and 25 ºC[165]. These membranes also

[163] Y. Kamiyama, N. Yoshioki, K. Matsui and K. Nakagome, *Desalination* **1984,** 51, 79-92.
[164] Light, W.G., Chu, R.C., Tran, C. N. *Desalination* **1987,** 64, 411 – 421.
[165] Allegrezza, A.E., Paraekh, B.S., Parise, P.L., Swiniarski, E.J., White, J.L., *Desalination* **1987,** 64, 285-264.

exhibited superior fouling and chlorine tolerance to that of aromatic polyamides. Blanco et al [166] studied the suitability of various sulfonated polysulfone for asymmetric membrane preparation. Sulfonated poly(ethersulfone) (PES) and polyethersulfone-cardio(PES-C) were prepared by a one-step process in sulfuric acid while sulfonated polysulfone (UDEL®) was prepared in chlorosulfonic acid due to its degradation in sulfuric acid. Asymmetric membranes were prepared by the DIPS technique with water as the non-solvent. Even though asymmetric membranes could be formed from these membranes, the fluxes and salt rejection were extremely low. In addition, asymmetric membranes from PES-C exhibited excellent stability in chlorine but bacteria and fungus development over a 7 month storage period caused a reduction in the permeability and flux[167]. However, all of these membranes have been prepared by post sulfonation reaction in either chlorosulfonic or sulfuric acid which encounter numerous synthetic challenges such as control of sulfonation, chain cleavage and crosslinking.

A relatively mild post sulfonation procedure utilizing sulfur trioxide and triethyl phosphate complex (SO_3-TEP) sulfonate to reduce these side reactions was illustrated by Nosey and Robeson [168] and later Johnson *et al.* who also found no evidence of a crosslinking side reaction using sulfur trioxide in a comprehensive study on functional membranes using SO_3-TEP for water desalination.[169] The success of SO_3-TEP was also used to prepare RO membranes based on commercially available UDEL® where the permselectivity of potassium chloride (KCl) through sulfonated polysulfone increased

[166] Blanco, J. F., Nguyen, Q.T., Schaetzel, P. *J. Appli. Polym. Sci.* **2002,** 84, 2461–2473.
[167] Blanco, J. F., Nguyen, Q.T., Schaetzel, P *J. Membr. Sci*. **2001,** 186, 267–279.
[168] A Noshay; L.M. Robeson, *J. Appl. Polym. Sci.* **1976**, 20, 1885-1903; C.L. Brousse; R. Cheapurlet; J.P. Quentin, *Desalination* **1976,** 18, 137-153.
[169] Johnson, B. C.; Yilgor, I.; Tran, C.; Iqbal, M.; Wightman, J.; Lloyd, D.; McGrath, J. E. *J. Polym. Sci. Polym. Chem. Ed.* **1984**, 22, 721.

with increasing degree of sulfonation.[170] Although the presence of a milder sulfonating agent could potentially minimize or even eliminate possible side reactions, lower reaction rates and less efficient sulfonations are associated with this process. Overall however, manufacturing reproducibility issues and inability to prepare a product with flux/rejection capabilities equivalent to aromatic polyamides associated with post sulfonated polysulfone have limited the success these membranes in the RO application.

To avoid these problems, researchers[171, 172, 173] are now investigating random sulfonated copolymers prepare by direct copolymerization of a disulfonated monomer as perspective alternatives. Recently, researchers at Virginia Tech have created a new copolymer membrane for RO that exhibit high salt rejection and stability against chlorine attack[171]. Polymer membranes are based on disulfonated poly(arylene ether) systems that were initially used as proton exchange membrane for fuel cells but are in the salt form and can be prepared in either dense, TFC, or asymmetric form. Dense and TFC membranes of 4, 4'-biphenol based poly(arylene ether sulfone)s have demonstrated that low degrees of sulfonation result in salt rejections as high as 99.2% can be achieved[172]. However, low fluxes and low water uptakes are also characteristic of these membranes. These properties can be improved making very thin membranes or membranes using polymers with higher sulfonation levels. Higher chlorine tolerance at high chlorine

[170] V. Deimede, G.A. Voyiatzis, J.K. Kallitsis, L. Qingfeng, N.J. Bjerrum,; *Macromolecules* **2000,** 33, 7609-7617.
[171] Membrane Technology "*UCLA and Virginia Tech develop novel desalination technologies*." March (**2007**).
[172] Park, H., Freeman, B., Zhang, Z., Sankir, M., McGrath, J.E. *Angew. Chem. Int. Ed.* **2008,** 47, 6019 – 6024.

concentrations (1000 ppm) over a wide range of pHs than commercially available polyamides TFC and a greater resistance to fouling[173, 99] has also been observed.

2.2. Introduction to Fuel Cells

A fuel cell is an electrochemical device that combines a fuels, such as hydrogen and methanol, and oxygen from air in the presence of a catalyst to generate electricity.[174,175] The primary by-products of fuel cells are water and heat, which make the technology very environmentally friendly (

Figure 1-17).[176] Most fuel cells are powered by hydrogen, but a variety of other primary fuels such as natural gas, methanol, and ethanol which generate protons or hydronium ions are also employed.[177] The core of a fuel cell is the membrane electrode assembly (MEA) which is composed of an ion-conducting electrolyte, an anode and a cathode. The efficiency of fuel cells generally ranges from 40 to 60%. However, this efficiency can be increased to 80% if the heat generated is used.[178]

The first fuel cell was invented by Sir William Grove in 1843.[6,179] Since then several other fuel cells systems have been developed. Fuel cells are classified in terms of the nature of the electrolyte and its operation conditions as either low-temperature or high-temperature fuel cells.[180] The properties of the electrolyte determine the operating temperature and the fuel used to generate electricity. The main types of commercially

[173] McGrath, J.E., Freeman, B., Baird, D. "Chlorine Resistant Reverse Osmosis (RO) Membranes: Scale-up, Characterization, Processing, and Evaluation" Proposal to the Office of Naval Research June, 2006.
[174] Appleby, A. J., Ed. *Fuel Cells: Trends in Research and Appli][cations*; Hemisphere Publishing Corp.: New York, 1987; p.281.
[175] Zalbowitz, M.; Thomas, S. "Fuel Cells: Green Power," Department of Energy, 1999 LA-UR-99-3231.
[176] Barbir, F.; Gomez, T., *Int. J. Hydrogen Energy* **1997**, 22, 1027-1037.
[177] Sopina, K. *Renewable Energy* **2006,** 31, 719-727.
[178] J.H. Hirschenhofer, D.B. Stauffer, R.R. Engleman, in Fuel Cells: A Handbook (Revision 3), DOE/METC-94/1006, 1994.
[179] William Grove writing to Michael Faraday, October 22, 1842.
[180] Appleby, A.J.; Foulks, F.R., *Fuel Cell Handbook*, Van Nostrand Reinhold, New York, 1989.

available fuel cells include alkaline fuel cell (AFC), phosphoric acid fuel cell (PAFC), molten carbonate fuel cell (MCFC), solid oxide fuel cell (SOFC), polymer electrolyte membrane fuel cell (PEMFC), and direct methanol fuel cell (DMFC).[181]

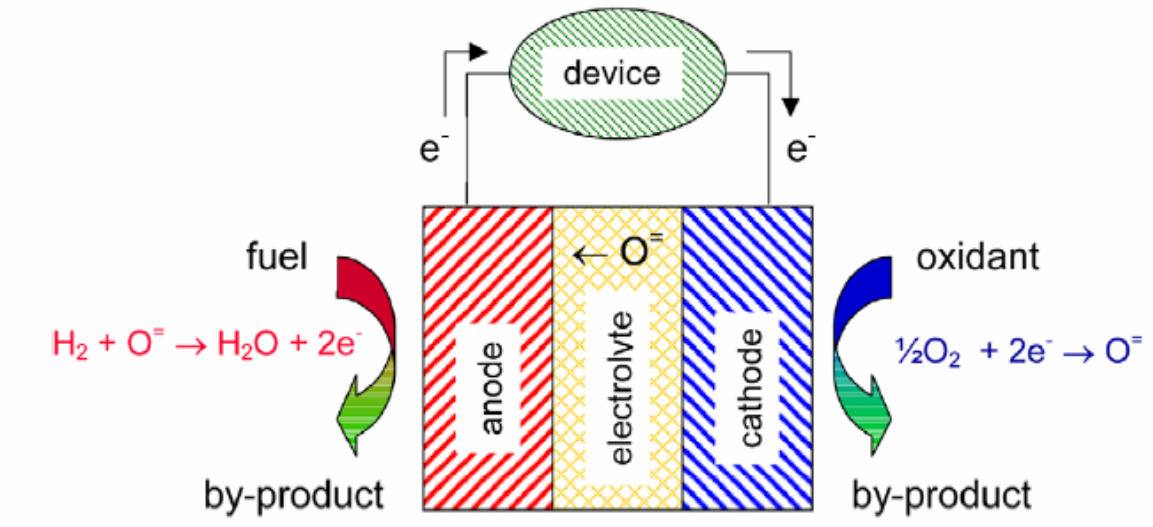

Figure 1-17. Basic scheme of the fuel setup and operation.[182] Reprinted from Acta Materialia, 51, Haile Sossina, Fuel cell materials and components, 5981-6000, Copyright (2003), with permission from Elsevier.

2.2.1. High Temperature Fuel Cell (HTFC)

High temperature fuel cells include MCFC and SOFC. High temperature operation at temperature above 500 °C causes the electrodes to become increasingly more tolerant to carbon monoxide (CO) in the fuel. However, more stable electrolyte materials that can withstand these extreme temperatures are required.

[181] Appleby, A. J., Ed. *Fuel Cells: Trends in Research and Applications*; Hemisphere Publishing Corp.: New York, 1987.
[182] Sossina, Haile. *Acta Materialia* **2003**, 51, 5981-6000.

2.2.1.1.Molten Carbonate Fuel Cells

The first MCFC was reported in 1960.[183] Sanyo has conducted research to develop MCFC stacks and systems.[184] Generally, the electrolytes utilized in MCFC are mixtures sodium carbonate with lithium carbonate (Li/Na) or potassium carbonate with lithium carbonate (Li/K) supported by a ceramic $LiAlO_2$ matrix.[185] The operation temperatures of MCFCs are in the range of 550-700 °C.[186] The anode and cathode in MCFCs are made of porous nickel and nickel oxide (NiO), respectively. However, the anode material has the susceptibility to creep while the NiO material in the cathode undergoes slow dissolution in the molten carbonate electrolytes.[187] Alternative materials such as $LiCoO_2$, $LiFeO_2$ and Li_2MnO_3 for the cathode and Cr-doped Ni for the anode are currently being investigated to resolve these problems.[188] The net transfer of CO_2 from the cathode side of the cell to the anode through the electrolyte is one of the major distinguish features of MCFCs.[189]

2.2.1.2.Solid Oxide Fuel Cells

[183] Mitchell, Will Jr. *Fuel Cells*; Academic Press Inc.: New York, 1963.
[184] Y. Miyake. *J. Power Sources* **1996,** 61, 149-153.
[185] a) Selman, R.J, *Energy* **1986**, 11, 153-208; b) Okada, O.; Yokoyama, K., *Fuel Cells* **2001**, 1 (1) 72-77.
[186] Minh, N, "High Temperature Fuel Cells", *Chemtech* **1991**, 21 (1), 32-37.
[187] Dicks, A. L. *Current Opinion in Solid State and Materials Science* **2004**, 8, 379-383.
[188] a) Escudero, M. J.; Rodrigo, T.; Daza, L.; *Catalysis Today* **2005**, 377, 107–108; b) Wijayasinghe, A.; Bergman, B.; Lagergren, C.; *Solid State Ionics* **2006,** 177, 165-173.
[189] Carrette, L.; Friedrich, K.A.; Stimming, U.; Fuel Cells: Principles, Types, Fuels, and Applications", *ChemPhysChem* **2000**, 1, 162.

SOFCs, operate at temperatures of 800–1000 °C and employ hard ion conducting ceramics as the electrolyte.[190] The high operating temperature of the conventional SOFC technology puts high demands both on materials, cell and system designs.[191] Cracking in the electrolyte and slow start are just some of the disadvantages associated with SOFCs extreme temperatures.[192] Stabilized zirconia--which is zirconium oxide (ZrO_2) doped with either calcium (Ca^{2+}), yttrium (Y^{3+}) or Sc^{3+}, is the most popular electrolyte used in SOFCs.[8,13] The presence of these metals is required to stabilize the ZrO_2 at the higher temperatures or to enhance ionic conductivity.[193] However, Y_2O_3 is principally chosen as the dopant. Anodes in SOFC are made from nickel while the cathodes are alloys containing metals and metal compounds such as cobalt, ferrite, maganite, lathananum or zirconium. SOFCs are being applied in large, high-power applications such as full-scale industrial stations and large-scale electricity-generating stations.[7,14]

2.2.2. Low Temperature Fuel cell (LTFC)

The primary kinds LTFC include AFC, PAFC, and PEMFC.[194] Low temperature fuel cells have better durability than HTFC and facilitate quick start up and shut down. However since protons and electrons at these temperatures are extremely slow generating, expensive noble metal catalysts are required to convert H_2 to H^+.

2.2.2.1.Alkaline Fuel Cells

[190] Carrette, L.; Friedrich, K.A.; Stimming, U.; *Fuel Cells* **2001**, 1, 5-38.
[191] Apfel, H.;, Rzepka, M.; Tu, H.; Stimming, U.; *J Power Sources* **2006**, 154, 370-378.
[192] Bujalski, W.; Paragreen, J.; Reade, G.; Pyke, S.; Kendall, K.; *J Power Sources* **2006**, 157, 745-749.
[193] Winters, M.; Brodd, R. J.; *Chem Rev* **2004**, 104, 4245-4270
[194] Appleby, A.J., *Energy* **1986**, 11, 13-94.

A Beacon fuel cell was developed as the first successful alkaline fuel cell at the University of Cambridge in the 1959[23]. The functional temperatures of AFCs are typically between 75 – 110 °C with potassium hydroxide solution (30 – 40 wt%) acting as the electrolyte.[195] However, temperatures up to ~250 ºC with an 85% KOH solution have also been reported.[196] Hydroxyl ions in AFC migrate from the cathode to the anode. Anion conducting polymer electrolytes such as polyether and polyepichlorhydrin as substitutes to KOH have also been proposed.[197]

A major problem associated with these polymer electrolytes is the lack of durability of these materials in an aqueous alkali. In general, ammonium groups such as benzyl trimethylammonium and N-alkyl pyridinium which are the most common anion exchange groups used in these materials, decompose in the concentrated alkali solution by the Hoffman degradation reaction.[198,199]

The electrodes may consist of an active electrocatalyst layer and a hydrophobic layer usually poly(tetrafluorethylene) (PTFE).[200] Inexpensive metals such as nickel and silver can be used as catalyst at the anodes and cathode, respectively.[201] Hence, the operation cost AFCs are lower due to smaller amounts of precious metal catalysts such as platinum

[195] Sheibley, D.W.; Martin, R.A, *Prog. Batteries Solar Cells* **1987**, 6, 155.
[196] Carrette, L.; Friedrich, K.A.; Stimming, U.; *ChemPhysChem* **2000**, 1, 162-193.
[197] Iojoiu, C.; Chabert, F.; Maréchal, M.; Kissi, N. El.; Guindet, J.; Snchez, Y. From polymer chemistry to membrane elaboration: A global approach of fuel cell polymeric electrolytes *J Power Sources* **2006**, 153, 198-209.
[198] Li, Lei, *J Mem Sci* **2005**, 262, 1-4.
[199] Sata, T.; Tsujimoto, M.; Yamaguchi, T.; Matsusaki, K.;*J Mem Sci* **1996**, 112, 161-170.
[200] McLean, G.F.; Niet, T.; Prince-Richard, S.; Djilali, N.; *Int. J Hydrogen Energy* **2002**, 27, 507-526.
[201] Gülzow, E.; Schulze, M.; Gerke, U.; *J. Power Sources* **2006,** 156, 1-7.

being used to achieve an equivalent reaction rate in other fuel cell systems (i.e., PEMFC and DMFC systems).[202]

Expensive purification of hydrogen and oxygen are, however, required for AFC because the poisoning of the catalyst and contamination from carbon dioxide (CO_2) and carbon monoxide (CO) may occur.[203] Unlike MCFC and SOFC the carbon dioxide produced in the cell and from air causes deterioration within the AFCs.[204] Equation 1-18 describes the reaction of CO_2 with the KOH electrolyte.

$$CO_2 + 2OH^- \rightarrow CO_3^{2-} + H_2O \qquad \textbf{Equation 1-18}$$

The continuous buildup of carbonates in the cell contaminates the electrolyte and disrupts the overall cell performance.

2.2.2.2.Phosphoric Acid Fuel Cell

The phosphoric acid fuel cell is fabricated by single stacked cells consisting of electrodes, an electrolyte matrix, and bipolar plate.[205] The PAFC electrolyte, primarily phosphoric acid (H_3PO_4) retained in a 0.1–0.2 mm thick silicon carbide (SiC) matrix works together with the catalyst for both for the oxidation of hydrogen fuel at the anode and oxygen reduction at the cathode.[206,207] The quantity of the electrolyte can be

[202] Burchardt,T.; Goue´rec, P.; Sanchez-Cortezon, E.; Karichev, Z.; Miners, J. H.; *Fuel* **2002**, 81, 2151-2155.
[203] K. Kordesch, K.; Gsellmann, J.; Kraetschmer, B., in *Power Sources 9*, J. Thompson, Ed., Academic Press, New York, 1983, p.381.
[204] Tomantschger, K.; McClusky, F.; Oporto, L.; Reid, A.; Kordesch, K., *J. Power Sources* **1986**, 18, 317-335.
[205] Appleby, A. J., Ed. *Fuel Cells: Trends in Research and Applications*; 1987, Hemisphere Publishing Corp.: New York; p. 281.
[206] Yoon, K.H.; Duk Yang, B.; *J of Power Sources* **2003**, 124, 47-51.
[207] Song, R.; Shin, D.; Kim, C.; *Int. J. Hydrogen Energy* **1998**, 23, 1049-1053.

modified in the matrix by adjusting SiC particle size distribution and the binder content in the matrix layer.[208]

The electrocatalyst in PAFCs is comprised of carbon-supported platinum along with PTFE binders. However, improved wettablity and increase porosity with poly(ether sulfone)s have been reported.[209] Conversely, at cell voltages above 0.8 V the catalyst become problematic because of platinum dissolution and carbon corrosion.[40] Further drawbacks of PAFCs include decrease lifetime due to contamination from CO and sulphur (S), larger and heavier design compared to other fuel cells of similar power, and the acid solution electrolyte that may corrode cell component leading to increased cost.[210] Although United Technologies Company is the main manufacturer of PAFCs, outstanding results from companies such as Toshiba and Fuji Electric have been documented.[15, 39]

PAFCs can be applied as dispersed power generation, electrical buses and trucks, and remote power stations. PAFC operate at moderate temperature of 150 to 200 °C with natural gases as the fuel at an efficiency of 40%.[211]

2.2.3. Proton Exchange Membrane Fuel Cells

PEMFCs are being investigated worldwide as alternative energy devices for applications in stationary, automotive, and portable power.[212] The first PEM technology

[208] Song, R.; Dheenadayalan, S.; Shin, D.; *J of Power Sources* **2002**, 106, 167-172.
[209] K.H. Yoon, J.H. Jang, Y.S. Cho, *J. Mater. Sci. Lett.* **1998**, 17, 1755-1758.
[210] Larminie, J.; Dickd, A.; *Fuel Cell Systems Explained.*; 2000, John Wiley and Sons Inc.: England; p. 137.
[211] Ghouse, M.; Abaoud, H.; Al-Boeiz, A.; AbdulHadi, M.; *Applied Energy* **1998**, 60, 153-167.
[212] a) Zalbowitz, M.; Thomas, S. "Fuel Cells: Green Power," Department of Energy, **1999** LA-UR-99-3231.; b) Dhathathreyan, K.S.; Sridhr, P.; Sasikumar, G.; Ghosh, K.K.; Velayuthan, G.; Rajalakshmi, N.;

was invented by General Electric as part of NASA's US Gemini space program in the early 1960s. Advancements in membrane materials and operations of PEMFC have aided in PEMFCs to be considered the most promising fuel cell candidates in terms of size, mode of operation and applications.[42] Current PEMFC systems generate higher specific power and power density compared to other fuel cells even at low temperature of 30 – 175°C.[213] However, typical operation temperatures of PEMFCs are in the range of 80 – 100 °C.[190]

A single fuel cell consists of membrane electrode assembly and two flow field plates for fuel and air. The MEA in a PEMFC is comprised of a proton exchange membrane (PEM) between two catalyzed porous PTFE-coated carbon paper gas diffusion layers (GDL).[214] Platinum, the most common catalysts in PEMFC, is bonded to the electrodes by painting or hot pressing at temperatures above the glass transition of the membrane. A detailed schematic of an MEA in a PEMFC is presented in Figure 1-18.

Subramaniam, C.K.; Raja, M.; Ramya, K., *Int. J. Hydrogen Energy* **1999**, 24, 1107-1115; c) Korgesch, K.; Simader, G., *Fuel Cells and Their Applications*, Wiley-VCH, Weinheim, 1996.

[213] Mathias, M.; Gasteiger, H.; Makharia, R.; Kocha, S.; Fuller, T.; Pisco, J.; Preprints of Symposia - American Chemical Society, Division of Fuel Chemistry **2004**, 49(2), 471-474.

[214] Hickner, M. A. *PhD. Thesis*, VPI & SU, 2003.

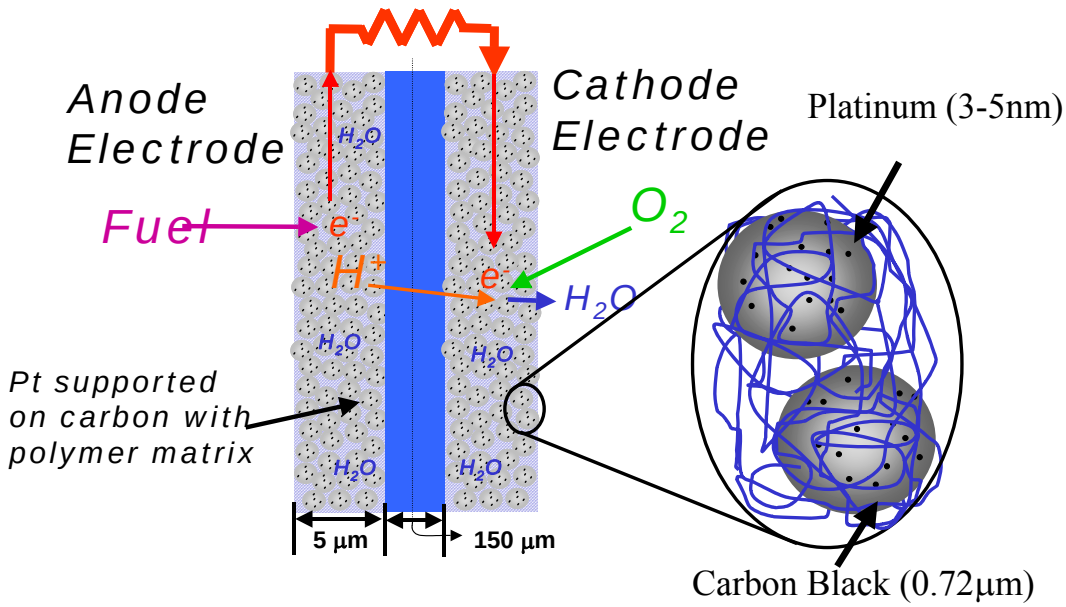

Figure 1-18. Components and setup for a Membrane Electrode Assembly (MEA) used in a PEMFC. Reprinted with permission from[215]. Copyright 2004 American Chemical Society.

In PEMFC, current is generated at the anode by applying a voltage across the cell causing hydrogen molecules to dissociate into protons and electrons in the presence of the platinum catalyst.[216] The hydrated membrane transports the protons to the cathode of the cell, while the electrons are transported to the current collectors. The protons subsequently combine by reacting with either pure oxygen or air, in the presence of a catalyst at the cathode, to form water.[40]

The electrochemical reactions in PEMFC vary according to the types of fuel utilized at the anode. The fuels incorporated at the anode include hydrogen or methanol. The electrochemical process associated with each type of fuel is described in Table 1-3..

[215] Hickner, M.A., Ghassemi, H., Kim,Y. S., Einsla, B. R., McGrath, J.E.Chem. Rev.**, 2004,** 104, 4587-4612.
[216] Liebhafsky, H.A.; Cairns, E..J., *Fuel Cells and Fuel Batteries*, John Wiley and Sons, Inc., New York 1968.

Table 1-3 Electrochemical reaction carried out in Hydrogen-Air and Methanol-Air PEMFC.[180]

Electrochemical	*Fuels Sources*	
Reactions	**Hydrogen /Oxygen**	**Methanol/Oxygen**
Anode	$H_2 \rightarrow 2H^+ + 2\ e^-$	$CH_3OH + H_2O \rightarrow CO_2 + 6H^+ + 6e^-$
Cathode	$½O_2 + 2H^+ + 2e^- \rightarrow H_2O$	$3/2\ O_2 + 6H^+ + 6e^- \rightarrow 3\ H_2O$
Overall	$H_2 + ½O_2 \rightarrow H_2O$	$CH_3OH + H_2O + 3/2\ O_2 \rightarrow CO_2 + 3\ H_2O$

2.2.3.1.Hydrogen/Air (H_2/Air) PEMFC

Hydrogen/Air PEMFC are the most attractive alternative to the internal combustion engine. Here a stream of pure or reformed hydrogen is oxidized at the anode generating protons and electrons while oxygen is simultaneously reduced at the cathode. The protons migrate through the PEM to the cathode combing with reduced oxygen (air) to produce water. The electrons are transmitted to the anode via an external circuit to produce electricity.

The operating temperatures of PEMFC range from 60-120 ºC with fuel efficiencies of 35-60%. When the waste heat (only recovered as hot water) from the cell is utilized the fuel efficiency can be as high as 90%. Some other advantages of PEMFC include rapid changes in power output to meet shifts in power demand and higher power density capabilities compared to other fuel cell that allow for compact and lightweight setup.

2.2.3.2.Direct Methanol Fuel Cell (DMFC)

DMFC are a category of proton exchange membrane fuel cells that utilizes about liquid methanol as the fuel. DMFCs were developed in the early 1990s at the Caltech/NASA Jet Propulsion Laboratory and the University of Southern California. Unlike H_2/air PEMFC, the fuel (methanol) is not reformed, but is instead fed directly to the fuel cell. Storage of liquid methanol is easier to transport and supply and is not as difficult as hydrogen storage.

As shown in Table 1-3**,** in a DMFC the hydrogen required for oxidation at the anode is pulled from the methanol by the platinum catalyst generating protons, electrons and carbon dioxide. The protons is transported via a PEM to the cathode where combines with electrons and reduced oxygen to form water.

These systems operate at temperatures between 30 ºC- 90 ºC. The low temperatures associated with DMFC require a more active catalyst to promote rapid oxidation of methanol to hydrogen ions and carbon dioxide. Thus higher catalyst loading are needed.

The need for water in DMFC, limits the energy density of the fuel leading to lower power output. Additionally, the permeation of methanol through current membrane materials lowers the overall efficiency of these systems. Therefore DMFC are suitable for low powered applications such as cell phones, laptop computers, and digital cameras.

2.2.3.3.Challenges Facing Proton Exchange Membrane Fuel Cells

Proton exchange membranes fuel cells (PEMFCs) are attractive alternative energy sources for transportation, stationary and portable power. However, the progress and commercialization of these systems have been extremely restricted due to various drawbacks including the cost of the system, water management, catalyst layer, carbon dioxide poisoning, and membrane materials. Each of these issues will be addressed below.

2.2.3.3.1. Cost of PEMFC System

The cost of PEMFC system has been estimated at $500-600/kW.[217] About 80% of the costs are attributed to the bipolar plates, platinum, and the electrodes. Membranes, peripheral parts and system assembly make up the remaining 20%. The individual cost of PEMFC system is shown in Table 1-4

Table 1-4. Individual cost requirements for PEMFC components[218]

Component	***Materials Used***	***Amount Required***	***Current Cost ($)***
Bipolar Plates	Graphite (single cell)	4mm	1650/ m^2
Electrodes	Nafion (Single cell)	0.8 mm	1423/ m^2

[217] Jung-Ho Wee. Renewable & Sustainable Energy Reviews **2007**, 11(8), 1720-1738.
[218] Tsuchiya H, Kobayashi O. *Int J Hydrogen Energy* **2004,** 29, 985–90.

Catalyst	Platinum	2-4mg/m^2	32-64/ m^2
Proton Exchange Membrane	Nafion	100 μm	500/m^2
Peripheral Parts	End plates, thrust bolts. Plastic frame	0.5 kg/ m^2	15.4/ m^2
Assembly	Hand assembly	-	385/50kW

After examining Table 1-4 it is understandable that fuel cell vehicles (FCV) are 10 times as expensive as traditional internal combustion engine vehicles. Many researchers are now investigating various techniques to reduce the cost of fuel cells. To reduce cost many researchers have suggested using lower catalyst loading on the electrodes; preparing bipolar plates from several kinds of materials including carbon composites or injection molding of graphite filled polymer and metals; or developing a alternative PEMs.[219] Barbir and Gomez also reported that a great reduction in cost could be achieved if mass production techniques were applied in the fuel cell manufacturing process.[220] This would ultimately reduce the cost of current fuel cells from $500/cell plus $1000/stack to $50/cell plus $150/stack.

2.2.3.3.2. Water Management

The formation of water during the fuel cell operation is one of the major issues that hinder the PEMFC performance. Electro-osmotic drag and back diffusion of water

[219] T.R.Ralph. *Platinum Metals Rev*, **1997,** 41,102-113.
[220] Barbir, F. and Gomez, T. *Int. J. Hydrogen Energy*. **1996,** 21, 891-901.

are factors that can cause negative consequences due to the formation water. The presence of water can lead to flooding of the PEM which decreases the surface area needed for efficient separation of hydrogen or water formation to take place.[221] Thus, water management is an important characteristic of PEM.

The PEM is an ion conducting polymer which is responsible for the transports protons from the anode to cathode and must prevent the significant diffusion of fuel and oxygen. However, good proton conduction can only occur when the PEM is correctly hydrated.[222] Thus the operation temperature of PEMFC typically is limited to below 100 ºC. The hydrated properties of PEMs are greatly affected by their mechanical properties and increases dramatically with temperature and water content.[223] To improve water management many researchers are now focusing on using air and fuel gas humidifiers and water recovery system in the current systems.[13, 14]

Non-hydrated proton exchange membranes have also been investigated. Non-hydrated membranes such as acid–base polymer complexes or basic polymers such as PBI [poly(benzimidazole)] in combination with sulfuric, phosphoric and various halide acids have also been investigated.[224] The performances of these non-hydrated membranes, however, are considerably inferior to that of Nafion[6] and other hydrated membranes. The use of non-hydrated membranes could also allow PEMFC operations to occur at high temperatures (>100 ºC).

---

[221] Rayment, C. and Sherwin, S. Introduction to Fuel Cell Technology, 2003.
[222] Choi, P.; Datta, R. *J Electrochem Soc* **2003**, 150(12), E601-E607.
[223] Kopitzke, R.W.; Linkous, C.A.; Anderson, H.R.; Nelson, G.L. Conductivity and Water Uptake of Aromatic-Based Proton Exchange Membrane Electrolytes, *J. Electrochem. Soc.* **2000**, *147*, 1677-1681.
[224] a) Hasiotis, C.; Diemede, V.; Kontoyannis, C. *Electrochimica Acta* **2001**, 46, 2401-2406; b) Ariza, M. J.; Jones, D. J.; Roziere, J. *Desalination* **2002,** 147,183-189.

2.2.3.3.3. Catalyst Layer

The primary catalysts used in PEMFCs are nanosized platinum particles supported on carbon. Platinum compared to other catalysts for PEMFC exhibit highly activated and stabilized electro-oxidation of hydrogen and reduction of oxygen. However, one of the main problems associated with Pt-based catalyst is the cost. Typically the Pt black catalyst loading on electrodes is 2-4 mg/cm^2 which ranges from \$32-64/cm^2 as shown in Table 1-4**.** The expense of Pt becomes an even greater problem in DMFC where higher cathode loading of platinum. To reduce PEMFC cost many researchers have investigated the use of lower Pt catalyst loading. This change is very apparent in hydrogen/air PEMFC where over the last decade the platinum content (or Pt loading) has been drastically reduced from ~4 mg/cm^2 (per electrode) to less than 0.4 mg/cm^2.[225] The use of hydrous phosphate and oxides that serve as catalytic support for platinum and allow lower catalyst loadings (0.02 mgPt/cm^2) to be utilized may also reduce cost.[226]

Wilson et al[227] prepared platinum black based cathode with 0.12 mg/cm^2 catalyst loading. These researchers mixed Nafion EW1100 (5 wt% in isopropanol and water with carbon supported Pt to prepare thin film catalyst layers. In the Ballard Mark V single cell and advanced-stack hardware employing cathode loading of ≤0.6 mgPt/cm^2 and anode loadings of ≤0.25 mgPt/cm^2 exhibited comparable performance to current MEA stacks with higher platinum black electrode loadings (4 mgPt/cm^2).[228] Low catalyst loadings

[225] Sossina M. Haile *Acta Materialia* 51 **2003,** 5981–6000.
[226] Lyons, K.S., Bouwman, P.J., Ugarte, P. Hydrogen, fuel Cells, and Infrastructure Technologies, FY 2003 Progress Report.
[227] Wilson, M.S., Valerio, J.A., Gpttesfeld, S. *Electrochimicia Acta* **1995,** 40, 355-363.
[228] Ralph, T.R., Hards, G.A., Keating, J.E., Campbell, S.A., Wilkinson, D.P., Davis, M., St-Pieere, J., Johnson, M.C. *J. Electrochem Soc.* **1997**, 144, 3845-3857.

(0.05 mgPt/cm^2) from a mixture of carbon supported Pt catalyst and polytetrafluoroethylene (PTFE) have also been investigated.[229]

High catalytic activity towards hydrogen oxidation and low carbon monoxide tolerance are needed. A number of studies have been conducted to improve the catalytic activity in PEMFC. Cho et al.[230] utilized carbon supported Pt (Pt/C) as the cathode catalyst in DMFC to improve the surface area and offer greater stability than Pt black. The single cell MEA performance of the MEA with 2.0 mg/cm^2 Pt/C demonstrated better performance than the MEA that had a higher Pt black loading (3.0 mg/cm^2). However compared to Pt/Au/C catalyst prepared by Wang et al[231], Pt/C had significantly lower methanol tolerance

Higher activity for methanol oxidation could be obtained when small amounts of Pt were added to tungsten carbide (WC).[232] Mesoporous WC was prepared by polycondensation of resorcinol and formaldehyde. Ammonium metatungstate salt was used as the tungsten source while cetyltrimethylammonium bromide was used as the surfactant. Platinum catalyst (7.5 wt%) was loaded on WC by borohydride reduction method in alkaline media. Recently, Ham et al[233] also demonstrated that two times higher catalytic activity of hydrogen oxidation at the anode in H_2/Air PEMFC when Pt supported on mesoporous tungsten carbide (WC) was used.

2.2.3.3.4. Carbon Monoxide Poisoning

[229] Ferreira, C. Srinivasan, S. Extended Abstracts Electrochemical Society, Spring Meeting, San Francisco, 94-1, 1994, 969.
[230] Cho, Y.., Park, H., Cho, Y.,Park, I., Sung, Y. *Electrochimica Acta*, **2008,** 53, 5909-5912.
[231] Wang, J., Yin, G., Wang, G., Wang, Z., Gao, Y. *Electrochemistry Communications* **2008,** 10, 831-834.
[232] Ganesan, R., Lee, J.S. *Angew. Chem. Int.* **2005,** 44, 6557-6560.
[233] Ham, D. J., Kim, Y.K., Han, Y.H., Lee, J.S. *Catalysis Today* **2008,** 113, 117-122.

Carbon monoxide (CO) is an impurity found in hydrogen feed when it is reformed from fossil fuels such as alcohol or hydrocarbons. The presence of CO is a major drawback form PEMFC because platinum is very susceptibility to carbon monoxide poisoning As shown in Equation 1-19 to Equation1-21, small amounts of carbon monoxide (approximately 10 ppm) can poison Pt surface by blocking active site for hydrogen oxidation resulting in lower catalytic activity and decreased cell performance due to reduced surface areas for efficient electro-oxidation to occur.[234]

.

$$H_2 + 2Pt \leftrightarrow 2H - Pt \qquad \textbf{Equation 1-19}$$

$$2H - Pt \leftrightarrow 2Pt + 2H^+ + 2e^- \qquad \textbf{Equation 1-20}$$

$$CO + Pt \leftrightarrow CO - Pt \qquad \textbf{Equation 1-21}$$

Carbon monoxide can be removed from the surface of the Pt catalyst by reaction with surface (S) hydroxyls (Equation 1-21 to Equation1-23):[235]

$$H_2O + Pt \leftrightarrow Pt - OH + H^+ + e^- \qquad \textbf{Equation 1-22}$$

$$CO - Pt + OH - S \rightarrow 2Pt + CO_2 + H^+ + e^- \qquad \textbf{Equation 1-23}$$

Alloys of Pt with ruthenium (Ru), Mo, Re and WC are used to remove carbon monoxide due to the ability of these metals to electroxidize CO absorbed onto Pt by

[234] Meland, A., Kjelstrup, S. *J. Electroanalytical Chemistry* **2007**, 610, 171-178; Sathe, B.R., Risbud, M.S., Patil, S., Ajayakumar, K.S., Naik, R,C., Mulla, I.S., Pillai, V.K. *Senors and Actuators* **2007,** A138, 376-383.
[235] Gardner, C.L., Ternan, M. *J. Power Sources* **2007,** 171, 835-841.

promoting the formation of surface hydroxyl ions on Pt through water activation. A detailed study on model catalyst with defined Pt to Ru surface compositions showed that the lowest overpotential in a PEM single cell was achieved by Pt/Ru catalyst in a 1:1 ratio.[236] Divisek et al demonstrated that enhanced CO tolerance up to 250ppm of CO was achieved with Pt/Ru alloys.[237] These researchers also showed that the addition of hydrogen peroxide (H_2O_2) to the humidification water at cell temperatures of 80 ºC exhibited the same performance on a current voltage curve as that of pure hydrogen. The enhanced performance with H_2O_2 is due to the oxidation of CO by active oxygen from H_2O_2 decomposition. Previously mentioned, higher temperature fuel cells can also be utilized to dramatically increase CO tolerance.

2.2.3.4.Proton Exchange Membrane (PEM) Materials

The challenge to find ideal polymeric materials that will provide desired properties for use as a proton conductor in PEMFCs has been investigated ever since the use of ion exchange electrolytes for fuel cells was suggested in the 19th century.[238,239] To date perfluorinated sulfonic acid copolymers have been the most widely studied as proton exchange membranes (PEMs) for fuel cells (Figure 1-19). Nafion, a poly (perfluorosulfonic acid) copolymer produced by DuPont, is the current state-of-the-art polyelectrolyte membrane used for fuel cells. It contains a hydrophobic fluorocarbon

[236] Gasteiger, H.A., Markovic, N., Ross, P.N. *J. Phys. Chem*. **1994,** 98, 617; Gasteiger, H.A., Markovic, N., Ross, P.N. *J. Phys. Chem*. 99 (**1995**) 8290; Gasteiger, H.A., Markovic, N., Ross, P.N. *J. Phys. Chem*. 99 (**1995**) 167.
[237] Divisek, J., Oetjen, H.-F., Peinecke, V., Schmidt, M., Stimming, U. *Electrochimica Acta*, 43 (**1998**) 3811-3815.
[238] Savadogo, J.O., *New Mat. Electrochem. System* **1997**, 1, 47.
[239] W.T. Grubb, Proceedings of the 11th Annual Battery Research and Development Conference, PSC Publications Committee, Red Band, NJ, p.5, (1957).

backbone and perfluoroether side chains containing a strong hydrophilic ionic pendant group, sulfonic acid. Nafion exhibits some excellent characteristics such as high proton conductivity (0.1 S/cm), good chemical and mechanical properties, and long term stability at high relative humidity.[240] However, drawbacks of many perfluorinated membranes include high cost, low conductivity at low humidity or high temperatures, and limited operation temperature (<100ºC).[241] In addition, high methanol permeability limits their usage in direct methanol fuel cells (DMFCs) and decreases the cell efficiency.[242]

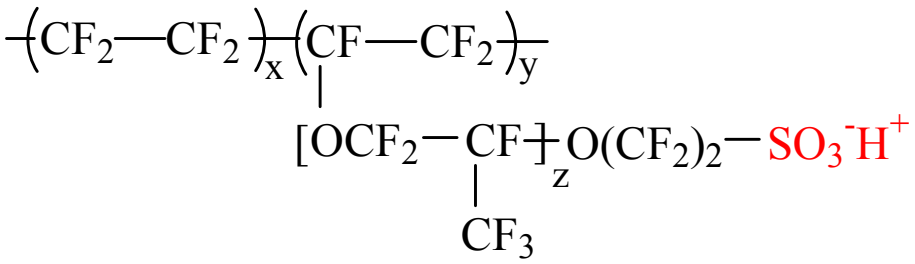

Figure 1-19. Structure of Nafion® perfluorosulfonic acid copolymer.[240]

To overcome these challenges, many researchers have developed various alternative ionomeric membrane materials that exhibit comparable performances to perfluorinated polymers. Alternative proton conductive materials are generally classified as perfluorinated ionomers, partially fluorinated polymers, and non-fluorinated membranes with aromatic backbone, non-fluorinated hydrocarbons, or blends.[243] Many of these materials are potentially less expensive, have higher operation temperatures,

[240] Mauritz, K.A.; Moore, R.B. State of Understanding of Nafion. *Chem. Rev.* **2004**, *104*, 4535-4586.
[241] Korgesch, K.; Simader, G., *Fuel Cells and Their Applications*, Wiley-VCH, Weinheim, 1996.
[242] Clagett, D.C. in *Encyclopedia of Polymer Science and Engineering,* H.F. Mark, N.M. Bikales, C.G. Overberger, G. Menges, Eds., Vol. 6, John Wiley and Sons, New York, 1986.
[243] Farrauto R.; Hwang, S.; Shore, L.; Ruettinger, W.; Lampert, J.;Giroux, T.; Liu, Y.; and Ilinich,O. *Annu. Rev. Mater. Res.* **2003**, 33, 1-27

and/or have lower methanol perm abilities. Since the focus of this fuel cell research is based on blend membranes, a literature review on this topic is appropriate.

2.2.3.4.1. Polymer Blends as Candidates for PEMFC

Polymer blends are recognized as a valuable means to combine the properties of two different polymers.[244] Polymer blending has been shown to improve many characteristics including impact strength, thermal behavior, and surface property.[245] Generally with respect to proton exchange membranes, polymer blending has been investigated to improve or modify properties such as mechanical strength, water swelling behavior, methanol permeability, and proton conductivity. Most commercial blends are either homogeneous, phase-separated, or a little of both[246]. Advantages of polymer blending includes reduction of cost since synthesis of new polymers is not required to obtain novel materials, improved processability of high temperature thermoplastics, and improved mechanical properties[247]. Several book reviews describe various aspects of the preparation of polymer blends.[248] However, the focus of this review will mostly be directed to copolymer blends.

---

[244] D. R. Paul and C. B. Bucknall, Eds. Polymer Blends. John Wiley & Sons Ltd, New York, 2000, pp. 1217. For example see: (a) JE Yoo and CK Kim *Polym Int.,* **2004**, **53**, 1950-1956; (b) Moon-Sung Kang, Jong Hak Kim, Jongok Won, Seung-Hyeon Moon and Yong Soo Kang, *J. Membr. Sci*. **2005**, 247(1-2), 127-135.

[245] Noshay, A.; McGrath, J. E. Block Copolymers: Overview and Critical Survey; Academic Press: New York, 1977.

[246] Utracki, L.A. Commercial Polymer Blends. Springer – Verlag 1998. Online version available at: http://www.knovel.com/knovel2/Toc.jsp?BookID=878&VerticalID=0

[247] a) A. Rudin, Elements of Polymer Science and Engineering, 2nd Ed., NY, Academic Press, 1999.; b) O. Olabisi, L. M. Robeson, and M. T. Shaw. Polymer-Polymer Miscibility, New York : Academic Press, 1979.

[248] a) Paul, D.R.; Bucknall, C., *Polymer Blends Vol.I. Formulation and Performance* John Wiley & Sons: New York, 1987; b) 189 Katime, I.A.; Iturbe, C.C., in *Polymeric Materials Encyclopedia,* J.C. Salamon, Ed., CRD Press, New York, 1996.

2.2.3.4.2. Sulfonated Copolymer Blends as PEMs in Fuel Cells

2.2.3.4.2.1.Sulfonated Polystyrene Blends

NASA was the first to initiate a crosslinked polystyrene sulfonic acid (PSSA) membrane in a PEMFC as an auxiliary power source in the Gemini program. However this membrane was oxidatively unstable under the system operating conditions.[249] Other forms of crosslinked and/or grafting PS as PEM for fuel cells have also been investigated.[250,251] Unfortunately, the high cost and inferior stability to perfluorinated membranes have fueled alternative routes such as blending to be investigated.[252]

Chen and Hong[253] studied the effect of microspheres of PSSA in blends of poly ethylene oxide and polystyrene. Along with providing proton conductivity, the PSSA could also can enhance the miscibility between PS and PEO without the need of introducing the amine end groups in PEO chains. However, relativity low proton conductivities (10^{-4} S/cm) were obtained from these blends. No comparison to Nafion membranes was reported.

Binary blends of sulfonated poly(2,6-dimethyl-1,4-phenylene) oxide (PPO-SH) and sulfonated polystyrene (PS-SH) with different degrees of sulfonation have also been prepared.[254] Total compatibility was only achieved obtained for the 50/50 blend composition of the PPO-SH and PS-SH both with 30% sulfonation (type III ionomers).

---

[249] Scott, D. S. and Hafele, W. *International Journal of Hydrogen Energy*, **1990**, 15, 727-737.
[250] Buchi, F.N.; Gupta, B.; Haas, O.; Scherer, G.G., *Electrochim. Acta* **1995**, 40, 345-353.
[251] Lehtinen, T.; Sundholm, G.; Holmberg, S.; Sundholm, F, Bjornbom, P.; Bursell, M., *Electrochim. Acta* **1998**, 43, 1881-1890.
[252] Ding, J.; Chuy, C.; Holdcroft, S., *Macromolecules* **2002**, 35, 1348-1355.
[253] L. Hong and N. Chen. *Journal of Polymer Science: Part B: Polymer Physics*, **2000**, 38, 1530-1538.
[254] Canovas, M. J.; Acosta, J. L.; Linares, A. *Macromolecular Chemistry and Physics*. **2005**, 206, 680-688.

The system formed by these two type III ionomers displayed lower water and methanol permeability values than those obtained for commercial Nafion. However, high contents of PS-SH lead to significant membrane deterioration in the presence of methanol and water.

Kim and Jung[255] observed similar trends in the methanol permeability and proton conductivity for the 50/50 composition of sulfonated poly(2,6-dimethyl-1,4-phenylene) oxide (SPPO) and sulfonated polystyrene (SPS) blends. The increase in these values at this composition has been attributed to the greater amorphous portions in the blends that facilitate swelling.

Proton conductive blend membranes of polyvinylidene fluoride and of sulfonated styrene–(ethylene-butylene)–styrene block copolymer (s-SEBS) have been examined.[256] Overall, the sulfonated styrene–(ethylene-butylene)–styrene block copolymer (s-SEBS) and PVDF blends exhibited extremely low IECs (1.8 to 0.59 meq/g) and proton conductivities (3.55×10^{-2} to 1.99×10^{-4} S/cm). The decreases in IEC and conductivity values were directly related to an increase in the PVDF content.

Lopez et al[257] prepared blends of polyvinylidene fluoride (PVDF) with sulfonated polystyrene-*co*-divinylbenzene in salt (PS-co-DVB-SO_3Na) or acid form (PS-co-DVB-SO_3H). The value of the PVDF/ PS-co-DVB-SO_3H blend exhibited IECs three times greater than Nafion 117. An enhancement in the permselectivity in higher concentrations of hydrochloric acid was also observed.

[255] Bokyung Kim, Bumsuk Jung. *Macromolecular Rapid Communication*. **2004**, 25, 1263-1267.
[256] A. Mokrini and M.A. Huneault. *J. Power Sources* **2006**, 154, 51-58.
[257] Lopez, M. L.; Compan, V.; Garrido, J.; . Riande, E.; and Acosta, J. L. *J. Electrochem. Soci.* **2001**, 148, E372-E377.

2.2.3.4.2.2.Sulfonated Perfluorinated Copolymers Blends

As previously stated, limitations of many perfluorinated membranes in PEMFC such as high methanol permeability and high cost has stimulated the development of alternative materials. Currently, research into perfluorinated copolymers blends with various other polymers has gained attention in an effort to control these problems. Blends of perfluorinated copolymers have been investigated primarily for DMFC because incorporation of these copolymers may not only lead to improvement in fuel efficiency but reduce interfacial resistance and improve adhesion to commercially available Nafion® electrodes.

Cho et al [258] investigated blends of vinylidene fluoride-hexafluoropropylene copolymer (P(VdF-co-HFP)) and Nafion in order to reduce the methanol crossover and the cost with retaining essential proton conductivity. Although, the methanol permeabilities of the blends were reduced with increasing P(VdF-co-HFP)) content, higher methanol uptake than that of the native Nafion was obtained for the blends. Further research by this group showed that the coating a Nafion membrane with poly(vinylidene fluoride) copolymer/Nafion blend resulted in a reduction in methanol cross-over and an enhanced cell performance due to improved compatibility with the electrodes.[259]

[258] Cho, K.Y.; Eom, J. Y.; Jung, H.Y.; Choi, N.S.; Lee, Y. M.; Park, J. K.; Choi, J. H.; Park, K. W.; Sung, Y. E. *Electrochimica Acta* **2004**, 50, 583-588.
[259] Cho, K.Y.; Jung, H.Y.; Choi, N.S.; Sung, K. A.; Kim, W. K.; Sung, S.J.; Park, J. K.; Choi, J. H.; Park, K. W.; Sung, Y. E. *Solid State Ionics* **2005**, 176, 3027-3030.

A laminated composite Nafion–Nafion/ polyvinylene difluoride (PVdF)–Nafion polymer electrolyte membrane has been prepared by Kim et al.[260] The membranes formed by blending and hot pressing, exhibited decreased methanol crossover with increased PVDF content.

J. Lin et al[261] also attempted to blend Nafion with small amount of vinylidene fluoride-hexafluoropropylene copolymer (P(VdFco-HFP)). A sharp drop in the proton conductivity by around two orders of magnitude compared with native Nafion membrane was observed even though the amount of the Nafion content in the blends was large.

Blends of perfluorinated polymers with high performance polymers such as PBI have also been investigated.[262] These blends take advantage of the acid-base interaction between the sulfonic acid group in Nafion and the imidazole nitrogen in PBI (Figure 25). Although water swelling decreased from 0.44 to 0.15 with only 8 wt% incorporation of PBI into Nafion, a decrease in proton conductivity was also observed. Increasing the PBI content in the blended membrane also increased the ohmic resistance resulting in decreased DMFC performance.

A reduction in the proton conductivity, water swelling and methanol permeability was also observed from poly(vinylidene fluoride) (PVDF) and sulfonated poly(ether ether ketone) (SPEEK).[263] As the methanol concentration increased, methanol permeability in the blends was also increased. At 30 vol% methanol concentration the blends became mechanically unstable.

---

[260]Kim, H. J.; Kim, H. J.; Shul, Y.G.; Han, H. S. *J. Power Sources* **2004,** 135, 66-71.
[261] Lin,J.; Ouyang, M.; Fenton, J.M.; Kunz, H.R.; Koberstein, J.T.; Cutlip, M.B. *J. Appli. Polym. Sci.* **1998**, 70, 121-127.
[262] Wycisk, R.; Chisholm, J.; Lee, J.; Lin, J.; Pintauro, P. N. *J. Power Sources* **2006,** 163, 9-17.
[263] Song Xue and Geping Yin. *Polymer* **2006**, 1-6.

2.2.3.4.2.3.Sulfonated Poly(arylene ether) Blends

Blends of sulfonated poly(arylene ethers) with other materials such as polyethersulfone (PES), polysulfone (PSf), or polybenzimidazoles (PBI) have been investigated as candidates for applications in PEMFCs.[264] Typically, many of these studies utilized unsulfonated copolymers to reduce the aqueous swelling of the sulfonated polymer blends[265]. However, it has been well documented that the majority of polymer pairs are thermodynamically immiscible due to small combinational entropy of mixing for high molecular weight copolymers.[266,267] Therefore, many polymer-blend pairs macrophase separate yielding poor adhesion at the interphase of the two polymers.

Manea and Mulder investigated blends of polyethersulfone (PES) with sulfonated polysulfone (SPAU) or sulfonated poly(etheretherketone) (SPEEK).[268] Microphase separation between the hydrophobic PES and the hydrophilic polymers lead to inhomogeneous blends. Nonetheless, these membranes still exhibited methanol permeabilities one to two orders of magnitude lower than Nafion 117 (1.3×10^4 Barrer in 25 % methanol). Therefore these membranes are attractive candidates for DMFC applications. Although this research group further demonstrated that methanol permeability one order of magnitude (2.1×10^3 Barrer) lower than Nafion could also be obtained for a PBI/SPSU (2:8) blend, these values were still higher than the previous PES/SPSU blends (1.7×10^3 Barrer).[269]

---

[264] Jochen Kerres. *J. Membr. Sci.* **2001**, 185, 3-27.
[265] K.D. Kreuer. *J. Membr. Sci.* **2001,** 185, 29-39.
[266] Charoensirisomboon, P., Inoue, T., Solomko, S.I, Sigalov, G.M., Weber, M. *Polymer* **2000**, 41 7033-7042.
[267] Tucker, R.T.; Han, C.C.; Dobrynin, A.V.; and Weiss, R.A. *Macromolecules* **2003**, 36, 4404-10.
[268] Carmen Manea and Marcel Mulder. *J. Membr. Sci.* **2002**, 206, 443-453.
[269] Carmen Manea and Marcel Mulder. *Desalination* **2002**, 147, 179-182.

Bowen et al[270] reported that miscible PES/SPEEK blends were achieved at polymer weight ratios of 0.02 – 40 wt% of SPEEK. The solution, containing 20wt% total polymer in NMP, remained homogenous at room temperature for at least two months. Lower miscibility was observed for blend solutions of PSU/SPEEK which became turbid after only two weeks when the weight ratio was increased to 0.25 wt%.

Miscible blends based on sulfonated poly(ether ketone ketone) (SPEKK) and PES (85/15 wt%) were prepared by Swier et al.[271] The increased miscibility between the two polymers which initially proved to be interfacially inhomogeneous was attributed to the excellent solvent properties of DMAc. The absence of strong specific interactions (hydrogen bonding or acid-base interaction) between the polymers was responsible for the polymers' incompatibility. Compared to neat SPEKK membranes, the blend exhibited reduced membrane swelling and increased membrane stability in the fuel cell environment.

Miscible blends of SPEKK/polyetherimide (PEI) blends were also prepared, however, limited solubility due to increased IEC (>0.8 meq/g) and higher degrees of sulfonation typically resulted in heterogeneous morphologies.[272] The absence of interfacial mixing and low mobility of both components at temperature above 200 °C resulted in no morphological changes to these blends.

Improvements to copolymer-copolymer miscibility can be achieved by promoting intermolecular interactions such as hydrogen bonding, dipole-dipole interaction, acid-

[270] Bowen, R. W.; Doneva, T. A.; and Yin, H. B. *J. Membr. Sci.* **2001**, 181, 253-263.
[271] Swier, S.; Ramani, V.; Fenton, J.M.; Kunz, H.R.; Shaw, M. T.; and Weiss, R.A. *J Membr. Sci* **2005**, 256, 122-133.
[272] Swier, S.; Shaw, M. T.; and Weiss, R. A.. *J. Membr. Sci.* **2006**, 270, 22-31.

base interactions, and covalent crosslinking.[267] As the bond strength of each interaction becomes stronger the polymer miscibility may be increased.

Kerres and colleagues [273] have conducted comprehensive studies on these interactions and their effects in various blends of sulfonated poly(arylene ether sulfone)s (SPAES)or sulfonated poly(ether ether ketone)s (SPEEK).

Blends comprised of sulfonated PSU (PSU-SO_3H) with unfunctionalized PSU UDEL® produced inhomogeneous, nontransparent membranes with poor mechanical stability and extremely low IEC's.[206a] Blend microphase separation was still apparent after hydrolysis when nonionic precursors (PSU-SO_3Cl, PSU-SO_3CH_3 or PSU-SO_3NH_2) of PSU-SO_3H were blended with unmodified PSU. The incompatibility was attributed insufficient entanglements between the polymers due to weak Van der Waals and dipole-dipole interactions. Furthermore, blends of unmodified PSU and PSU-SO_3CH_3 or PSU-SO_3NH_2 displayed excessive swelling or could not be hydrolyzed in sulfonic acid groups, respectively.

Cui, Kerres, and Eigenberger [274] also investigated blends of SPEEK with polysulfone UDEL®-ortho-sulfone-diamine (PSU-NH_2), polyamide PA Trogamid P, or poly(etherimide) PEI Ultem. Hydrogen bonding between the polymers was used to obtain miscible blends illustrated by single T_gs 5-20 K higher than SPEEK. However, blends of SPEEK and polyamide PA Trogamid P or poly(etherimide) PEI Ultem exhibited excessive swelling at elevated temperatures and decreased hydrolytic instability of the PA amide bonds and the PEI imide bonds in acidic conditions. Although

[273] a) Zhang, W.; Tang, C.-M.; and Kerres, J. *Separation and Purification Technology* **2001**, 209,22-23; b) Walker, M.; Baumgärtner, K.-M.; Kaise, M. Kerres, J.; Ullrich, A.; Räuchle, E. *J. Appli. Polym. Chem.* **1999**, 74, 67-73; c) Jochen A. Kerres. *J. Membr. Sci.* **2001**, 185, 3-27.
[274] Cui, W.; Kerres, J.; and Eigenberger, G. *Separation and Purification Technology* **1998**, 14, 145-154.

PEEK/PSU-NH_2 blends exhibited good proton conductivities, these values were still lower than the PA or PEI blends due to the polysalt formation which partial block the SO_3^- groups required for transport.

The drawbacks associated with the previous blends have lead these researchers to investigate more strongly bonded, acid–base blend systems from sulfonated poly(ether ether ketone) or poly(arylene ether sulfone) with different kinds of basic polymers, such as polybenzimidazole, aminated polysulfone (PSU-NH_2), poly(4-vinylpyridine), and polyethylenimine.[275] These acid base blends exhibit specific interactions (H-bonding and salt pairs formation) that increase compatibility between these polymeric materials resulting in high thermal stabilities (270-350 °C) and low swelling ratios.

Short term fuel cell test (maximum 300 h) on the SPSU/PBI blend membranes demonstrated reduced methanol permeability at temperature up to 100 °C and similar cell performance to Nafion 112 in a H_2/O_2 fuel cell. Additionally, membranes containing PBI proved to be the most mechanically stable under fuel cell operating conditions. In general, however, frequent delamination of these membranes from the catalyst layer led to higher cathode humidification being required to obtain optimum performance than Nafion based membrane electrode assemblies.[276]

Diemede et al[277] studies of PBI/SPSU blends also showed that these blends displayed excellent miscibilities. However, these researchers found that miscibility was dependent on the PBI ratio and the degree of sulfonation of SPSU in the blend. Higher degrees of sulfonation (20 and 44 %) and larger PBI ratios exhibited broad T_gs in region

[275] Kerres, J.; Ullrich, A.; Meier, F.; Haring, T. *Solid State Ionics* **1999**, 125, 243-249.
[276] Jorissen, L.; Gogel, V.; Kerres, J.; Garche, J. *J. Power Sources* **2002**, 105, 267-273.
[277] Diemede, V.; Voyiatzis, G.A.; Kallitsis, J.K.; Qingfeng, L.; Bjerrum, N.J. *Macromolecules* **2000**, 33, 7609-7617.

between those of the pure polymers indicating enhanced miscibility. Increasing the PBI content in the blend also shifted the T_gs to higher temperatures.

Further research on the effect of doping levels of phosphoric acid of PBI/SPSU blend membranes was also conducted.[278] It was observed that blends with lower degrees of sulfonation and higher PBI content yielded higher doping levels. These doping levels were increased at higher temperatures but degradation of the membrane due to the presence of higher PBI concentration was observed.[279] Moreover, durability test of the impregnated membranes showed that a weight loss of 25-35 % of H_3PO_4 (85 %) was observed within 10 h. This weight loss remained stable for several days. In all cases the blends demonstrated conductivities greater than 2×10^{-2} S/cm. These values increased as function of temperature and doping levels. For the doping level of $\geq$ 1000 % the conductivity of the blend at 80 °C relative humidity was comparable (7×10^{-2} S/cm) or higher (2.1×10^{-1} S/cm) than Nafion which shows conductivities of 7×10^{-2} S/cm and 1.7×10^{-1} S/cm at 80 and 100 °C, respectively. However, at these doping levels the membranes become mechanically instable (soften).

Kerres et al[280] have also prepared a group of novel basic polymers via lithiation reactions of PSU followed by subsequent reactions with aromatic ketone, aldehydes, or carboxylic ester groups. Blends of these polymers with SPEEK displayed good proton conductivity and good thermal stabilities, though complete molecular miscibility, was not observed as in the previous blends,

[278] Hasiotis, C.; Diemede, V.; Kontoyannis, C. *Electrochimica Acta* **2001**, 46, 2401-2406.
[279] Hasiotis, C.; Qingfeng, L.; Diemede, V.; Kallitsis, J.K.; Kontoyannis, C.; Bjerrum, N.J. *J. Electrochem. Soc.* **2001**, 148(5), A513-A519.
[280] J. Kerres and A. Ullrich. *Separation and Purification Technology* **2001**, 1, 22-23.

Covalently crosslinked blend membranes from polyaryl sulfinates and polyaryl sulfonates where the sulfinate groups were crosslinked by alkylation with ,4-diiodobutane and ionically cross-linked blend membranes polyaryl sulfonates and PBI or basic PSUs have also been synthesized.[281] In addition to high proton conductivities and decreased membrane swelling, these membranes also exhibited DMFC performance comparable to Nafion 105 although the connection between the blend membranes and electrodes was rather poor. Significantly lower methanol permeation rates were also observed.

More recently these researchers investigated the effect of inorganic particles (SiO_2)[281] and two heteropolyacids[282] to these blends. Kerres et al showed that ionically cross-linked hydrocarbon membranes which has been filled with a highly disperse siliconium dioxide that inhibits methanol permeability but displayed fuel cell performance comparable to Nafion 105. However, the inferior adhesion of these polymers to Nafion electrodes resulted in discontinuity in the ion path and decreased cell longevity due to delamination between the hydrocarbon based PEM membranes from the Nafion electrode.

The two heteropolyacids, monobdophosphoric acid $H_3PMo_{12}O_40 \cdot xH_20$ (MPA) and tungstophosphoric acid $H_3PW_{12}O_40 \cdot xH_20$ (TPA) were added to blend of sulfonated poly(ether ketone) and PBI in an attempt to reduce the specific H^+ resistance. Instead, increased swelling and decreased IEC values were associated with TPA incorporation while a blue discoloration occurred when MPA was used. Both TPA and MPA leached out of the membrane when subjected to aqueous post treatments.

[281] Kerres, J.; Zhang, W.; Ullrich, A.; Tang, C.-M.; Hein, M.; Gogelb,V.; Freyb, T.; Jorissen, L.*Desalination* **2002**, 147, 173-178.
[282] Kerres, J.; Tang, C.-M.; Graf, C. *Ind. Eng.Chem. Res.* **2004**, 43, 4571-4579.

CHAPTER 2. HYDROCARBON AND PARTIALLY FLUORINATED SULFONATED COPOLYMER BLENDS AS FUNCTIONAL MEMBRANES FOR PROTON EXCHANGE MEMBRANE FUEL CELLS

Natalie Y. Arnett,[a] William L. Harrison,[b] Anand S. Badami,[a] Abhishek Roy,[a] Ozma Lane,[a] Frank Cromer,[a] Limin Dong,[c] and James E. McGrath[a]

[a]Department of Chemistry, Virginia Polytechnic Institute and State University, Blacksburg, VA 24061, USA

[b]NanoSonic, Inc, 1485 South Main Street, Blacksburg, Va. 24060

[c]deceased

Reprinted from "*Journal of Power Sources* **2007,** 172, 20–29." with permission from Elsevier.

To whom correspondence should be conducted: *jmcgrath@vt.edu, Tel: 540-231-5976

Fax: 540-2318517

Abstract

Polymer blending is recognized as a valuable technique used to modify and improve the mechanical, thermal, and surface properties of two different polymers or copolymers. This paper investigated the solution properties and membrane properties of a biphenol-based disulfonated poly (arylene ether sulfone) random copolymer (BPS-35) with hexafluoroisopropylidene bisphenol based sulfonated poly (arylene ether sulfone) copolymers (6FSH) and an unsulfonated biphenol-based poly (arylene ether sulfone)s. The development of blended membranes with desirable surface characteristics, reduced water swelling, and similar proton conductivity are presented.

Polymer blends were prepared both in the potassium salt forms from N, N-dimethylacetamide (DMAc). Water uptake, specific conductivity, thermogravimetric analysis (TGA), differential scanning calorimetry (DSC), and contact angles were used to characterize the blended films. Surface enrichment of the fluorinated component is illustrated by an significant increase in the water-surface contact angle was observed when 10wt% 6FBPA-00 (106^{o}) was added to BPS 35 (80^{o}). Water weight gain was reduced by a factor of two.

Keywords: Poly(arylene ether sulfone) (PAES); Copolymer blends; Radel®; Nafion®; Proton exchange membrane fuel cell (PEMFC)

1. Introduction

Proton exchange membrane fuel cells (PEMFCs) are being investigated worldwide as alternative energy devices for applications in stationary, automotive, and portable power.[283,284,285] PEMFCs convert chemical energy directly into electrical energy using a series of electrochemical redox reactions.

To date perfluorinated sulfonic acid copolymers, such as Nafion® produced by DuPont, have been the most widely studied proton exchange membranes (PEMs) in fuel cells. Drawbacks of many perfluorinated membranes include high cost,[286] limited operation temperature (<100ºC).[287] In addition, high methanol permeability limits usage in direct methanol fuel cells (DMFCs).[288] Therefore, many alternative nonfluorinated and partially fluorinated membranes that exhibit comparable performance to perfluorinated polymers have been investigated. These materials are potentially less expensive, have higher operation temperatures, and lower methanol permeabilities.[289,290]

Poly(arylene ether sulfone)s represent a promising group of alternative PEMs for direct methanol and hydrogen/air fuel cells. A series of sulfonated poly(arylene ether

[283] Zalbowitz, M.; Thomas, S. "Fuel Cells: Green Power," Department of Energy, 1999 LA-UR-99-3231.
[284] Dhathathreyan, K.S.; Sridhr, P.; Sasikumar, G.; Ghosh, K.K.; Velayuthan, G.; Rajalakshmi, N.; Subramaniam, C.K.; Raja, M.; Ramya, K., *Int. J. Hydrogen Energy* **1999,** 24, 1107-1115.
[285] Korgesch, K.; Simader, G., Fuel Cells and Their Applications, Wiley-VCH, Weinheim, 1996.
[286] Pourcelly, G.; Gavach, C. In Proton Conductors; Colomban, P., Ed.; Cambridge University Press: London, 1992; pp. 295.
[287] M.K. Daletou, N. Gourdoupi, J.K. Kallitsis, *J Membr Sci.* **2005**, 252, 115-122.
[288] C. Manea, M. Mulder, *J Membr Sci.,* **2002**, 206, 443-453.
[289] M. A Hickner, H. Ghassemi, Y. S. Kim, B. R. Einsla, J.,E. McGrath, *Chem. Rev*., **2004**,104, 4587-4612
[290] a) A. Roy, M. A. Hickner, X. Yu, Y. Li, T. E. Glass, J. E. McGrath, J. Poly. Sci. Part B: Poly Phys, **2006**, 44, 2226-2239; b) O. Olabisi, L. M. Robeson, and M. T. Shaw. Polymer-Polymer Miscibility, New York: Academic Press, 1979.

sulfone) copolymers have been reported by McGrath et al.[291][292] The high molecular weight sulfonated copolymers exhibit excellent film forming behavior, high glass transition temperatures, and proton conductivities greater than 0.1 S/cm. Previous research [293] has shown that aromatic membranes displayed fuel cell performance comparable to Nafion. However, the adhesion of these polymers to DMFC Nafion electrodes was inferior. This produces undesirable high frequency resistance (HFR) and decreased cell longevity due to delamination between the hydrocarbon based PEM membrane and the Nafion electrode.[294]

Polymer blends are recognized as a valuable means to combine the properties of two different polymers.[295,296] Polymer blending improves many characteristics including impact strength, thermal behavior, and surface character.[297] Advantages of polymer blending may include reduction of cost since synthesis of new polymers is not required to obtain novel materials, improved processability of high temperature thermoplastics, and improved mechanical properties. [298] Furthermore, due to the different possible microstructures within the blend, the surface composition can be significantly different

[291] W.L. Harrison,; F. Wang, J.B Mecham, V.A. Bhanu, M. Hill, Y. S. Kim, J. E. McGrath, *J Polym Sci Part A: Polym Chem*., **2003,** 41, 2264-2276.
[292] F. Wang, M. Hickner, . Y.S. Kim, T. A. Zawodzinski, J. E. McGrath, *J. Membr. Sci*., **2002,** 197, 231-242.
[293] J. Kerres, W. Zhang, A. Ullrich, C. M. Tang, M. Hein, V. Gogel, T. Frey, L Jörissen,. *Desalination* **2002**, 147, 173-178.
[294] M.S. Wilson, Membrane catalyst layer for fuel cells, US Patent 5211984, 1993.
[295] D. R. Paul and C. B. Bucknall, Eds. Polymer Blends. John Wiley & Sons Ltd, New York, 2000, pp. 1217.
[296] For example see: (a) JE Yoo and CK Kim *Polym Int.,* **2004**, 53, 1950-1956; (b) Moon-Sung Kang, Jong Hak Kim, Jongok Won, Seung-Hyeon Moon and Yong Soo Kang, *J. Membr. Sci.,* **2005**, 247, 127-135.
[297] A. Noshay, J. E. McGrath, Block Copolymers: Overview and Critical Survey; Academic Press, New York, 1977.
[298] A. Rudin, Elements of Polymer Science and Engineering, second ed., Academic Press, New York, 1999; b) O. Olabisi, L. M. Robeson, and M. T. Shaw. Polymer-Polymer Miscibility, Academic Press, New York, 1979.

from the bulk. This possibility can be desirable as in the case of blends of fluorinated polymers due to their hydrophobic surface properties.[299]

Blends of sulfonated poly(arylene ether) with polyethersulfone (PES), polysulfone (PSf), or polybenzimidazoles (PBI) have been investigated as potential candidates for applications in PEMFCs.[300] Typically, many of these studies utilized unsulfonated copolymers to reduce the aqueous swelling of the sulfonated polymer blends.[301] However, it has been well documented that the majority of polymer pairs are thermodynamically immiscible.[302] Therefore, many polymer-blend pairs macrophase separate yielding poor adhesion at the interphase of the two polymers.

Manea and Mulder investigated blends of polyethersulfone (PES) with sulfonated polysulfone (SPAU) or sulfonated poly(etheretherketone) (SPEEK).[288] Phase separation between the hydrophobic PES with the hydrophilic polymers lead to undesirable inhomogeneous blends.

Bowen et al[303] reported that miscible PES/SPEEK blends were achieved at polymer weight ratios of 0.02 – 40 wt% of SPEEK. The solution, containing 20wt% total polymer in NMP, remained homogenous at room temperature for at least two months. Lower miscibility was observed for blend solutions of PSU/SPEEK which became turbid after only two weeks when the weight ratio was increased to 0.25 wt%.

[299] P. Charoensirisomboon, T. Inoue, S.I Solomko, G.M. Sigalov, M. Weber, *Polymer* **2000**, 41, 7033-7042.
[300] a) S. Swier, V. Ramani, J.M. Fenton, H.R. Kunz, M. T. Shaw, and R.A. Weiss, J Membr. Sci., 256 (2005) 122-133. b) W. Cui, J. Kerres, G. Eigenberger, *Sep. Purif. Technol.*, **1998**, 14, 145-154.
[301] K.D. Kreuer. *J. Membr. Sci*., **2001**, 185, 29-39.
[302] D. Gan, W. Cao, Z. Wang, *J Fluor. Chem.* **2002**, 116, 59-63.
[303] R.W. Bowen, T. A. Doneva, H. B. Yin, *J. Membr. Sci*., **2001**, 181, 253-263.

Blends based on sulfonated poly(ether ketone ketone) SPEKK/polyetherimide (PEI) and SPEKK/PES (85/15 wt%) and have been prepared by Swier et al.[304] SPEKK/polyetherimide (PEI) blends displayed limited solubility due to increased IEC (>0.8 meq/g) and higher degrees of sulfonation typically resulted in heterogeneous morphologies. On the other hand, SPEKK/PES blends which initially proved to be interfacially inhomogeneous, exhibited increased miscibility between the two polymers in DMAc. The absence of strong specific interactions (hydrogen bonding or acid-base interaction) between the polymers was responsible for the polymers' incompatibility in the solid state.

Improvements to copolymer-copolymer miscibility can be achieved by promoting intermolecular interactions such as hydrogen bonding, dipole-dipole interaction, acid-base interactions, and covalent crosslinking.[267] Kerres and colleagues[305] have conducted comprehensive studies on these interactions and their effects in various blends of sulfonated poly(arylene ether sulfone)s (SPAES)or sulfonated poly(ether ether ketones)s (SPEEK). These researchers determined that increasing the bond strength of each interaction between the blend components led to increased copolymer-copolymer miscibility.

This paper reports the development of fluorinated and non-fluorinated directly copolymerized poly(arylene ether sulfone) random copolymers blended membranes with desirable surface characteristics and reduced water swelling).

---

[304] a) S. Swier, M. T. Shaw, R. A.. Weiss,. *J. Membr. Sci.*, **2006**, 270, 22-31; b) S.; Swier, V. Ramani, J.M. Fenton, H.R. Kunz, M. T. Shaw, R.A. Weiss, *J Membr. Sci*, **2005**, 256, 122-133.

[305] a) W. Zhang, C.-M. Tang, J. Kerres, *Separation and Purification Tech.,* **2001**, 209, 22-23; b) M. Walker, K.-M. Baumgärtner, M. Kaise, J. Kerres, A. Ullrich, E. Räuchle, J. Appl Polym. Chem., 74 (1999) 67-73; c) J.A. Kerres. *J. Membr. Sci.,* **2001**, 185, 3-27.

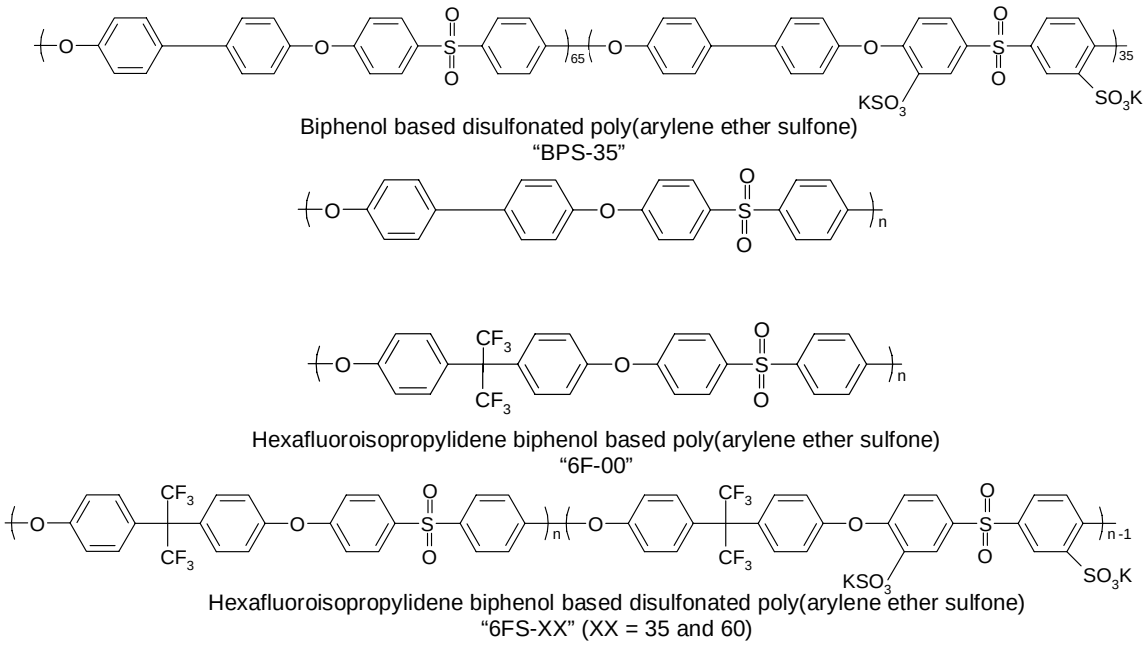

Figure 2-1 Chemical structures of the directly copolymerized poly(arylene ether sulfone) disulfonated random copolymers utilized.

2. Experimental

2.1. Materials

4,4'-Hexafluoroisopropylidenediphenol (6F BPA), received from Ciba, was purified by sublimation and dried under vacuum. Eastman Chemical provided high purity 4,4'-biphenol (BP) which was dried at 50 ºC under vacuum before each use. Solvay Advanced Polymers supplied highly purified 4,4'-dichlorodiphenylsulfone (DCDPS) and polyphenylene sulfone (Radel®). 4,4'-Dichlorodiphenylsulfone was dried at 60 ºC under vacuum before each use. N-Methyl-2-pyrrolidinone (NMP) (Aldrich) was

vacuum distilled from calcium hydride onto molecular sieves, then stored under nitrogen. N,N-Dimethylacetamide (DMAc) (Aldrich) was distilled under vacuum from phosphorous pentoxide and stored over molecular sieves under nitrogen. Potassium carbonate was vacuum-dried at 150 ºC prior to polymerization. Toluene obtained from Aldrich was used as received. The detailed synthesis of 3,3'-disulfonate-4,4'-dichlorodiphenylsulfone monomer (SDCDPS) has been reported.[291]

2.2. Copolymer Synthesis by Direct Copolymerization

Similar copolymerization procedures were used to synthesize BP or 6F BPA copolymers.[306] A typical copolymerization for the sulfonated copolymers is described using the 6FS-60 system. First, 6F-BPA (1.8494 g, 5.5 mmol), DCDPS (0.6318 g, 2.2 mmol), and SDCDPS (1.6211 g, 3.3 mmol) were added to a 3-neck flask equipped with an overhead mechanical stirrer, nitrogen inlet and a Dean-Stark trap. Potassium carbonate (0.8707 g, 6.3 mmol), and DMAc (18 mL) were introduced to afford a 20% (w/v) solids concentration. Toluene (usually DMAc/Toluene = 2/1, v/v) was used as an azeotroping agent. The reaction mixture was refluxed at 150 ºC for 4 h to dehydrate the system. The temperature was raised slowly to 190 ºC by controlled removal of the toluene. The reaction was allowed to proceed for 30 h or until a viscous solution was observed. The solution was cooled to room temperature and the copolymer was isolated by coagulation in stirring deionized water. The precipitate was stirred overnight at 60 ^{o}C to remove most of the salts. The copolymer was then collected by vacuum filtration and dried in a vacuum oven at 120 ºC for 24 h. Similar procedures with appropriate

[306] W.L. Harrison, M. Hickner, Y.S. Kim, J.E. McGrath. *Fuel Cells*, **2005,** 5, 201-212.

monomers and comonomer ratios were used to prepare the BPS-35, 6FS-35 and the 6F-00 copolymers and have been previously reported.[307,308]

2.3. Polymer Blending and Membrane Acidification

Separate solutions of the copolymers at different weight ratios with a total combined solution concentration of 5% w/v were prepared in DMAc. The 6F copolymer solutions were added to BPS-35 solutions and stirred at 80 ºC for 1 h. Solutions were hot filtered through a 0.45 μm PTFE filter onto clean glass substrates. The membranes were dried gradually via a heating lamp with increasing intensity for 24 h and then under vacuum at 100 °C for 24 h. The copolymer blend membranes in the potassium salt form were converted to the acid form by first boiling in 0.5 M H_2SO_4 for 2 h and immediately followed by extraction in boiling deionized water for 2 h described in earlier studies as "Method 2".[309]

2.4. Characterization

2.4.1. ^{1}HNMR

[307] Wang, F.; Hickner, M.; Ji, Q.; Harrison, W.; Mecham, J.; Zawodzinski, T. A.; McGrath, J. E. *Macromol Symp.*, **2001**, 175, 387.
[308] Kim, Y. S.; Wang, F.; Hickner, M.; Zawodzinski, T. A.; McGrath, J. E. *J. Membr. Sci.*, **2003**, 212, 263-282.
[309] Y.S. Kim, F. Wang, M. Hickner, S. McCartney, W.L. Harrison, Y.T. Hong, T.A. Zawodzinski, and J.E. McGrath, *J. Polym. Sci., Part B: Polym. Phys.*, **2003**, 41, 2816-2828.

^{1}H NMR analysis was conducted on a Varian Unity 400 spectrometer to determine monomer purity and degree of sulfonation in the copolymers. All spectra were obtained from a 10% solution (w/v) in a DMSO-d_6 solution at room temperature.

2.4.2. Intrinsic Viscosity

The intrinsic viscosities were determined in NMP with 0.05 M lithium bromide (LiBr) at 25 °C with an Ubbelohde viscometer (0.05 M). LiBr was used to control ionic aggregates associated with the sulfonated copolymers and minimize the ionic effect.

2.4.3. Fourier Transform Infrared (FTIR) Spectroscopy

FTIR spectra were recorded on a Brunker Tensor 27 FTIR Spectrometer using thin polymer films in the acid form. The samples were dried at 100-110 ^{o}C for up to 48 hours before collecting the spectra. All spectra were measured at a resolution of 2 cm^{-1} and represent the average of 32 scans.

2.4.4. Turbidity Measurements

The clarity of the blended membranes was obtained from qualitative visual observations. The blended membranes were characterized in both the salt and acid forms to understand the effect of hydrothermal treatment (Method 2 acidification).

2.4.5. Aqueous Potentiometric Titrations

Aqueous potentiometric titrations were carried out on a Schott Instruments TA20 plus titration unit for ion-exchange capacities measurements of the blended membranes. The acidified membrane was placed in a concentrated 1M solution of sodium sulphate and stirred for 24 hrs. The solution was then titrated with a standard sodium hydroxide solution at 0.02 mL/second and potential stretches from simple endpoint titrations were recorded.

2.4.6. Water Uptake

The water uptake of the blended membranes was performed by immersing the membranes in deionized water at room temperature for 24 h. The wet membranes were then blotted to remove surface water droplets and quickly weighed. These membranes were then vacuum dried at 90 ºC for 24 h and weighed again. The water uptake (%) of the membranes was calculated by:

$$WaterUptake = \frac{W_{wet} - W_{dry}}{W_{dry}} \times 100\% \qquad 1$$

where W_{wet} is the weight of the wet membrane and W_{dry} represents the weight of the dry membrane.

2.4.7. Proton Conductivity

A Solartron (1287 + 1252) impedance/gain phase was used to measure the proton conductivity of each film in the acid form over a frequency range of 10 Hz to 1 MHz under fully hydrated conditions. The resistance of each film was measured at ~25 ^{o}C using the conductivity cell.[290a]

2.4.8. Thermogravimetric Analysis (TGA)

The thermooxidative stabilities of the membranes (10 – 15 mg) were determined using a TA Instruments TGA Q 500. Both the salt and acid form blended membranes were vacuum dried at 100 ^{o}C for 12 h prior to analysis. Before TGA characterization the membranes were placed in the TGA furnace at 150 ^{o}C in a nitrogen atmosphere for 30 minutes. The samples were evaluated over the range of 30 to 700 ^{o}C at a heating rate of 10 ^{o}C/min in air.

2.4.9. Differential Scanning Calorimetry (DSC)

The glass transition temperatures (T_g) of the films were obtained on a TA Instrument DSC Q 1000. Scans were conducted under nitrogen at a heating rate of 10 ^{o}C/min. Second heat T_g values are reported as the midpoints of the changes in the slopes of the baselines.

2.4.10. Dynamic Mechanical Analysis (DMA)

Membranes were cut into dogbones with length of 20 mm, width of 4 mm, and thickness ranging between 0.05 to 0.1 mm and analyzed on a DMA 2980 instrument. The dogbone samples were placed in vacuum oven for 24 hours at 120ºC to extract excess water. The dogbones were then placed in thin film tension clamps tested between 100 to 300 ºC at 1 Hz.

2.4.11. Contact Angles

The "instantaneous" (1-5 sec) contact angle measurements were obtained on a Ten Angstroms (FTA 32) instrument that utilized the sessile-drop method. Contact angle was a quantitative method used to determine the hydrophobicity or hydrophilicity of the film surface. Deionized water was dropped on the surface of the membranes at room temperature and the contact angle of the drops was determined. Measurements were carried out on both the air/membrane interface and the membrane glass interface.

2.4.12. Tapping Mode Atomic Force Microscopy (TP-AFM)

Tapping Mode Atomic Force Microscopy (TP-AFM) images of the blends were obtained using a Digital Instruments MultiMode scanning probe microscope with a NanoScope IVa controller. A silicon probe (Veeco) with an end radius of <10 nm and a force constant of 5 N/m was used to image samples. Samples were dried under vacuum at 100 °C for 12 h and then equilibrated at 50% relative humidity for at least 12 h before

being imaged immediately at room temperature in a relative humidity of approximately 15-20%.

2.4.13. X-ray Photoelectron Spectroscopy (XPS)

Samples for XPS were placed under vacuum at 80 ºC for 24 h and then placed in a sealed container at room temperature before characterization. Samples were kept under vacuum in a Perkin Elmer 5400 X-ray photoelectron spectrometer (XPS) at room temperature for 1 h before they were analyzed for surface fluorination. A magnesium filament with a 13 kV source and 0.100 eV broad scan/0.025 eV narrow scan resolution was used in all acquisitions. Samples were oriented to achieve an electron take-off angle of 45º corresponding to a sampling depth of 5 nm.

3. Results and Discussion

Two series of copolymers have been synthesized via nucleophilic aromatic step or polycondensation reactions. Biphenol and 6F BPA were, respectively, reacted with DCDPS and SDCDPS in NMP in the presence on potassium carbonate. The copolymer compositions and degrees of sulfonation were controlled by varying the molar stoichiometries of the DCDPS and SDCDPS. An example of preparation of poly(arylene ether sulfone) polymer and copolymers is described below (Figure 2-2). The unsulfonated and sulfonated copolymers produced ductile transparent films from DMAc on glass plates.

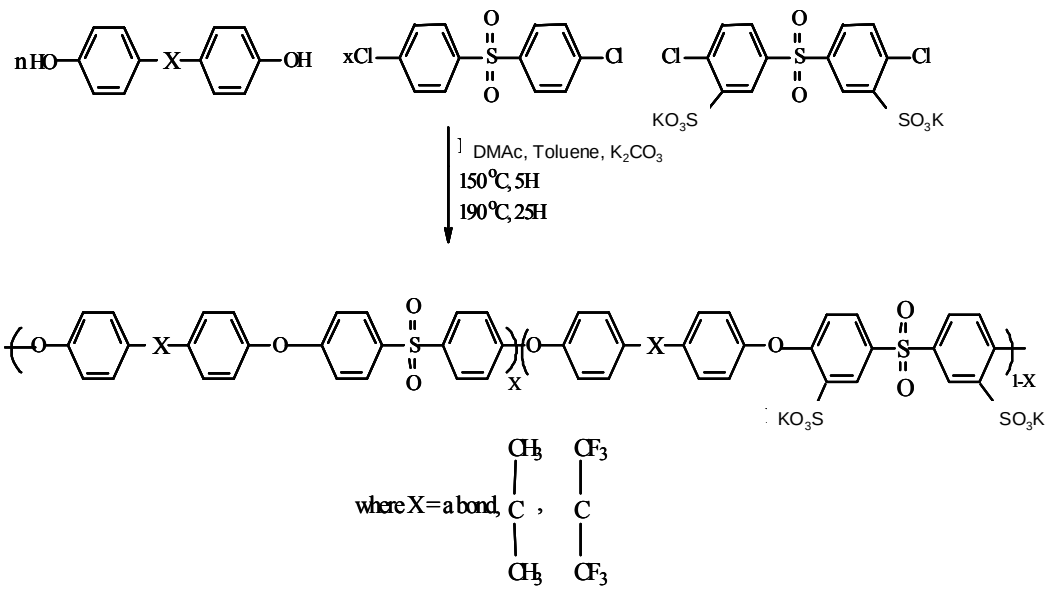

Figure 2-2. Sample synthesis of disulfonated poly(arylene ether sulfone) copolymers via direct copolymerization

NMR and FTIR were essential tools to investigate the sulfonated poly(arylene ether sulfone) copolymers structural compositions and functional groups. Proton NMR integration was utilized to confirm successful incorporation of the 60 or 35 mol% SDCDPS comonomer into the copolymers. The sulfonation values for the copolymers used and their intrinsic viscosities are recorded in Table 2-1. All degrees of disulfonation determined by ^{1}H NMR was in good agreement with the molar feed ratios of SDCDPS, which verifies incorporation of the sulfonated comonomer into the copolymers.

Table 2-1 Summary of general characteristics of polymers and copolymers used to prepare blends

Copolymer Composition	***IV***	***Degree of Sulfonation***
Radel®	0.6	0

BPS-35	1.1	35
6F-00	0.6	0
6FS-35	0.57	35
6FS-60	0.45	60

Tough, ductile polymer blend membranes were obtained from DMAc solutions. BPS-35 was blended with various weight percentages of the unsulfonated partially fluorinated polymer (6F-00), or the partially fluorinated copolymers, 6FS-35 or 6FS-60, containing 35 or 60 mol% of SDCDPS respectively. Higher weight fractions (> 10 wt%) of these polymers into BPS-35 initially resulted in microphase separation which was determined by DSC. Visible macrophase separation was seen above 20 wt%. Therefore, low weight percentages (0-10 wt%) of the blends were investigated to eliminate the possibility of phase separation. Blends of commercially available polyphenylene sulfone (Radel®) with BPS-35 were also prepared to evaluate the effect of the unsulfonated polymer on the water uptake of membranes. The films were analyzed in both the salt and acidified form

3.1. Turbidity and optical clarity

The optical clarity of the membranes was inspected visually as a preliminary means of identifying compatibility between the polymers. Observation of clarity and miscibility of salt and acid form membranes are listed in Table 2-2. Low weight percentages (0-5 wt%) of the 6F moiety in BPS-35 resulted in transparent films. As the amounts of 6F polymers or copolymers were increased to 10 wt%, some hazing on the outer edges of the membranes in the salt form was observed. The addition of 5 to 10 wt% of Radel into the blends yielded cloudy membranes. Higher ratios (> 10 wt%) of 6F

moieties and Radel into the blends resulted in opaque films with large regions of *macrophase* separation.

The clarity of the blended membrane after hydrothermal treatment (Method 2 acidification) was also investigated. Previous research has shown that Method 2 acidification of disulfonated PAES membranes lead to the formation of larger hydrophilic domains with more phase continuity.[309] In the polymer blends comprised of 5 wt% of 6F-00 and 6FS-60 in BPS-35, no obvious differences in membrane clarity were observed after being subjected to Method 2 acidification process. The incorporation of 10 wt% of these copolymers in BPS-35 caused the membranes to become cloudy. This cloudiness was also apparent at lower weight percents (5 wt%) of 6FS-35 in the blends. However, blended membranes containing even 5-10 wt% of Radel became transparent after undergoing Method 2 acidification.

Table 2-2. The effect of blend compositions on the optical clarity and appearance of blended membranes in the salt and acid forms

Composition (wt%)	***Optical Clarity (Salt)[a]***	***Optical Clarity (Acid)[b]***
BPS-35	T	T
BPS-35/6F-00		
98/2	T	T
95/5	T	T
90/10	H	C
0/100	T	T
BPS-35/6FS-35		
98/2	T	T
95/5	T	H
90/10	C	C
0/100	T	T
BPS-35/6FS-60		
98/2	T	T
95/5	T	H
90/10	H	H

0/100	T	T
BPS-35/ Radel®		
98/2	T	T
95/5	C	T
90/10	C	T
0/100	T	T

a. The appearance of membrane upon direct release from glass substrate
b. The appearance of membrane after undergoing Method 2 acidification
c. The abbreviations for each membrane indicate the level of optical clarity observed where T = transparent; H = white discoloration on membrane outer edges; C = cloudy; O = opaque.

FTIR was used to probe and elucidate information on the surface of the copolymer blends. Chen and Gardella reported the use of ATR-FTIR to quantitatively analyze the surface of polystyrene/polystyrene-co-poly(dimethylsiloxane) blends.[310] As shown in Figure 2-3, a definite trend was observed with increasing concentrations of 6FS-35 into the blends. The appearance of absorption bands between 900-970 cm^{-1} and also at 1539 cm^{-1} which may be associated with the symmetrical and asymmetrical stretches of the hexafluoroisipropylidene group peaks clearly indicate practical compatibility of 6FS-35 into BPS-35. The continual increase in the intensity of these peaks was also seen as a function of 6FS-35 weight fraction and could possibly corroborate with the surface enrichment from the partially fluorine containing copolymer.

[310] Chen, J.; Gardella, J.A., "Quantitive ATR FTIR Analysis of Surface Segregation of Polymer Blends of Polystyrene/poly(dimethsiloxane)-co-polystyrene", *Appl. Spectro*. 1998, 52(3), 361.

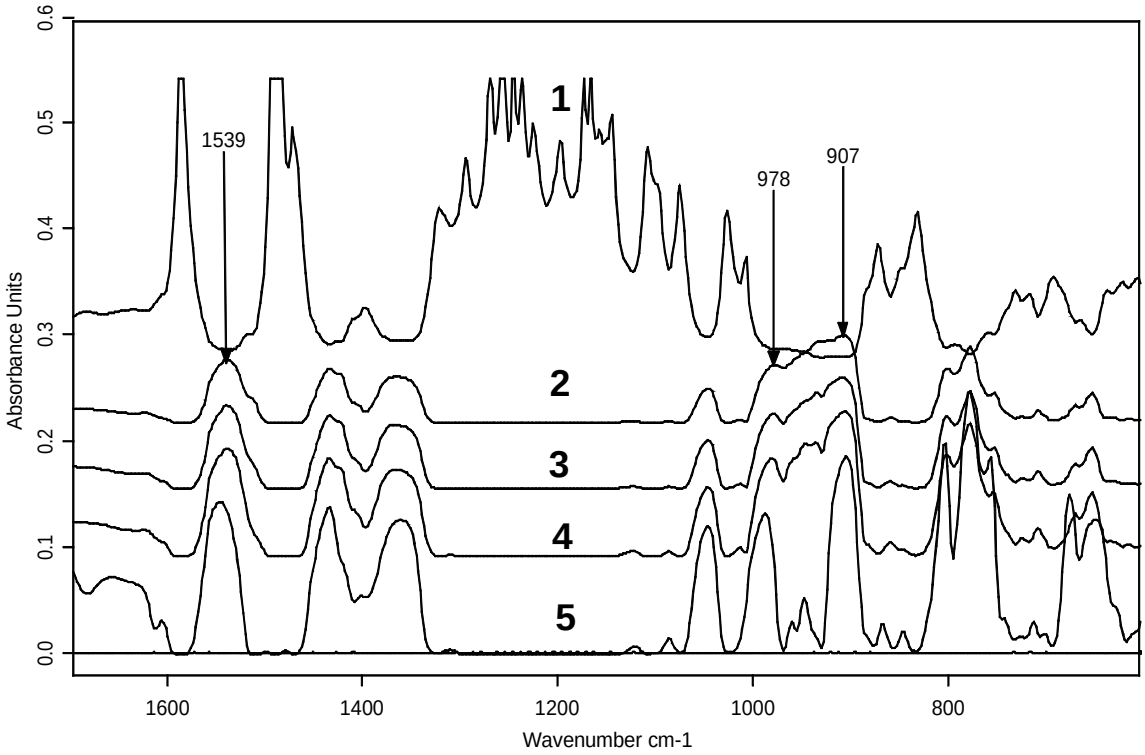

Figure 2-3. FTIR spectra of selected BPS-35/6FS-35 blend compositions. 1) BPS35; 2) 98 wt% BPS35/2 wt% 6FS-35; 3) 95 wt% BPS35/5 wt% 6F00; 4) 90 wt% BPS35: 10 wt% 6F00; 5) 6FS-35

3.2. Water uptake

The presence of water in PEMs is vitally important to transport and the overall PEMFC performance and dependent on several parameters such as degree of sulfonation, temperature, and relative humidity.[306] A decrease in the water uptake was observed in all the blends membranes except those containing 6FS-60 where the reverse effects occurred (See Table 2-3). These changes were a function of weight percents. Additionally, the 6F-00 and Radel series were more effective in reducing the sorption of water in the

membrane. From the table, a 15 % greater reduction in water uptake values compared to BPS-35/6FS-35 can be seen with the addition of 2 to 10 wt% 6F-00 into the blends. This was expected due to the absence of conducting sulfonic acid groups on these polymers that increased membrane hydrophobicity and decreased IEC.[311]

Table 2-3 Summary of the water uptake and specific conductivity of selected poly(arylene ether sulfone) copolymer blend

Composition wt%	*IEC (mequiv/g)*	*Water Uptake (wt%)*	*Conductivity* (S/cm)*
BPS-35	1.33	39	0.08
BPS35/6F00			
98/2	1.30	33	0.06
95/5	1.29	27	0.06
90/10	1.20	18	0.06
0/100	0	0	0
BPS35/6FS-35			
98/2	1.37	33	0.06
95/5	1.34	28	0.06
90/10	1.32	24	0.06
0/100	0.85	20	0.05
BPS35/6FS-60			
98/2	1.40	48	0.12
95/5	1.51	57	0.13
90/10	1.76	90	0.14
0/100	2.19	400	0.15
BPS35/ Radel®			
98/2	1.32	35	0.07
95/5	1.30	31	0.07
90/10	1.23	21	0.07
0/100	0	0	0

The decrease in the water uptake and IEC with increasing concentration of these polymers can be seen morphologically with TM-AFM. An example of this change is shown in the phase images of BPS-35/ 6FS-35 series (Figure 2-4) where the dark phases

[311] Y.S. Kim, M. A. Hickner, L. Dong, B. S. Pivovar, J.E. McGrath, *J. Membr. Sci*., **2004**, 243, 317–326.

represent the soft hydrophilic ionic domains and the lighter phases the hard hydrophilic domains. As seen, the addition of larger concentration of 6FS-35 the domains sizes of the hydrophilic regions become smaller. The decrease in hydrophilic domain sizes directly correlates with a reduction in water uptakes from 33 to 24 wt% when 2 to 10 % of 6FS-35 was added.

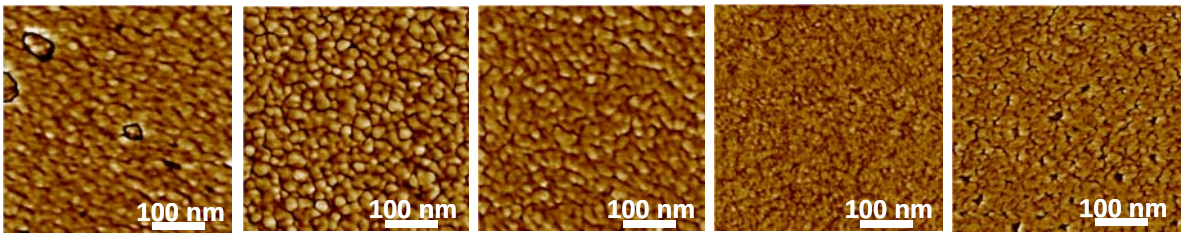

Figure 2-4. The effect of 6FS-35 incorporation on the TM-AFM phase images of selected BPS-35/Radel blended membranes in the acid form. a) BPS35; b) 98 wt% BPS-35/2 wt% 6FS-35; c) 95 wt% BPS35/5 wt% 6FS-35; d) 90 wt% BPS35/10 wt% 6FS-35; e) Radel.

In the 6FS-60 series the reverse effects (i.e. increased water uptake values) in water uptake were observed. The increase in the water uptakes is due to the highly hydrophilic nature of 6FSH-60, which may be further amplified by the introduction of hydrogen bonding with water. Consequently, increasing the weight fraction of 6FS-60 in the blends resulted in membranes with higher degrees of swelling and extremely poor membrane integrity in the wet state.

3.3. Proton Conductivity

The proton conductivities of the BPSH-35/6F00, BPSH-35/6FS-35 and BPSH-35/6FS-60 all followed similar trends as observed for the water uptakes (Table 3). However, these differences in proton conductivity were a function of weight fractions only in the BPSH-35/6FSH-60 series. A reduction in conductivities from 0.08 S/cm for BPSH-35 to 0.06 S/cm occurred with increasing weight percentages 6F-00 and 6FS-35. A decrease in proton conductivity from 0.08 for BPSH-35 to 0.07 and 0.06 S/cm with increasing weight percentages 6F-00 and 6FS-35 or BP-00, respectively was also observed. Lower proton conductivities with incorporation of the 6F moieties were expected due to the hexafluoroisopropylidene connecting units that increase the hydrophobicity along the backbone segments.[291] In an effort to reduce water uptake without adversely affecting the proton conductivity and minimize the possibility of phase separation only small weight fractions of these polymers were introduced into the blends. Additionally, a reduction in IEC values (See Table 2-3) with the introduction of a nonconductive material in an ionic polymer should cause a decline in the proton conductivity of the membrane. This trend was seen in blends of sulfonated poly(ether ketone ketone) (SPEKK) with poly(ether imide) (PEI)[312] or polyvinylidene fluoride (PVDF).[313] Interestingly, however, the conductivities of these samples, which should have closely followed those of the water uptake and IEC, remained unchanged as the concentration of unsulfonated polymer was increased from 2 -10 wt%. Further investigations are underway to determine the reasoning behind this trend.

Higher proton conductivities from 0.12 to 0.14 S/cm exhibited by BPSH-35/6FSH-60 membranes were directly related to the higher IEC and water uptake values

[312]] J. V. Gasa, R. A. Weiss, M.T. Shaw, *J. Polym. Sci., Part B: Polym. Phys.*, **2006**, 44, 2253-2266.
[313] S. Ren, G. Sun, C. Li, Z. Wu, W. Jin, W,Chen, Q. Xin, X. Yang, *Materials Letters*, **2006**, 60, 44-47.

of the acidified 6FSH-60 compared to BPSH-35. Although these values are comparable or better than to commercial Nafion, higher water sorption characteristics associated with these membranes cause excessive swelling. Therefore, the utilization of BPSH35/6FSH-60 membranes as successful PEMs is virtually impossible since the swelling properties of these membranes far exceed those required for practical PEMFC applications. For these reasons we have primarily focused the attention in this study to blends comprised of BPS-35 with 0 to 10 wt% of 6F-00, 6FS-35, and Radel.

3.4. Proton Conduction Under Partially Hydrated Conditions

The hydrated properties of disulfonated PAESs can be dramatically increased by both temperature and water content.[314] Figure 2-5 illustrates the effect of hydration level and chemical structure on proton conductivity at 80 ºC between 30 to 90% relative humidity (RH). BPSH-35 was used as a control. As seen, the addition of 10 wt% unsulfonated 6F-00 and Radel resulted in a small but constant decrease in proton conductivity. Furthermore, the incorporation of 6F-00 into the blend yielded higher proton conductivities as a function of relative humidity even though these membranes exhibited lower water uptake and proton conductivity values. This phenomenon which has been reported[315] is caused by the increased hydrophobicity of the 6F backbone resulting in shorter conduction pathway and increased "free water" content. As with many disulfonated copolymers that have been previously investigated, low proton conductivities (0.01 S/cm) at low relative humidities (~ 20%) were observed. This could

[314] R.W. Kopitzke, C.A. Linkous, H.R. Anderson, G.L. Nelson, *J. Electrochem. Soc.,* **2000**,147, 1677-1681.
[315] Yu Seung Kim, Brian Einsla, Mehmet Sankir, William Harrison, Bryan S. Pivovar. *Polymer* **2006**, 47, 4026–4035.

possibly be overcome by preparing blocks copolymers between PAES with high levels of disulfonation (>60%) and unsulfonated homopolymers. The clearly defined hydrophilic/hydrophobic microstuctures of these block copolymers may facilitated proton conduction even at low relative humidities.

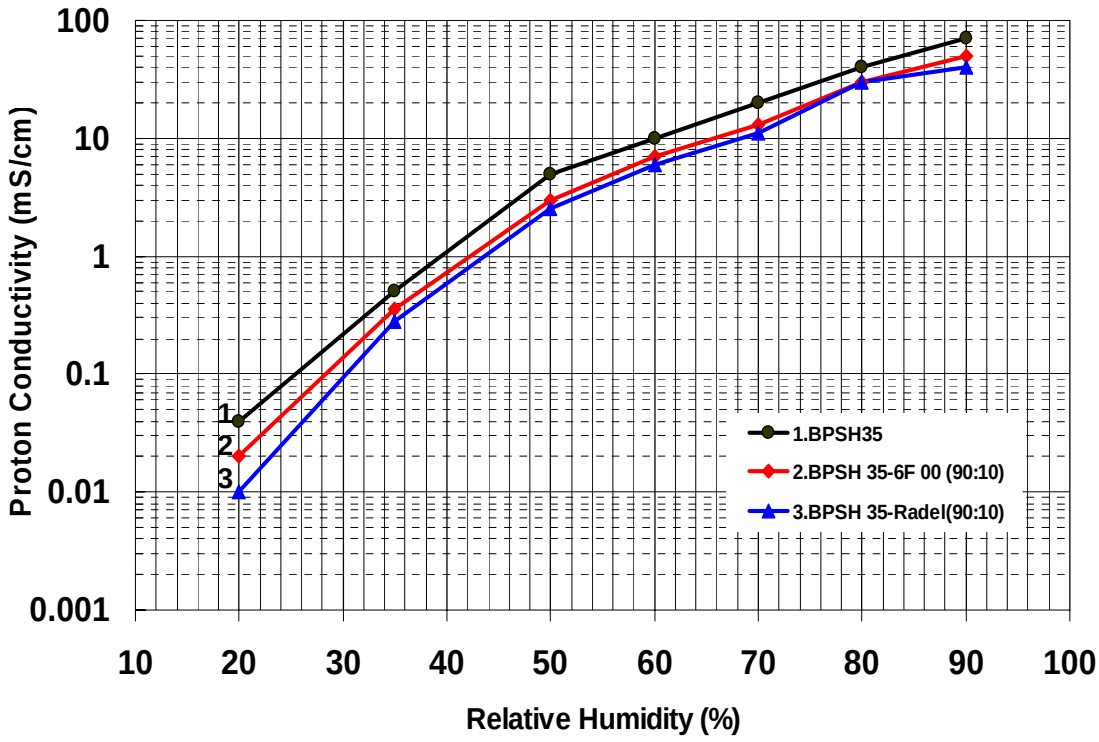

Figure 2-5. Influence of temperature and chemical structure on proton conductivity at 100% relative humidity of blended membranes with 10 wt% of unsulfonated homopolymers.

3.5. TGA

The influence of blend composition of the acidified membranes on the thermo-oxidative stability from 50 to 700 ^{o}C was explored. In the salt form, the same high thermal stabilities up to 500 ^{o}C were observed for all the blended membranes. The acidified membranes were clearly influenced by the copolymer composition and the weight percent blend compositions.

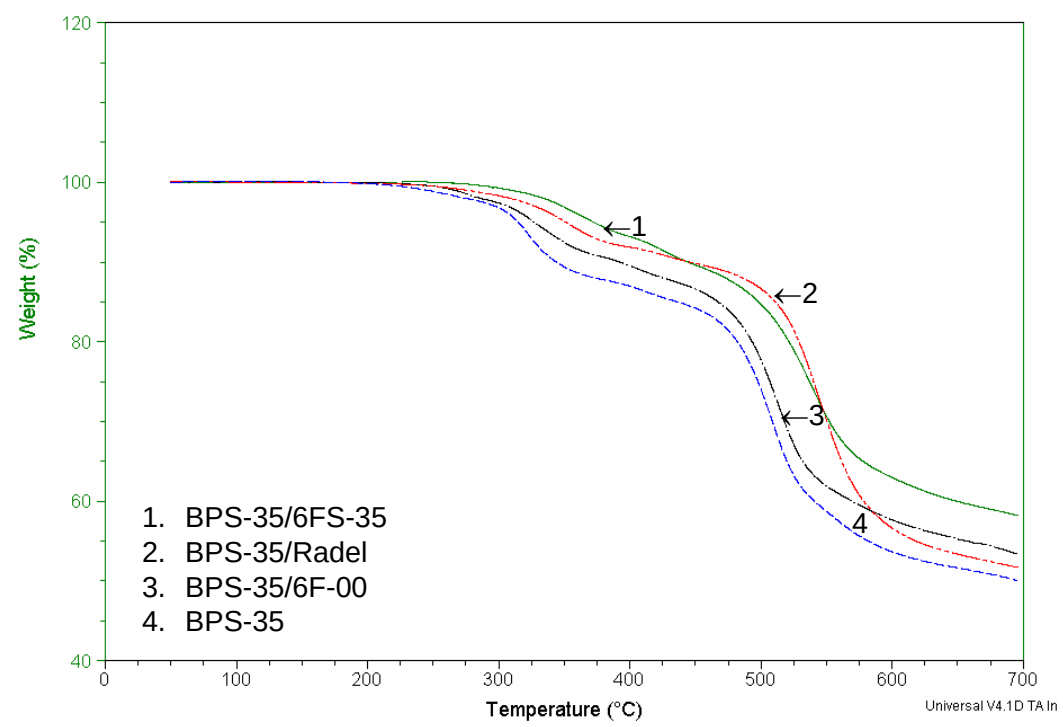

Figure 2-6. Effect of chemical composition on the decomposition temperatures on 90/10 blended membranes.

From Figure 2-6, it can be seen that the addition of 10 wt% of 6FS-35 lead a higher decomposition temperature (371 ^{o}C) compared to the other blends of the same weight fractions. From the graph, all the copolymers in the acid form exhibited a two-step

degradation profile with the first weight loss being assigned to the desulfonation process and the second weight loss peak to main chain polymer degradation.[316][317]

A summary of the thermal properties of the blended membranes is given in Table 2-4.

Table 2-4 Summary of the thermal properties by TGA and DSC of blended membranes in acid form

Composition wt%	*TGA* (T_d, °C, 5% wt loss)	*DSC* (T_g,°C)
BPS-35	265	264
BPS35/6F00		
98/2	295	262
95/5	307	261
90/10	321	260
0/100	485	194
BPS35/ Radel®		
98/2	289	263
95/5	313	263
90/10	346	261
0/100	500	220

The thermo-oxidative stability of the all blends increased as a function of weight fractions with the highest thermal stabilities being displayed by BPS-35/6FS-35 series. This was unexpected since the presence of higher concentrations of sulfonic acid groups might have been expected at lower degradation temperatures. The enhanced thermal stability of these membranes may be due to crosslinking of the sulfonic acid group by crosslinking. Unpublished DMA data from these blends illustrates this possible crosslinking occurring in both the disulfonated copolymers and blended membranes due

[316] J. P. Quentin, Sulfonated Polyarylether Sulfones, U.S. 3,709,841, Rhone-Poulenc, January 9, 1973.
[317] R. Nolte, K. Ledjeff, M. Bauer, R. Mulhaupt, *J. Membr. Sci.,* **1993**, 83, 211.

to shifts in the glass transition to higher temperatures after several experimental runs. Kerres et al [318] observed good thermal stabilities in crosslinked sulfonated blend membranes of poly(ethersulfone) PSU Udel™ with pendant sulfinic (PSU-SO_2H) and sulfonic (PSU-SO_3H) acid groups. The improved thermal stability could be observed using TGA where a 5% weight loss for the PSU-SO_2H/PSU-SO_3H (70:30) crosslinked membranes resulted in a 60 ^oC increase compared membranes that only had 30 % PSU-SO_2H. A similar trend of unexpectedly high desulfonation temperatures (>350 ^oC) for 6F poly(arylene ether sulfones) copolymers containing less than 40 percent degree of disulfonated has been previously reported.[291] By monitoring of the sulfonic acid peak at 1030 cm^{-1} with FTIR these researchers showed that a decrease in peak intensity when the film is exposed to 260 ^oC for 30 minutes could be observed.

3.6. DSC

The thermal properties (T_g) of the blends as a function of composition were investigated using DSC. DSC analyses were conducted on the membranes in the acid form. Figure 2-7 shows selected DSC thermoscans (2nd heat) of BPS-35/6F-00 as a function of weight percent. As shown, larger amounts of 6F-00 in the blends lead to small but subtle shifts in the T_gs to lower temperatures. The decrease in T_g was expected since the introduction of a unsulfonated copolymers into the blends would decrease molecular bulkiness and diminishes intermolecular interaction by hydrogen bonding of SO_3H groups (ionomer

[318] J. Kerres, W. Cui, R. Disson, Wolfgang Neubrand, *J. Membr. Sci.* 1998, 139, 211-225.

effect).[319] The thermoscan suggested some miscibility between the copolymers was obtained because only a single T_g was observed for each blend. Although the same type of shifts in the DSC spectra were also observed for blends containing Radel, higher glass transition temperatures were observed. Higher weight fractions of unsulfonated copolymers or 6FS-35 into BPS-35 first resulted in microphase separation above 20 wt%, ultimately progressing into clearly defined macrophase separation at about 50 wt%. This can be observed by the appearance of two T_g peaks in DSC scans.

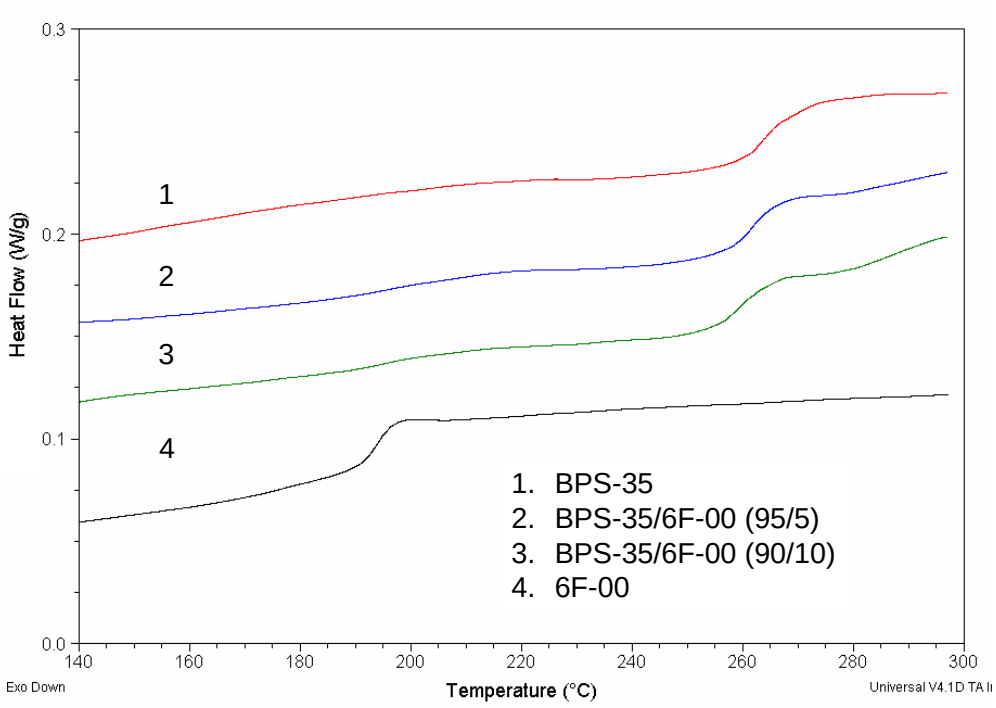

Figure 2-7. Influence of weight fractions on thermal transition on acid form BPS-35/6F-00 membranes.

[319] S. M. J. Zaidi, S. D. Mikhailenko, G. P. Robertson, M. D. Guiver, S. Kaliaguine, *J. Membr. Sci.* **2000**, 173, 17-34.

Furthermore, it is well known that ion-containing copolymers display complex thermal transitions due to the presence of aggregates by the sulfonic acid (of varying sizes) and the influence to the 'normal' polymer transitions.[320,321] As previously stated crosslinks can possibly be formed in these membranes at temperatures above 230 °C. The presence of crosslinks in these membranes can hinder the internal rotations within the polymers making it more difficult to determine the glass transition temperatures of these membranes in the acid form using DSC. DMA which is a more sensitive technique than DSC was used to detect the glass transition (T_g) in the acidified BPS-35/6FS-35 membranes. As shown in Table 2-5 the blends of BPS35/6FS-35 exhibited the same decrease in glass transition temperatures as higher concentrations of 6FS-35 were introduced. Notably, these T_g temperatures were higher than the aforementioned membranes. The reason for this was that these blends were analyzed in the salt instead of the acid form which resulted in shifts of the glass transition temperatures to higher temperatures after several runs.

Table 2-5. Summary of the thermal properties of BPS-35/6FS-35 blends

Composition wt%	***TGA*** ***(T_d, °C, 5% wt loss)***	***DMA*** ***(Storage Modulus T_g,°C)***
BPS-35	265	279
BPS35/6FS-35		
98/2	355	276
95/5	367	271
90/10	371	263
0/100	350	235

[320] M. Ehramann, R. Muller, J.C. Galin, C.G. Bazuin, *Macromol.* **1993**, 26, 4910-1918.
[321] A. Eisenberg, J. Kim, Introduction to Ionomers, Wiley-Interscience Pub., 1998; (b) G. L. Wilkes, M. R. Tant, K. A. Mauritz, Eds. Ionomers: Synthesis, Structure, Properties and Applications, Blackie Academic and Professional, New York, 1997.

3.7. Surface Properties of Blended Membranes

Contact angle experiments were conducted on the various copolymer blend systems to explore the surface properties, including hydrophobicity, of the cast membranes. The data may provide information on the nature of the surface and confirm the surface enrichment of the fluorine atoms in the membranes. Linemann et al used fluoropolymers as a means to reduce surface energy in latex blends of fluorinated acrylates with poly(*n*-butyl methacrylate) for water, oil, and soil repellence.[322] In blends of BPS-35 with 6F-00 and 6FS-35, higher contact angles were observed as the ratio of the partially fluorinated in the blend was increased. Figure 2-8 illustrates the effect of increasing 6F-00 concentration on the instantaneous contact angle. As the weight fraction of 6F-00 in the blends was increased (from 0 to 10 wt%) the contact angle changed by 21 degrees on the air side of the membranes. The contact angle for the blends with 6F polymers are listed in table.

From the table, the air and glass side of the membranes refer to the air/membrane and glass/membrane interfaces, respectively. The higher contact angles associated with increasing 6F-00 concentration may be attributed to increased amounts of the fluorine moieties on the membrane surfaces leading to enhanced hydrophobicity. Compared to the air/solid interface, lower contact angles on the glass/solid interface can be attributed to an increase in the surface energy. Furthermore, lower contact angle values in the BPS-

[322] R. F. Linemann, T. E. Malner, R. Brandsch, G. Bar, W. Ritter, R. Mulhupt, *Macromol.,* **1999,** 32(6), 1715-1721.

35/6FS-35 blends were also seen due to the presence of higher concentration of sulfonic acid groups that increased surface hydrophilicity.

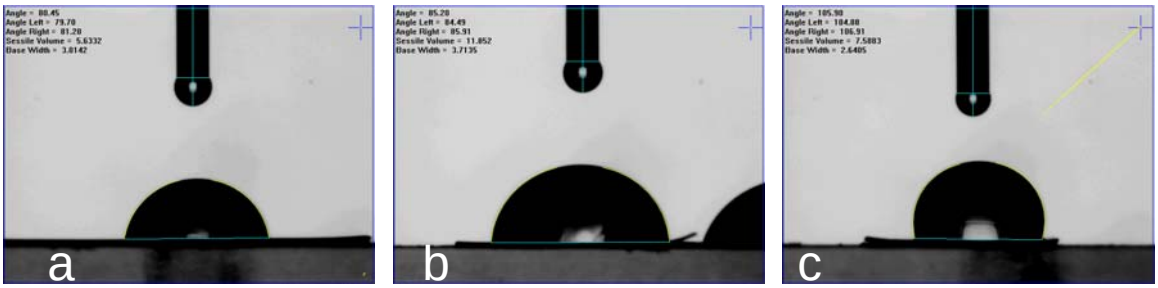

Figure 2-8. The effect of 6F00 incorporation on the water contact angles of selected BPS35:6F00 blend membranes. a) BPS35 (80°); b) 98 wt% BPS35:2 wt% 6F00 (85°); c) 90 wt% BPS35: 10 wt% 6F00 (106°)

The calculated amounts of fluorine atoms present on the surface of these films were confirmed by XPS and are recorded in Table 2-6. Although no general trend occurred as a function of weight fraction, a difference in the fluorine content on the air and glass surfaces of the membranes was observed. The changes in the quantitative amounts of fluorine on each surface directly correspond with angular changes observed by contact angle. This affirms that an enrichment of fluorine atoms on the surface of the membranes occurred leading to reduced surface energy and an increase in contact angle. As with the contact angles, the fluorine content on the air/membrane interface were notable higher than those on the glass/membrane interface in all the blend compositions.

Table 2-6 Summary of the surface properties of fluorinated blended membranes by contact angles and XPS.

Composition (wt%)	***Contact Angle***		***XPS***	
BPS35/6F00	*Air side*	*Glass side*	*Air side*	*Glass side*
100/0	80	64	0.1	0.0
98/2	85	70	8.4	0.0
95/5	87	77	0.2	0.3
90/10	106	78	10.9	0.0
0/100	109	89	10.2	9.9
BPS35/6FS35				
98/2	83	69	10.4	0.4
95/5	87	73	-	-
90/10	91	77	6.5	2.2
0/100	93	87	7.4	1.3

4. Conclusions

A series of random copolymer blends composed of varying weight percent BPS-35 with 6F polyether sulfone, 6FS-35, and 6FS-60 have been made. The partially miscibility between the 6F containing copolymers and BPS-35 was observed by the appearance and increase of the appearance of hexafluoroisipropylidene group symmetrical and asymmetrical infrared peaks between 900-970 cm^{-1} and also at 1539 cm^{-1}. In the salt form, low weight percentages (0-5 wt%) of the 6F moiety in BPS-35 resulted in transparent films whereas the addition of 5 to 10 wt% of Radel into the blends yielded cloudy membranes. No changes in the optical clarity of membranes with 6F-00 and 6FS-60 were seen after being subjected to Method 2 acidification.

A decrease in the water uptake was observed in all the blends membranes except those containing 6FS-60 and were directly correlated to morphological and IECs changes as function of weight fraction. Introduction of 6F-00, 6FS-35 and Radel into the blends intially lead to reduction in proton conductivities although these conductivities remained constant as the concentration of unsulfonated polymer was increased from 2 -10 wt%. Compared to BPSH-35 a small but constant decrease in proton conductivity with 10 wt% of 6F-00 and Radel was also seen at 80 ºC under relative humidity conditions. However, an increased in conductivity occurred as relative humidity was raised from 30 to 90%.

The thermo-oxidative stability and thermal properties (T_g) of the all blends were found to be a function of weight fractions. The self enrichment of the fluorine atoms on the both the air and glass surface of the membranes was confirmed using contact angle and XPS measurements.

Acknowledgements

The authors of this paper would like to gratefully acknowledge the National Science Foundation Partnership for Innovation and the Nissan Motor Company for funding.

CHAPTER 3. THE EFFECT OF STRUCTURE, COMPOSITION, AND MORPHOLOGY ON THE PERFORMANCE OF DISULFONATED POLY(ARYLENE ETHER SULFONE) RANDOM COPOLYMER BLENDS FOR DIRECT METHANOL FUEL CELLS.

Natalie Y. Arnett[a], William L. Harrison[b], Abhishek Roy[a], Ozma Lane[a], and James E. McGrath[a]

[a]Macromolecules and Interfaces Institute

Virginia Polytechnic Institute and State University, Blacksburg, VA 24061

[b]NanoSonic, Inc, 1485 South Main Street, Blacksburg, Va. 24060

Abstract

The purpose of this research was to systematically investigate the properties and characteristics of disulfonated poly(arylene ether sulfone) (PAES) copolymer blends for PEMFCs. Several blends between biphenol based disulfonated PAES (BPS-35) and various fluorine containing polymers were studied. Fluorine containing polymers used in this research include hexafluoroisopropylidene biphenol based PAES (6F-00), hexafluoroisopropylidene biphenol based disulfonated PAES (6FS-35), hexafluoroisopropylidene biphenol based poly (phenyl phosphine oxide) (6FPPO), and poly(vinylidene fluoride) (Kynar®). .

The development of blended membranes with desirable surface characteristics, reduced methanol permeability and decreased water swelling has been reported. Polymer blends were prepared in the potassium salt forms primarily from N, N-dimethylacetamide (DMAc). Water uptake, proton conductivity, thermogravimetric analysis (TGA), differential scanning calorimetry (DSC), contact angle, methanol permeability, and direct methanol fuel cell performance were used to characterize the blended films.

1. Introduction

Polymer blends are recognized as a valuable means to combine the properties of two different polymers[337, 323]. Previous research into a series of disulfonated random copolymer blends fabricated by varying weight percent biphenol based disulfonated PAES (BPS-35) with hexafluoroisopropylidene biphenol based PAES (6F-00), hexafluoroisopropylidene biphenol based disulfonated PAES (6FS-35), and Radel R displayed an initial reduction in proton conductivities[324]. Unexpectedly however, the conductivities remained constant as the concentration of unsulfonated polymer was increased from 2 to 10 wt.%. A self-enrichment of fluorine atoms on the both the air and glass surface of the membranes was also observed.

Miscibility in polymer blends is linked to the thermodynamic concept of homogeneity, to the existence of a single phase and to property isotropy. In other words, a miscible blend is the genuine dissolution of one polymer in the other.[323] Polymer incompatibility arises from very small entropy gained by mixing different kinds of long chains. The miscibility of two polymers is governed by changes to the Gibbs free energy of mixing (G_m).[325] For a reversible system at a given temperature (T),

$$\Delta G_m = \Delta H_m - T\Delta S_m \quad .$$

[323] O. Olabisi, L. M. Robeson, and M. T. Shaw. Polymer-Polymer Miscibility, New York : Academic Press, 1979

[324] Arnett, N.Y. Harrison, W.L., Badami, A.S., Roy, A., Lane, O., Cromer, F., Dong, L., McGrath, J. E. *Journal of Power Sources* **2007,** 172, 20–29.

[325] Folkes, M.J. and Hope, P.S., Eds. "Polymer Blends and Alloy." Blackie Academic & Professional, London, 1993.

where H_m is the enthalpy of mixing and S_m is the entropy of mixing. If ΔG_m is positive the two polymers will be immiscible whereas for spontaneous mixing ΔG_m must be negative.

There are a number of molecular variables that contribute to compatibility of polymer-polymer blends. These parameters include polarity, specific group interaction, blending temperature, and polymer to polymer ratios.[326] Temperature is important factor in controlling polymer-polymer miscibility because if ΔG_m needs to be negative for thermodynamic mixing, then

$$\Delta H - T\Delta S < 0$$

implies that exothermic mixtures will spontaneously mixing at $\Delta H<0$ whereas endothermic mixtures will only occur at high temperatures.

Polarity becomes an important issue in polymers that are similar in structure and/ or polarity since they are less likely to repel one another.[327] Blends comprosed of sulfonated polysulfone (PSU-SO_3H) and unfunctionalized PSU (UDEL®) produced inhomogeneous, nontransparent membranes with poor mechanical stability and extremely low IECs.[328] Blend microphase separation was still apparent after hydrolysis when nonionic precursors (PSU-SO_3Cl, PSU-SO_3CH_3 or PSU-SO_3NH_2) of PSU-SO_3H were blended with unmodified PSU. The incompatibility was attributed to insufficient entanglements between the polymers due to weak van der Waals and dipole-dipole interactions. Furthermore the blends of unmodified PSU and PSU-SO_3CH_3 or PSU-SO_3NH_2 displayed excessive swelling or did not hydrolyzed, respectively.

---

[326] Shanaike, G.O. and Simon, G.P., EDs. Polymer Blends and Alloys. Mercel Dekker, New York, 1999.
[327] Coleman, M.M., Graf, J.F., and Painter, P.C. "Specific Interactins and the Miscibility of Polymer Blends: A Practical Guide for Predicting and Designing Blends." Technomic Publishing Company, Pennsylvania, 1991.
[328] Cui, W.; Kerres, J.; and Eigenberger, G. *Separation and Purification Technology* **1998**, 14, 145.

Improvements to copolymer-copolymer miscibility can be achieved by promoting intermolecular interactions such as hydrogen bonding, dipole-dipole interaction, acid-base interactions, and covalent crosslinking.[329] As the bond strength of each interaction becomes stronger, the polymer miscibility may be increased. Cui, Kerres, and Eigenberger[330] investigated blends of SPEEK with polysulfone UDEL®-ortho-sulfone-diamine (PSU-NH_2), polyamide PA Trogamid P, or poly(etherimide) PEI Ultem. Hydrogen bonding between the polymers was used to obtain miscible blends as illustrated by single T_gs 5-20 K higher than SPEEK.

More strongly bonded, acid–base blend systems from sulfonated poly(ether ether ketone) or poly(arylene ether sulfone) with different kinds of basic polymers, such as polybenzimidazole, aminated polysulfone (PSU-NH_2), poly(4-vinylpyridine), and polyethylenimine have also been prepared.[331] These acid base blends exhibit specific interactions (H-bonding and salt pairs formation) that increase the compatibility between these polymeric materials resulting in high thermal stabilities (270-350 °C) and low swelling ratios.

Varying the ratio of polymers may also induce miscibility. In a 50:50 polymer blend, two polymers may be completely immiscible. However, if a smaller amount of one of the polymers is added into the blend mixture, miscibility can be achieved. Chen and Yang[332] showed that in liquid crystalline poly(aryl ether ketone) (LC-PAEK) and poly(aryl ether ether ketone) (PEEK) blends that the composition of the blends has great

[329] Tucker, R.T.; Han, C.C.; Dobrynin, A.V.; and Weiss, R.A. *Macromolecules* **2003**, 36, 4404.
[330] Cui, W.; Kerres, J.; and Eigenberger, G. *Separation and Purification Technology* **1998**, 14, 145.
[331] Kerres, J.; Ullrich, A.; Meier, F.; Haring, T. *Solid State Ionics* **1999**, 125, 243.
[332] Chen, J. Lui, X. Yang, D. *J. Appl. Polym. Sci.* **2006,** 102, 4040-4044

effect on the phase behavior and structure. Thin films of pure LC-PAEK and PEEK crystallized from the melts exhibit typical mosaic and spherulitic structures, respectively. For the blends with higher LC-PAEK contents (>50%), the two components are miscible at the molecular level in the melting state, and a phase separation takes place during the cooling process. In PEEK-rich blends, LC-PAEK is rejected into the boundary of PEEK spherulites.

The development of blended membranes of BPS-35 with fluorine containing copolymer such as 6F-00, 6FS-35, hexafluoroisopropylidene biphenol based poly (phenyl phosphine oxide) (6FPPO) and poly(vinylidene fluoride) (Kynar®) is reported in this chapter. The effect of the various chemical structures and their concentration in the blends on membranes properties and fuel cell performance will also be investigated. The chemical structures of these copolymers are presented in Figure 3-1. The introduction of these copolymers into the blends led to reduced methanol permeability, desirable surface characteristics and reduced water swelling.

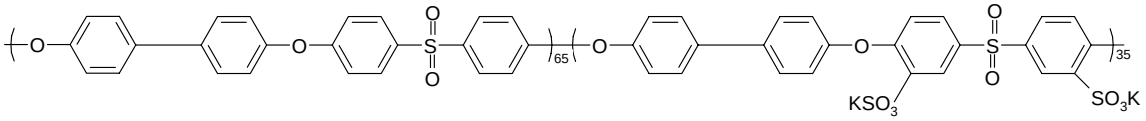

Biphenol based disulfonated poly(arylene ether sulfone)
"BPS-35"

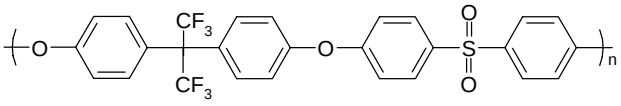

Hexafluoroisopropylidene biphenol based poly(arylene ether sulfone)
"6F-00"

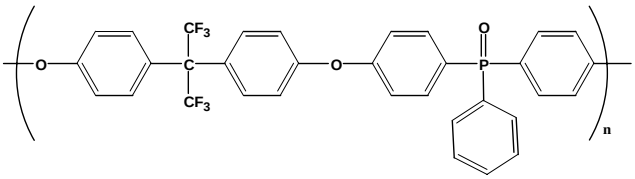

Hexafluoroisopropylidene biphenol based poly (phenyl phosphine oxide)
"6FPPO"

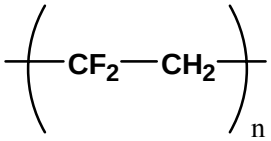

Poly(vinylidene fluoride)
"Kynar 761"

Figure 3-1.Chemical structures of the fluorine-containing copolymers utilized

2. Experimental

2.1. Materials

4,4'-Hexafluoroisopropylidenediphenol (6F BPA), received from Ciba, was purified by sublimation and dried under vacuum. Eastman Chemical provided high purity 4,4'-biphenol (BP) which was dried at 50 ºC under vacuum before each use. Solvay Advanced Polymers supplied highly purified 4,4'-dichlorodiphenylsulfone (DCDPS). 4,4'-Dichlorodiphenylsulfone was dried at 60 ºC under vacuum before each use. Kynar 761 polymer was kindly donated by ARKEMA. N-Methyl-2-pyrrolidinone (NMP) (Aldrich) was vacuum distilled from calcium hydride onto molecular sieves, then

stored under nitrogen. N,N-Dimethylacetamide (DMAc) (Aldrich) was distilled under vacuum from calcium hydride and stored over molecular sieves under nitrogen. Undistilled NMP and DMAc were used to prepare the blends. Potassium carbonate was vacuum-dried at 150 ºC. Toluene obtained from Aldrich was used as received. The detailed synthesis of 3,3'-disulfonate-4,4'-dichlorodiphenylsulfone monomer (SDCDPS) has been reported.[291]

2.2. Copolymer Synthesis by Direct Copolymerization

Similar copolymerization procedures were used to synthesize BP or 6F BPA copolymers. A typical copolymerization for the sulfonated copolymers is described using the 6FS-35 system. First, 6F-BPA (3.1608 g, 9.4 mmol), DCDPS (1.7599 g, 6.1 mmol), and SDCDPS (1.6211 g, 3.3 mmol) were added to a 3-neck flask equipped with an overhead mechanical stirrer, nitrogen inlet and a Dean-Stark trap. Potassium carbonate (0.8707 g, 6.3 mmol), and DMAc (18 mL) were introduced to afford a 20% (w/v) solids concentration. Toluene (usually DMAc/Toluene = 2/1, v/v) was used as an azeotroping agent. The reaction mixture was refluxed at 150 ºC for 4 h to dehydrate the system. The temperature was raised slowly to 190 ºC by controlled removal of the toluene. The reaction was allowed to proceed for 30 h or until a viscous solution was observed. The solution was cooled to room temperature and the copolymer was isolated by coagulation in stirring deionized water. The precipitate was stirred overnight at 60 ^{o}C to remove most of the salts. The copolymer was then collected by vacuum filtration and dried in a vacuum oven at 120 ºC for 24 h. Similar procedures with appropriate monomers and

comonomer ratios were used to prepare the BPS-35, 6FS-35 and the 6F-00 copolymers and have been previously reported.[307,308]

2.3. Polymer Blending and Membrane Acidification

Separate solutions of the copolymers (potassium salt form) at different weight ratios were prepared in DMAc (5 wt/v%). The 6F copolymer solutions were added to BPS-35 solutions and stirred or 80 °C for 1 h. Solutions were filtered through a 0.45 μm PTFE filter onto clean glass substrates. The membranes were dried gradually via a heating lamp for 24 h and then under vacuum at 100 °C for 24 h. Blend membrane systems were converted from the potassium salt form to the acid form by first boiling in 0.5 M H_2SO_4 for 2 h and immediately followed by extraction in boiling deionized water for 2 h as described earlier.[309]

2.3.1. Blending of Acidified Copolymers

The membranes were prepared from BPS35 and 6FS35 films that were first acidified by Method 2 acidification method. After acidification the membranes were equilibrated in deionized water for 2 days at RT and then dried again in vacuum oven for 2 days at 100 °C. Separate solutions of BPSH-35 and 6FSH-35 copolymers were then prepared in DMAc (10 wt%) and the 6FSH-35 solutions were added to the BPSH-35 solutions, stirred at 80°C for 1 hour. The solutions were hot filtered and cast onto glass plates and

dried first with an IR lamp and then in the vacuum oven for 24 hours at 100 ºC. Finally the membranes were subjected to a second "Method 2 "acidification

2.4. Characterization

2.4.1. Turbidity Measurements

The clarity of the blended membranes was obtained from qualitative visual observations. The blended membranes were characterized in both the salt and acid forms to understand the effect of hydrothermal treatment (Method 2 acidification).

2.4.2. Aqueous Potentiometric Titration

Aqueous potentiometric titrations were carried out on a Schott Instruments TA20 plus titration unit for ion-exchange capacities measurements of the blended membranes. The acidified membrane was placed in a concentrated 1M solution of sodium sulphate and stirred for 24 hrs. The solution was then titrated with a standard sodium hydroxide solution at 0.02 mL/second and simple endpoint titrations were recorded.

2.4.3. Water Uptake

The water uptake of the blended membranes was performed by immersing the membranes in deionized water at room temperature for 24 h. The wet membranes (W_{wet}) were then blotted to remove surface water droplets and quickly weighed (W_{dry}). These membranes were then vacuum dried at 90 ºC for 24 h and weighed again. The water uptake (%) of the membranes was calculated by:

$$WaterUptake = \frac{W_{wet} - W_{dry}}{W_{dry}} \times 100\% \qquad 1$$

where W_{wet} is the weight of the wet membrane and W_{dry} represents the weight of the dry membrane.

2.4.4. Proton Conductivity

A Solartron (1287 + 1252) impedance/gain phase with window cell geometry was used to measure the proton conductivity of each film in the acid form at 30 ^{o}C over a frequency range of 10 Hz to 1 MHz under fully hydrated conditions. In determining proton conductivity in liquid water, membranes were equilibrated at 30 ^{o}C in DI water for 24 h prior to testing. For determining proton conductivity under partially hydrated conditions, membranes were equilibrated in a humidity-temperature oven (ESPEC, SH-240) at the specified RH and 80 ^{o}C for 24 h before each measurement.

2.4.5. Thermogravimetric Analysis

The thermooxidative stabilities of the membranes (10 – 15 mg) were determined using a TA Instruments TGA Q 500. Both the salt and acid form blended membranes were vacuum dried at 100 ^{o}C for 12 h prior to analysis. Before TGA characterization the membranes were placed in the TGA furnace at 150 ^{o}C in a nitrogen atmosphere for 30 minutes. The samples were evaluated over the range of 30 to 700 ^{o}C at a heating rate of 10 ^{o}C/min in air.

2.4.6. Differential Scanning Calorimetry

The glass transition temperatures (T_g) of the acidified membranes were obtained on a TA Instrument DSC Q 1000. Scans were conducted under nitrogen at a heating rate of 10 ^{o}C/min. Second heat T_g values are reported as the midpoints of the changes in the slopes of the baselines.

2.4.7. Contact Angles

The "instantaneous" (1-5 sec) contact angle measurements were obtained on a Ten Angstroms (FTA 32) instrument that utilized the sessile-drop method. Contact angle was a quantitative method used to determine the hydrophobicity or hydrophilicity of the film surface. Deionized water was dropped on the surface of the membranes at room temperature and the contact angle of the drops was determined. Measurements were carried out on both the air/membrane interface and the membrane glass interface.

2.4.8. Tapping Mode Atomic Force Microscopy

Tapping Mode Atomic Force Microscopy (TP-AFM) images of the blends were obtained using a Digital Instruments MultiMode scanning probe microscope with a NanoScope IVa controller. A silicon probe (Veeco) with an end radius of <10 nm and a force constant of 5 N/m was used to image samples. Samples were dried under vacuum at 100 °C for 12 h and then equilibrated at 50% relative humidity for at least 12 h before being imaged immediately at room temperature in a relative humidity of approximately 15-20%.

3. Results and Discussion

Poly(arylene ether sulfone) random copolymers were prepared by reacting either biphenol (BP), or 6F BPA, systematically with varied ratios of DCDPS and SDCDPS. BPS-35 was blended with 0-10 wt% of 6F-00, 6FS-35, 6FPPO, or Kynar 761 ($PVDF_2$). The films were analyzed in acidified forms. The introduction of 6FPPO into the blends could possibly improve polymer-polymer compatibility with BPS-35 through specific interactions of sulfonic acid groups with triphenyl phosphine oxide group. The introduction of flexible, thermally and oxidative stable polyvinylidene fluoride ($PVDF_2$) into copolymer blends could essentially lower the modulus of the resulting proton exchange membrane, as well as reduce its water swelling, which will be applicable to humidity cycling and real proton exchange membrane fuel cell systems.

3.1. Influence of Amorphous Copolymer Structures

The optical clarity of the membranes was inspected visually as a preliminary means of identifying compatibility between the polymers (See Table 3-1). In the salt form, low weight percentages (0-5 wt%) of the 6F-00, 6FS-35, and 6FPPO moieties in BPS-35 resulted in transparent films. Increased turbidity and large regions of *macrophase* separation were observed when higher ratios (>80 wt%) of 6F moieties were introduced into the blends. Although increase turbidity, which could be a sign of immiscibility, was observed at 10 wt% of these polymers no obvious regions of phase separation could be detected as shown by TM-AFM (Figure 3-2). Immiscibity between two copolymers was visually observed by the formation of large circles ("islands") throughout the entire membranes. Figure 3-2 clearly shows the absence of these "islands" throughout the membrane morphology.

Water uptake and conductivity as a function of blend compositions were investigated. Previous research has shown that the incorporation fluorine moiety into a polysulfone membrane leads to lower water uptake but greater proton conductivity compared to BPS-30 control.[333] A summary of the hydrated properties of these blends are listed in

Table 3-2**.** As expected, a reduction in the water uptake for the unsulfonated 6F-00 and 6FPPO was also observed due to a decrease in the IEC of the blend. In the 6FS-35 blend series a decrease in the water uptake and conductivity was also observed as the concentration of the 6FS-35 increased.

A reduction in conductivities was also observed when higher concentrations of these copolymers were introduced into the blends. However, the conductivities of these

[333] Kim, Y. S.; Einsla, B.; Sankir, M.; Harrison, W.; Pivovar, B. S. *Polymer* **2006**, 47, 4026.

samples remained unchanged as the concentration of 6F-00 and 6FS-35 was increased from 2 to 10 wt%. A continual decrease in the proton conductivities with increasing weight percent of 6FPPO was observed. This decrease can be attributed to an increase in hydrogen bonding between the phosphine oxide and sulfonic acid groups as the concentration of 6FPPO increases in the blend.

Table 3-1. Optical properties of blend membranes

Composition (wt%)	***Optical Clarity (Salt)[a]***	***Optical Clarity (Acid)[b]***
BPS-35	T	T
BPS-35/6F-00		
98/2	T	T
95/5	T	T
90/10	H	C
0/100	T	T
BPS-35/6FS-35		
98/2	T	T
95/5	T	H
90/10	C	C
0/100	T	T
BPS-35/6FPPO		
98/2	T	T
95/5	T	T
90/10	C	C
0/100	T	C

a. The appearance of membrane upon direct release from glass substrate
b. The appearance of membrane after undergoing Method 2 acidification
c. The abbreviations for each membrane indicate the level of optical clarity observed where T = transparent; H = white discoloration on membrane outer edges; C = cloudy; O = opaque.

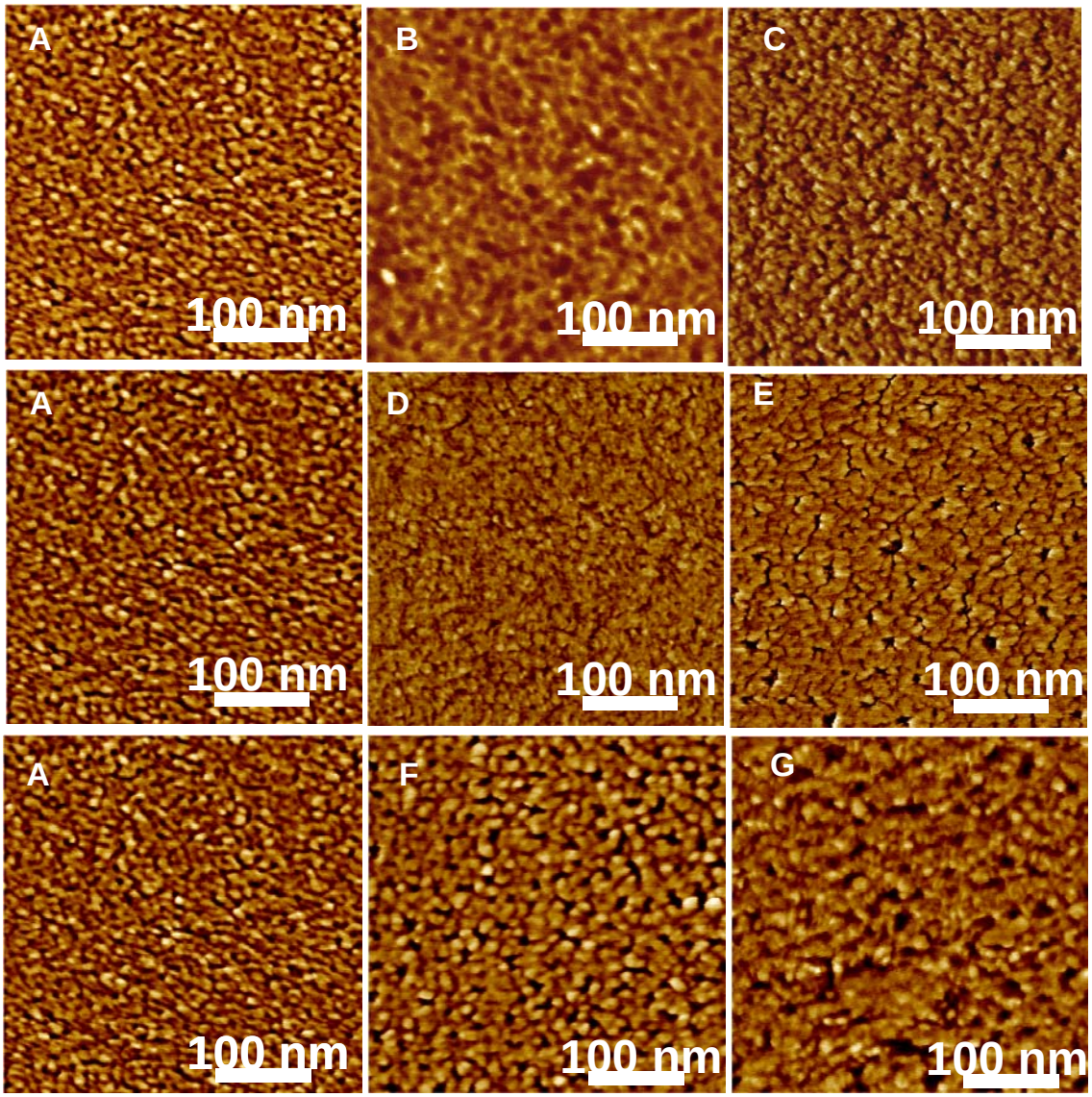

Figure 3-2. TM-AFM Phase Images of BPS-35 with 10 wt% various 6F-copolymers. Image A represents BPSH-35; B represent 10 wt% 6FS-00; C represents 6FS-00; D represent 10 wt% 6FS-35; E represents 6FS-35; F represent 10 wt% 6FPPO; G represents 6FPPO.

To improve polymer-polymer miscibility through possible hydrogen bonding, blending of the copolymers in the acid form was also investigated. These investigations

were conducted using BPSH-35/6FSH-35 blend membranes. The membranes were prepared from BPS35 and 6FS35 films that were first acidified by Method 2 acidification method. The properties of these membranes are presented in Table 3-3. No changes in the optical clarity before or after acidification were observed. Compared to the previous BPS35/6FS-35 blends that were blended in the salt form, these membranes have much lower water uptake and proton conductivity. However, the water uptake and proton conductivity values remained essentially unchanged as the concentration of 6FSH-35 was increased.

Table 3-2. Hydrated Properties of BPS-35 and Different Amorphous Copolymers

Composition wt%	***IEC (mequiv/g)***	***Water Uptake (wt%)***	***Conductivity (S/cm)***
BPS-35	1.33	39	0.08
BPS35/6F00			
98/2	1.30	33	0.06
95/5	1.29	27	0.06
90/10	1.20	18	0.06
0/100	0	0	0
BPS35/6FS-35			
98/2	1.37	33	0.06
95/5	1.34	28	0.06
90/10	1.32	24	0.06
0/100	0.85	20	0.05
BPS35/6FPPO			
98/2	1.29	32	0.07
95/5	1.27	29	0.06
90/10	1.22	30	0.03
0/100	0	0	0

The proton conductivity as a function of relative humidity was also studied and the effect of hydration level and 6FS-00 concentration on proton conductivity at 80 ºC between 30 to 90% relative humidity (RH) is shown in Figure 3-3.

Table 3-3. Properties of BPSH-35/6FSH-35 blend membranes

Blend Ratio (wt%)	***BPSH-35/6FSH-35***			
	Clarity (Salt)	*Clarity (Acid)*	*Water Uptake (wt%)*	*Conductivity[1] (S/cm)*
100 : 0	T	T	32	0.07
98 : 2	T	T	23	0.04
95 : 5	C	C	24	0.04
90 : 10	C	C	23	0.04
0 : 100	T	T	18	0.05

a. The appearance of membrane upon direct release from glass substrate.
b. The appearance of membrane after undergoing Method 2 acidification.
c. The abbreviations for each membrane indicate the level of optical clarity observed where T = transparent; C = cloudy.
d. Proton conductivity measurements were carried out at 30 ºC in DI H_2O.

As with the proton conductivities at 30 ºC the addition of up to 10 wt% unsulfonated 6FS-00 also resulted in a small but constant decrease in proton conductivity as a function of relative humidity. Furthermore, the proton conductivity in the random copolymer (BPSH-35) and blended membranes drops significantly at lower RH values. This trend that is characteristic of disulfonated random copolymers occurred due to the lack of connectivity among sulfonic acid groups for proton transport under partially hydrated conditions. The incorporation of 20 wt% 6FS-00 contributed to a greater decline in proton conductivities at lower relative humidities. At this ratio, phase separation between the two polymers became apparent

.

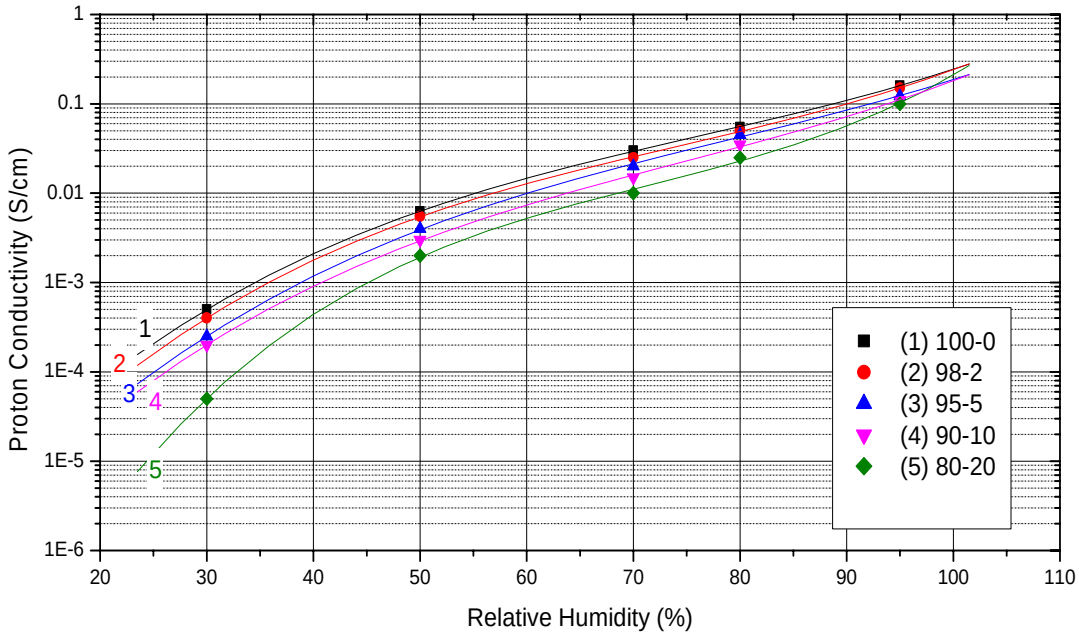

Figure 3-3. Proton conductivity under partially hydrated conditions as a function of 6F-00 blend compositions (80°C).

The influence of blend composition of the acidified membranes on the thermo-oxidative stability from 50 to 700 ^{o}C was explored. The acidified membranes were clearly influenced by the copolymer composition and the weight percent blend compositions. A summary of the thermal properties of the blended membranes is listed in Table 3-4. The thermo-oxidative stability of the all blends increased as a function of weight fractions.

The thermal properties (T_g) of the blends as a function of composition were also investigated using DSC (See Table 3-4). DSC measurements were conducted on the membranes in the acid form and the values were compared to theoretical calculations determined by the Fox equation. Larger amounts of these fluorine containing polymers in the blends lead to small but subtle shifts in the T_gs to lower temperatures. The detection

of one T_g and the close correlation of the experimental to theoretical values indicates good miscibility between the copolymers.

Table 3-4. Summary of the thermal properties by TGA and DSC of blended membranes of BPS-35 with Various Amorphous Copolymers in acid form

Composition (wt%)	*TGA (T_d, ºC, 5% wt loss)*	*Theoretical[1] T_g (ºC)*	*Experimental[2] T_g (ºC)*
BPS-35	286	264	264
BPS-35/6F-00			
98/2	295	262	262
95/5	307	259	261
90/10	321	254	260
0/100	485	194	194
BPS-35/6FS-35			
98/2	355	263	276
95/5	367	262	271
90/10	371	260	263
0/100	400	235	235
BPS-35/6FPPO			
98/2	310	262	262
95/5	326	260	260
90/10	315	256	259
0/100	479	207	207

2. Theoretical calculations were determined using the Fox equation; $1/T_g = (w_a/T_{ga}) + (w_b/T_{gb})$ where w_a is the weight fraction of BPS-35 in the blends, T_{ga} is the glass transition temperature of BPS-35, w_b is the weight fraction of fluorine containing copolymer in the blends and T_{gb} is the glass transition temperature of the fluorine containing copolymer.
3. Experimental T_g were determined from DSC, 2nd heat 10 ºC /min.

3.2. Influence of Semi-crystalline Structure

Poly(vinylidene fluoride) ($PVDF_2$) is a very useful thermoplastic that combines an excellent chemical resistance and good physical and thermal stability. The properties of BPS-35 and $PVDF_2$ blends are listed in Table 3-5.

Low concentrations (5 wt%) of $PVDF_2$ resulted in cloudy membranes. Both the acid and salt forms of these membranes became opaque at concentrations above 5 wt%. The opaqueness of these membranes is directly related to poor optical clarity of $PVDF_2$ due to its crystalline nature.

Table 3-5. Properties of BPS-35/ $PVDF_2$ blends

Blend Ratio (wt%)	***BPS-35 /$PVDF_2$***			
	Clarity (Salt)	*Clarity (Acid)*	*Water Uptake (wt%)*	*Conductivity[1] (S/cm)*
100 : 0	T	T	39	0.08
98 : 2	C	C	33	0.07
95 : 5	C	C	29	0.07
90 : 10	C	O	27	0.05
80 : 20	O	O	24	0.04
0 : 100	C	C	0	0

a. The appearance of membrane upon direct release from glass substrate.
b. The appearance of membrane after undergoing Method 2 acidification.
c. The abbreviations for each membrane indicate the level of optical clarity observed where T = transparent; C = cloudy; O = opaque.
d. Proton conductivity measurements were carried out at 30 ºC in DI H_2O.

Figure 3-4 shows the TM-AFM phase images of BPSH-35/$PVDF_2$ blends with increasing $PVDF_2$ concentration. As with the amorphous copolymer, no phase separation was observed when 10 wt% of $PVDF_2$ was introduced into the blend. The water uptake and proton conductivities decreased with increasing $PVDF_2$ concentration. As with blends of BPS-35 with 6FS-00 or 6FS-35, a decrease in the water jguptake and proton conductivities with increasing $PVDF_2$ concentration were observed. Furthermore, the conductivities of these samples at 30 ºC in liquid water remained unchanged, as the concentration of $PVDF_2$ was increased from 2 to 10 wt%.

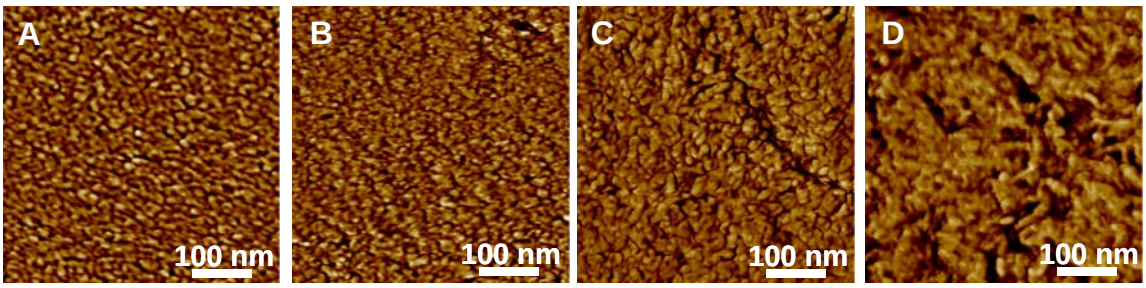

Figure 3-4. TM-AFM phase images of A) BPSH-35; B) BPSH-35/$PVDF_2$ (98/2) blend membrane; C) BPSH-35/$PVDF_2$ (90/10) blend membrane; D) $PVDF_2$

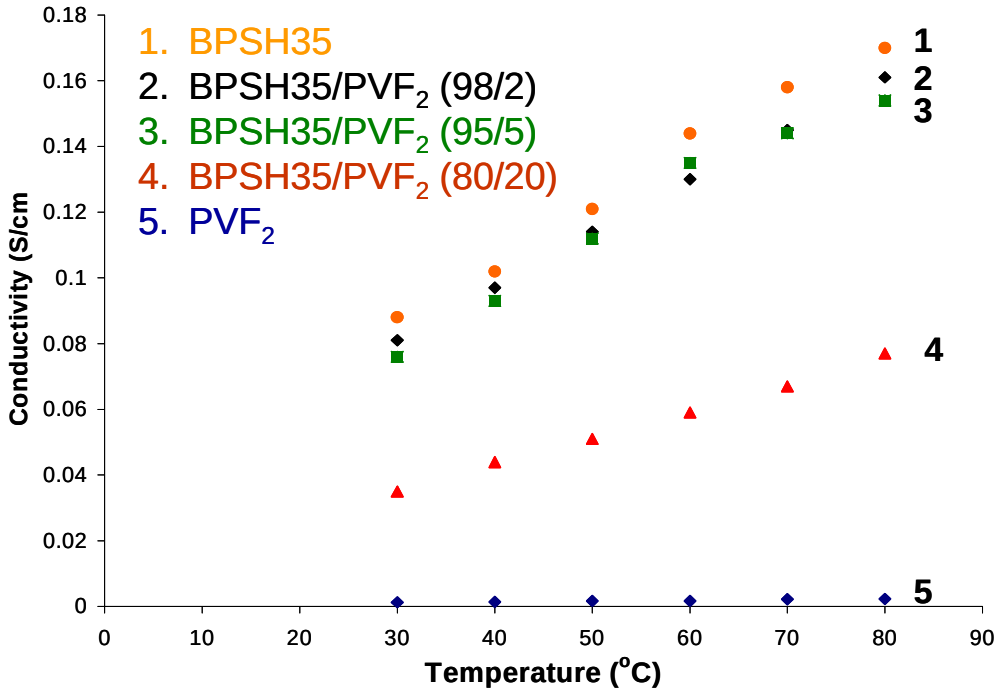

Figure 3-5. Proton conductivity vs. temperature curve for BPSH-35/$PVDF_2$ blends in liquid water

In spite of a similar trend in the proton conductivities from 30 to 80 ºC (Figure 3-5), a large reduction in proton conductivity even at elevated temperature due to

decreasing polymer-polymer compatibility and increasing hydrophobic character was demonstrated by the blends containing 20 wt% of $PVDF_2$.

4. Conclusions

A series of copolymer blends composed of various weight percent of 6F-00, 6FS-35, 6FPPO, and $PVDF_2$ to BPS-35 have been made. Low weight percentages (0-5 wt%) of the 6F-00, 6FS-35, and 6FPPO moieties in BPS-35 resulted in transparent films. Both the acid and salt forms of $PVDF_2$ blended membranes became opaque at concentrations above 5 wt%. As seen by TM-AFM, the partially fluorinated copolymers are compatibility with BPS-35 up to 10 wt%. The water uptake of the blends decreased with increasing the ratio of the partially fluorinated moieties, but a modest decrease in the proton conductivities was observed. Higher incorporation of the partially fluorinated resulted in modest shifts to the T_g of the blends

CHAPTER 4. DIRECT METHANOL FUEL CELL PERFORMANCE OF POLY(ARYLENE ETHER SULFONE) BLEND MEMBRANES

Natalie Y. Arnett[a], William L. Harrison[b], Melinda Einsla[c], and James E. McGrath[a]

[a]Macromolecules and Interfaces InstituteVirginia Polytechnic Institute and State University, Blacksburg, VA 24061

[b]NanoSonic, Inc, 1485 South Main Street, Blacksburg, Va. 24060

[c]Los Alamos National Laboratories, Los Alamos, NM 87545

Abstract

This chapter reports the results of the investigated DMFC properties of the BPS-35 blend with 6F-00, 6FS-35, 6FPPO and Kynar®. The introduction of 10 wt% of the fluorinated copolymers caused considerable reduction in methanol permeability compared to Nafion 1135. The introduction of 10 wt% 6F-00 showed very promising fuel cell performance similar to Nafion® 212 at a 0.5 M methanol feed concentration. The high frequency resistance (HFR) of the Nafion® membrane was 0.080 cm^2, while that of BPS-35/6F-00 (90/10) blend membrane was 0.081 cm^2. As the methanol increased from 0.5 to 5 M. this membrane began to out perform Nafion® 1135. Nafion® 1135 performance at 5 M is so poor due to its low methanol tolerance that it can no longer be found on the performance curve. All the other blended membranes however, had much higher HFRs and thus poorer performance than both Nafion and BPSH-35.

BPSH-35/6FS-00 (90/10) membrane also displayed better performance than the BPSH-35.

1. **Introduction**

Direct methanol fuel cells (DMFCs) are being investigated worldwide as attractive power sources for small portable electronics[1334]. DMFCs convert chemical energy from methanol directly into electrical energy using a series of electrochemical redox reactions. Perfluorinated sulfonic acid copolymers, such as Nafion® produced by DuPont, are the most widely used proton exchange membranes (PEMs) in fuel cells. The use of many perfluorinated membranes in DMFCs is limited due to high methanol permeability that causes fuel waste and significant loss of performance at the cathode.

Many alternative nonfluorinated and partially fluorinated membranes such as the series of disulfonated poly(arylene ether sulfone) (PAES) random copolymers have been reported by McGrath et al.[335, 336]. These cheap materials have higher operation temperatures and lower methanol permeabilities[337].

The purpose of this chapter is to report the DMFC properties of the blended BPS-35 with 6F-00, 6FS-35, 6FPPO and Kynar® membranes. The effect of the various chemical structures and their concentration in the blends on fuel cell performance will also be described. The chemical structures of these copolymers were presented in Chapter 3 (Figure 3-1).

---

[334] M. Zalbowitz, S. Thomas. Fuel Cells: Green Pwer, Department of energy, 1999, LA-UR-99-3231

[335] Harrison, W.L.; Wang, F.; Mecham, J.B; Bhanu, V.A.; Hill, M.; Kim, Y. S.; McGrath, J. E. *J Polym Sci Part A: Polym Chem* **2003**, 41, 2264-2276.

[336] A. Roy, M.A. Hickner, X. Yu, Y. Li, T.E. Glass, J.E. McGrath, *J. Polym. Sci. B: Polym. Phys.* **2006,** 44, 2226–2239;

[337] Hickner. M. A.; Ghassemi, H.; Kim, Y. S.; Einsla, B. R.; McGrath, J.,E.; Alternative Polymer Systems for Proton Exchange Membranes (PEMs) *Chem. Rev*., **2004,** 104, 4587-4612.

2. **Experimental**

Membrane electrode assemblies (MEAs) of the acidified membranes were prepared from standard catalyst inks using unsupported Pt–Ru catalyst for anode and Pt catalyst for cathode as developed at Los Alamos National Laboratory[8]. The anode and cathode catalyst loading was approximately 9 Pt/Ru and 6 Pt mg/cm^2, respectively. Limiting methanol crossover currents through the membrane inside a cell were measured to estimate methanol permeability. DMFC performance was conducted at a cell temperature of 80 °C. Methanol solutions between 0.5 and 5 M were fed into the anode, while humidified nitrogen at 500 sccm and ambient pressure was supplied to the cathode.

3. **Results and Discussion**

High methanol permeability (methanol crossover) is one of the major draw backs of current PEM.[338] Methanol crossover in the PEM causes a decrease to the overall cell efficiency and lifetime. The reaction of methanol at the cathode results in a loss of fuel and cathode voltage and is referred to as a mixed potential. Figure 4-1 illustrates that the introduction of 10 wt% of the fluorinated copolymers caused considerable reduction in methanol permeability compared to Nafion 1135.

[338] Deluca, Nicholas W., Elabd, Y.A. *J. Polym. Sci. Part B: Polym. Phys.* **2006,** 44, 2201–2225.

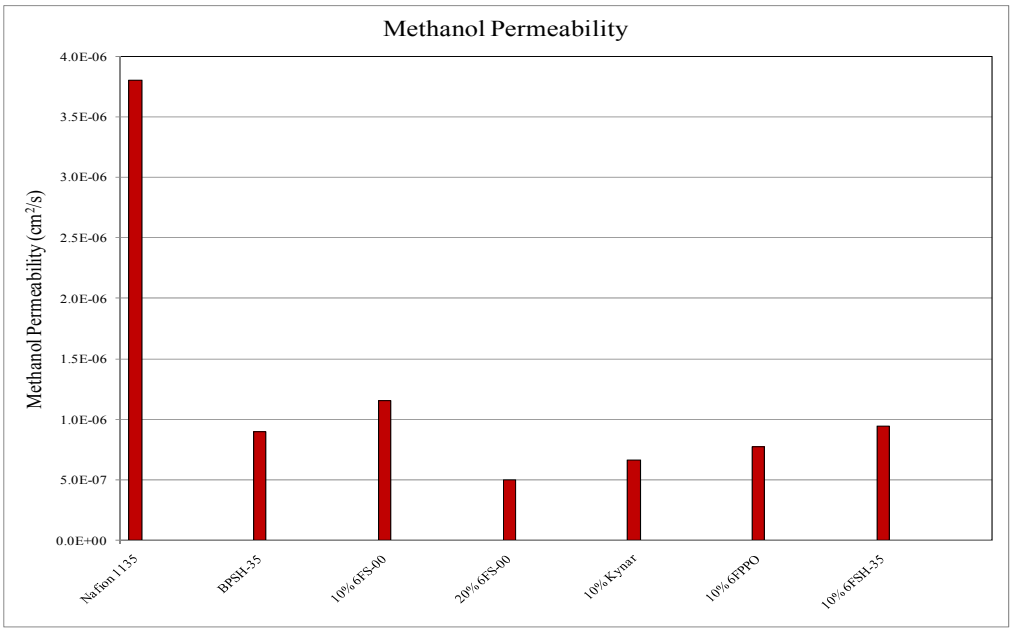

Figure 4-1. Effect of fluorinated copolymers incorporations on methanol permeability

Several researchers have proposed that the incompatibility and excessive swelling of many hydrocarbon based poly(arylene ether)s sulfonated membranes to typical perfluorosulfonic acid electrodes may cause the delamination of the electrode layer from the membranes and the reduction in fuel cell performance.[339, 340] Figure 4-2 shows that the introduction of 10 wt% 6F-00 showed very promising fuel cell performance similar to Nafion® 212 at a 0.5 M methanol feed concentration. The high frequency resistance (HFR) of the Nafion® membrane was 0.080 cm^2, while that of BPS-35:6F-00 (90:10) blend membrane was 0.081 cm^2. Additionally, this membrane also displayed better performance than the BPSH-35 as shown by the lower HFR value. Lower HFR values lead to higher proton conductivity and better adherence of membranes to electrodes.[341]

[339] M.S. Wilson, Membrane catalyst layer for fuel cells, US Patent 5211984, **1993**.
[340] S. Mukerjee, et al, *Journal of Membrane Science* **2003,** 219, 123-136.
[341] Cornelius, C., Fujimoto, Cy. H., Hickner, M. DOE Hydrogen Program: *FY 2005 Progress Report*, 804-810.

Superior fuel cell performance of fluorine containing copolymers due to decreased ohmic losses compared to the BPS-30 control has been previously reported[333]. This improved performance could also be attributed to enhanced compatibility between the partially fluorine component in the blends and the Nafion electrodes. However as shown in Table 4-1 all the other blended membranes had much higher HFRs and thus poorer performance than both Nafion and BPSH-35. The inferior performance of these membranes could be attributed to their lower proton conductivity and IEC values.

Table 4-1. Summary of Open Circuit Voltage (OCV) and High Frequency Resistance (HFR) of BPS-35 blends with Fluorine Containing Polymers compared to Nafion® 212.

Polymer (wt%)	***OCV (V)***	***HFR (W-cm^2)***
Nafion® 212	0.81	0.080
BPSH-35	0.81	0.096
10% 6FS-00	0.80	0.081
20% 6FS-00	0.80	0.232
10% Kynar	0.85	0.187
10% 6FPPO	0.85	0.172
10% 6FSH-35	0.81	0.100

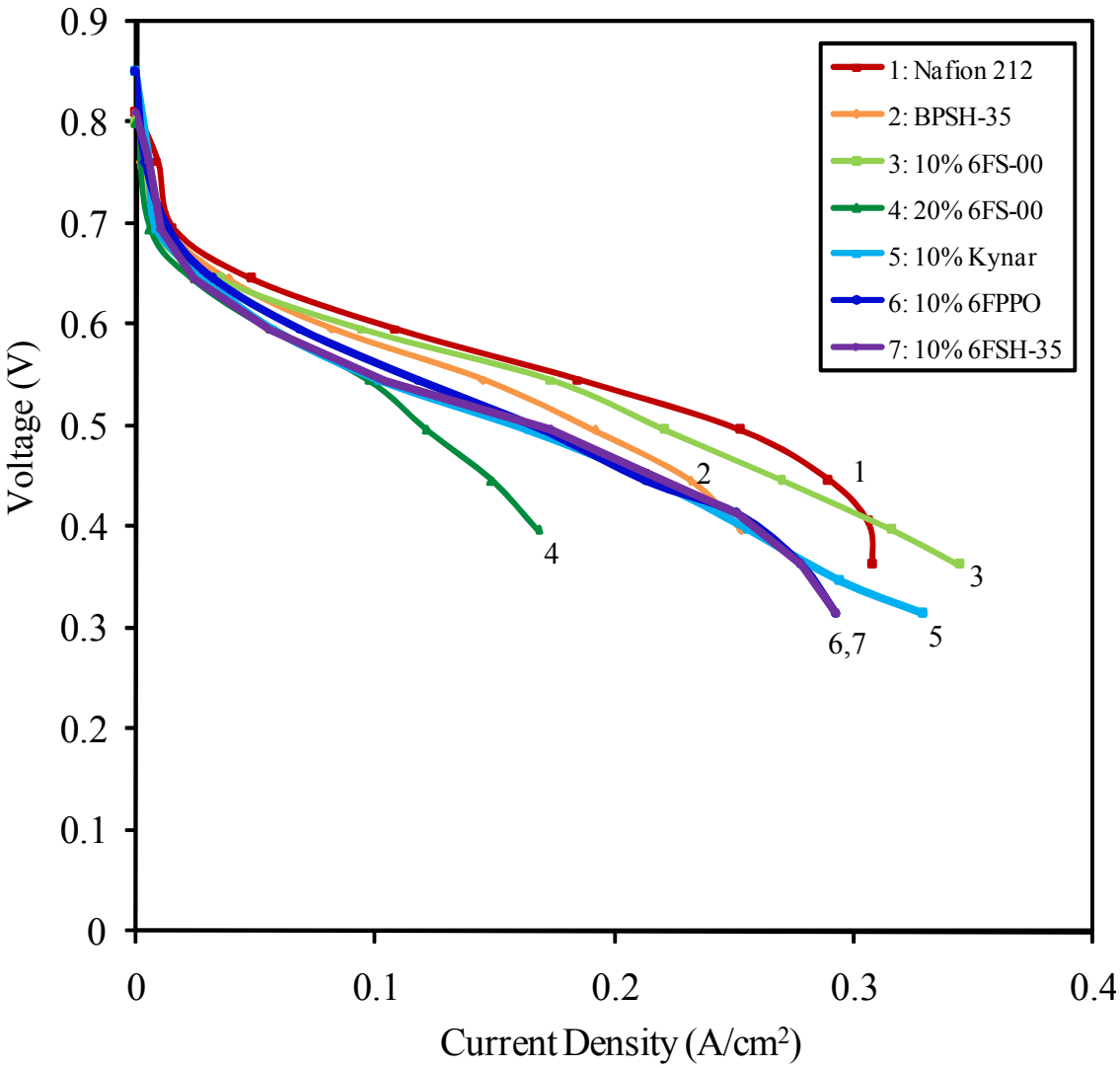

Figure 4-2. Effect of fluorinated copolymers incorporations on DMFC performance 0.5 M in methanol at 80 °C

Typically, low methanol concentrations (0.5 M) are used in the DMFC to combat high methanol crossover. However, low methanol concentrations limit the overall cell potential. If higher methanol concentration could be used a significantly higher cell voltage could be achieved. Figure 4-4 shows the influence of methanol concentrations on

blends with 10 and 20 wt% of 6FS-00. These membranes were compared to both Nafion 1135 and BPSH-35. As shown, the introduction of 10 wt% 6FS-00 showed comparable performance to Nafion® 1135 and BPSH-35 in 0.5 M methanol. As the methanol increasing from 0.5 to 5 M,. this membrane began to out performed Nafion® 1135. Nafion® 1135 performance at 5 M is so poor due to its low methanol tolerance that it can no longer be found on the performance curve. The poor performance of the blend membranes containing 20 wt% of 6FS-00 is due to phase separation between BPS-35 and 6FS-00 which occurs at this concentration as illustrated by the appearance of a second T_g (See).

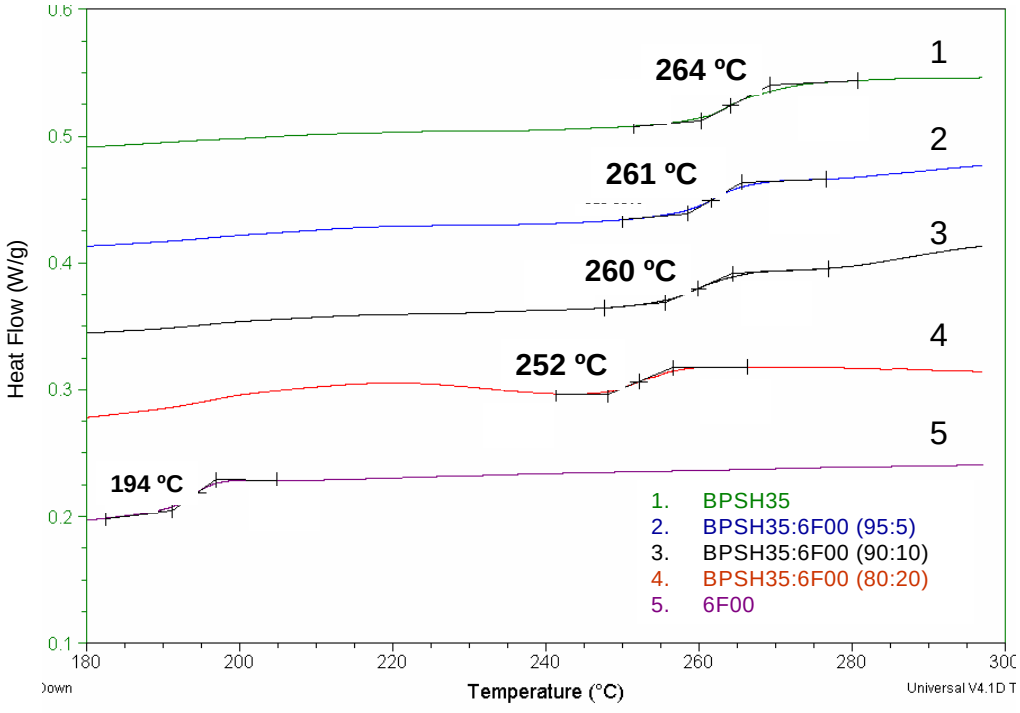

Figure 4-3. Influence of weight fractions on thermal transition on acid form BPSH-35/6FS-00 membranes.

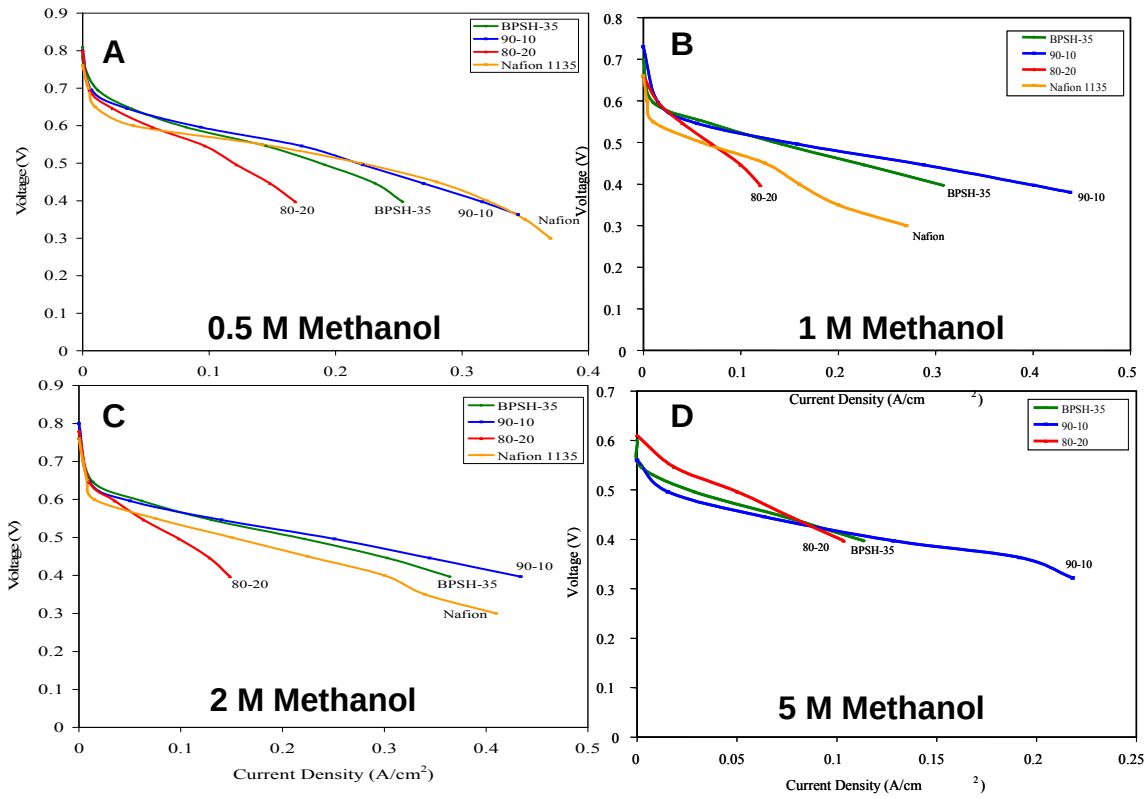

Figure 4-4. The influence of increasing methanol concentration on BPSH-35/6FS-00 blend membranes

5. Conclusions

DMFC performance of the 10 wt% 6F00 exhibited comparable performance to Nafion 212 and 1135. Better fuel cell performance was illustrated at higher methanol concentrations. The introduction of 10 wt% of the fluorinated copolymers caused considerable reduction in methanol permeability. However, phase separation in the membranes with 20wt% 6FS-00 resulted in poor DMFC performance. Methanol permeability lower than Nafion 1135 was observed in all the blends

CHAPTER 5. PREPARATION AND CHARACTERIZATION OF CHLORINE-RESISTANT DISULFONATED POLY(ARYLENE ETHER SULFONE) BLEND MEMBRANES FOR REVERSE OSMOSIS AND NANOFILTRATION

Natalie Y. Arnett[a], Ho Bum Park[b], Benny Freeman[b], and James E. McGrath[a]

[a]Macromolecules and Interfaces Institute

Virginia Polytechnic Institute and State University, Blacksburg, VA 24061

[b]Department of Chemical Engineering

The University of Texas at Austin, Austin, TX 78712

Abstract

The susceptibility of commercially available polyamide membranes to chlorine attack is one of the major drawbacks of the reverse osmosis industry. Disulfonated biphenol based poly(arylene ether sulfone)s (BPS-XX) which have shown excellent chlorine resistances are an attractive alternative to polyamide membranes. Blends of biphenol-based disulfonated poly (arylene ether sulfone) random copolymer (BPS-35) with hexafluoroisopropylidene bisphenol based sulfonated poly (arylene ether sulfone) copolymers (6FS-XX) and commercially available Radel R have been prepared. Blend membranes have been analyzed in both the potassium salt and acid forms. In the salt form these membranes displayed good sodium chloride salt rejections above 92%. The highest salt rejections of 97.2 and 98.0% were obtained from BPS35:Radel R (90:10) and BPS-35:6FS-35 (95:5) blends, respectively.

1. Introduction

Reverse osmosis and nanofiltration membranes have been developed for the purification of drinking water, wastewater treatment, and separation of nonaqueous solutions. Generally, NF membranes are prepared from charged polymers containing carboxylic or sulfonic groups while RO membranes are prepared from non-ionic materials such as cellulose acetate, polyamide, and polysulfones[342]. NF membranes have been development in the RO area because these membranes typically have much higher water fluxes at low pressures and good rejection of organic compounds compared to traditional RO membranes. The differences in salt rejection mechanism for NF membranes are responsible for the improvements in membrane performance.

Salt rejection of RO membranes are based on assumptions from the solution-diffusion model (SDM) whereas the major factor in determining salt rejection in NF ("loose RO") membranes is both molecular size and Donnan exclusion (ion repulsion)[121]. Donnan exclusion is the phenomenon where charged groups tend to exclude ions of the same charge while being freely permeable to ions of the opposite charge[343]. Also called low-pressure reverse osmosis membranes, NF membranes lose their selectivity at salt concentrations above 1000 or 2000 ppm salt in the feed water and high pressures.

The most common membranes for RO and NF are thin film composites comprised of interfacially polymerized polyamide on a porous polysulfone (UDEL) support. One of the major disadvantages of commercially available polyamide membranes is their susceptibility to undergo chlorine attack. Disulfonated poly(arylene ether sulfone)s which have shown excellent chlorine resistances are an attractive alternatives to

[342] Peeters, J.M.M., Boom, J.PMulder,., M.H.V., H. Strathmann *J. Membr. Sci.* **1998,** 145, 199-209.
[343] Frederick George Donnan. *J. Membr. Sci.* **1995,** 100, 45-55.

polyamide membranes[172]. These researchers demonstrated that increasing the sulfonation level in disulfonated copolymers would increase the water permeability but an increase in salt passage due to excessive swelling also occurs. A decrease in salt rejection at with increasing degree of sulfonation was also recorded.

In this research the preparation and characterization of chlorine-resistant disulfonated poly(arylene ether sulfone) blend membranes will be studied. Blends of biphenol-based disulfonated poly (arylene ether sulfone) random copolymer (BPS-35) with hexafluoroisopropylidene bisphenol based sulfonated poly (arylene ether sulfone) copolymers (6FS-35) and commercially available Radel R have been prepared. Previous research has focused on utilizing these blends in PEMFC. PEMFC studies into a series of disulfonated random copolymer blends composed of varying weight percent biphenol based disulfonated PAES (BPS-35) with fluorine containing polymers and Radel R exhibited good miscibility between the polymers and reduced water uptakes as the concentration of unsulfonated polymer was increased from 2 to 10 wt.%[7]. The reduction in the water uptake for these membranes could also cause an improvement in the salt rejection

2. Experimental

2.1. Materials

4,4'-Hexafluoroisopropylidenediphenol (6F BPA), received from Ciba, was purified by sublimation and dried under vacuum. Solvay Advanced Polymers supplied highly purified 4,4'-dichlorodiphenylsulfone (DCDPS) and polyphenylene sulfone

(Radel®). 4,4'-Dichlorodiphenylsulfone was dried at 60 ºC under vacuum before each use. N-Methyl-2-pyrrolidinone (NMP) (Aldrich) was vacuum distilled from calcium hydride onto molecular sieves, then stored under nitrogen. N,N-Dimethylacetamide (DMAc) (Aldrich) was distilled under vacuum from phosphorous pentoxide and stored over molecular sieves under nitrogen. Potassium carbonate was vacuum-dried at 150 ºC prior to polymerization. Toluene obtained from Aldrich was used as received.

2.2. Copolymer Synthesis by Direct Copolymerization

Similar copolymerization procedures were used to synthesize the BPS-35 and 6FS-35 copolymers. These procedure have been previously reported.[308,309]

2.3. Polymer Blending and Membrane Acidification

Separate solutions of the copolymers at different weight ratios were prepared in DMAc (5 wt/v%). The 6F copolymer solutions were added to BPS-35 solutions and stirred or 80 °C for 1 h. Solutions were filtered through a 0.45 μm PTFE filter onto clean glass substrates. The membranes were dried gradually via a heating lamp for 24 h and then under vacuum at 100 °C for 24 h. Blend membrane systems were converted from the potassium salt form to the acid form by first boiling in 0.5 M H_2SO_4 for 2 h and immediately followed by extraction in boiling deionized water for 2 h as described earlier.[311]

2.4. Characterization

The clarity of the blended membranes was obtained from qualitative visual observations. The blended membranes were characterized in both the salt and acid forms to understand the effect of hydrothermal treatment (Method 2 acidification).

The water uptake of the blended membranes was performed by immersing the membranes in deionized water at room temperature for 24 h. The wet membranes were then blotted to remove surface water droplets and quickly weighed. These membranes were then vacuum dried at 90 ºC for 24 h and weighed again. The water uptake (%) of the membranes was calculated by:

$$WaterUptake = \frac{W_{wet} - W_{dry}}{W_{dry}} \times 100\% \qquad 1$$

where W_{wet} is the weight of the wet membrane and W_{dry} represents the weight of the dry membrane.

Tapping Mode Atomic Force Microscopy (TP-AFM) images of the blends were obtained using a Digital Instruments MultiMode scanning probe microscope with a NanoScope IVa controller. A silicon probe (Veeco) with an end radius of <10 nm and a force constant of 5 N/m was used to image samples. Samples were dried under vacuum at 100 °C for 12 h and then equilibrated at 50% relative humidity for at least 12 h before being imaged immediately at room temperature in a relative humidity of approximately 15-20%.

Water and salt transport properties were determined using a Millipore MilliQ system (Billerica, MA). The water permeability was measured in a high-pressure (up to 1000 psi) dead-end filtration system (Sterlitech TM HP4750 stirred cell, Sterlitech Corp., WA) and calculated using

$$P_W = \frac{V \cdot l}{A \cdot t \cdot \Delta p}$$

where P_w is the water permeability,V is the volumetric water flux, t is the unit time, A is the area of the membrane, l is the membrane thickness and Δp is the difference in pressure.

Salt rejection experiments using NaCl were conducted in a dead-end system using feed solutions containing 2000 mg L^{-1} of NaCl (2000 ppm). The salt rejection (R) was calculated as a function of the salt concentration in the permeant (C_{jl}) and the salt concentration in the feed water (C_{jo}) using a digital conductivity meter (Oakton® CON 110, Cole Parmer, Vernon-Hills, NJ). The salt rejection were measure using

$$R = \frac{1 - c_{jl}}{c_{jo}} \times 100\%$$

and the data was reported at a feed pressure of 1000 psig (approximately 70 bar); the permeant pressure was atmospheric.

3. Result and Discussion

Tough, ductile polymer blend membranes were obtained from DMAc solutions. BPS-35 was blended with various weight percentages of the Radel® R or 6FS-35. As shown by TM-AFM in Figure 5-1, the incorporation of up to 10 wt% of Radel in the blends showed no obvious regions of phase separation. Above 20 wt% visible regions of macrophase separation was observed. All the films were analyzed in both the salt and acidified form.

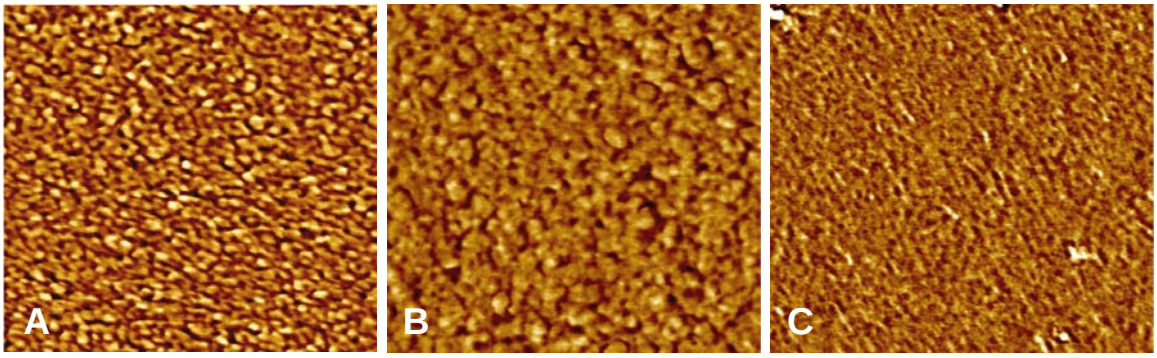

Figure 5-1. TM-AFM Phase Images of BPSH-35 with 10 wt% Radel R. Image A represents BPSH-35; B represent 10 wt% Radel; C represents Radel R

The optical clarity of the membranes was inspected visually as a preliminary means of identifying compatibility between the polymers. Observation of clarity of BPS-35/Radel R and BPS-35/6FS-35 blended membranes in salt and acid form are listed in Table 5-1 and Table 5-2, respectively. Low weight percentages (0-5 wt%) of the 6FS-35 in BPS-35 resulted in transparent films in both the salt and acid form. As the amounts of 6FS-35 increased to 10 wt%, some hazing on the outer edges of the membranes in the salt form was observed. After acidification these membranes became cloudy. The addition of 5 to 10 wt% of Radel into the blends yielded cloudy membranes in the salt form. However, these membranes became transparent after undergoing Method 2 acidification. Higher ratios (> 10 wt%) of 6FS-35 and Radel into the blends resulted in opaque films with large regions of *macrophase* separation.

Table 5-1. Properties of BPS-35/Radel R blend membranes

BPS35: BP00 Blend ratio	***Clarity***	***Water Uptake***	***Water permeability***	***NaCl rejection***

(wt%)		*(wt%)*	*(L·μm/m^2·h·bar)*	*(%)**
BPS35 (acid)	T	39	2.52	86.2
98:2 (acid)	T	35	3.45	86.8
95:5 (acid)	T	31	3.14	87.3
90:10 (acid)	T	21	2.20	90.2
BPS35 (salt)	T	17	0.35	94.9
98:2 (salt)	T	15	1.69	94.5
95:5 (salt)	C	15	1.24	95.8
90:10 (salt)	C	12	0.71	97.2

a. The appearance of membrane upon direct release from glass substrate.
b. The appearance of membrane after undergoing Method 2 acidification.
c. The abbreviations for each membrane indicate the level of optical clarity observed where T = transparent; C = cloudy.

Table 5-2. Properties of BPS-35/6FS-35 blend membranes

BPS35: 6FS-35 Blend ratio (wt%)	***Clarity***	***Water Uptake (wt%)***	***Water permeability (L·μm/m^2·h·bar)***	***NaCl rejection (%)****
BPS35 (acid)	T	39	2.52	86.2
98:2 (acid)	T	33	4.15	86.3
95:5 (acid)	H	28	5.24	85.7
90:10 (acid)	C	24	4.23	83.4
BPS35 (salt)	T	17	0.35	94.9
98:2 (salt)	T	16	0.95	93.5
95:5 (salt)	T	15	0.86	98.0
90:10 (salt)	C	15	0.83	92.6

a. The appearance of membrane upon direct release from glass substrate.
b. The appearance of membrane after undergoing Method 2 acidification.
c. The abbreviations for each membrane indicate the level of optical clarity observed where T = transparent; H = white discoloration on membrane outer edges; C = cloudy.

Water uptake as a function of blend compositions was investigated and a summary of the hydrated properties of these blends is listed. (See Table 6-1 and Table 5-2). As expected the water uptake of the blended membranes in the salt form were

lower than those in the acid form. In both cases, a decrease in the water uptake was observed as the concentration of the Radel R and 6FS-35 was increased.

The water permeability and salt rejection properties of BPS-35/Radel R blend membranes in the salt and acid form are presented in Figure 5-2. The numerical values corresponding to these properties are recorded in Table 5-1. The figure shows that in the blend membranes, as the concentration of the Radel R increases from 2 to 10 wt%, water permeability through the membrane decreases. This is true in both the salt and acid forms and was due to the increase in hydrophobic nature of the membrane as the content of the Radel R increases.

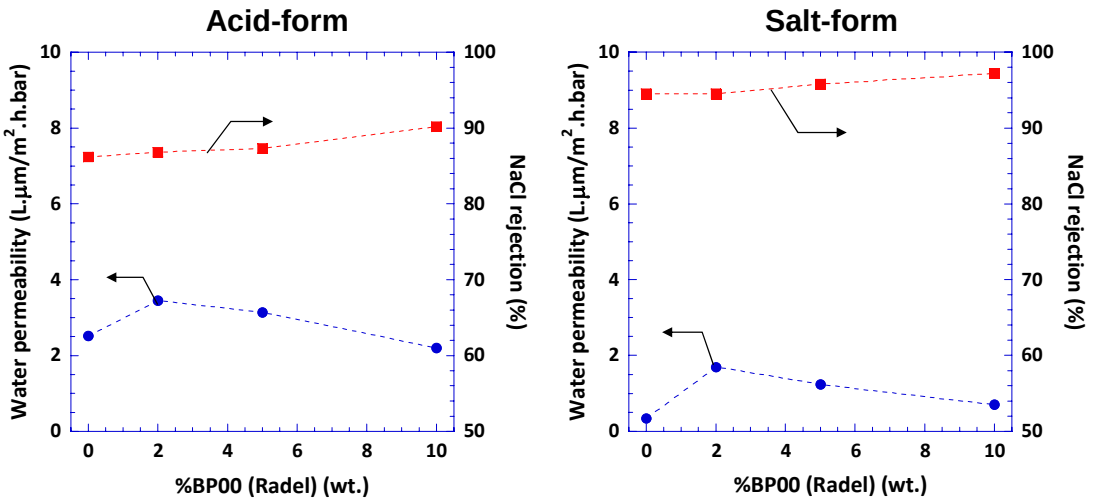

Figure 5-2. Water permeability and salt rejection properties of BPS-35/Radel R blend membranes in the salt and acid form.

Higher water fluxes were observed for the acidified membranes. The water permeability of these membranes increased from 3.4 to 2.2 L·µm/m^2·h·bar as the concentration of Radel R increased from 2 to 10 wt%, respectively. The higher water permeability for the

acidified membranes was due to the formation of larger hydrophilic domains that increased the hydrophilicity of the acidified membranes[344]

Figure 5-1 also demonstrates that increasing the concentration of Radel R caused an increased in the NaCl rejection. Salt rejection of the blend membranes was measured using a 2000 ppm NaCl in a crossflow filtration at a 400 psi and 25 ºC. Unlike the water permeability, the highest salt rejection values were obtained from the blend membranes in the salt form. The reduction in the water uptake that essentially decreased salt passage through the membrane was responsible for the higher salt rejections at higher concentrations of Radel R. Salt rejections over 80% were observed for all of the acidified membranes while the salt rejection of the membranes in the salt form was above 90%[121]. Thus the use of these blends in NF and RO is possible since the salt rejection in nanofiltration membranes is typically between 20 and 80% while the salt rejection of RO membranes is above 90%. The highest salt rejection of 97.2 % were obtained from BPS35:Radel R (90:10) blend.

As shown in Figure 5-3 and Table 5-2, higher water permeabilities and lower salt rejection were also observed for the BPS-35/6FS-35 acidified membranes. However, these blends did not follow a particular trend in terms of 6FS-35 concentration. This is illustrated by BPS-35/6FS-35 (95/5) acidified membranes showing higher water permeabilities than BPSH-35 and the BPS-35/6FS-35 (98/2) membranes. In the salt form BPS-35/6FS-35 (95/5) membrane also demonstrated the highest salt rejection of 98% while the lowest salt rejection (92.6%) was shown by BPS-35/6FS-35 (90/10) blend membranes. The irregularity in water permeability may be a result of changes in the

[344] Y.S. Kim, F. Wang, M. Hickner, S. McCartney, W.L. Harrison, Y.T. Hong, T.A. Zawodzinski, and J.E. McGrath, *J. Polym. Sci., Part B: Polym. Phys.,* **2003,** 41, 2816-2828.

thickness of the membranes. Boussu et al[144] illustrated that membranes with thinner top layer (~0.5 µm) had higher water permeability (19 L·µm/m^2·h·bar) than membranes that had thicker skin layer (~3 µm) that had water permeability of 10 L·µm/m^2·h·bar. Since thinner membranes correspond to higher water permeability, the increase in water permeability for the BPS-35/6FS-35 (95/5) membranes could have been due to these membranes were thinner.

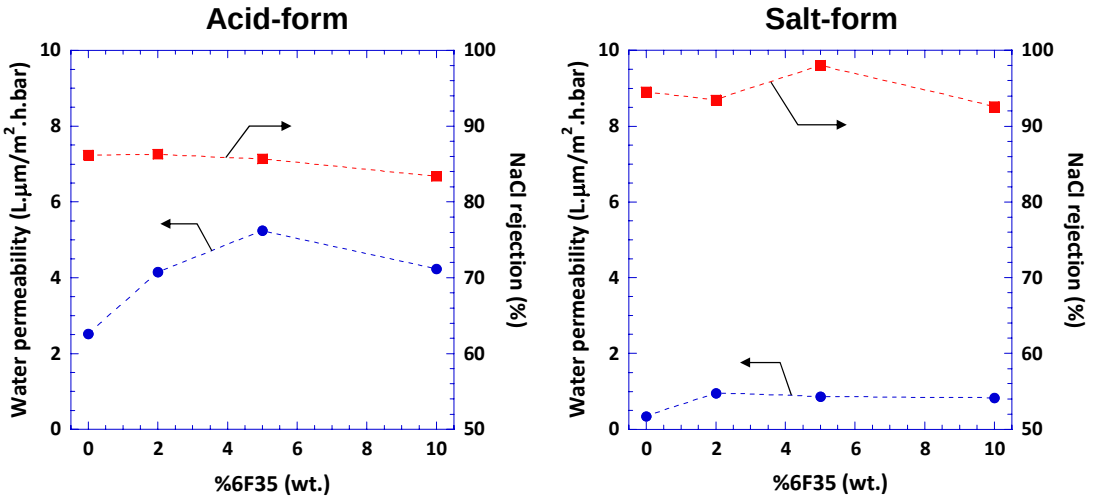

Figure 5-3. Water permeability and salt rejection properties of BPS-35/6FS-35 blend membranes in the salt and acid form.

4. Conclusions

Tough, ductile polymer blend membranes between BPS-35 with 2–10 wt% of Radel® R or 6FS-35 were prepared. As expected the water uptake of the blended membranes in the salt form was lower than those in the acid form. However, a decrease in the water uptake as the concentration of the Radel R and 6FS-35 was increased was observed in

both membranes. Higher water permeabilities and lower salt rejection values were also observed for the acidified blend membranes. In BPS-35/Radel R membranes the changes water permeabilities and salt rejection were a function of blend ratio with 10 wt% of Radel R demonstrating the lowest water permeability but highest salt rejection in the salt form. The opposite effect was observed for acidified membranes. No particular trend in terms of 6FS-35 concentration was observed.

CHAPTER 6. PREPARATION AND CHARACTERIZATION OF ASYMMETRIC DISULFONATED POLY(ARYLENE ETHER SULFONE) MEMBRANES BY DIFFUSION INDUCED PHASE SEPARATION PROCESS: PART I – Preparation of Asymmetric Membrane Via Polar Aprotic Solvent

Natalie Y. Arnett, Chung Hyun Lee, Ozzie Lane, and James E. McGrath

[a]Macromolecules and Interfaces InstituteVirginia Polytechnic Institute and State University, Blacksburg, VA 24061

Abstract

Asymmetric membranes based on disulfonated biphenol based poly(arylene ether sulfone)s (BPS-20) from various polar aprotic solvents have been prepared by diffusion induced phase separation technique (DIPS). Polar aprotic solvents investigated include NMP, DMAc, DMF, and DMSO. The purpose of this research was to systematically study of the preparation of disulfonated poly(arylene ether sulfone) copolymer asymmetric membranes from polar aprotic solvents. Although the formation of an asymmetric morphology can be accomplished from all these solvents except DMSO, the appearance of macrovoids or finger-like projection were also observed. The occurrence of these macrovoids was reduced by increasing the drying temperature and concentration of the polymer solution.

Various coagulation baths were investigated to achieve suitable asymmetric morphology. The order of solvent (NMP)/non-solvent demixing from fastest to slowest to

form asymmetric membranes in different non-solvents was as follows: acetone > acetone:isopropyl alcohol (IPA) (50:50)> methyl ethyl ketone (MEK) > IPA> ethanol > methanol > methyl isobutyl ketone (MIBK) > acetone: water (H_2O) (50:50) ≥ H_2O. Different non-solvent mixtures comprised of water or IPA with acetone were also studied.

1. Introduction

Phase inversion occurs by bringing the initially thermodynamically stable polymer solution to an unstable state by solvent/nonsolvent exchange *during* the coagulation step. The resulting asymmetric membrane structure generally contains a defect free thin skin layer supported on a porous sublayer. The skin layer should be as thin (0.1 to 1 μm) as possible to maximize the membrane selectivity and productivity. The substructure should provide sufficient mechanical strength to support the delicate skin layer during high-pressure operation. This can be accomplished by eliminating macrovoids or fingerlike projection from the sublayer structure which collapse under pressure.

The importance of asymmetric membranes by diffusion induced phase separation (DIPS) was first demonstrated by Loeb and Sourirajan in 1963.[140] The formation of these membranes was accomplished by first dissolving the polymer in an appropriate solvent, followed by casting of the polymer solution onto a glass substrate. After some predetermined evaporation time, the substrate was immersed into a coagulation (non-solvent) bath to induce phase separation. Although relatively simple to prepare in concept, the formation of stable asymmetric structures from various polymers has been shown to be extremely complicated practically. The complexity of preparing asymmetric membranes lies in the ability to essentially alter the membrane morphology through various experimental parameters such as polymer concentration, solvent, or nonsolvent.

Kossau et al[144] illustrate the effect of some of these parameters on the structure of polyethersulfone (PES) asymmetric membranes from DMF or NMP. Asymmetric membranes with thinner top layers and higher water flux were achieved from NMP. Higher polymer concentrations in DMF lead to a less porous membrane with less fingerlike pores, an increase in the overall membrane thickness [14 wt% (50 μm) versus 20wt% (60 μm)], and lower water permability. The increase viscosity slowed down the diffusional exchange between solvent and non-solvent and leads to a higher polymer concentration at the interphase between polymer solution and non-solvent bath. A change in the polymer chemical structure from PES to polysulfone (PSU) generated larger pores but lower water fluxes.[345]

The purpose of this research was to develop a systematically study the preparation of disulfonated poly(arylene ether sulfone) (BPS-20) copolymer asymmetric membranes by DIPS. Asymmetric membranes were prepared from BPS-20 random copolymer to improve the overall water flux through the membranes that was shown to be extremely low for dense membrane (20 μm). Since the water permeability through a membrane is directly related the thickness, the formulation of asymmetric membranes with thin skin layers could improve the water flux with adversely effecting the salt rejection ,shown to be greater than 99 % for this copolymer. Several preparation factors based on various experimental parameters such as solvent choice, non-solvent bath, and polymer structure were studied to find the optimal conditions to obtain an asymmetric nanoporous membrane.

[345] C. Barth; M.C. Gonçalves; A.T.N. Pires; J. Roeder; B.A. Wolf. *Journal of Membrane Science* **2000,** 169, 287–299.

The characteristic solubility behavior and subsequent non-solvent selection for BPS-20 was used to generate three dimensional (ternary) solubility parameter diagrams developed by Hansen.[346] Hansen assumed that the total cohesive energy which holds a liquid together (energy of evaporation) can be divided into contributions from dispersion forces, E_d, permanent dipole-permanent dipole interactions, E_p, and hydrogen bonding E_h. Dividing each component by the molar volume of a solvent gives the following equation

$$\delta^2 = \delta_d{}^2 + \delta_p{}^2 + \delta_h{}^2$$

where δ is the overall solubility parameter, $\delta_d{}^2$ is the dispersive component of the solubility parameter, $\delta_p{}^2$ the permanent-dipole-permanent dipole component of the solubility parameter, $\delta_h{}^2$ the hydrogen bonding component of the solubility parameter. The subsequent solubility of the polymer was plotted in terms of each specific interaction (δ_d, δ_p, δ_h) of various solvents using a triangular graphing based on the first power relationship technique.[347]

$$F_i = \delta_i / (\delta_d + \delta_p + \delta_h)$$

where *i* represents is the subsequent dispersion, polar or hydrogen bonding component of the solubility parameter. The use of this first power relationship improves the distribution of points representing the organic liquids and leads to the generation of a "solubility envelope" for a particular polymer. A "solubility envelope" is the region of polymer solubility determined experimentally by various solvents that dissolve the polymer. Utilizing these three component solubility parameters in conjunction with ternary plots can facilitate a more efficient and precise selection of casting solution components and composition.

---

[346] Hansen, Charles M. *I & E C Product Research and Development* **1969,** 8(1), 2-10.
[347] J.P. Teas, Graphical analysis of resin solubilities, J. Paint Technol., **1968,** 40, 19-25.

2. Experimental

2.1. Materials

Eastman Chemical provided high purity 4,4'-biphenol (BP) which was dried at 50 ºC under vacuum before each use. Solvay Advanced Polymers supplied highly purified 4,4'-dichlorodiphenylsulfone (DCDPS), polyphenylene sulfone (Radel®), and polysulfone (UDEL®). 4,4'-Dichlorodiphenylsulfone was dried at 60 ºC under vacuum before each use. N-Methyl-2-pyrrolidinone (NMP) (Aldrich), N,N-Dimethylacetamide (DMAc), dimethylformamide (DMF), dimethylsulfoxide (DMSO) were purchased from Aldrich and used with further purification. All of the non-solvents evaluated were used with further purification and purchased from either Fisher Scientific or Aldrich. The detailed synthesis of 3,3'-disulfonate-4,4'-dichlorodiphenylsulfone monomer (SDCDPS) has been reported [9]

2.2. Non-solvent Selection

Solutions (30 wt%) of BPS-20 were prepared in NMP. BPS-20 solution was coated onto a glass stirring rod and immersed in the various non-solvents at room temperature for phase inversion. Large asymmetric membranes were only prepared from non-solvents that illustrated fast coagulation. The solutions were cast onto glass plates and dried with an IR lamp at 35 ºC for 30 min. The membranes were coagulated in a

non-solvent 1 hour and placed in DI water at RT for 24 hours. The membranes were dried at room temperature for 24 hours.

2.3. Solvent Selection

Solutions (30 wt%) of BPS-20 were prepared in various polar aprotic solvents (NMP, DMAc, DMF, and DMSO). Upon dissolution, the mixtures were placed in the cold room for 24 hours to remove air bubbles. The solutions were then cast onto glass plates, smoothed with a doctor blade **(**0.381 mm**),** and dried with an IR lamp at 35 ºC for 30min. The membranes were coagulated in acetone for 1 hour and placed in DI water at RT for 24 hours. Finally the membranes were dried at room temperature for 24 hours.

2.4. Influence of polymer concentration, drying time and drying temperature

Disulfonated biphenol based poly(arylene ether sulfone)s asymmetric membranes dissolved in NMP were studied as function of the drying time, concentration, and drying temperature. The experimental procedures for each parameter are presented below. To study the effect of polymer concentration solutions (25, 30, 35, and 40 wt%) of BPS-20 were prepared in either NMP. Next the solutions were cast onto glass plates and dried with an IR lamp at 35 ºC for 30 minutes.

The influence of drying time was accomplished by first preparing solutions (25 wt%) of BPS-20 were prepared in NMP. The solution was cast onto glass plates and dried with an IR lamp at 35 ºC for 30, 45, or 60 min.

The effect of drying temperatures was determined using a 30 wt% solution of BPS-20 prepared in NMP. The solutions were cast onto glass plates and dried at room temperature or with an IR lamp at 35 or 45 ºC for 30.min.

All the membranes were then coagulated in acetone for 1 hour and placed in DI water at RT for 24 hours after each parameter was modified. Lastly, the membranes were dried at room temperature for 24 hours.

2.5. Generation of Solubility Parameter Ternary Phase Diagrams

Three-phase solubility parameter diagrams were generated utilizing the solubility of the polymer in terms of each specific interaction (δ_d, δ_p, δ_h) of various solvents using a triangular graphing based on the first power relationship technique[348] The location of the solubility envelope within the triangular diagram was determined by preparing 15 wt % polymer solutions in various liquids at 25°C. Each of the solution was coagulated in various non-solvents for 1 hour and placed in DI water at RT for 24 h. The placements of various non-solvents in reference to the solubility envelope were also determined.

2.6. Characterization

2.6.1. Scanning Electron Microscopy

Top and cross section of the asymmetric membranes were imaged using a LEO (Zeiss) 1550 field emission Scanning Electron Microscopy (FE-SEM) at 5 eV. The samples

[348] J.P. Teas, Graphical analysis of resin solubilities, J. Paint Technol., **1968,** 40, 19-25.

were freeze fractured under cryogenic conditions using liquid nitrogen and coated with 8-10 nm gold before being tested.

3. Results and Discussion

The purpose of changing various preparation factors was to determine whether or not a stable asymmetric membrane with a thin dense surface layer (0.1 -1 μm) could be obtained from disulfonated bisphenol based poly(arylene ether sulfone)s (BPS-20) by DIPS. The phase inversion casting method is intrinsically connected to the asymmetry of the membranes and allows the tailoring of very distinct structures upon the variation of the casting solution composition (system of solvents, concentration or types of polymers.) and of the casting parameters (evaporation time, coagulation media (non-solvent), etc.). BPS-20 was chosen for these experiments because it exhibited high salt rejections (+99 %) but very low water fluxes as a dense membrane. Formation of a stable asymmetric membrane with a thin dense surface layer utilizing BPS-20 could ultimately improve the overall flux through the membranes without sacrificing the high salt rejection properties.

Membranes were formed on glass plates with any support to study the effect of these factors on the final asymmetric structure. Polar aprotic solvents were used to dissolve BPS-20. The different preparation factors based on the casting composition and the casting parameters within each of these areas were investigated.

3.1.1. Effect of non-solvent

The determination of an effective non-solvent is a key to the formation of an asymmetric structure. Generally water is used to induce phase separation in both unsulfonated and post-sulfonated PAESs[345]. Water is a good non-solvent because it induces rapid phase separation (shown by membrane changing from clear to opaque) and is completely miscible with the polymer solvents. As shown in Table 6-1, this was also illustrated in these studies with Radel R, UDEL, and post sulfonated Radel R (PSRR-35) with a 35% degree of sulfonation. A rapid change in the appearance of Radel R, UDEL, and PSRR-35 from clear to opaque was also observed in various alcohol and ketones, although UDEL formed a gel in ethanol. The morphology as illustrated by SEM of Radel R coagulated in water is presented in Figure 6-1. The appearance of long finger-like projections (macrovoids) throughout the membrane was observed. Under applied pressure these macrovods collapse and decrease the water flux through the membranes. Therefore, the removal of macrovoids from the membrane sublayer will likely improve the water flux characteristics.

The preparation of asymmetric membranes from disulfonated PAESs (BPS-20) coagulated in water did not occur because water caused gelation of the membrane. Therefore to achieve asymmetric formation for these copolymers other types of non-solvents were investigated. The establishments of a suitable coagulation medium (non-solvent) relies on the ability of the solvent and non-solvent to instantaneous demix. This can be observed by the rapid conversion of the transparent polymer solution to an opaque film. The order of solvent (NMP)/non-solvent demixing from fastest to slowest to form asymmetric membranes from BPS-20 in different non-solvents was as follows: Acetone

>Acetone:IPA (50:50)> MEK > IPA> Ethanol > Methanol > MIBK > Acetone: H_2O (50:50) ≥ H_2O.

Table 6-1. General Observation of Unsulfonated, Post Sulfonated, and Disulfonated PAESs in Various Non-solvents

Non-Solvent	***BPS-20***	***Udel***	***Radel R***	***PS-Radel R 35***
Water (H_2O)	G	O	O	O
Methanol	G	O	O	O
Ethanol	O	G	O	O
Isopropanol (IPA)	O	O	O	O
Acetone	O	O	O	O
Acetone/(H_2O) (50:50	G	O	O	O
Acetone/ IPA (50:50	O	O	O	O
Methyl Ethyl Ketone (MEK)	O	O	O	O
Methyl Isobutyl Ketone (MIBK)	G	O	O	O

1. Abbreviations include: O = Opaque; G = Gelled

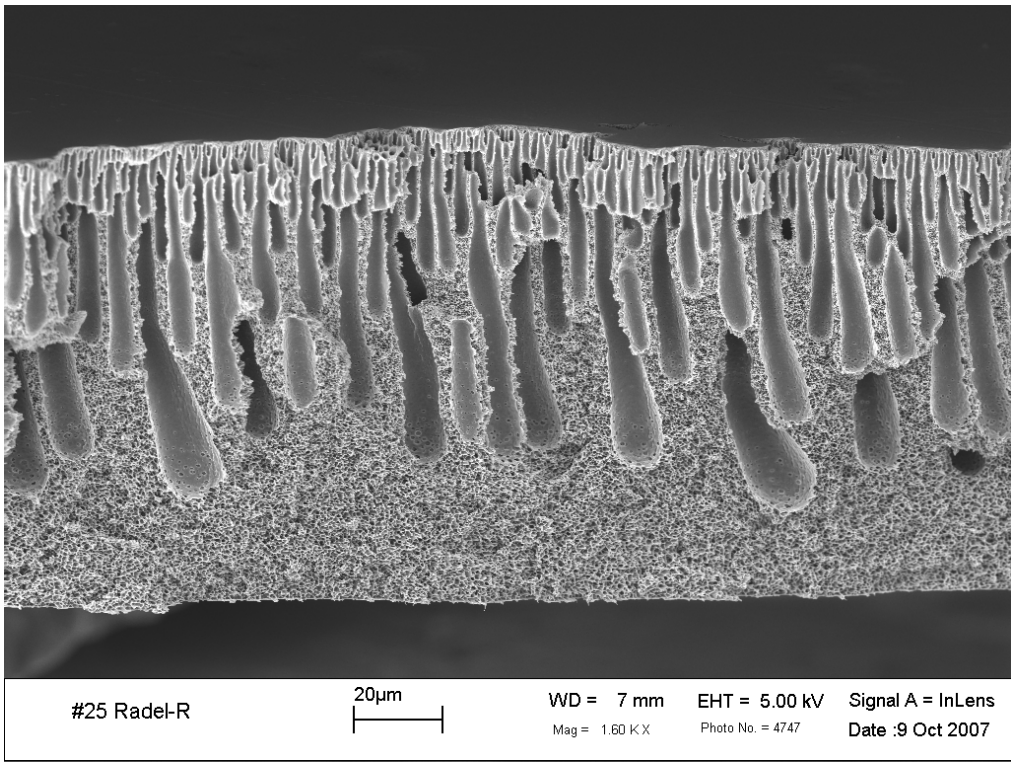

Figure 6-1. SEM cross-section of Radel R dissolved in NMP and coagulated in deionized water.

Moreover, several researchers have proposed that skin layer thickness and overall structure of asymmetric membranes are determined by the kinetics of the coagulation process.[345, 351, 352] These researchers showed that instantaneous liquid-liquid demixing during coagulation resulted in thin-skinned membranes, whereas delayed liquid-liquid demixing gave rather thick-skinned membranes. Delayed demixing (>1 min) and gelation in alcohols which have typically been used as alternative to water, were observed. The fastest coagulation of BPS-20 occurred in acetone. Figure 6-2 illustrated that instantaneous demixing between NMP and acetone lead to much thinner dense surface layer (5.12 µm) that were half the thickness of the membranes coagulated in IPA (10.85 µm).

Increasing the length of the alcohol chain from methanol to IPA changed the membrane structures from a gel to opaque at higher sulfonations. The opposite effect was observed when the length of the ketones was increased.

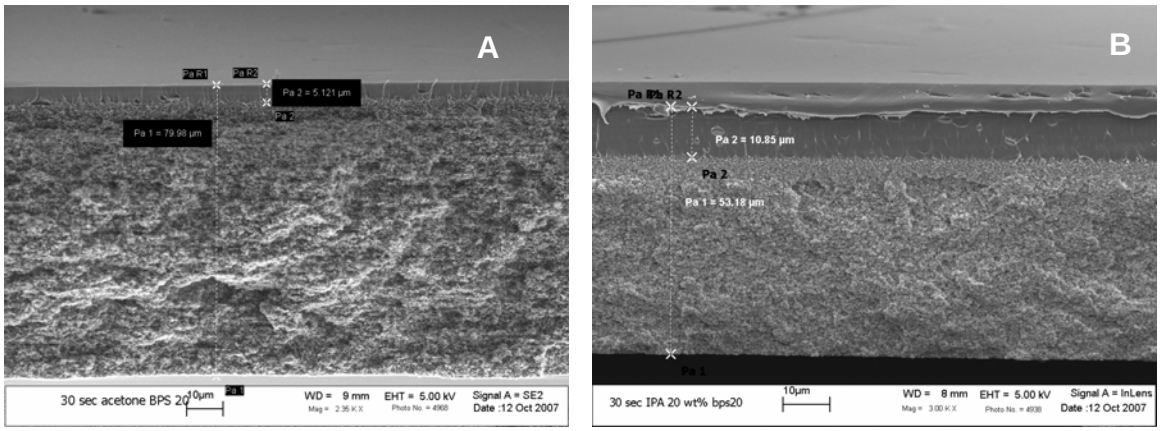

Figure 6-2. SEM cross-section of BPS-20 (20 wt%) asymmetric membrane dissolved in NMP and coagulated in A) Acetone B) IPA and dried at room temperature for 30 sec.

3.1.2. Polymer Selection

The ideal polymer copolymer used in DIPS are tough, amophorous, high molecular weight (30,000 – 45,000 Daltons) thermoplastics with a glass transition temperatures (>50 °C) above the expected use temperature.[121] The choice of polymer is very important because not only does it determine the morphology of the resulting membranes but it also influences the solvent and non-solvent selections. Over the years, many types of amorphous disulfonated PAESs random copolymers with high glass transition temperatures have been synthesized. Table 6-2 lists the observations of various

unsulfonated and disulfonated biphenol based and partially fluorinated (6FS-XX) in various non-solvents.

The unsulfonated Radel-R, Udel (See Table 6-2), and 6F polysulfone coagulated in water was very rapid. All of the biphenol based PAES membranes with various degrees of sulfonation exhibited rapid coagulation in acetone. However, no change to the appearance of 6FS-XX membranes was observed in acetone. In fact no suitable non-solvent for the partially fluorinated PAESs could be found. The lack of liquid-liquid demixing between acetone and NMP with these copolymers may be due to the high affinity of the fluorine groups in these copolymers for acetone. Phase separation in ethanol was observed for these membranes however the rate of coagulation was too slow (> 10 min) to conduct any reliable membrane studies.

Table 6-2. General observation of PAESs in various non-solvents

Non-Solvent	***BPS-10***	***BPS-20***	***BPS-35***	***6FS-00***	***6FS-10***	***6FS-20***
Water (H_2O)	G	G	G	O	G	G
Methanol	O	G	G	O	H	G
Ethanol	O	O	O	O	O	O
Isopropanol (IPA)	O	O	O	H	H	H
Acetone/ IPA (50:50)	O	O	O	NC	NC	NC
Methyl Ethyl Ketone (MEK)	O	O	O	G	G	NC
Methyl Isobutyl Ketone (MIBK)	NC	G	G	H	H	H

1. Abbreviation defined include G = Gelled; H = Hazy; NC = No Change.

Normally, macrovoids or finger like projections are present in membranes prepared by DIPS and are generally due to low polymer concentrations.[349] The appearance of big finger like projections occurred in disulfonated biphenol based poly(arylene ether sulfone)s and unsulfonated copolymers dissolved in NMP and coagulated rapidly in acetone or water, respectively. The development of these projections led to an unstable membrane morphology which at high pressures results in reduced water flux due to a collapse of these large macrovoids by mechanical compression.[350] Thus the elimination of macrovoids from the membrane structure is very important.

Slower coagulation times at higher sulfonations were observed. The appearance of these large finger-like projections throughout the membranes can be observed in the biphenol based PAES (Figure 6-3) at different sulfonation levels. The change in the amount and size of these projections with increasing degree of sulfonation was caused by the decrease rate of exchange.[351] At higher sulfonation levels there is an increased tolerance of the polymer solution for higher acetone content without phase separation. The greater affinity of the disulfonated PAESs at higher sulfonation levels to acetone leads to a longer time for the solvent exchange between the acetone bath and the polymer solution before the BPS-35 becomes gelled and vitrified

[349] Lee, K-W., Seo, B-K., Nam, S-T., Han, M-J. *Desalination* **2003,** 159, 289-296.
[350] Michael E. Williams. "*A Brief Review of Reverse Osmosis Membrane Technology*" EET Corporation and Williams Engineering Services Company, Inc., 2003.
[351] Blanco, J-F, Sublet, J., Nguyen, Q. T., Schaetzel, P. *J. Membr. Sci*. **2006**, 283.27–37.

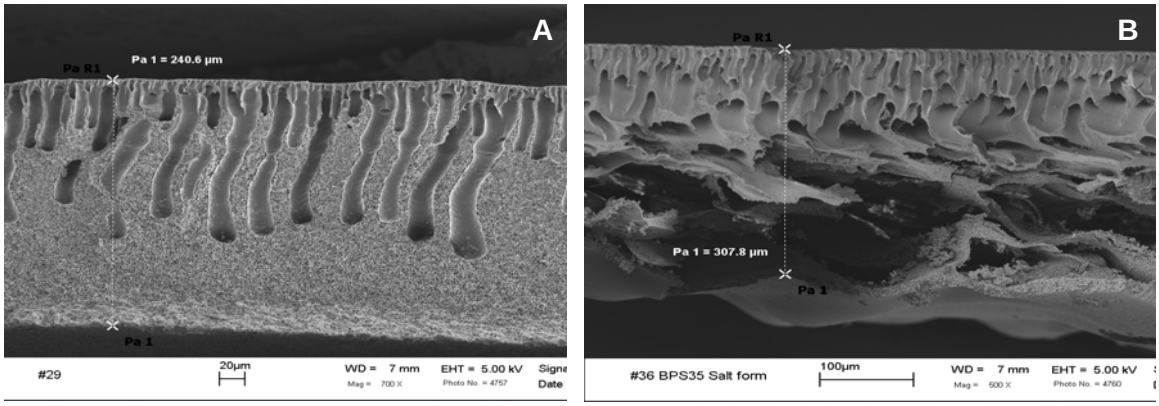

Figure 6-3. SEM cross-section of A) BPS-20 (20 wt%) and B) BPS-35 (20 wt%) asymmetric membranes dissolved in NMP and coagulated in acetone.

3.1.3. Solvent Choice

Generally the best casting solution solvents for disulfonated PAESs are aprotic solvents such as dimethyl formamide (DMF), *N*-methyl pyrrolidone (NMP), dimethyl acetamide (DMAc), and dimethylsulfoxide (DMSO)**.** The asymmetric membrane formation was carried out using BPS-20 (30 wt%) dissolved in these well-known polar aprotic solvents. Figure 6-4 illustrates the influence of different aprotic solvents on morphology.

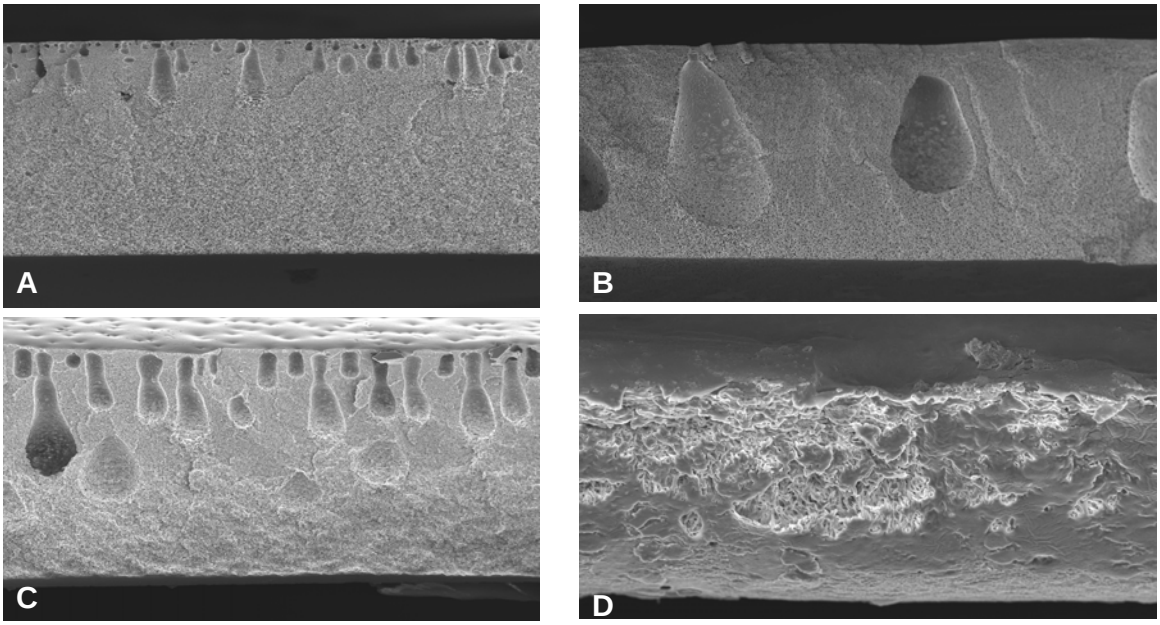

Figure 6-4. SEM cross-section of BPS-20 in the sodium salt form dissolved in A) NMP, B) DMF, C) DMAc, and D) DMSO , Concentration = 30 wt-%.; Drying temperature = 35°C; Drying time = 30 min.

The formation of an asymmetric morphology can be accomplished from all these solvents except DMSO. The use of DMSO leads to a more dense membrane that is free of pores and gel-like in character. Furthermore the use of DMSO also delayed the solidification of BPS-20 showing a very slow transition rate (> 1 min.) in acetone. Additionally, dissolution of the copolymer in NMP led to a decrease number and sizes of macrovoids present in the membranes.

Ternary phase diagrams based on experimental observations (Table 6-1 and Table 6-2) and the solubility parameters of these solvents in reference to BPS-20 have been developed. Figure 6-5 demonstrates the envelope corresponding to the region of polymer solubility as defined by the aprotic solvents found to dissolved BPS-20.

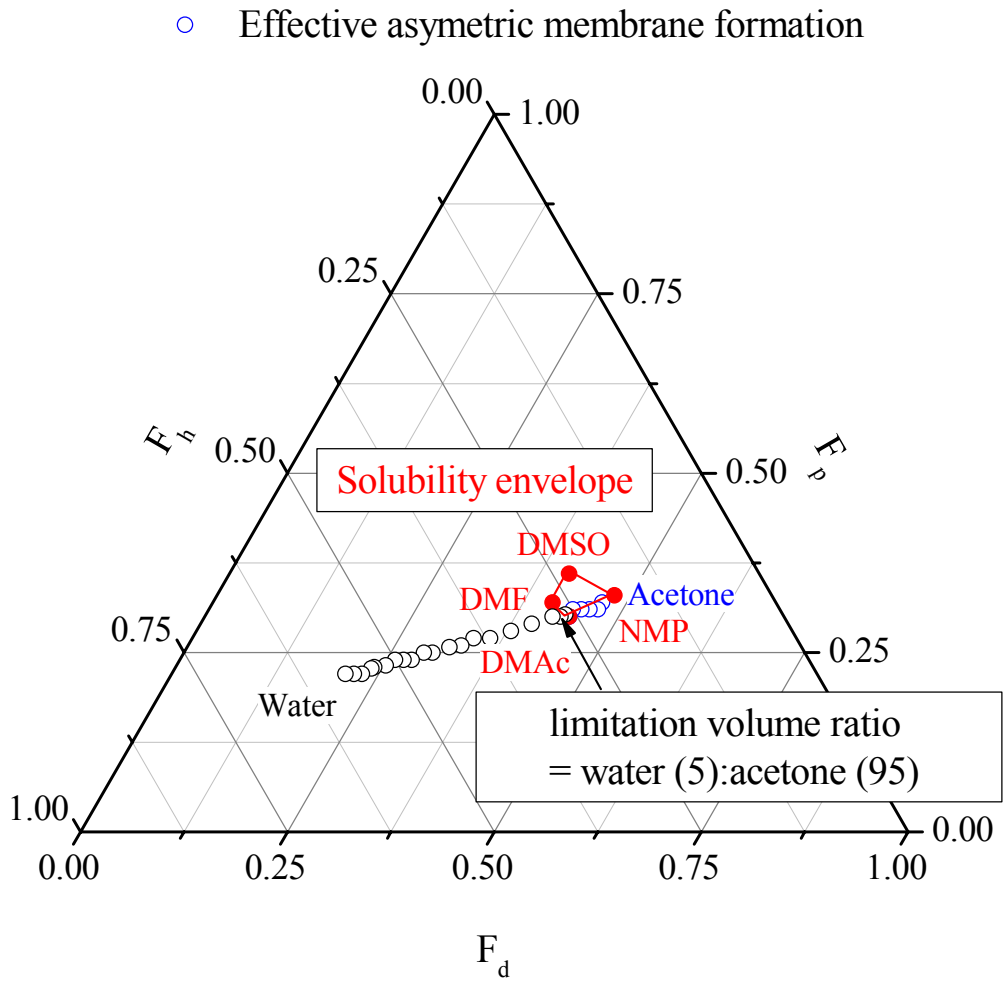

Figure 6-5. Three dimensional phase diagram of BPS-20 asymmetric membrane formation from polar aprotic solvents and coagulated in non-solvent mixtures of water-acetone at ambient temperature.

As previously discussed phase transition of BPS-20 membranes prepared from NMP, DMAc, and DMF occurred without gelation at a fast rate in acetone. Slower transition rates were observed when water or IPA was used. The use of water as a non-solvent also caused gelation of BPS-20.

Focusing on the location of these non-solvents to convert BPS-20 into asymmetric membranes it is noted that acetone which is a good non-solvent for BPS-20 is located on the edge of the "Solubility Envelope" (3D phase diagram) whereas water which caused gelation of this copolymer is located far away from the envelope. Fast conversion of BPS-20 could also be obtained in mixtures containing acetone with water below 5 vol.%. Higher water content resulted in slower phase transition (> 25 sec.). This means that the composition of non-solvent mixtures near the "Solubility Envelope" should be selected for the favorable asymmetric membrane formation.

Mixtures of acetone and IPA were also investigated. As noted in Figure 6-6, IPA like water was not located close to the solubility envelope due to its slow exchange rate. Although good asymmetric morphology free of macrovoids could be obtained with higher volumes of IPA (70 vol%), thicker top surfaces (1.8 μm) which would decrease water flux were also formed. Figure 6-7 demonstrates the effect of acetone:IPA mixtures on the morphology of BPS-20 asymmetric membranes. SEM images on the left correspond to the entire membrane in various non-solvent mixture ratios of acetone to IPA. While the SEM images on the right correspond to the surfaces and relative thickness of each membranes.

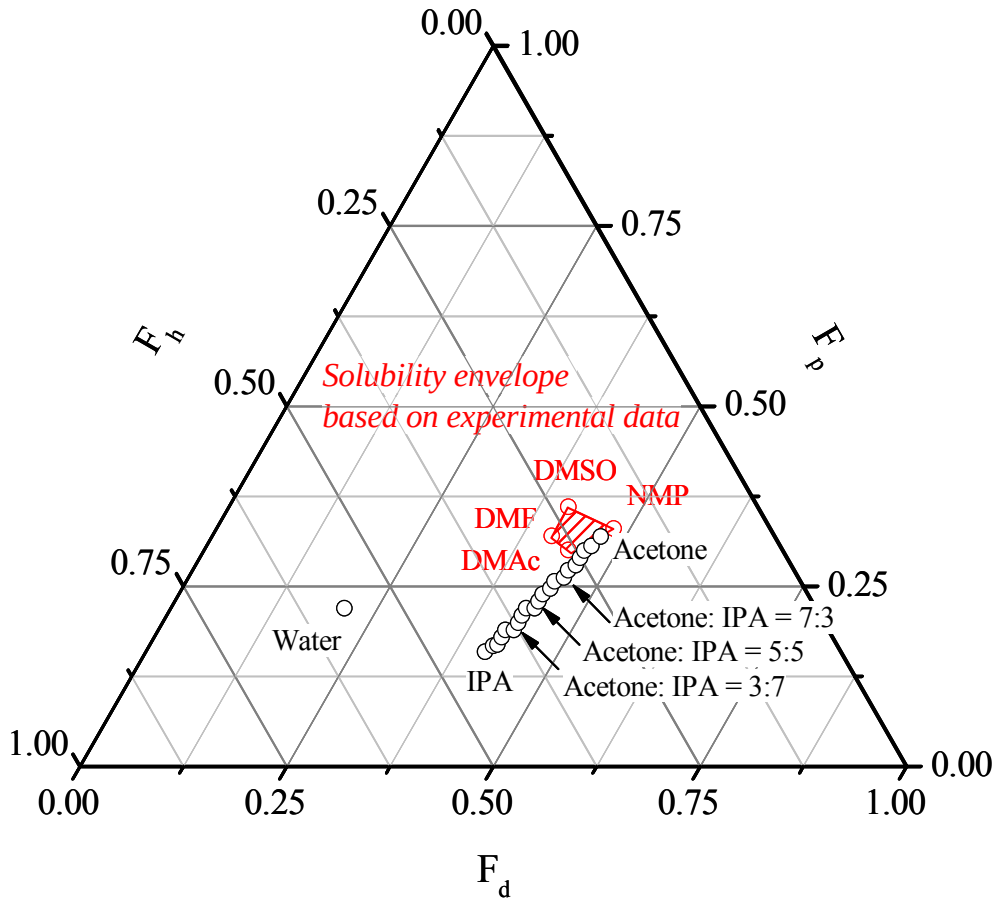

Figure 6-6. Three dimensional phase diagram of BPS-20 asymmetric membrane formation from polar aprotic solvents and coagulated in non-solvent mixtures of acetone : IPA at ambient temperature.

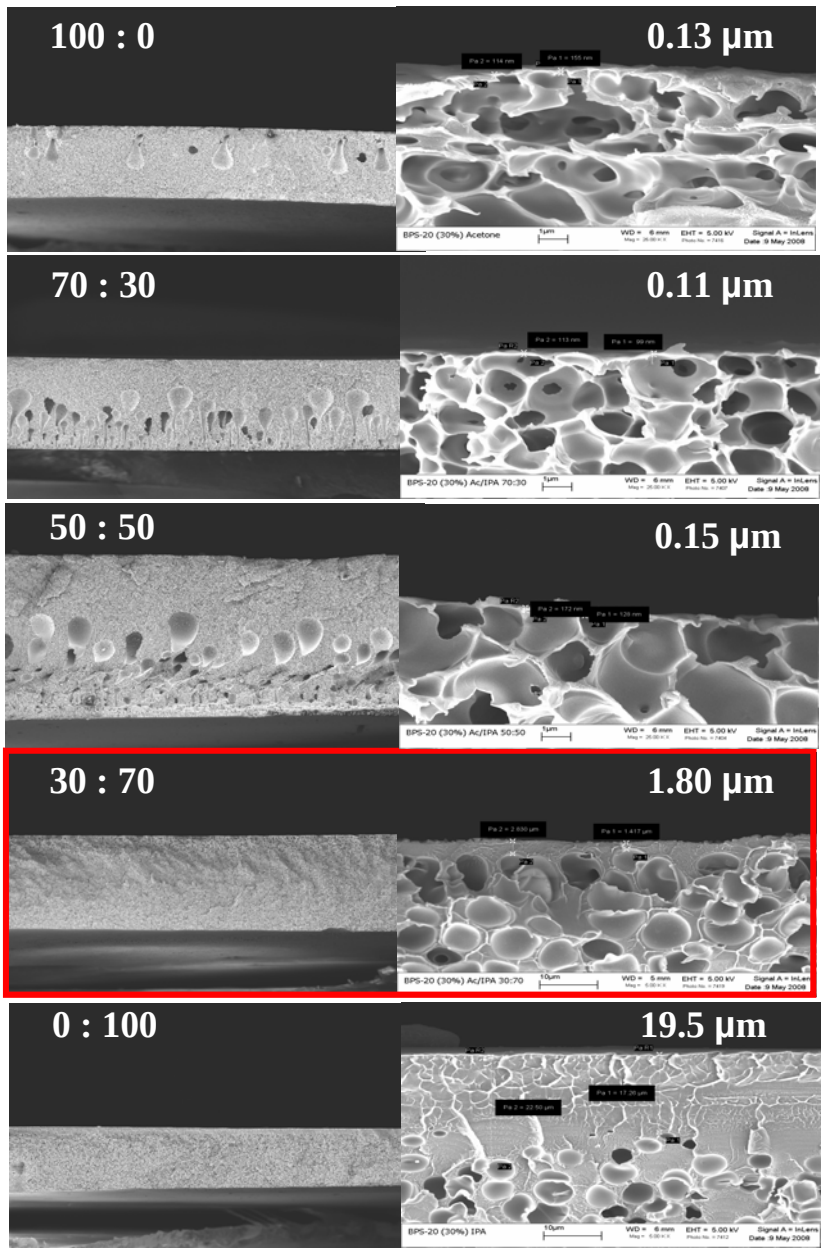

Figure 6-7. Asymmetric membrane formation and relative surface thickness of BPS-20 from non-solvent mixture of acetone:IPA at ambient temperature.

Note that solvents located at a long distance from the tie line should be excluded owing to their slow transition rate. Interestingly, DMSO exhibiting a poor phase transition is far from the tie line composed of available non-solvent mixtures.

Considering each solvent location in phase diagrams, DMAc seems to be the best solvent when 5 wt% of water is used while NMP would be the best solvent if pure acetone is used.

3.1.4. Effect of the polymer concentration, drying time, and drying temperature

The occurrence of macrovoids was reduced by increasing the drying temperature and concentration of the polymer solution. All the membranes were prepared from BPS-20 in NMP. Figure 6-8 illustrates the effect of increasing the drying temperature on asymmetric structure. Increasing the drying temperature from 25 °C (A) to 35 °C (B) for 30 minutes greatly reduced the size of the macrovoids. Longer drying times at 35 °C for 45 (C) minutes resulted in the disappearance of the macrovoids.

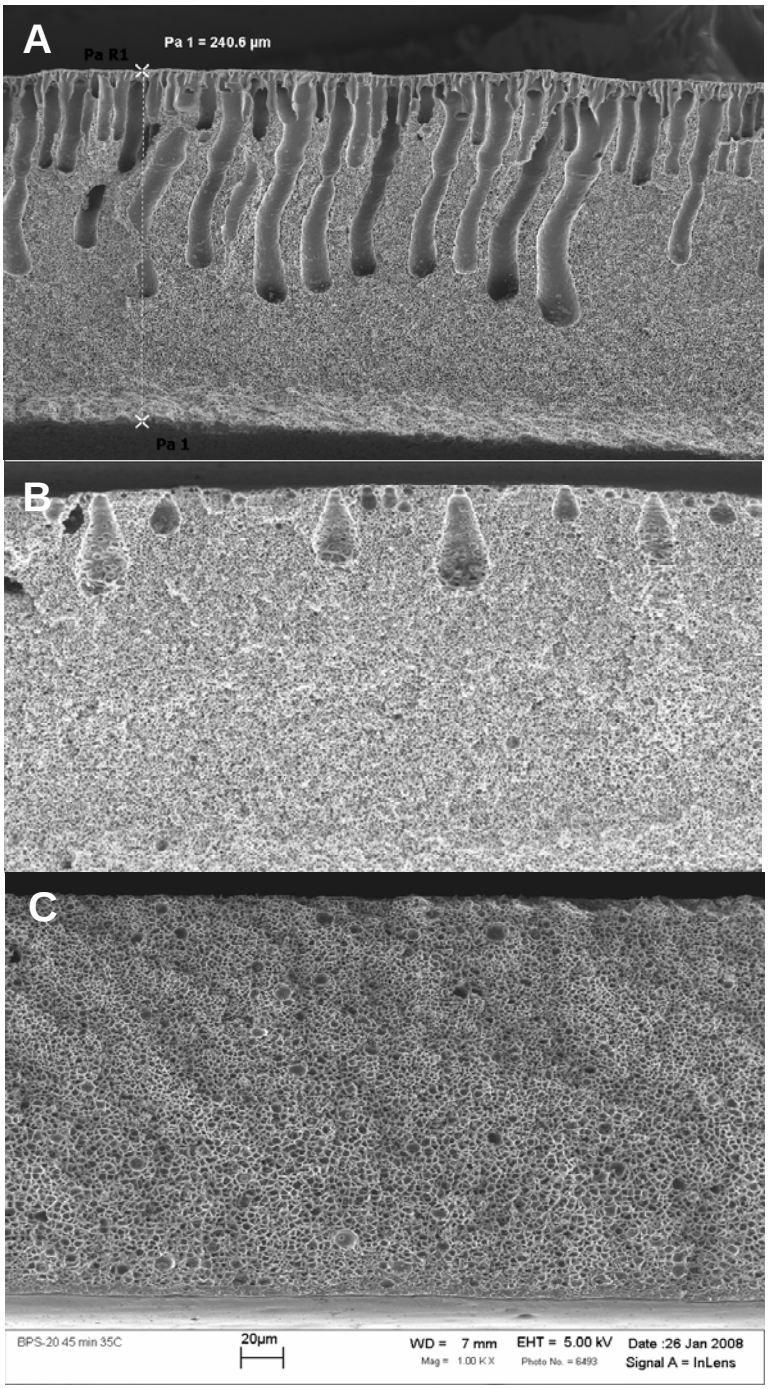

Figure 6-8. SEM images of BPS-20 (30 wt%) asymmetric membrane dissolved in NMP and coagulated in acetone as a function of drying temperature. A) BPS-20 dried at room temperature for 30 minutes B) BPS-20 dried at 35 °C for 30 minutes C) BPS-20 dried at 35 °C for 45 minutes

Similar changes to the membrane morphologies were exhibited when the concentration of the membranes were increased from 25 to 40 wt%. Specifically that higher polymer concentration led to the removal of macrovoids from the membranes. In addition, higher concentrations also resulted in fewer defects on the surface of the membrane. This effect is illustrated in Figure 6-9 which showed that increasing the polymer concentration from 25 to 30 wt% caused a reduction of defects or pinhole.

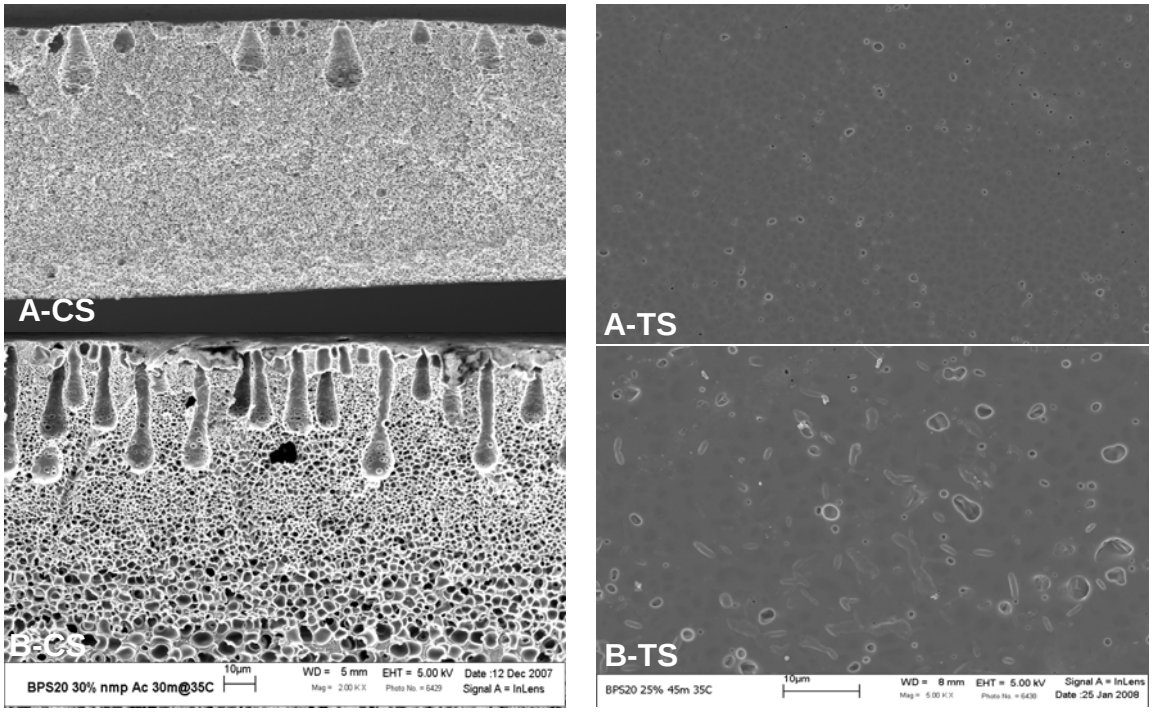

Figure 6-9. Cross-section (CS) and top surface (TS) SEM images of A) 30 wt% BPS-20 in NMP and B) 25 wt% BPS-20 in NMP

A correlation between drying time and polymer concentration in terms of the dense top layer thickness was observed. All the membranes were dissolved in NMP and dried at 35 ºC. Figure 6-10 demonstrates that at higher concentration and longer drying

time the thickness of the dense top layer increased whereas thinner top layers were achieved at low concentration and shorter drying times. Along with thicker top surfaces, the use of higher concentration and longer drying time also eliminated the appearance of macrovoids throughout the membranes.

Conc (wt%)/ Time (min)	30	45	60
30	50 nm	66 nm	71 nm
35	62 nm	78 nm	95 nm
40	71 nm	110 nm	163 nm

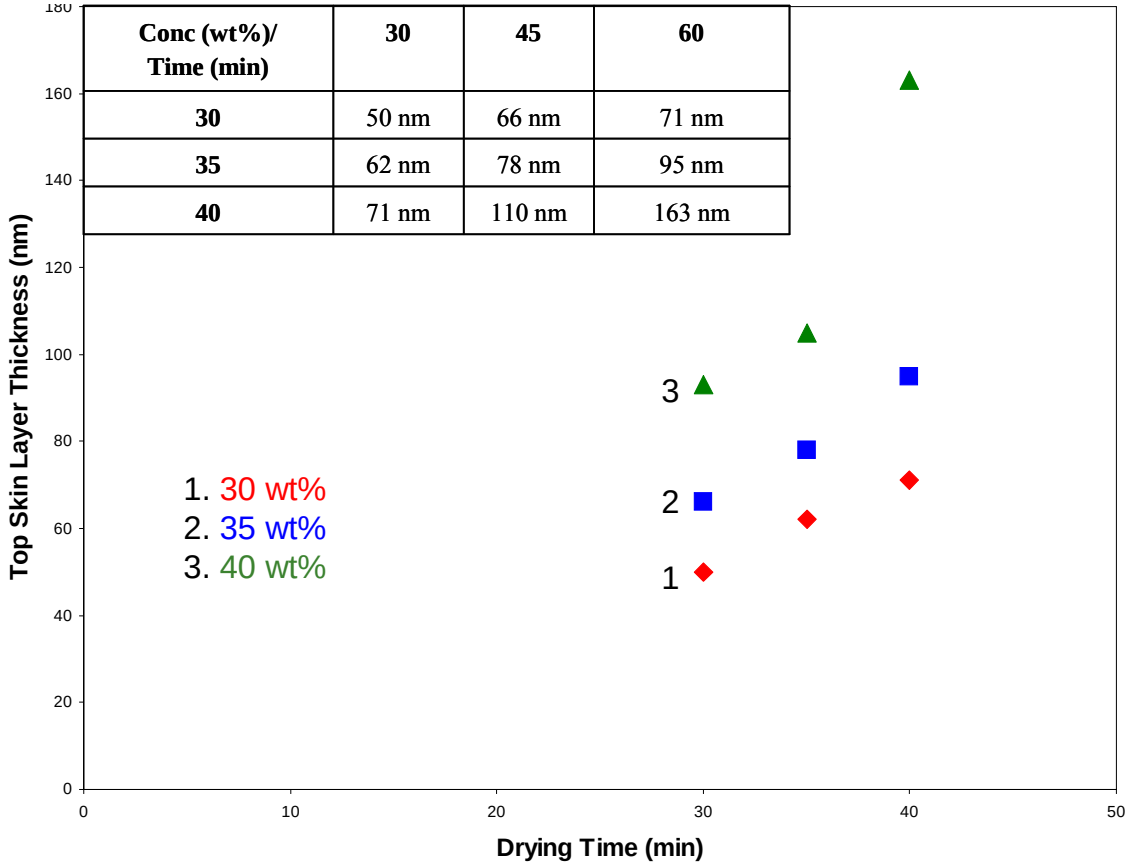

Figure 6-10. The effect of polymer concentration and drying time on the skin thickness of BPS-20 asymmetric membranes

The increase in the surface thickness and decrease porosity of the final film was due to an increase in the polymer concentration at the interface of the casting film

4. Conclusions

Asymmetric membranes based on disulfonated biphenol based poly(arylene ether sulfone) random copolymer (BPS-20) from various NMP, DMAc, and DMF have been accomplished. The appearance of macrovoids or finger-like projection present in these membranes were controlled by increasing the drying temperature and concentration of the polymer solution. The use of DMSO which exhibited delayed liquid-liquid demixing (> 1 min.) in acetone formed a dense membrane structure that was free of pores and gel-like in character. Utilizing these three component solubility parameter in conjunction with ternary plots facilitated a more efficient and precise selection of casting solution components and composition. Ternary phase diagrams based on the solubility parameter the solvents and non-solvent used were in agreement with experimental observation

Acetone was the best non-solvent for all of the biphenol based PAES membranes with various degrees of sulfonation. The order of solvent (NMP)/non-solvent demixing from fastest to slowest to form asymmetric membranes in different non-solvents was as follows: Acetone > Acetone:Isopropyl alcohol (IPA) (50:50)> methyl ethyl ketone (MEK) > IPA> Ethanol > Methanol > methyl isobutyl ketone (MIBK) > Acetone: water (H_2O) (50:50) ≥ H_2O. Fast conversion of BPS-20 could also be obtained in mixtures containing acetone with water below 5 vol.%. Although good asymmetric morphology free of macrovoids could be obtained with higher volumes of IPA (70 vol%), thicker top surfaces (1.8 μm) that would decrease water flux were formed. No suitable non-solvent for the partially fluorinated PAESs could be found.

.

CHAPTER 7. PREPARATION AND CHARACTERIZATION OF ASYMMETRIC DISULFONATED POLY(ARYLENE ETHER SULFONE) MEMBRANES BY DIFFUSION INDUCED PHASE SEPARATION PROCESS: PART II – Preparation of Asymmetric Membrane Via Cosolvent Mixtures

Natalie Y. Arnett, Chung Hyun Lee, Ozzie Lane, and James E. McGrath

[a]Macromolecules and Interfaces InstituteVirginia Polytechnic Institute and State University, Blacksburg, VA 24061

Abstract

The formation of asymmetric membranes has been prepared using of two nonsolvents serving as a cosolvent system. Disulfonated biphenol based poly(arylene ether sulfone)s (BPS-20) which has shown excellent chlorine resistances and good salt rejections were chosen as the copolymer for this research. The purpose of this research was to investigate systematically the properties of BPS-20 asymmetric membranes prepared by diffusion induced phase separation (DIPS) from various cosolvent systems.

Several preparation factors based on various experimental parameters such as cosolvent choice, non-solvent bath, casting solution concentration, and drying time were studied to find the optimal circumstances to obtain an asymmetric nanoporous membrane. SEM images showed the formation of a stable phase separated morphology consisting of a dense skin layer and a porous support. Stable asymmetric structures were obtained

from THF/FAm (80:20 and 76:24) cosolvent mixture. Acetone was the most promising coagulant for the BPS-20 copolymers.

1 Introduction

The use of two nonsolvents serving as a cosolvent system in the formation of asymmetric phase inversion membranes from BPS-20 was investigated. The cosolvent system comprised of tetrahydrofuran (THF) as a non-solvent and formamide (FAm) as swelling agent has been previously studied by Kinzer et al[352]. Kinzer and collegues showed that membranes with a dense, thick skin layer, comprising approximately 15 to 40 percent of the overall membrane thickness, and supported by a porous sponge-like substructure was formed from THF/FAm cosolvent mixtures. These membranes were coagulated in isopropyl alcohol. A cosolvent system was utilized in this work to replace the traditional solvent-nonsolvent systems that dissolved not only the sulfonated copolymers but the unsulfonated copolymers which are typically used as a porous/woven support for many asymmetric membranes.

The purpose of this research was to investigate systematically the properties of BPS-20 asymmetric membranes prepared by diffusion induced phase separation (DIPS) from various cosolvent systems. In the initial work THF was chosen as one of the nonsolvents due to its volatile nature at ambient conditions whereas the swelling agent formamide was chosen due to its experimentally determined compatibility with THF. Based on investigations by Kinzer et al[352], an 80/20 and 76/24 ratio of THF to FAm were highlighted in this research. However, the high volatility of THF became a problem when preparing larger membranes. Therefore low volume concentrations of THF to

[352] Kinzer, K., Lloyd, D.R., Gay, M.S., Wightman, J.P., Johnson, B.C., McGrath, J.E. *J. Membr. Sci.,* **1985,** 22, l-29.

FAM and other cosolvent systems based on FAm with various higher boiling ethers have also been examined. As before the formation of a stable asymmetric morphology as a function of the casting composition and the casting parameters were explored. Several preparation factors based on various experimental parameters such as cosolvent choice, non-solvent bath, casting solution concentration, and drying time were studied to find the optimal circumstances to obtain an asymmetric nanoporous membrane. Three dimensional (ternary) solubility parameter based triangular graphing technique based on BPS-20 behavior in various cosolvent systems has been constructed.

2 Experimental

2.1 Materials

Eastman Chemical provided high purity 4,4'-biphenol (BP) which was dried at 50 ºC under vacuum before each use. Solvay Advanced Polymers supplied highly purified 4,4'-dichlorodiphenylsulfone (DCDPS). 4,4'-Dichlorodiphenylsulfone was dried at 60 ºC under vacuum before each use. All solvents and non-solvents utilized in this study were purchased from either Fisher Scientific or Aldrich and used without further purification.

2.2 Non-solvent Selection

Solutions (30 wt%) of BPS-20 were prepared in THF/FAm. Upon dissolution BPS-20 solution was coated onto glass stirring rod and immersed in the various non-

solvent at room temperature for phase inversion. Large asymmetric membranes were only prepared from non-solvents that illustrated fast coagulation. The solutions was cast onto glass plates and dried with an IR lamp at room temperature for 30 sec. The membranes were coagulated in a non-solvent 1 hour and placed in DI water for 24 hours. The membranes were dried at room temperature for 24 hours.

2.3 Selection of Cosolvent System

BPS-20 was dissolved in different cosolvent mixtures to afford a 15 wt% solution. All the cosolvent systems contained formamide in various ratios with several types of ethers. Some of the ethers investigated included tetrahydrofuran (THF), 1, 4-Dioxane, 2-methyltetrahydrofuran (MeTHF), cyclopentyl methyl ether (CPME), monoglyme (MG), and diglyme(DG). The solutions were prepared in a sealable container in the following order: formamide, BPS-20, and ether. The solutions were placed in the cold room for 24 hours and then cast onto glass plates. The addition of the ether last into the container and placing the solution in the cold room was carried out to minimize ether evaporation losses. After casting onto glass plates, the membranes were immediately placed into an acetone non-solvent bath for 1 hour. The membranes were stored in deionized water for 24 h to remove any residual acetone and then dried at room temperature for 24 hours.

2.4 Influence of polymer concentration, drying time and drying temperature

Disulfonated biphenol based poly(arylene ether sulfone)s asymmetric membranes dissolved in THF/FAm (80/20) were studied as function of the drying time, concentration, and drying temperature. The experimental procedures for each parameter are presented below. To study the effect of polymer concentration solutions (15, 20, and 25 wt%) of BPS-20 were prepared in THF/FAm cosolvent mixtures. Next the solutions were cast onto glass plates and dried with an IR lamp at 35 ºC for 30 minutes.

The influence of drying time was accomplished by first preparing solutions (25 wt%) of BPS-20 were prepared in THF/FAm cosolvent mixtures. The solution was cast onto glass plates and dried with an IR lamp at 35 ºC for 30, 60, or 90 seconds.

All the membranes were then coagulated in acetone for 1 hour and placed in DI water for 24 hours after each parameter was modified. Lastly, the membranes were dried at room temperature for 24 hours.

2.5 Generation of Solubility Parameter Ternary Phase Diagrams

Three-phase solubility parameter diagrams were generated utilizing the solubility of the polymer in terms of each specific interaction (δ_d, δ_p, δ_h) of various solvents using a triangular graphing based on the first power relationship technique[353] The location of the solubility envelope within the triangular diagram was determined by preparing 15 wt % polymer solutions in various liquids at 25°C. Each of the solution were coagulated in various non-solvents for 1 hour and placed in DI water for 24 h. The placements of various non-solvents in reference to the solubility envelope were also determined.

[353] J.P. Teas, Graphical analysis of resin solubilities, J. Paint Technol., **1968,** 40, 19-25.

2.6 Characterization

2.6.1 Scanning Electron Microscopy

Top and cross section of the asymmetric membranes were by using a LEO (Zeiss) 1550 field emission Scanning Electron Microscopy (FE-SEM) at 5 eV. The samples were freeze fractured under cryogenic conditions using liquid nitrogen and coated with 8-10 nm gold before tested.

3 Results and Discussion

3.1 Effect of non-solvent

Good phase separated morphology was seen for the disulfonated BPS-20 copolymer dissolved in THF/Formamide (80:20; 76:24) solutions. As shown in Figure 7-1, the film is asymmetric in nature with a finely porous open-pore substructure. No macrovoids are observed in this or any other film resulting from THF/FAm casting solutions. Moreover, the appearance of macrovoids in the membranes were not observed when different non-solvents were used.

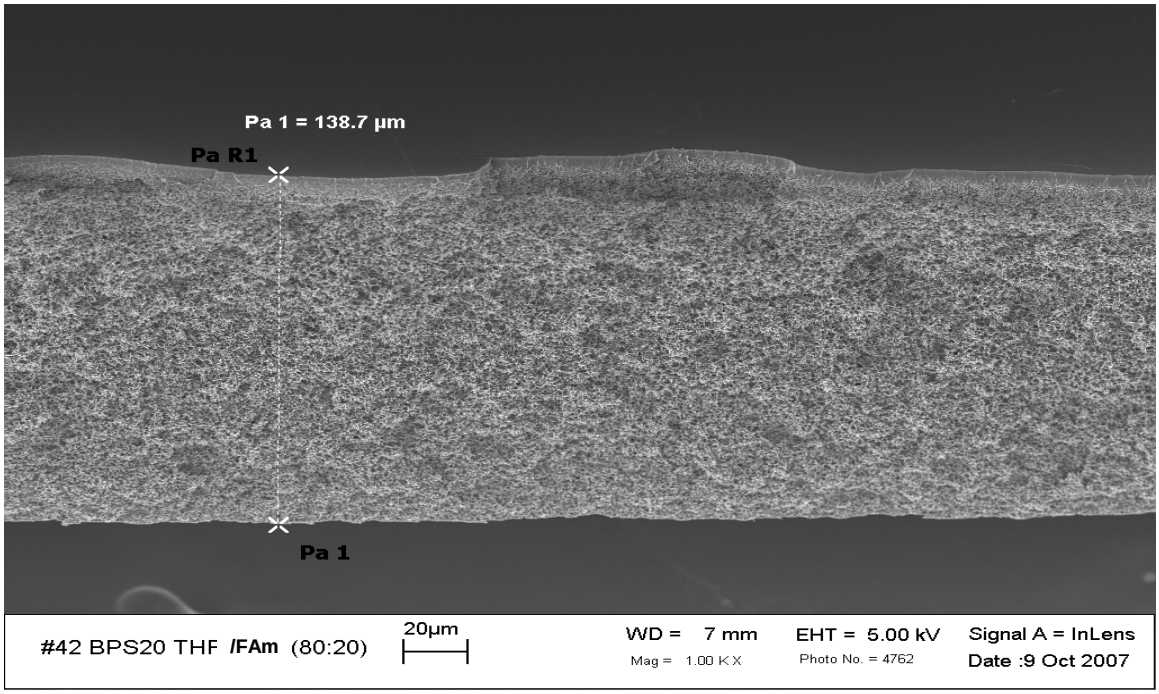

Figure 7-1. SEM cross-section of BPS-20 asymmetric membranes from THF/FAm (80/20) cosolvent system.

The preparation of asymmetric membranes was accomplished from various non-solvents. The observations in these non-solvents at ambient temperatures are listed in Table 7-1. The order of phase inversion from fastest to slowest in different non-solvents was as follows: Acetone > MEK > MIBK > Ethanol > IPA> Methanol > H_2O. The difference in the rate of phase inversion was directly related to the changes in the surface layers of the membrane. As shown in Figure 7-2 the skin layer thickness of a membrane coagualated in acetone gave a membrane with a surface thickness of 5.1 µm. The surface thickness of membranes is doubled (10.8 µm) when IPA was used.

Although similar observations were made in both an 80/20 and 76/24 THF/FAm compositions, a thinner top layer (2.4 µm) was formed when BPS-20 was cast from a 76/24 cosolvent mixture of THF/Formamide. An 80/20 cosolvent system formed a 5.7

μm skin layer. The increase in surface thickness was caused by an increased polymer concentration at the surface of the membrane due to faster evaporation time with higher concentration of THF in the system.

Table 7-1. Observations of Asymmetric Formation of BPS-20 from THF/FAm Cosolvent Systems.

Non-solvent	***THF/FAm (76/24)***	***THF/FAm (80/20)***
Water (H_2O)	G	G
Methanol	O	O
Ethanol	O	O
Isopropanol (IPA)	O	O
Acetone	O	O
Methyl Ethyl Ketone (MEK)	O	O
Methyl Isobutyl Ketone (MIBK)	O	O

1. All the membrane were formed from 15 wt % solutions of BPS-20 at 25°C.
2. Abbreviated defined include G = gel; O = opaque.

Solubility diagrams based on these observations and the solubility of BPS-20 in THF/FAm at different ratios is shown in Figure 7-3. The best regions of solubility for the THF/FAm systems could be determined from the phase diagrams. Casting solution compositions located on opposite sides of the solubility envelope were chosen in order to study the effect of initial casting solution location on membrane performance. Notice that BPS-20 dissolved in 80:20 and 76/24 THF/FAm cosolvent systems are located in close proximity to the solubility envelope boundary. Moving to lower concentration of THF in the systems causes the solubility to be shifted outside of the envelope. Furthermore, the location of acetone close to the solubility envelope proves that it was the best non-solvents when BPS-20 was dissolved in THF/FAM. The placement of water

and IPA far from the solubility envelope further exemplified that the use of these non-solvent was still not possible.

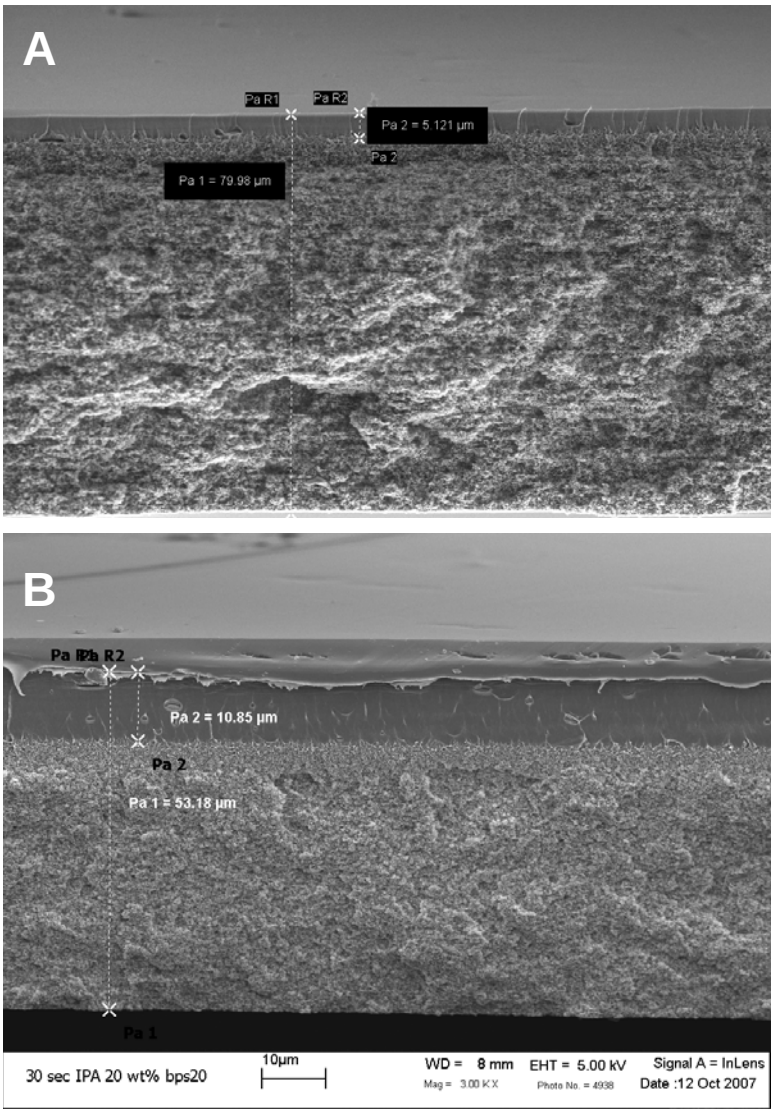

Figure 7-2. SEM images of BPS-20 (20 wt%) asymmetric membrane dissolved in THF/FAm (76:24), dried at room temperature for 30 sec, and coagulated A) Acetone B) IPA.

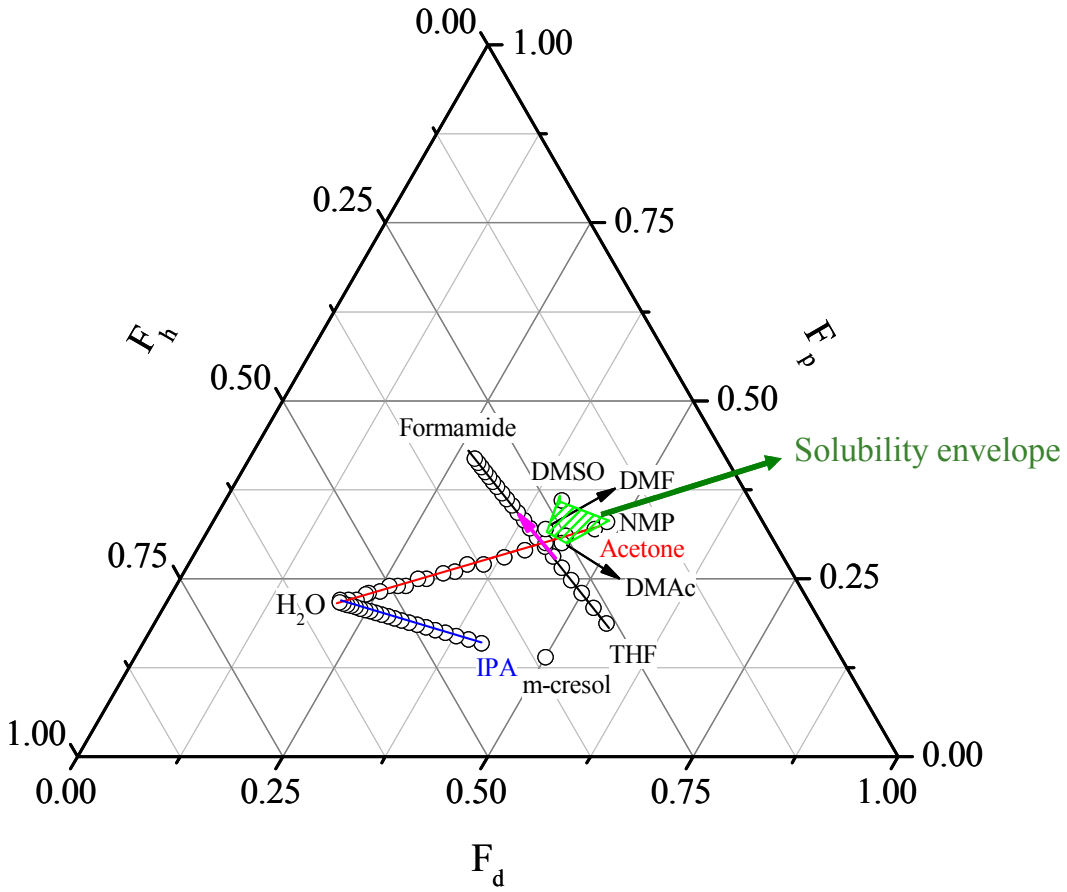

Figure 7-3. Three dimensional phase diagram of BPS-20 asymmetric membrane formation from THF/FAm cosolvent systems at ambient temperature.

3.1.1 Effect of the polymer concentration and drying time

Unlike the membranes that were prepared from aprotic solvents, the formation macrovoids in these membranes was not dependent on the polymer concentration or drying time. Thus polymer concentration and drying times were studied to determine the effect of these parameters on the surface thicknesses. Drying temperatures higher than

room temperature were not investigated due to the low boiling point of THF. All the membranes were coagulated in acetone at ambient temperatures.

The general asymmetric structure of films allowed to evaporate for 30, 60, and 90 seconds before immersion into acetone is shown in Figure 7-4. Thinner skins (2 μm) were obtained for membranes prepared with shorter drying times (<30 sec). The loss of THF from the surface of the film caused the polymer concentration in this region to increase to the point of precipitation. When sufficient time is allowed for an integral polymer skin layer to form before immersion into acetone, a porous membrane with a dense skin will be formed. Increasing the evaporation period to 60 sec resulted in dense skin layers being formed on both the top surfaces and throughout the film with small region of finely porous open-pore sponge structure in between.[354] Longer drying times (>90 sec) lead to the formation of dense membranes that exhibited no asymmetric character. An increase in time results in an increase in the polymer concentration not only on the surface of the membranes but also in the bulk. This not only caused a thicker skin layer to be formed but also resulted in the dense skin layers throughout different areas of the film beside that surface.

[354] Kinzer, K., Lloyd, D.R., Wightman, J.P., McGrath, J.E. *Desalination*, **1983,** 46, 327-334.

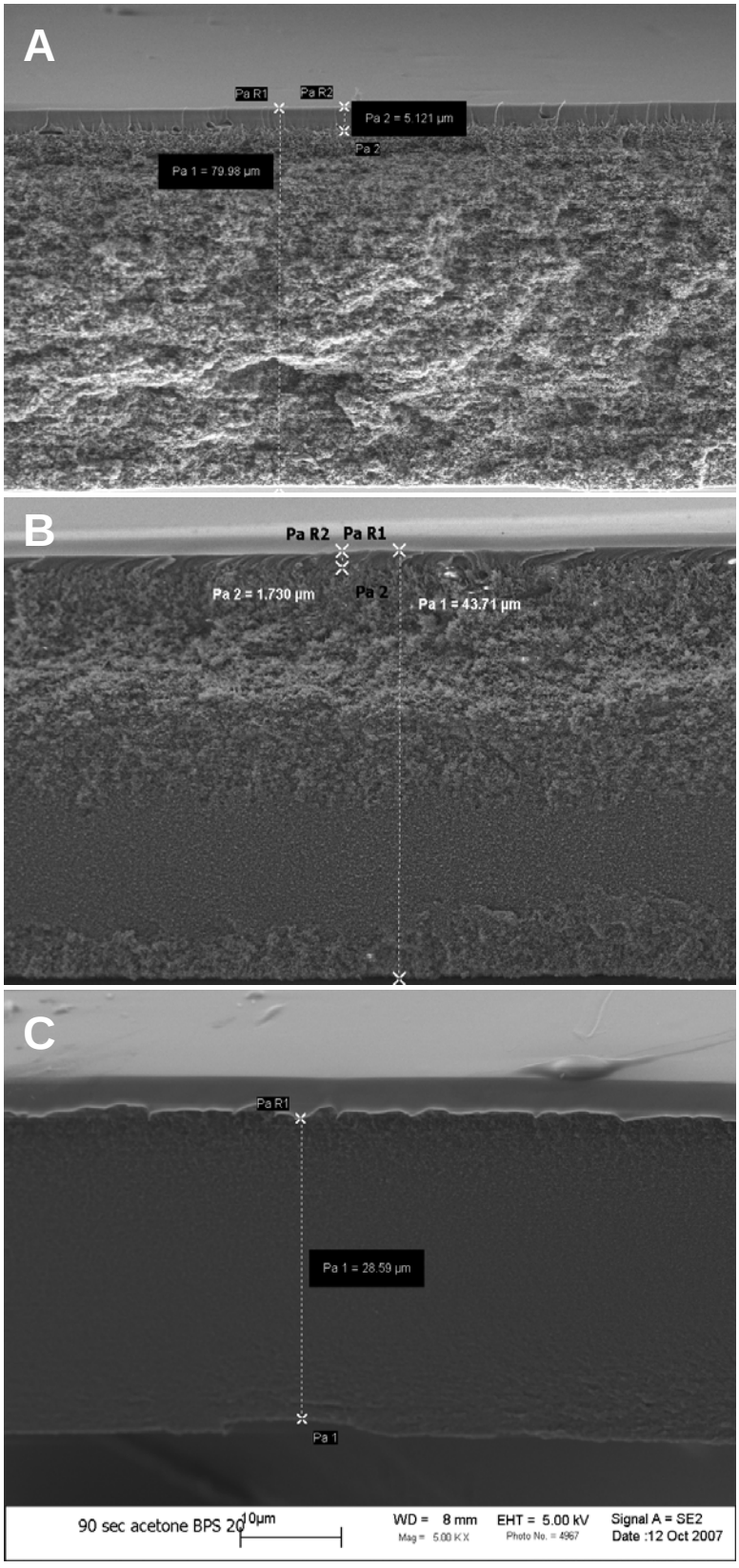
A
Pa R1
Pa R2
Pa 2 = 5.121 µm
Pa 2
Pa 1 = 79.98 µm
B
Pa R2
Pa R1
Pa 2 = 1.730 µm
Pa 2
Pa 1 = 43.71 µm
C
Pa R1
Pa 1 = 28.59 µm
Pa 1
90 sec acetone BPS 20
10µm
WD = 8 mm
Mag = 5.00 K X
EHT = 5.00 kV
Photo No. = 4967
Signal A = SE2
Date :12 Oct 2007

Figure 7-4. SEM images of BPS-20 (15 wt%) asymmetric membrane dissolved in THF/FAm (76:24), coagulated in acetone, and dried at room temperature for A) 30 sec, B) 60 sec, and C) 90 sec.

Concentrations under 15 wt% gave membranes with poor mechanical properties. Table 7-2 illustrated the effect of increasing polymer concentration on skin thickness. These membranes were prepared from BPS-20 solutions **(**THF/FAm 76:24**)** and dried for 30 sec in air. As the concentration of the membrane increase from 15 to 25 wt% thicker skin layer ranging between 2 to 8 μm, respectively were generated. Increasing the viscosity of the polymer solution hampers the diffusional exchange between the co-solvent and non-solvent resulting in a higher polymer concentration at the interface of the casting film and hence an increase in the thickness of the dense top layer.[355]

Table 7-2. The effect of concentration on the skin layer measurements for asymmetric membranes prepared from BPS-20 in THF/FAm (76:24)

Concentration (wt%)	***Skin Thickness (μm)***
15	2
20	5
25	8

3.1.2 Effect of Cosolvent System

[355]Domenech-Cardo, M.T., Aura-Castro, E. *Studies in Conservation* **1999,** 44, 19-28.

The properties of BPS-20 in other cosolvent systems based on FAm with various higher boiling ethers was also investigated. These systems were investigated in an effort to replace the highly volatile THF that made preparing larger membranes very difficult. A summary of the solubility properties of BPS-20 in different cosolvent mixtures is listed in Table 7-3. From this table it is obvious that the formulation of a good cosolvent system is not trivial due to the fact that only four of the cosolvents systems studied had the ability to complete dissolve BPS-20. The systems that dissolved BPS-20 included THF/FAm, 1,4-Dioxane (D)/ FAm, monoglyme (MG)/FAm, and, diglyme (DG)/ FAm.

Table 7-3. Cosolvent systems utilized to determine the BPS-20 solubility

Cosolvent	***100/0***	***50/50***	***76/24***	***80/20***	***0/100***
THF/FAm	NS	S	S	S	SA
Ethylene glycol/FAm	NS	SA	SA	SA	SA
Diethylene glycol/FAm	NS	SA	SA	SA	SA
triethylene glycol/FAm	NS	SA	SA	SA	SA
hexane/ Fam	NS	NS	NA	NA	SA
Cyclohexane/ FAm	NS	NS	NA	NA	SA
Ethyl acetate/ FAm	NS	NS	NS	NS	SA
2-Methyltetrahydrofuran (MeTHF)/FAm	NS	NS	NS	NS	SA
Cyclopentyl methyl ether (CPME)/ FAm	NS	NS	NS	NS	SA
1,4-Dioxane (D)/FAm	NS	NS	S	S	SA
Monoglyme (MG)/FAm	NS	NS	S	S	SA
Diglyme (DG)/FAm	NS	NS	S	S	SA

1. All the membranes were formed from 15 wt % solutions of BPS-20 at 25°C.
2. Abbreviated defined include S= soluble; SA = swelling agent; NS = not soluble; NA = not available

The formation of asymmetric membranes from soluble cosolvent systems was possible in acetone and methyl ethyl ketone (See Table 7-4). Instantaneous demixing between these non-solvents and the different cosolvent systems lead to asymmetric membrane formation.

However, unlike the THF/FAm systems the preparation of asymmetric membranes resulted in formation large macrovoids throughout the membrane structure.

Table 7-4. Observation of Asymmetric Formation of BPS-20 from Different Cosolvent Systems.

Non-solvent/Cosolvent	*THF/FAm*	*MG/FAm*	*DG/FAm*	*D/FAm*
Water (H_2O)	G	G	G	G
Methanol	O	O	G	O
Ethanol	O	O	G	O
Isopropanol (IPA)	O	O	G	O
Acetone	O	O	O	O
Methyl Ethyl Ketone (MEK)	O	O	O	O
Methyl Isobutyl Ketone (MIBK)	O	O	O	G

1. Abbreviation defined include G = Gelled; H = Hazy; NC = No Change.

A ternary solubility parameter phase diagram based on these soluble co-solvent systems in various non-solvents is presented in Figure 7-5. The use of monoglyme or dioxane in an 80/20 ratio with FAm shifts the tie lines away from the solubility envelope and moves more toward the region characterized by gel-formation. The shift of these systems toward gel-formation gives us a better understand to why a stable asymmetric morphology was not obtained as in the case of the THF/FAm and further substantiates the reliability of these ternary phase solubility parameter diagrams to determine good solvents and non-solvents for stable asymmetric formation.

- Conventional solubility envelope

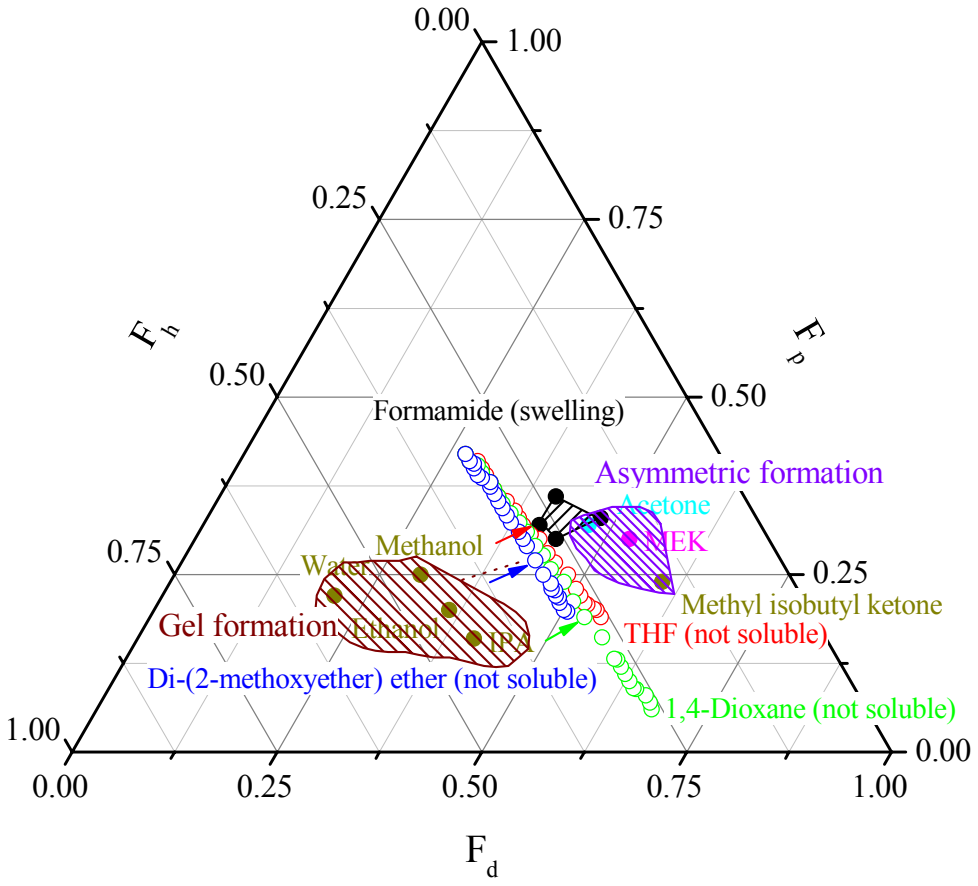

Figure 7-5. Three dimensional phase diagram BPS-20 asymmetric membrane from cosolvent systems containing 20 vol% of FAm and coagulated in acetone at ambient temperature

4 Conclusions

The asymmetric membranes were prepared using two nonsolvents when combined served as a cosolvent system. Only four of the cosolvents systems THF/FAm, 1,4-Dioxane (D)/ FAm, monoglyme (MG)/FAm, and, diglyme (DG)/ FAm had the ability to complete dissolve BPS-20. However, unlike the THF/FAm systems the preparation of

asymmetric membranes from these other cosolvent systems caused large macrovoids to form throughout the membrane. The shift of these systems toward gel-formation gives us a better understand to why a stable asymmetric morphology was not obtained as in the case of the THF/FAm and further substantiated the reliability of ternary phase solubility parameter diagrams to determine good solvents and non-solvents for stable asymmetric formation.

Good phase separated morphology was seen for the disulfonated BPS-20 copolymer dissolved in THF/Formamide (80:20; 76:24) solutions and coagulated in acetone. Thicker skins were formed from casting solution with high polymer concentrations (25 wt%). Thinner skins (2 μm) were obtained for membranes prepared with shorter drying times (<30 sec). Longer drying times (>90 sec) lead to the formation of dense membranes that exhibited no asymmetric character.

CHAPTER 8. PREPARATION OF THIN FILM COMPOSITE MEMBRANES BASED ON DISULFONATED POLY(ARYLENE ETHER SULFONE) RANDOM COPOLYMERS FOR DESALINATION BY REVERSE OSMOSIS

Natalie Y. Arnett[a], Chung Hyun Lee[a], Ozzie Lane[a], Bryan McCloskey[b], Benny Freeman[b], and James E. McGrath[a]

[a]Macromolecules and Interfaces Institute

Virginia Polytechnic Institute and State University, Blacksburg, VA 24061

[b]Department of Chemical Engineering

The University of Texas at Austin, Austin, TX 78712

Abstract

The purpose of this research was to prepare ultra-thin TFC based on 4, 4'-biphenol based poly(arylene ether sulfone)s (BPS-20) using a combination of a solution casting and a brush-coating technique. The thin film composite membranes based on BPS20 (BPS-TFC) were fabricated using 0.1-1 wt% BPS20 solution in Di(EG) on the top of Udel® backing, air-drying at 70 °C for 2 hr (Control), and thermal-treating in vacuum oven from 90 to 190 °C for 2 hr. Increasing the number of applied coats from 1 to 3 times greatly improve the membrane surface smoothness resulting in the formation of dense, pinhole free skin layer with average thickness (t_{avg}) of ~550 nm. Although the removal of DiEG could be achieved at 150 °C, this temperature would ultimately result in

a decrease in the water flux due to extreme reduction of pore size of the Udel® backing. Therefore, 90 ^{o}C was chosen as the maximum thermal treatment temperature for these TFC. The addition of 20 wt% of glycerin contributed to opening the pores of the Udel® backing as illustrated by the increase in water flux from 0 to approximately 600 L/m^{2}hr. A multilayer technique may be the route to successfully preparing ultra-thin, defect-free TFC.

1. Introduction

Polyamide thin film composites (TFC) are the most widely used membranes in desalination. TFCs for reverse osmosis (RO) desalination are multilayered membranes comprised of ultra-thin skin polyamide top layer (20-100 nm) on top of a polysulfone porous support and reinforced by a non-woven fabric[121]. The polyamide top layer is formed via interfacial polymerization of *a* diamine (e.g. *m*-phenylene diamine, MPD) in aqueous phase and di- or –tri- chloride (e.g. trimesoyl chloride, TMC) in organic phase. Compared to traditional cellulose acetate (CA) asymmetric membranes, the top layer of TFC are usually much thinner resulting in higher selectivity and fluxes. TFC membranes also offer additional advantages over CA membranes including enhance stability over larger pH range and higher temperatures and reduced fouling.

The major limitation of polyamide TFC membranes is their sensitivity to chlorine. Polyamide membranes are believed to degrade by chlorination first undergoing N-chlorination through chlorine attack on amidic nitrogen followed by ring chlorination through intermolecular rearrangement[160]. Ring chlorination disrupts hydrogen bonding between the chains and degrades the polymer matrix via chain scission. Thus in a RO system, water has to be dechlorinated before passing through the polyamide TFC and then rechlorinated before distribution. Ultimately affording more complicated system setups and increasing production cost.

TFC based on disulfonated poly(arylene ether sulfone) (PAES) random copolymers are attractive alternatives to polyamide RO membranes. Recent research has shown that dense membranes prepared from disulfonated PAES exhibit high salt

rejection (99%) and stability against chlorine attack at low sulfonation levels (20%)[356,357]. The high tolerance of these copolymers to chlorine could possible reduce costs with the RO setup by essentially eliminating both the dechlorination and rechlorination steps. However, low fluxes and low water uptakes are also characteristic of these membranes. These properties can be greatly improved by preparing TFC from these copolymers. Thus the purpose of this research was to prepare ultra-thin TFC based on 4, 4'-biphenol based poly(arylene ether sulfone)s (BPS-20) using a combination of a solution casting and a brush-coating technique. Different variables such as casting solvents, treatment of the polysulfone support, and the amount of surface coats applied will be investigated. The effect of these variables on the performance of these TFC will be reported.

2. Experimental

1.1 Materials

Eastman Chemical provided high purity 4,4'-biphenol (BP) which was dried at 50 ºC under vacuum before each use. Solvay Advanced Polymers supplied highly purified 4,4'-dichlorodiphenylsulfone (DCDPS), polyphenylene sulfone (Radel®), and polysulfone (UDEL®). 4,4'-Dichlorodiphenylsulfone was dried at 60 ºC under vacuum before each use. Diethylene glycol, ethylene glycol, propylene glycol, 2-methyl-2,4-pentanediol were purchased from Aldrich and used with further purification. The detailed synthesis of

[356] Membrane Technology. "UCLA and Virginia Tech develop novel desalination technologies." March (2007).
[357] Park, H., Freeman, B., Zhang, Z., Sankir, M., McGrath, J.E. *Angew. Chem. Int. Ed.* **2008,** 47, 6019 – 6024.

3,3'-disulfonate-4,4'-dichlorodiphenylsulfone monomer (SDCDPS) has been reported[93]. BPS-20 random copolymer was supplied by Akron Polymer Systems.

1.2 Casting Solvent Selection and TFC Fabrication

Casting solvents were chosen based on three-phase solubility parameter diagrams previously discussed. Solutions (0.1-7% wt%) of BPS-20 were prepared in diethylene glycol at 60 ºC for 8 hours. The solubility of BPS-20 in other glycols such as ethylene glycol, propylene glycol, 2-methyl-2,4-pentanediol (hexylene glycol) was also investigated for comparison. The solutions were then applied onto a pretreated porous polysulfone support (Dow) using both a doctor blade and a camel hair paint brush at ambient temperatures. The membranes were then imaged using SEM.

1.3 Pretreatment of Polysulfone Porous Support

Polysulfone porous support was pretreated by soaking the support in water, isopropanol (IPA), IPA:glycerin (80:20) mixture, and diethylene glycol for 24 hrs. The effect of the membrane drying and thermal treatment was investigated. The experimental procedures for each parameter are presented below.

The influence of membrane drying was accomplished by placing the polysulfone support in the appropriate solvents and allowing it to no air time or to dry in air for approximately 1 hr.

The effect of drying temperatures was determined using dense membranes. Dense membranes were used to understand the thermal behavior of BPS-20 in Di(EG) because it is hard to isolate only a submicron skin layer from the composite. This membrane was prepared by casting a 7 wt% BPS20-Di(EG) solution onto a glass plate and dried at room temperature or in the vacuum oven at 70, 90, 130, 150, 170, and 190 ºC for 2 hrs.

1.4 Generation of Solubility Parameter Ternary Phase Diagrams

Three-phase solubility parameter diagrams were generated utilizing the solubility of the polymer in terms of each specific interaction (δ_d, δ_p, and δ_h) of various solvents using a triangular graphing based on the first power relationship technique[358] The location of the solubility envelope within the triangular diagram was determined by preparing 20 wt % polymer solutions in various liquids at elevated temperatures.

1.5 Characterization

1.5.1 Scanning Electron Microscopy

Top and cross section of the TFC membranes were by using a LEO (Zeiss) 1550 field emission Scanning Electron Microscopy (FE-SEM) at 5 eV. The samples were freeze fractured under cryogenic conditions using liquid nitrogen and coated with 8-10 nm gold before tested.

[358] J.P. Teas, Graphical analysis of resin solubilities, J. Paint Technol., **1968,** 40, 19-25.

1.5.2 Bubble Point Test

The approximate maximum pore size of a the polysulfone support was determined using a ASTM Standard E-128 "Bubble Point" test carried out on a Perm-porometer. The 'Bubble Point' test is used to correlate the measured bubble point pressure value to the calculated maximum pore size[359]. A piece of polysulfone was submerged in isopropyl alc The calculated maximum pore was then multiplied by a pore shape correction factor to estimate the filter rating.

1.5.3 RO Performance of Thin Film Composite (TFC) Membranes

Water and salt transport properties were determined using a Millipore MilliQ system (Billerica, MA). The water flux of the Udel® backing was measured in a high-pressure (up to 1000 psi) dead-end filtration system (Sterlitech TM HP4750 stirred cell, Sterlitech Corp., WA). Salt rejection experiments using sodium chloride (NaCl) were conducted in a cross-flow system using feed solutions containing 2000 mg L^{-1} of NaCl (2000 ppm). The salt rejection (R) was calculated as a function of the salt concentration in the permeant (C_{jl}) and the salt concentration in the feed water (C_{jo}) using a digital conductivity meter (Oakton® CON 110, Cole Parmer, Vernon-Hills, NJ).

3. Results and Discussion

3.1. Casting Solvent Selection and Thin Film Composite Preparation

[359] http://www.chandeisenmann.com/tech_info/bubble_point.asp

Solvent selection is an important aspect required to successfully prepare TFC. An appropriate solvent should not only completely dissolve a selected material for a dense skin layer but should also be insoluble for the porous Udel® backing. Ternary phase diagram are effective resources used to determine efficient and precise selection of casting solution components and composition. A region of solubility for BPS-20 copolymer has already been developed and discussed in the previous chapters. However, this solubility envelope was based on polar aprotic solvents such as NMP that act as good solvents for Udel® support. Thus other solvents based on ternary diagrams that were good solvents for BPS-20 and good non-solvents for Udel® backing were selected. Preliminary research has shown that formic acid has the ability to dissolve BPS-20 under elevated temperature. Utilizing this data has allowed the solubility envelope for BPS-20 to be expanded to various solvents under elevated temperatures (Figure 8-1). Some potential solvent alternatives for BPS-20 at elevated temperatures are listed in Table 8-1.

Limited solubility has been observed for these solvents at 60 °C for several hours. The highest dissolution amount (7 wt%) of BPS-20 was observed in diethylene glycol. This was due to Di(EG) having the highest hydrophilic concentration (0.75) of all the solvents. Hence, the hydrophilic concentration was determined as the ratio of the number of hydrophilic groups [hydroxyl (OH) or oxygen (O)] functionalities present in the compound to the amount of carbons present. Decreasing the hydrophilic concentration from 0.67 to 0.33 resulted from decreased solubility (1 wt%) to insolubility, respectively.

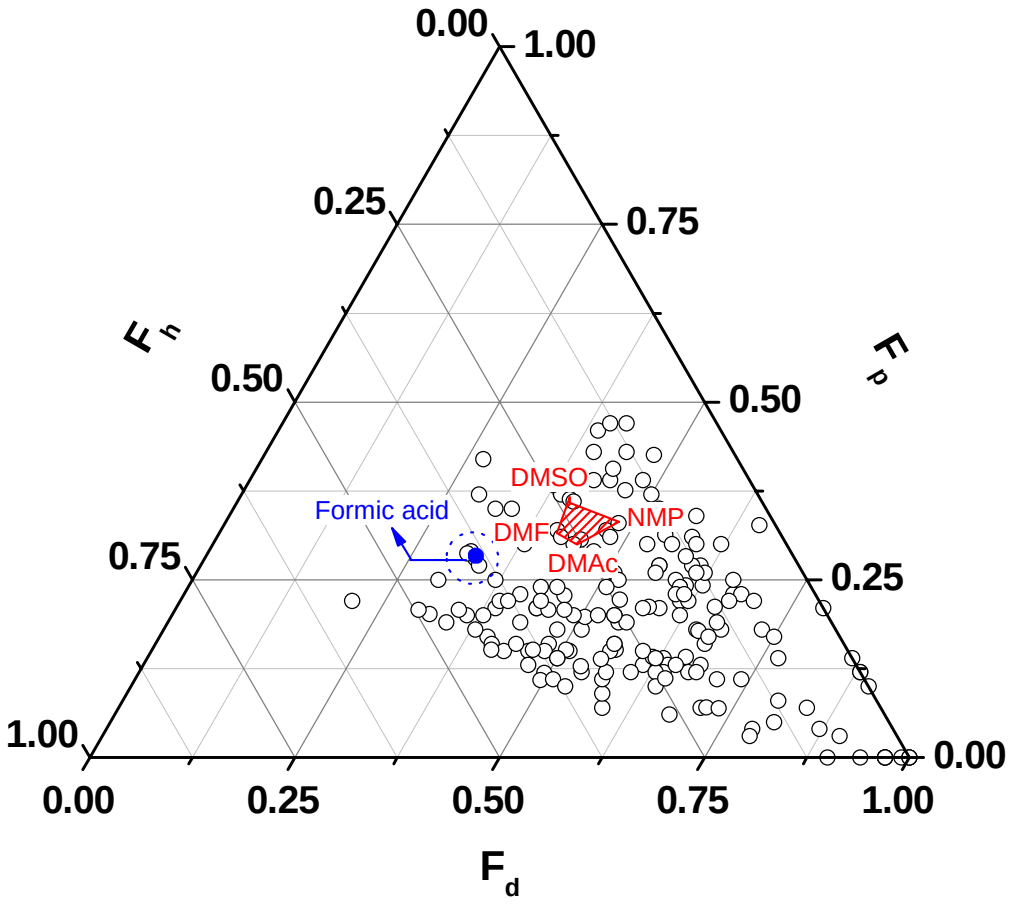

Figure 8-1. Ternary Phase Solubility Parameter Diagram Illustrating the Placement of Formic Acid in Relation to Predetermined Solubility Envolope for BPS-20

The placement of Di(EG) and EG on the solubility diagrams in relation to the predetermined solubility envelope for BPS-20 is presented in Figure 8-2. By comparing Figure 1 and 2 it is apparent that the placement of Di(EG) lies very close to that of formic acid. Since the highest concentration of BPS-20 could be obtained in Di(EG), the preparation of BPS20-TFC was carried out utilizing this solvent. Additionally, Di(EG) was also found to be a good solvent and non-solvent for BPS20 and Udel® backing, respectively.

Table 8-1. Properties of Some Alternative Solvents for BPS-20 Used to Prepare Thin Film Composites

Name	***Structure***	***Boiling Point (°C)***	***Hydrophilic Concentration[a]***	***Solubility of BPS-20[b]***
Diethylene glycol [Di(EG)]	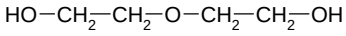	244	0.75	Soluble up to 7 wt%
Propylene glycol (PG)	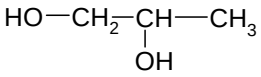	188	0.67	Soluble up to 1 wt%
Hexylene glycol (HG)	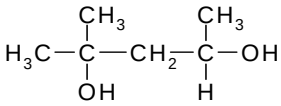	198	0.33	Insoluble

a. Hydrophilic concentrations of the solvents were determined by number of hydrophilic group (-OH or –O-)/ Number of carbon.

b. Solubility test were accomplished in the relevant solvent at 60 °C until dissolution.

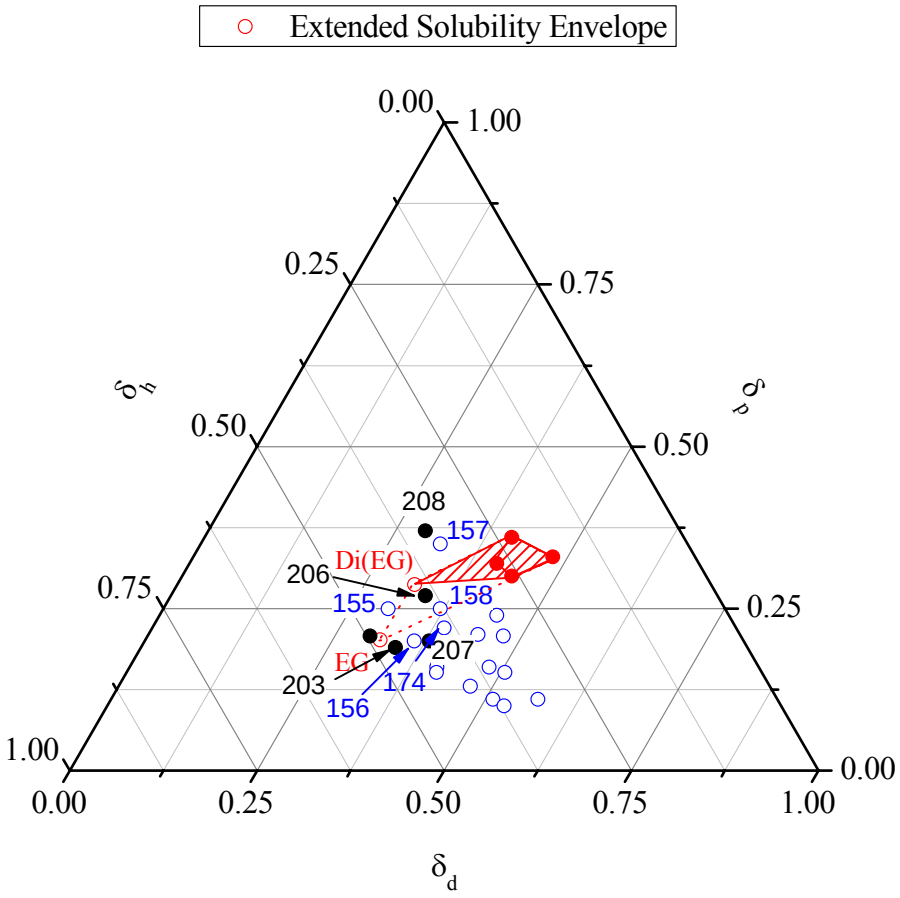

Figure 8-2. Classification of Potential Solvents for BPS-20 based on Ternary Phase Solubility Parameter Diagram

Complete dissolution of BPS20 in Di(EG) at low concentration only occurs after heating over 60 ^{o}C for approximately 8 hrs. However, this solution state does remain stable at R.T. Figure 8-3 demonstrates that faster dissolution times can be achieved when copolymers with higher sulfonation levels are used. This faster dissolution time is related to the high compatibility of Di(EG) with hydrophilic sulfonic acid groups in di-sulfonated polymer matrix (BPS20). At higher sulfonation levels, a higher concentration of sulfonic

acid groups are present in the copolymer matrix causing increased interactions with Di(EG) resulting in improved BPS-20 solubility and faster dissolution times.

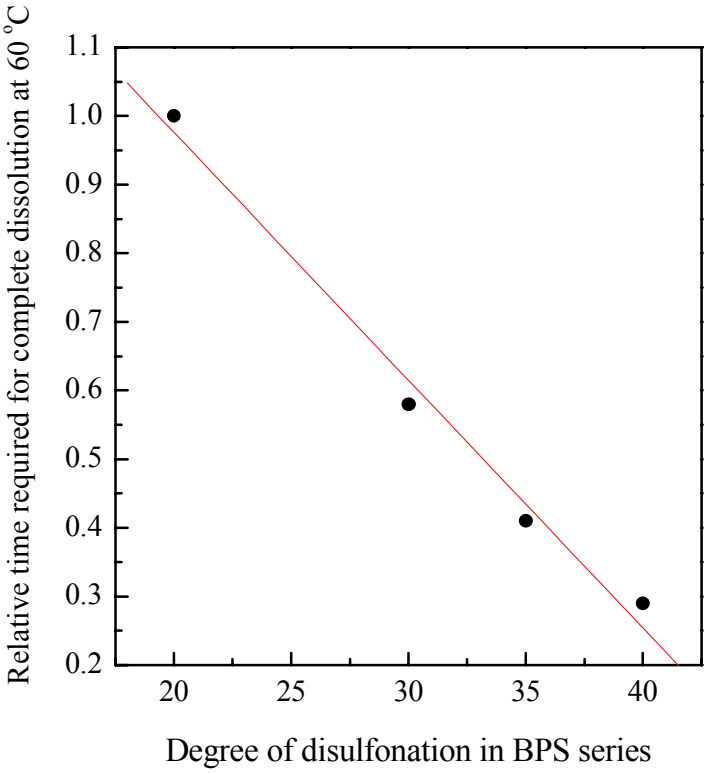

Figure 8-3. Solubility of Biphenol based Disulfonated PAES Random Copolymers with Various Degrees of Sulfonation in Di(EG) at 60 °C.

The thin film composite membranes based on BPS20 (BPS-TFC) were fabricated by the combination of solution casting with a doctor blade and brush-coating 0.1-1 wt% BPS20 solution in Di(EG) on the top of Udel® backing, air-drying at 70 °C for 2 hr (Control), and thermal-treating in vacuum oven from 110 to 190 °C for 2 hr. Figure 8-4 illustrates the effect of the number of coating on the surface properties of BPS-20-TFC.

As seen increasing the number of applied coats from 1 to 3 times greatly improved the membrane surface smoothness and reduced the amount of surface defects.

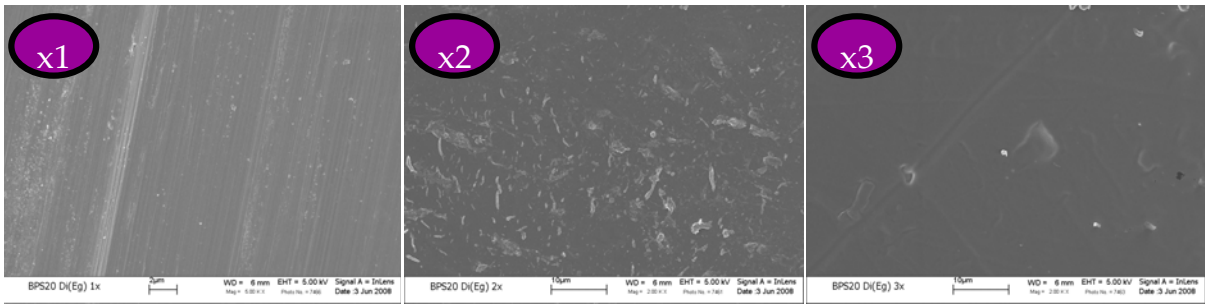

Figure 8-4. SEM images illustrate the effect of the number of brush coatings on the surface smoothness of BPS-TFC.

The surface and cross-section SEM images of BPS20-TFC are shown in Figure 8-5 Brush-coating (3x) with a low concentration (0.5% w/v) of BPS20-Di(EG) solution resulted in the formation of dense, pinhole free skin layer with average thickness (t_{avg}) of ~550 nm. However, penetration of BPS20 solution into porous backing layer during coating process was observed. This can potentially clog the pores of the porous Udel® backing, ultimately reducing water flux through the membrane.

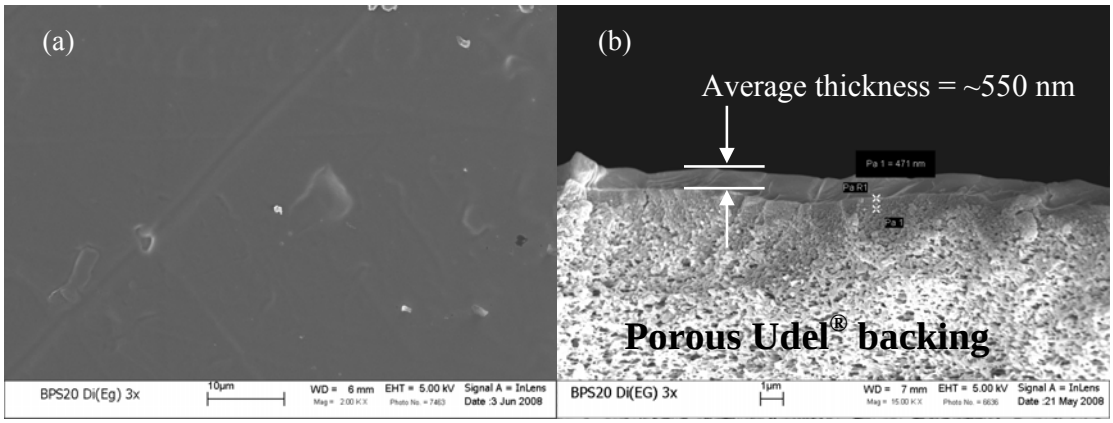

Figure 8-5. SEM images of a BPS20-TFC membrane, thermally treated at 130 ^{o}C for 2 hr and brush-coated 3x (a) surface (×500) (b) cross-section (×15,000).

Remember that Di(EG), has a high compatibility with water molecules. Therefore any remaining Di(EG) molecules in TFC membranes can be exchanged with water molecules via phase inversion. This can result in pore formation within the dense layer and decrease salt rejection. Hence, it is important to remove the remaining Di(EG) from the TFC membrane. This can be accomplished by thermal treatment of the TFC.

Figure 8-6 shows the thermal evaporation behavior of BPS20 in Di(EG). A dense membrane was used to understand the thermal behavior of BPS-20 in Di(EG) because it is hard to isolate only a submicron skin layer from the composite. In spite of high boiling point of Di(EG), it can be expected that most of Di(EG) would be removed at lower temperatures than its boiling point due to boiling point depression under vacuum. As observed in Figure 8-6, the residual content of Di(EG)-water mixture in BPS20 membrane decreases with high annealing temperatures. Additionally, comparable TGA thermograms were observed when the membrane was thermally treatment at 170 and 150 ^{o}C. Thus, it is possible that thermal treatment in vacuum at 150 ^{o}C for 2 hr should be an

adequate temperature to effective remove Di(EG) to form pore free dense membranes under RO conditions.

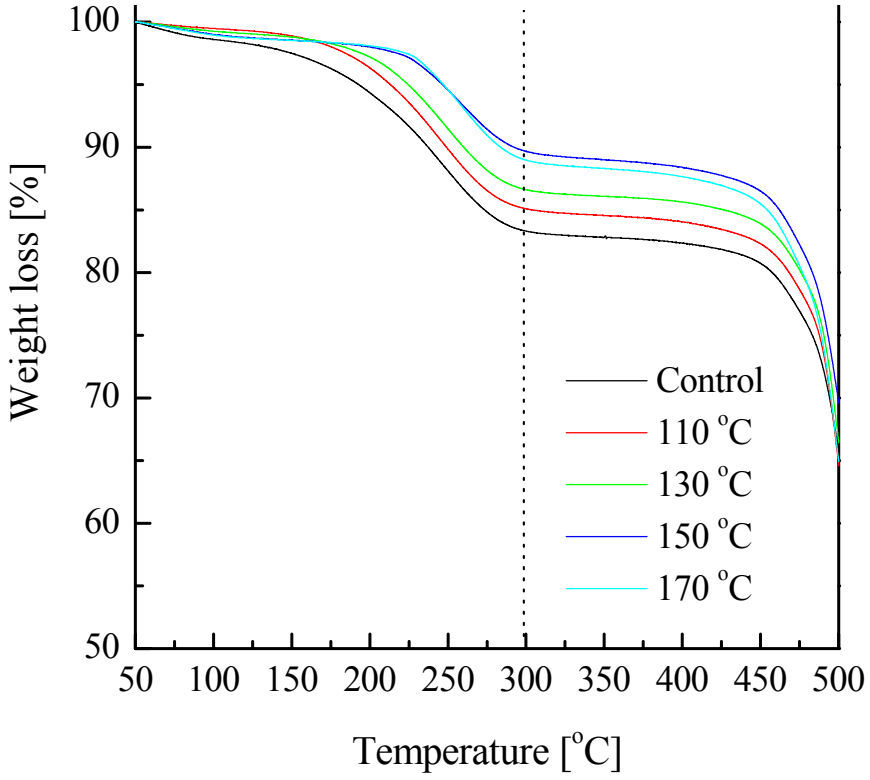

Figure 8-6. TGA thermograms of BPS-20 subjected to different thermal-treatment temperatures.

3.2. Pretreatment of Polysulfone Porous Support

The properties of the Udel® backing in TFC have a great effect on the overall performance of the membrane. The potential of shrinkage of the pores or even penetration, as shown before, from the polymer mixture into the pores can occur. One possible source of pore shrinkage may occur during thermal treatment of the TFC.

Therefore, the Udel® backings were placed in the vacuum oven at the appropriate temperature for 2 hrs and then a bubble point test was carried out in IPA on these supports to understand the effect its thermal treatment on pore size. The results from the bubble point test are presented in Figure 8-7. A slight increase in the maximum size of the pores (1-6) was observed as the temperature was increased to 150 ^{o}C (6). The pore size (0.0282 μm) at 150 ^{o}C decreases as the thermal treatment temperature was increased to 170 (7) and 190 (8) ^{o}C. At these temperatures the sizes of the pore were reduced to 0.0194 and 0.0157 μm, respectively. These results show that 90 ^{o}C should be the maximum thermal treatment temperature for these TFC since thermal treatment of the Udel® backing at 150 ^{o}C caused the large reduction in pore sizes as illustrated by the drop in the water flux. .

To diminish the probability of the pores shrinking, the polysulfone support was pretreated in some type of pore stabilizing solvent. The effectiveness of these solvents in stabilizing the pore can be observed by changes in the water flux. The effects of various stabilizing solvents on the water flux are illustrated in Figure 8-8. The solvents investigated include water, IPA, IPA/glycerin (80/20 by weight) mixture, and Di(EG). When these porous supports are pretreated and not dried, high water flux values are observed. However when the polysulfone support was air dried for 2 hrs after it has been pretreated with water and IPA, the water permeation through membranes essentially stopped as shown by the zero water flux values. This could due to the pores in the support completely collapsing after being exposed to these drying conditions. On the other hand, the addition of 20 wt% of glycerin contributed to opening the pores of the Udel® backing even after drying for 2 hrs in air. This was illustrated by the raise in the

water flux from 0 to approximately 600 L/m^{2}hr. However, this flux decreased as the drying temperature was increased to 150 for 2 hrs.

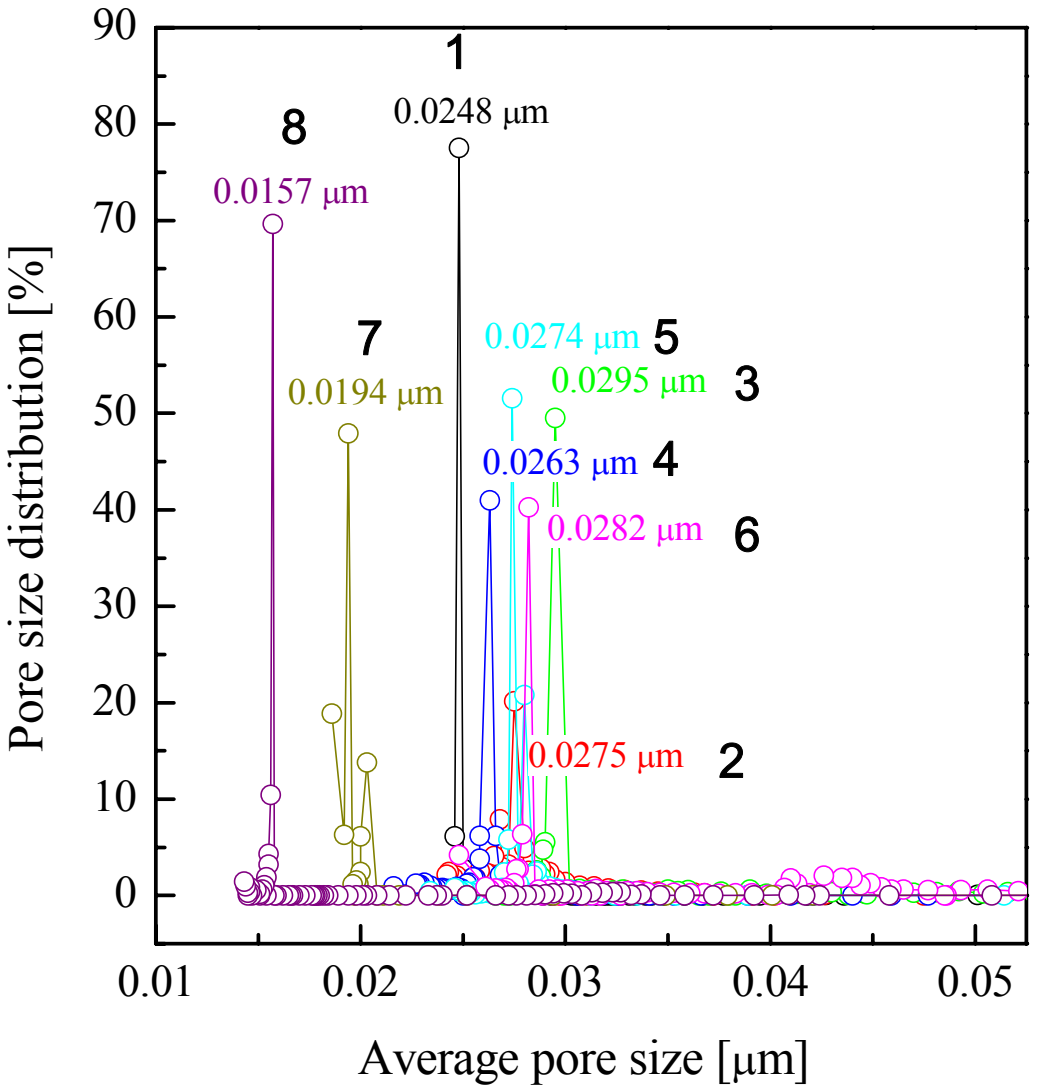

Figure 8-7. Maximum pore sizes from untreated and thermally treated Udel® backing; 1) Control with no thermal treatment; 2) Thermal treatment at 70 °C; 3) Thermal treatment at 90 °C; 4) Thermal treatment at 110 °C; 5) Thermal treatment at 130 °C; 6) Thermal treatment at 150 °C; 7) Thermal treatment at 170 °C; 8) Thermal treatment at 190 °C

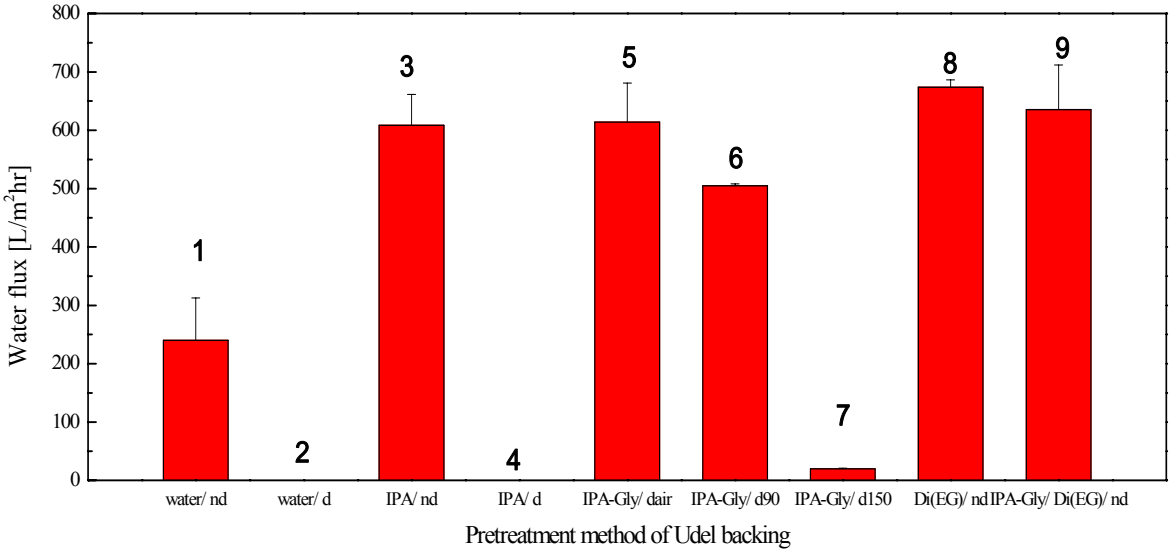

Figure 8-8. The effect of pore stabilizing solvents on the water flux through polysulfone support; 1) Pretreated with water and not dried (nd); 2) Pretreated with water and air dried (d) for 2 hrs; 3) Pretreated with IPA and not dried; 4) Pretreated with IPA and air dried for 2 hrs; 5) Pretreated with IPA/glycerin (Gly) (80/20) and air dried for 2 hrs; 6) Pretreated with IPA/glycerin (Gly) (80/20) and dried for 2 hrs at 90 ^{o}C; 7) Pretreated with IPA and dried for 2 hrs at 150 ^{o}C; 8) Pretreated with Di(EG) and not dried; 9) Pretreated with IPA/Glycerin (80/20)/Di(EG) and not dried

3.3. RO Performance of Thin Film Composite (TFC) Membranes

Generally, disulfonated copolymers in protonated form with high degree of sulfonation (DS) are highly water-permeable as compared with those in salted form with low DS. Table 8-2 lists the hydrated properties of BPS-20 and BPS-30 dense membranes in the salt and acid from. Although higher salt rejection values were demonstrated by BPS-20 and BPSH-20, the water fluxes were still low. The salt rejection values for BPS-

20 and BPSH-20 were 99.2% and 98.7%, respectively. In comparison, BPS-30 copolymers offered higher water permeability values but salt rejection of 96.2% for BPS-30 and 92.1% for BPSH-30.

Table 8-2. Hydrated and Reverse Osmosis Properties of BPS-20 and BPS-30 Random Copolymers in the Salt and Acid Forms.

Sample	Water Uptake (wt%)	Density (g/cm^3)	IEC (meq/g)	Water Permeability ($Lmm^{-2}h^{-1}bar$)	NaCl Rejection (%)
BPS-20	4.5	1.324	0.92	0.03	99.2
BPSH-20	18.1	1.353	0.92	0.21	98.7
BPS-30	9.1	1.349	1.34	0.18	96.2
BPSH-30	30.7	1.370	1.34	1.2	92.1

A submicron-coated skin layer gives clear evidence that an ultra-thin, dense selective layer leads a significant increase in water flux as well as in salt rejection. Figure 8-9 demonstrated the effect of the concentration of BPS-20 in Di(EG), the number of coatings and acidification on the salt water flux (highlighted in red) and salt rejection (highlighted in green) properties. BPS-20 copolymer was used to prepare these TFC and the membranes were acidified in 2 M H_2SO_4 at 65 ^oC for 4 hr. A lower temperature acidification technique was used to maintain the integrity of the TFC.

Coating the Udel backing with two coats Figure 8-9 (graph 1) of 1 wt% BPS-20 in Di(EG) resulted in salt rejections as high as 97%. After this TFC was acidified Figure 8-9 (graph 2) however, the salt rejection decreased to 94% while the salt water flux

doubled. The change in these values could be due to the improved water permeability in the surface membrane of the TFC after exposure to acidification procedure.

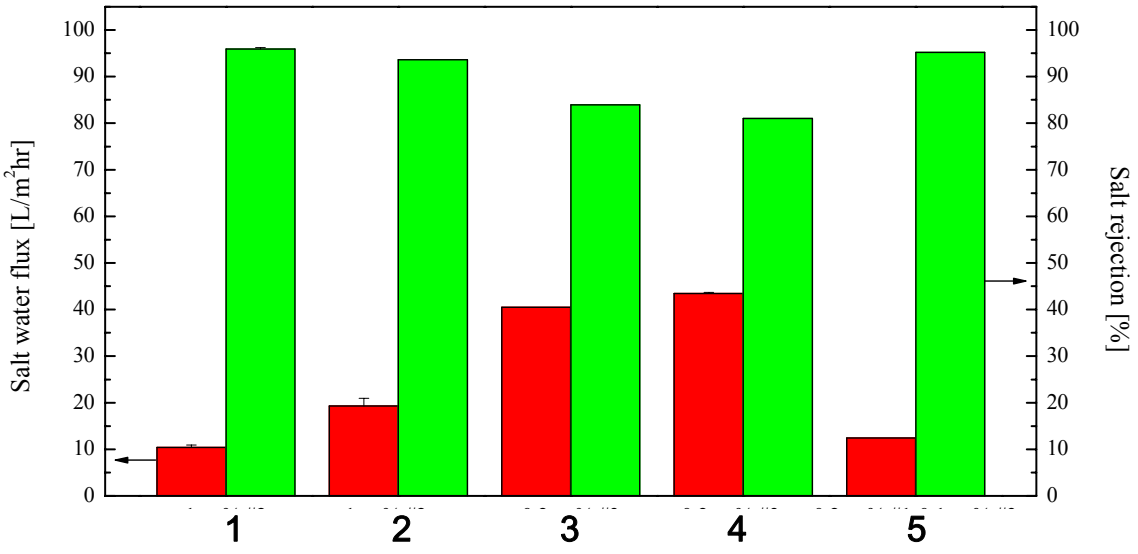

Figure 8-9. Water Flux and Salt rejection Properties of Various BPS-20 TFC Thermally Treated at 90°C. 1) Coated (2x) with 1 wt% BPS-20 in Di(EG); 2) Coated (2x) with 1 wt% BPS-20 in Di(EG) and acidified; 3) Coated (3x) with 0.2 wt% BPS-20 in Di(EG); 4) Coated (3x) with 0.2 wt% BPS-20 in Di(EG) and acidified; 5) First Coated (3x) with 0.1 wt% BPS-20 in Di(EG) and then coated (1x) with 0.2 wt% BPS-20 in Di(EG).

By using a dilute BPS-20 solution it is possible to achieve a thin membrane thickness and may be even the same RO performance when a pinhole free skin layer would be formed. This was not the case as illustrated in Figure 8-9 (graph 3 and 4) where TFCs were prepared by applying 3 coats of 0.2 wt% of BPS-20 in Di(EG) solution. The decrease in salt rejection to approximately 80% and the increase in salt water flux (approximately 40%) showed that pinholes or defects may be present in the skin layer

that allow salt to pass easily through the membrane. In Figure 8-9 (graph 5) a multilayer TFC was prepared by first applying 3 coats of a 0.1% BPS-20 solution to the polysulfone backing followed by one coat of 0.2 wt% solutions. The 0.2 wt% solution was applied to increase salt rejection and decrease salt water flux by possibly sealing any pinholes that may have formed in the underlying layers. This membrane showed comparable salt rejection and salt water flux values as graph 1, demonstrating that a multilayer technique may be the route to successfully preparing ultra-thin, defect-free TFC.

4. Conclusions

The preparation of TFC based on disulfonated PAES was accomplished. Membranes were prepared using low concentrations of BPS-20 in Di(EG) brush coated onto Udel support and thermally treated in the vacuum oven at various temperatures. Compared to other glycols the highest dissolution amount (7 wt%) of BPS-20 was observed in Di(EG). A minimum of three layers of BPS20-Di(EG) solution (0.5% w/v) are required to form dense, pinhole free skin layer. Thermal treatment in vacuum at 90 ^{o}C for 2 hr should be an adequate temperature to effectively remove Di(EG) from the skin layer without causing any extreme shrinkage of the pores in the polysulfone support. Soaking the Udel backing in IPA: glycerin (80:20) mixture contributed to expansion of the pores in the support layer. This was illustrated by the raise in the water flux from 0 to approximately 600 L/m^{2}hr. A multilayer technique may be the route to successfully preparing ultra-thin, defect-free TFC.

CHAPTER 9. OVERALL CONCLUSIONS

The preparation of copolymer blends between BPS-35 and various fluorine containing copolymer was accomplished at low concentrations (≤10 wt%). TM-AFM images and the existence of one T_g confirmed that compatibility between these copolymers was possible. A small reduction in proton conductivity was observed with increasing concentrations of the fluorine containing copolymers. However, no further change in the conductivities was observed in BPS-35/6FS-00, BPS-35/6FS-35, BPS-35/Radel R blend membranes as the concentration was increased from 2 to 10 wt%. A similar change was only observed up to 5 wt% for the BPS-35/$PDVF_2$ membranes. DMFC performance of the blends showed low methanol permeabilities compared to Nafion 1135. Comparable DMFC performance in 0.5 M methanol was only obtained from BPSH-35/6FS-00 (90/10) membranes. At higher methanol concentration these membranes actually outperformed Nafion 1135.

The use of BPS-35/6FS-35 and BPS-35/Radel R blend membranes in the potassium salt and acid forms for reverse osmosis and nanofiltration was also investigated. In the salt form these membranes displayed good sodium chloride salt rejections above 92%. However, low fluxes were also characteristic of these membranes. The highest salt rejections of 97.2 and 98.0% were obtained from BPS35:Radel R (90:10) and BPS-35:6FS-35 (95:5) blends, respectively.

Asymmetric membranes have been prepared from BPS-20 copolymers dissolved in both aprotic solvents and co-solvent mixtures. A region of solubility based on the solubility of BPS-20 in aprotic solvents has been determined. Acetone, which lied

closely to the outer edges of the solubility envelope was determined to be the best non-solvent to prepare asymmetric membranes. The use of aprotic solvents resulted in thin skin layers, however unstable morphologies containing macrovoids and surface defects were also observed. Stable morphologies but thick skin layers were obtained from THF/FAm co-solvent mixtures. To control the thickness of the skin, higher boiling point ether was utilized. The use of these cosolvents systems result in unstable morphologies similar to those observed when aprotic solvents were used. These mixtures fell well outside the solubility envelope.

Thin film composites were prepared from dilute concentration (0.1-1wt%) of BPS-20 in Di(EG). A minimum of three layers of BPS20-Di(EG) solution were required to form dense, pinhole free skin layer. Thermal treatment in vacuum at 90 ^{o}C for 2 hr was found to be an adequate temperature to effectively remove Di(EG) from the skin layer without causing any extreme shrinkage of the pores in the polysulfone support. The presence of glycerin as a pore stabilizing solvent contributed to expansion of the pores in the support layer. This was illustrated by an increase in the water flux from 0 to approximately 600 L/m^{2}hr.

CHAPTER 10. SUGGESTED FUTURE RESEARCH

The structure property relationships investigated during this research emphasize the importance of a thin skin formation in asymmetric and thin film composites (TFC) on RO performance. Earlier research showed that the BPS systems exhibited high salt rejection (+99%) and low water fluxes at low degrees of sulfonation (20%) when dense membranes (~ 20 μm) were used[172]. As demonstrated in Chapter 5, this trend was also observed in blends of BPS-35 with Radel R and 6FS-35. The water fluxes of both types of membranes were improved when the salt form was coverted to the acid form, however salt rejection decreased. Since the thickness of the membranes is directly related to the selectivity other types of such as asymmetric membranes and thin film composites that formed thin skin (~1 μm or less) were investigated. TFC were prepared by brush coating BPS-20 in diethylene glycol solutions onto porous polysulfone support. Asymmetric membranes also prepared from BPS-20 solutions in various cosolvents using a DIPS technique with acetone as the non-solvent. TFC composites prepared from BPS-20 copolymers with thin skin layer (~500 nm) also resulted in an improvement in the water fluxes without adversely affecting salt rejection. So how is it possible to combine the properties of these materials to achieve both high salt rejection and high water flux?

A multilayer technique may be the route to successfully prepare ultra-thin, defect-free phase separated TFC membranes with improved RO performances In a multilayered process it is not only possible to utilize BPS copolymers with higher degrees of sulfonation but the use of asymmetric membranes is also possible. In the first example, two layers would be brush coated onto a polysulfone support. The first layer could be

BPS or some other type of random poly(arylene ether sulfones) (See Figure 1-8, pg 29 for structural variations) with low degrees of sulfonations and in the salt form coated with another highly sulfonation (~40%) copolymer. The lower sulfonated copolymer layer would be responsible for high salt rejection while the higher sulfonated copolymers would increase the water flux. This highly sulfonated copolymer layer could be in the salt or acid form since both would have higher water fluxes. Another possible type of multilayer TFC could be forming an asymmetric membrane from a disulfonated copolymer and then brush coating it with a low sulfonated (< 20%) copolymer. An asymmetric membrane prepared from a disulfonated copolymer would not only serve as the support material but would also aid in improving the water permeability. The proposed membranes composition is illustrated below in Figure 10-1:

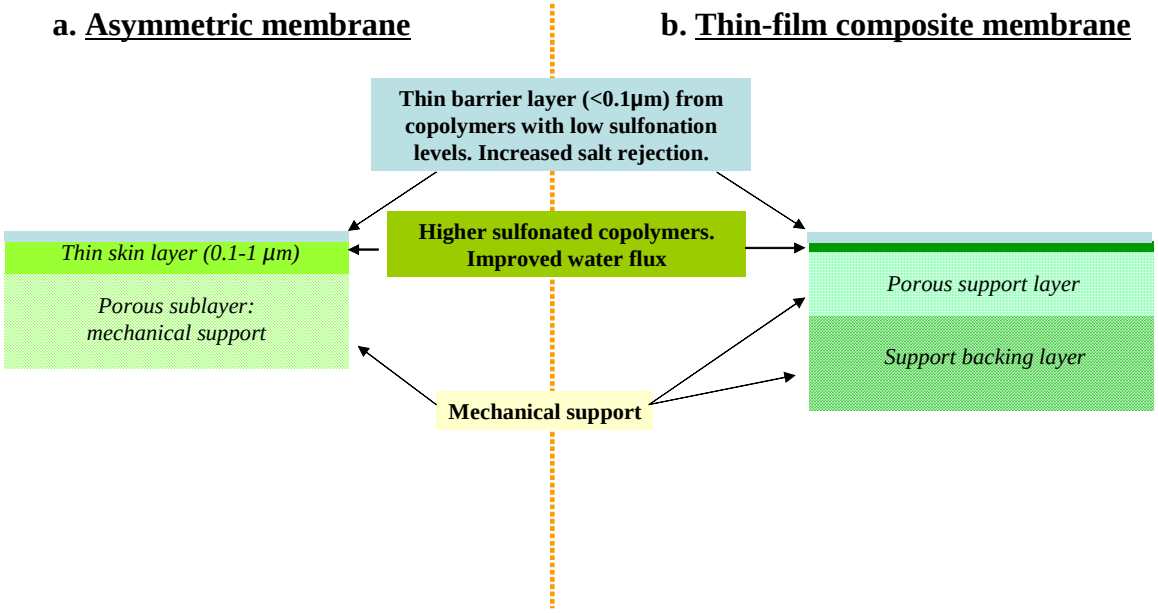

Figure 10-1. Variations in the layers compositions of proposed multilayered TFC membranes**.**